

This electronic thesis or dissertation has been downloaded from the King's Research Portal at <https://kclpure.kcl.ac.uk/portal/>



## The effects of Low-dose IL-2 immunotherapy on immune cells in Amyotrophic Lateral Sclerosis – an incurable motor neuron disease with immune driven pathologies

Mickunas, Marius

*Awarding institution:*  
King's College London

The copyright of this thesis rests with the author and no quotation from it or information derived from it may be published without proper acknowledgement.

### END USER LICENCE AGREEMENT



Unless another licence is stated on the immediately following page this work is licensed

under a Creative Commons Attribution-NonCommercial-NoDerivatives 4.0 International

licence. <https://creativecommons.org/licenses/by-nc-nd/4.0/>

You are free to copy, distribute and transmit the work

Under the following conditions:

- Attribution: You must attribute the work in the manner specified by the author (but not in any way that suggests that they endorse you or your use of the work).
- Non Commercial: You may not use this work for commercial purposes.
- No Derivative Works - You may not alter, transform, or build upon this work.

Any of these conditions can be waived if you receive permission from the author. Your fair dealings and other rights are in no way affected by the above.

### Take down policy

If you believe that this document breaches copyright please contact [librarypure@kcl.ac.uk](mailto:librarypure@kcl.ac.uk) providing details, and we will remove access to the work immediately and investigate your claim.

**The effects of Low-dose IL-2  
immunotherapy on immune cells in  
Amyotrophic Lateral Sclerosis – an  
incurable motor neuron disease with  
immune driven pathologies**

*by*

**MARIUS MICKUNAS**

A thesis submitted for the degree of Doctor of Philosophy

Department of Immunobiology

School of Immunology & Microbial Sciences

King's College London

May 2021

## Abstract

Amyotrophic lateral sclerosis (ALS) is a rare neurological disorder characterised by the loss of motor neurons that control voluntary muscles, leading to progressive paralysis and death. There is no cure, and approved drugs prolong survival by 3-6 months only. The events that trigger ALS are poorly understood, however recent findings indicate a role for inflammation and a lack of immune regulation in the prognosis of ALS.

To this end we carried out the first placebo-controlled, low-dose (LD) interleukin-2 (IL-2) immunotherapy trial in ALS patients with the aim of improving regulatory T cell (Treg) numbers. IL-2 therapy has been used to expand Treg *in vivo* but the expansions observed vary greatly between individuals and an improvement in Treg function is not always observed.

The aim of this project was to assess the effects of IL-2 on lymphoid and myeloid cell number, phenotype, function and IL-2 signalling. We observed significant expansion of Treg, natural killer (NK) cells, effector T cells and cytotoxic T lymphocytes in blood. The data also show changes in monocyte subsets in those receiving the highest dose of IL-2. Comprehensive phenotyping showed significant expansion of highly activated and proliferative Treg subsets and suggested an induction of Treg generation in the thymus. IL-2 also expanded NK subsets that have been shown to have disease modifying actions in other conditions, while assessment of monocyte phenotypes show a reduction in non-classical monocyte subset with high migratory potential. *In vitro* co-culture assays showed a significant increase in Treg suppressive function. While IL-2 signaling analysis showed a significant decrease in IL-2 signaling in Treg, and increased IL-2 signaling in cytotoxic T lymphocytes at the highest dose of IL-2.

In this thesis, we have shown that IL-2 therapy can effectively improve Treg number and function and, is safe and well tolerated in ALS patients. However, more work is needed to determine the dose/frequency or delivery system of IL-2 for optimal Treg expansion and maintenance of elevated numbers. Furthermore, the clinical efficacy of IL-2 in ALS is unknown but is currently being assessed in a phase II clinical trial.

## Acknowledgements

First and foremost, I would like to thank my first supervisor Professor Timothy Tree to whom I have the utmost gratitude for allowing me to undertake a PhD project in the subject area of immunology. His mentorship and positivity has guided me through the highs and lows of this PhD and has undoubtedly shaped my development as a researcher. I would also like to thank my second supervisor Professor Mark Peakman for his advice and ideas during lab meetings. I wish to thank the members of my PhD thesis committee: Dr Deena Gibbons, Dr Susan John and Dr Marc Martinez-Llordella for their advice and thoughtful discussion.

Thank you to all the members of the Tree group for making the last 4 years wonderful and full of laughs but more importantly for the help, advice, support and positivity when I was struggling to make some of the experimental protocols work. A particular thanks to Jennie Yang who has spent many hours teaching me flow cytometry. Everyone in DIIID for helpful scientific discussion, sharing of laboratory equipment, reagents, blood donations and fantastic baked goods.

I am fortunate to have a beautiful family, my mother, brother, my wife Florencia and our three beautiful children who pushed me and believed in me, especially in dark times where my own self-belief was at a low and without them this thesis would not have materialised.

Finally, I would like to dedicate this thesis to my partner Florencia and our three children, Sam, Luna and Oliver who are simply wonderful.

## Table of Contents

|   |    |
|---|----|
| <i>List of figures .....</i>  | 8  |
| <i>List of tables.....</i>  | 12 |
| <i>Abbreviations.....</i>   | 13 |
| <i>Chapter 1. Introduction.....</i>   | 19 |
| <i>    1.1. Amyotrophic Lateral Sclerosis – a fatal motor neuron disorder. ..</i> | 19 |
| <i>        1.1.1. Clinical presentation and diagnosis.....</i>                    | 20 |
| <i>        1.1.2. Genetic association with ALS.....</i>                           | 21 |
| <i>    1.2. Currently approved treatment in ALS.....</i>                          | 23 |
| <i>        1.2.1. Riluzole.....</i>   | 23 |
| <i>        1.2.2. Edaravone.....</i>  | 24 |
| <i>    1.3. ALS Research. ....</i>  | 26 |
| <i>        1.3.1. ALS Mouse model(s). ....</i>                                    | 26 |
| <i>        1.3.2. Biomarkers in ALS diagnosis and prognosis.....</i>              | 27 |
| <i>            1.3.2.1. Neurofilaments.....</i>                                   | 28 |
| <i>        1.4. ALS and the immune system.....</i>                                | 30 |
| <i>            1.4.1. The immunogenetics of ALS.....</i>                          | 31 |
| <i>            1.4.2. The innate immune system in ALS.....</i>                    | 32 |
| <i>                1.4.2.1. Monocytes and microglia.....</i>                      | 32 |
| <i>                1.4.2.2. NK Cells.....</i>                                     | 36 |
| <i>                1.4.2.3. Cytokines. ....</i>                                   | 37 |
| <i>                    1.4.2.3.1. MCP-1.....</i>                                  | 38 |
| <i>                    1.4.2.3.2. CX3CL1.....</i>                                 | 39 |
| <i>            1.4.3. ALS and the adaptive immune system. ....</i>                | 41 |
| <i>                1.4.3.1. CD8<sup>+</sup> T cells.....</i>                      | 43 |
| <i>                1.4.3.2. Treg.....</i>   | 43 |
| <i>        1.5. The role of IL-2 in Treg generation and function.....</i>         | 49 |
| <i>            1.5.1. Origins of IL-2.....</i>                                    | 50 |
| <i>            1.5.2. Production of IL-2 .....</i>                                | 50 |
| <i>            1.5.3. The IL-2R.....</i>  | 51 |
| <i>            1.5.4. Expression of IL-2R .....</i>                               | 52 |
| <i>            1.5.5. Signaling downstream of the IL-2R.....</i>                  | 54 |
| <i>            1.5.6. Pleiotropic effects of IL-2.....</i>                        | 56 |

|  |            |
|--|------------|
| <b>1.5.7. Clinical trials utilising low-dose IL-2.....</b>   | <b>58</b>  |
| <b>1.6. Clinical trials in ALS.....</b>  | <b>60</b>  |
| <b>1.7. Immuno-modulation in ALS (IMODALS) clinical trial. ....</b>  | <b>62</b>  |
| <b>1.8. Aims of this thesis.....</b>   | <b>66</b>  |
| <b>Chapter 2. Investigating the effects of IL-2 therapy on immune cells in peripheral blood of ALS patients.....</b>                   | <b>67</b>  |
| <b>2.1. Introduction.....</b>  | <b>67</b>  |
| <b>2.2. Materials and methods.....</b>   | <b>69</b>  |
| <b>2.3. Results.....</b>   | <b>71</b>  |
| <b>2.3.1. Designing analysis templates to identify the major leukocyte populations in whole blood.....</b>                             | <b>71</b>  |
| <b>2.3.2. Data concordance between analysts.....</b>   | <b>76</b>  |
| <b>2.3.3. Significant increases in total lymphocytes, CD3<sup>+</sup> and CD4<sup>+</sup> T cells as a result of IL-2 therapy.....</b> | <b>79</b>  |
| <b>2.3.4. Significant expansion of Treg by IL-2 in ALS patients. ....</b>  | <b>87</b>  |
| <b>2.3.5. IL-2 therapy expanded non-Treg cells bearing the IL-2R subunits.</b>   | <b>89</b>  |
| <b>2.3.6. Reduced numbers and frequencies of monocyte subsets at the height of IL-2 therapy.....</b>                                   | <b>96</b>  |
| <b>2.4. Discussion.....</b>  | <b>104</b> |
| <b>Chapter 3. Evaluating the effects of LD-IL-2 on Treg suppressive function in vitro. ....</b>  | <b>111</b> |
| <b>3.1. Introduction.....</b>  | <b>111</b> |
| <b>3.2. Materials and methods.....</b>   | <b>116</b> |
| <b>3.3. Results.....</b>   | <b>121</b> |
| <b>3.3.1. Quality control.....</b>   | <b>121</b> |
| <b>3.3.2. Significant correlations between Treg frequencies in fresh blood and cryopreserved PBMC.....</b>                             | <b>122</b> |
| <b>3.3.3. Improvement in Treg suppressive function after IL-2.....</b>   | <b>124</b> |
| <b>3.3.4. Sustained increase in Treg function three weeks after IL-2. ....</b>   | <b>129</b> |
| <b>3.3.5. Is expression of CD25 on Treg associated with increase in Treg suppressive function? .....</b>                               | <b>135</b> |
| <b>3.4. Discussion.....</b>  | <b>142</b> |
| <b>Chapter 4. Investigating the effects of LD-IL-2 therapy on IL-2 signalling in Treg and non-Treg cells.....</b>                      | <b>149</b> |
| <b>4.1. Introduction.....</b>  | <b>149</b> |
| <b>4.2. Materials and methods.....</b>   | <b>151</b> |

|  |            |
|--|------------|
| <b>4.3. Results.....</b>   | <b>158</b> |
| <b>4.3.1. Optimisation of experimental protocol.....</b>   | <b>158</b> |
| <b>4.3.2. Determining the concentrations of IL-2 needed for stimulation of different lymphocyte subsets.....</b>   | <b>161</b> |
| <b>4.3.3. Experimental quality control.....</b>  | <b>162</b> |
| <b>4.3.4. IL-2 signalling at day 1 in Treg and non-Treg cells did not correlate with the expansions observed at day 64 in these cell types.....</b>      | <b>163</b> |
| <b>4.3.5. Reduced IL-2 signalling in Treg following IL-2 therapy.....</b>  | <b>166</b> |
| <b>4.3.6. Increased IL-2 signalling in CD8<sup>+</sup> T cells following IL-2 therapy.</b>   | <b>173</b> |
| <b>4.3.7. Assessment of IL-2 signalling via STAT proteins in whole blood monocytes from healthy donors.....</b>  | <b>176</b> |
| <b>4.4. Discussion.....</b>  | <b>181</b> |
| <b>Chapter 5. Comprehensive phenotyping of Treg and non-Treg cells before and after LD-IL-2.....</b>   | <b>193</b> |
| <b>5.1. Introduction.....</b>  | <b>193</b> |
| <b>5.2. Materials and methods.....</b>   | <b>198</b> |
| <b>5.3. Results.....</b>   | <b>206</b> |
| <b>5.3.1. Experimental quality control.....</b>  | <b>207</b> |
| <b>5.3.2. Parent populations of Treg, NK and monocytes are comprised of several, heterogenous subpopulations in IMODALS trial participants....</b>       | <b>208</b> |
| <b>5.3.3. Treg, NK and monocyte subpopulation analysis in QC PBMC across the experimental batches.....</b>   | <b>210</b> |
| <b>5.3.4. LD-IL-2 selectively activates specific Treg subpopulations, some of which are maintained for up to three months after the final dose. ....</b> | <b>212</b> |
| <b>5.3.5. In ALS patients, IL-2 expands CD56<sup>bright</sup> NK subpopulations associated with an immunoregulatory, NK2, phenotype.....</b>             | <b>223</b> |
| <b>5.3.6. IL-2 therapy induced a decrease in monocytes with high migratory potential.....</b>  | <b>227</b> |
| <b>5.4. Discussion.....</b>  | <b>231</b> |
| <b>Chapter 6. Integrated analysis and final discussion.....</b>  | <b>242</b> |
| <b>6.1. Integrated analysis of chapter data.....</b>   | <b>242</b> |
| <b>6.1.1. Overview of PCA analysis.....</b>  | <b>244</b> |
| <b>6.1.2. PCA analysis on Treg at day 64.....</b>  | <b>246</b> |
| <b>6.1.3. PCA analysis on Treg and non-Treg cells at day 64.....</b>   | <b>249</b> |
| <b>6.1.4. PCA analysis on Treg at all timepoints where they are altered.....</b>   | <b>252</b> |
| <b>6.1.5. Summary of PCA analyses.....</b>   | <b>254</b> |
| <b>6.2. Summary of thesis findings and outstanding questions.....</b>  | <b>255</b> |

|   |            |
|---|------------|
| <b>6.3. Concluding remarks and future directions.....</b> | <b>259</b> |
| <b>References.....</b>                                    | <b>264</b> |

## List of figures

|   |    |
|---|----|
| <i>Figure 1-1 Neurofilament release into bodily fluids .....</i>  | 29 |
| <i>Figure 1-2 Summary of adaptive immunity findings in ALS. ....</i>  | 41 |
| <i>Figure 1-3 Mechanisms of Treg mediated suppression. ....</i>   | 46 |
| <i>Figure 1-4 Summary of Treg findings in ALS.....</i>  | 49 |
| <i>Figure 1-5 Transcription factors that regulate the expression of IL2 gene. ....</i>                      | 51 |
| <i>Figure 1-6 IL-2R subunits on the cell surface.....</i>   | 52 |
| <i>Figure 1-7 Transcription factors that regulate the expression of IL2RA, IL2RB and IL2RG genes.....</i>   | 54 |
| <i>Figure 1-8 Signaling pathways downstream of the IL-2R. ....</i>  | 56 |
| <i>Figure 1-9 The pleiotropic effects of IL-2 within the mammalian immune system.</i>                       | 57 |
| <i>Figure 1-10 IMODALS clinical trial profile.....</i>  | 65 |
| <i>Figure 2-1 Gating scheme for staining panel 1.....</i>   | 72 |
| <i>Figure 2-2 Gating scheme for panel 2. ....</i>   | 73 |
| <i>Figure 2-3 Gating scheme for monocyte phenotypes in panel 3. ....</i>                                    | 74 |
| <i>Figure 2-4 Gating scheme for monocyte phenotypes in panel 4. ....</i>                                    | 75 |
| <i>Figure 2-5 Pearson correlation coefficient for CD3, CD4 and CD8 T cells between analyst 1 and 2.....</i> | 77 |
| <i>Figure 2-6 Person correlation coefficient for Treg, Teff and NK cells between analyst 1 and 2.....</i>   | 78 |
| <i>Figure 2-7 Analysis methods used to investigate changes in immune cells after IL-2 therapy.....</i>      | 79 |
| <i>Figure 2-8 The effects of LD-IL-2 on total lymphocyte number.....</i>                                    | 81 |
| <i>Figure 2-9 The effects of LD-IL-2 on B cell number and frequency.....</i>                                | 82 |
| <i>Figure 2-10 The effects of LD-IL-2 on CD3 T cell number and frequency.....</i>                           | 84 |
| <i>Figure 2-11 The effects of LD-IL-2 on CD4 T cell number and frequency.....</i>                           | 86 |
| <i>Figure 2-12 The effects of LD-IL-2 on Treg cell number and frequency.....</i>                            | 88 |
| <i>Figure 2-13 The effects of LD-IL-2 on Teff cell number and frequency.....</i>                            | 90 |

|   |     |
|---|-----|
| <i>Figure 2-14 The effects of LD-IL-2 on CD8 T cell number and frequency.....</i>   | 91  |
| <i>Figure 2-15 The effects of LD-IL-2 on NK cell number and frequency. ....</i>   | 93  |
| <i>Figure 2-16 The effects of LD-IL-2 on CD56bright NK cell number and frequency.</i>   |     |
| .....   | 94  |
| <i>Figure 2-17 The effects of LD-IL-2 on CD56+CD16+ NK cell number and frequency. ....</i>  | 95  |
| <i>Figure 2-18 The effects of LD-IL-2 on total monocyte cell number and frequency.</i>  |     |
| .....   | 97  |
| <i>Figure 2-19 The effects of LD-IL-2 on classical monocyte cell number and frequency. ....</i>   | 98  |
| <i>Figure 2-20 The effects of LD-IL-2 on intermediate monocyte cell number and frequency. ....</i>  | 99  |
| <i>Figure 2-21 The effects of LD-IL-2 on alternative monocyte cell number and frequency. ....</i>   | 101 |
| <i>Figure 2-22 The effects of LD-IL-2 on CD163+CCR2- alternative monocyte cell number and frequency.....</i>                              | 103 |
| <i>Figure 3-1 Treg micro-suppression assay protocol. ....</i>   | 115 |
| <i>Figure 3-2 Gating strategy for sorting Tregs, Teff and B cells. ....</i>   | 119 |
| <i>Figure 3-3 Simple linear regression analysis of Treg frequency in whole blood and cryopreserved PBMC. ....</i>                         | 123 |
| <i>Figure 3-4 Assessment of mean Teff proliferation at day 1 and day 64 in IMODALS treatment groups. ....</i>                             | 125 |
| <i>Figure 3-5 Assessment of % suppression at Treg:Teff ratio of 1:2 at day 1 and day 64 in IMODALS treatment groups. ....</i>             | 127 |
| <i>Figure 3-6 Assessment of % suppression at Treg:Teff ratio of 1:4 at day 1 and day 64 in IMODALS treatment groups. ....</i>             | 128 |
| <i>Figure 3-7 Assessment of mean Teff proliferation at days 85 and 169 versus day 1 in IMODALS treatment groups. ....</i>                 | 130 |
| <i>Figure 3-8 Assessment of % suppression at Treg:Teff ratio of 1:2 at days 85 and 169 versus day 1 in IMODALS treatment groups. ....</i> | 132 |
| <i>Figure 3-9 Assessment of % suppression at Treg:Teff ratio of 1:4 at days 85 and 169 versus day 1 in IMODALS treatment groups. ....</i> | 134 |
| <i>Figure 3-10 Assessment of CD25 MFI on Treg at day 1 and day 64 in IMODALS treatment groups. ....</i>                                   | 137 |

|   |     |
|---|-----|
| <i>Figure 3-11 Analysis of percentage change in Treg expression of CD25 and suppressive function.....</i>   | 139 |
| <i>Figure 3-12 Assessment of CD25 MFI on Treg at days 85 and 169 versus day 1 in IMODALS treatment groups.....</i>  | 141 |
| <i>Figure 4-1 Representative gating scheme for analysis of barcoded IMODALS patient samples.....</i>  | 157 |
| <i>Figure 4-2 Incompatibility of certain monoclonal antibodies with BD perm buffer III.</i><br>.....  | 159 |
| <i>Figure 4-3 pSTAT5 expression by different populations of white blood cells in response to increasing concentrations of exogenous IL-2.....</i>                           | 161 |
| <i>Figure 4-4 Simple linear regression analysis of Treg and non-Treg cell percent change in number at day 64 and pSTAT5 expression at day 1 in the 1MIU IL-2 group.....</i> | 164 |
| <i>Figure 4-5 Simple linear regression analysis of Treg and non-Treg cell percent change in number at day 64 and pSTAT5 expression at day 1 in the 2MIU IL-2 group.....</i> | 166 |
| <i>Figure 4-6 Assessment of pSTAT5+ Treg at day 1 and day 85 in IMODALS treatment groups.....</i>   | 168 |
| <i>Figure 4-7 Simple linear regression analysis of percent change in the expression of pSTAT5 and CD25 MFI on Treg in the 2MIU group.....</i>                               | 170 |
| <i>Figure 4-8 Assessment of pSTAT5+CD45RA- Treg at day 1 and day 85 in IMODALS treatment groups.....</i>  | 172 |
| <i>Figure 4-9 Assessment of pSTAT5+ CD8+ T cells at day 1 and day 85 in IMODALS treatment groups.....</i>   | 174 |
| <i>Figure 4-10 Assessment of pSTAT5+CD45RA- CD8+ T cells at day 1 and day 85 in IMODALS treatment groups.....</i>   | 175 |
| <i>Figure 4-11 Induction of CD25 expression in whole blood monocytes by GM-CSF and IFN-<math>\gamma</math>. ....</i>  | 178 |
| <i>Figure 4-12 Assessment of IL-2 signalling in whole blood monocytes.....</i>  | 180 |
| <i>Figure 5-1 Gating scheme for Treg and Teff in immunophenotyping panel 1.</i>   | 203 |
| <i>Figure 5-2 Gating scheme for NK and monocytes in immunophenotyping panel 2.....</i>  | 204 |
| <i>Figure 5-3 Summary of the data analysis protocol for assessing changes in Treg, Teff, NK and monocyte subpopulations as a result of IL-2 therapy.....</i>                | 206 |

|  |     |
|--|-----|
| <i>Figure 5-4 Unbiased hierarchical clustering analysis of Treg, NK and monocyte subpopulations of IMODALS trial participants.</i> | 209 |
| <i>Figure 5-5 QC PBMC Treg, NK and Monocyte subpopulation analysis in experimental batches.</i>                                    | 211 |
| <i>Figure 5-6 Analysis of change in Treg subpopulation frequency and their expression profiles at day 64.</i>                      | 213 |
| <i>Figure 5-7 The effects of IL-2 therapy on CD45RA+Helios+CD31+Ki-67+ Treg at day 64.</i>   | 215 |
| <i>Figure 5-8 Analysis of change in Treg subpopulation frequency and their expression profiles at day 85.</i>                      | 217 |
| <i>Figure 5-9 The effects of IL-2 therapy on CD45RA+Helios+CD31+ Treg at day 85.</i>   | 219 |
| <i>Figure 5-10 Analysis of change in Treg subpopulation frequency and their expression profiles at day 169.</i>                    | 221 |
| <i>Figure 5-11 The effects of IL-2 therapy on CD45RA+Helios+CD31+ Treg at day 169.</i>   | 222 |
| <i>Figure 5-12 Analysis of change in NK subpopulation frequency and their expression profiles at day 64.</i>                       | 224 |
| <i>Figure 5-13 Analysis of change in NK subpopulation frequency and their expression profiles at day 85 and 169.</i>               | 226 |
| <i>Figure 5-14 Analysis of change in monocyte subpopulation frequency and their expression profiles at day 64.</i>                 | 228 |
| <i>Figure 5-15 The effects of IL-2 therapy on CD163+CCR2-CX3CR1+ monocytes at day 64.</i>  | 230 |
| <i>Figure 6-1 Analysis of percentage change in Treg number and suppressive function.</i>   | 243 |
| <i>Figure 6-2 PCA analysis of findings significantly altered by IL-2 therapy at day 64 in Treg cells.</i>                          | 248 |
| <i>Figure 6-3 PCA analysis of findings significantly altered by IL-2 therapy at day 64 in Treg and non-Treg cells.</i>             | 251 |
| <i>Figure 6-4 PCA analysis of Treg findings at clinical trial visits where they were significantly altered.</i>                    | 253 |
| <i>Figure 6-5 Flow cytometry analysis of matched PBMC and CSF samples from ALS patients in the MIROCALS trial.</i>                 | 262 |

## List of tables

|   |     |
|---|-----|
| Table 1-1 Brief summary of the main inclusion and exclusion criteria used for patient randomisation in IMODALS.....                   | 63  |
| Table 1-2 Demographic and baseline characteristics of IMODALS trial participants.....   | 64  |
| Table 2-1 Details of flow cytometry antibodies used in fresh blood immunophenotyping panels 1 and 2.....                              | 69  |
| Table 2-2 Details of flow cytometry antibodies used in fresh blood immunophenotyping panels 3 and 4.....                              | 70  |
| Table 3-1 Fluorescently labelled antibodies used for preparing the master mix for surface staining of PBMC.....                       | 117 |
| Table 3-2 Analysis of QC PBMC variables across the 11 experimental repeats of IMODALS PBMC suppression assays.....                    | 122 |
| Table 4-1 Details of surface and intracellular monoclonal antibodies used to stain the IMODALS PBMC.....                              | 155 |
| Table 4-2 Summary of target-clone-conjugate combinations tested for compatibility with perm buffer III during assay optimisation..... | 160 |
| Table 4-3 Analysis of QC 1 variables measured across the experimental batches.  | 162 |
| Table 4-4 Analysis of QC 2 variables measured across the experimental batches.  | 163 |
| Table 5-1 Monoclonal antibody details used in immunophenotyping panel 1 to stain IMODALS PBMC.....                                    | 200 |
| Table 5-2 Monoclonal antibody details used in immunophenotyping panel 2 to stain IMODALS PBMC.....                                    | 202 |
| Table 5-3 Parameters used in FlowSOM analysis of Treg, Teff, NK and Monocytes.....  | 205 |
| Table 5-4 Frequencies of Treg, Teff, NK, Monocytes, B Cells and DC of QC PBMC used in IMODALS sample flow cytometry.....              | 207 |
| Table 6-1 List of immune parameters used in PCA analysis.....   | 245 |

## Abbreviations

|                        |   |
|------------------------|---|
| <b>AA</b>              | Alopecia Areata                             |
| <b>AD</b>              | Alzheimer's Disease                         |
| <b>ADP</b>             | Adenosine Diphosphate                       |
| <b>ALL</b>             | Acute Lymphoblastic Leukaemia               |
| <b>ALS</b>             | Amyotrophic Lateral Sclerosis               |
| <b>ALSFRS-R</b>        | ALS Functional Rating Scale – Revised       |
| <b>AMP</b>             | Adenosine Monophosphate                     |
| <b>AP-1</b>            | Activator Protein-1                         |
| <b>APC</b>             | Antigen Presenting Cell                     |
| <b>AUC</b>             | Area Under the Curve                        |
| <b>BCR</b>             | B Cell Receptor                             |
| <b>BSA</b>             | Bovine Serum Albumin                        |
| <b>Ca<sup>2+</sup></b> | Calcium                                     |
| <b>cAMP</b>            | cyclic AMP                                  |
| <b>CD</b>              | Cluster of Differentiation                  |
| <b>CD15s</b>           | Sialyl Lewis x                              |
| <b>CFSE</b>            | Carboxyfluorescein Succinimidyl Ester       |
| <b>CMV</b>             | Cytomegalovirus                             |
| <b>CNS</b>             | Central Nervous System                      |
| <b>CTLA-4</b>          | Cytotoxic T-Lymphocyte-Associated Protein 4 |
| <b>DC</b>              | Dendritic Cells                             |
| <b>DMSO</b>            | Dimethyl Sulfoxide                          |
| <b>DNA</b>             | Deoxyribonucleic Acid                       |
| <b>EDTA</b>            | Ethylenediaminetetraacetic Acid             |

|                                 |  |
|---------------------------------|--|
| <b>EGR1</b>                     | Early Growth Response Protein 1                  |
| <b>ELF1</b>                     | E74-Like Factor 1                                |
| <b>ERK</b>                      | Extracellular Signal-Related Kinase              |
| <b>ETS1</b>                     | Erythroblast Transformation Specific Protein 1   |
| <b>EWS</b>                      | Ewing Sarcoma Gene                               |
| <b>FACS</b>                     | Fluorescence-activated cell sorting              |
| <b>fALS</b>                     | Familial Amyotrophic Lateral Sclerosis           |
| <b>FBS</b>                      | Foetal Bovine Serum                              |
| <b>FDA</b>                      | Food and Drug Administration                     |
| <b>FoxP3</b>                    | Forkhead Box Protein 3                           |
| <b>FTD</b>                      | Frontotemporal Dementia                          |
| <b>FVC</b>                      | Forced Vital Capacity                            |
| <b>GABP</b>                     | GA-Binding Protein                               |
| <b>GM-CSF</b>                   | Granulocyte-macrophage colony-stimulating factor |
| <b>GVHD</b>                     | Graft Versus Host Disease                        |
| <b>GWAS</b>                     | Genome-Wide Associate Studies                    |
| <b>HFE</b>                      | Haemochromatosis                                 |
| <b>HLA</b>                      | Human Leukocyte Antigen                          |
| <b>IDO</b>                      | Indoleamine 2,3-Dioxygenase                      |
| <b>IL-1</b>                     | Interleukin-1                                    |
| <b>IL-1<math>\beta</math></b>   | Interleukin-1 $\beta$                            |
| <b>IL-2</b>                     | Interleukin-2                                    |
| <b>IL-2R</b>                    | IL-2 Receptor                                    |
| <b>IL-2R<math>\alpha</math></b> | IL-2R Alpha Chain                                |
| <b>IL-2R<math>\beta</math></b>  | IL-2R Beta Chain                                 |

|                                  |                                      |
|----------------------------------|--------------------------------------|
| <b>IL-2R<math>\gamma</math>c</b> | IL-2R Common Gamma Chain             |
| <b>IL-4</b>                      | Interleukin-4                        |
| <b>IL-6</b>                      | Interleukin-6                        |
| <b>IL-10</b>                     | Interleukin-10                       |
| <b>ILC2</b>                      | Type 2 Innate Lymphoid Cells         |
| <b>IFN<math>\gamma</math></b>    | Interferon Gamma                     |
| <b>kDA</b>                       | Kilodalton                           |
| <b>KIF5A</b>                     | Kinesin Family Member 5A             |
| <b>KO</b>                        | Knockout                             |
| <b>LAG3</b>                      | Lymphocyte-Activation Gene 3         |
| <b>LD-IL-2</b>                   | Low Dose IL-2                        |
| <b>MAPK</b>                      | Mitogen Activated Protein Kinase     |
| <b>M-CSF</b>                     | Macrophage colony-stimulating factor |
| <b>MFI</b>                       | Median Fluorescence Intensity        |
| <b>MG</b>                        | Myasthenia Gravis                    |
| <b>MHC</b>                       | Major Histocompatibility Complex     |
| <b>MIU</b>                       | Million International Units          |
| <b>mL</b>                        | Milliliter                           |
| <b>MND</b>                       | Motor Neuron Disease                 |
| <b>mRNA</b>                      | messenger RNA                        |
| <b>MS</b>                        | Multiple Sclerosis                   |
| <b>mSOD1</b>                     | mutant SOD1                          |
| <b>NFAT</b>                      | Nuclear Factor of Activated T Cells  |
| <b>NF-H</b>                      | Neurofilament Heavy Chains           |
| <b>NF-L</b>                      | Neurofilament Light Chains           |

|                |  |
|----------------|--|
| <b>NF-M</b>    | Neurofilament Medium Chains                                |
| <b>NF-κB</b>   | Nuclear Factor κ-light-chain-enhancer of Activated B Cells |
| <b>NK Cell</b> | Natural Killer Cell  |
| <b>NK1</b>     | Natural Killer Type-1                                      |
| <b>NK2</b>     | Natural Killer Type-2                                      |
| <b>OCT-1</b>   | Octamer Transcription Factor                               |
| <b>P70 S6K</b> | Ribosomal Protein. S6 Kinase                               |
| <b>PAMPs</b>   | Pathogen-Associated Molecular Patterns                     |
| <b>PBMC</b>    | Peripheral Blood Mononuclear Cell                          |
| <b>PBS</b>     | Phosphate-Buffered Saline                                  |
| <b>PC</b>      | Principal Component  |
| <b>PCA</b>     | Principal Component Analysis                               |
| <b>PD</b>      | Parkinson's Disease  |
| <b>PD-1</b>    | Programmed Cell Death Protein 1                            |
| <b>PHA</b>     | Phytohaemagglutinin  |
| <b>pNF-H</b>   | Phosphorylated Neurofilament Heavy Chains                  |
| <b>PCR</b>     | Polymerase Chain Reaction                                  |
| <b>PRR</b>     | Pattern Recognition Receptor                               |
| <b>PRRs</b>    | Positive Regulatory Region                                 |
| <b>PSF</b>     | Penicillin Streptomycin Fungizone                          |
| <b>pSTAT5</b>  | Phosphorylated STAT5                                       |
| <b>pTreg</b>   | Peripheral Treg  |
| <b>QC</b>      | Quality Control  |
| <b>RA</b>      | Rheumatoid Arthritis                                       |

|                        |  |
|------------------------|--|
| <b>RNA</b>             | Ribonucleic Acid   |
| <b>RPMI</b>            | Roswell Park Memorial Institute 1640 Medium              |
| <b>RRMS</b>            | Relapsing Remitting Multiple Sclerosis                   |
| <b>RTE</b>             | Recent Thymic Emigrants                                  |
| <b>SALT</b>            | Severity of Alopecia Tool                                |
| <b>sALS</b>            | Sporadic Amyotrophic Lateral Sclerosis                   |
| <b>SD</b>              | Standard Deviation                                       |
| <b>SLE</b>             | Systemic Lupus Erythematosus                             |
| <b>SLO</b>             | Secondary Lymphoid Organs                                |
| <b>SOD1</b>            | Superoxide Dismutase 1                                   |
| <b>SP1</b>             | Specificity Protein 1                                    |
| <b>STAT5</b>           | Signal Transducer and Activator of Transcription 5       |
| <b>T1D</b>             | Type 1 Diabetes  |
| <b>TCGF</b>            | T Cell Growth Factor                                     |
| <b>TCR</b>             | T Cell Receptor  |
| <b>TDP-43</b>          | Trans-activation Response Element DNA-binding Protein 43 |
| <b>TGF-β</b>           | Transforming Growth Factor Beta                          |
| <b>Teff</b>            | Effector T Cells   |
| <b>T<sub>FH</sub></b>  | T Follicular Helper Cell                                 |
| <b>T<sub>H1</sub></b>  | T Helper 1 Cells   |
| <b>T<sub>H2</sub></b>  | T Helper 2 Cells   |
| <b>T<sub>H17</sub></b> | T Helper 17 Cells  |
| <b>TLR</b>             | Toll-Like Receptor                                       |
| <b>TNF-α</b>           | Tumour Necrosis Factor-alpha                             |

|                   |   |
|-------------------|---|
| <b>TREC</b>       | T Cell Receptor Excision Circle               |
| <b>Treg</b>       | Regulatory T Cells                            |
| <b>tTreg</b>      | Thymic Treg                                   |
| <b>UMAP</b>       | Uniform Manifold Approximation and Projection |
| <b>WT1</b>        | Wilms Tumour Suppressor                       |
| <b>δALSFRS</b>    | Change in ALSFRS Score                        |
| <b>γδ T Cells</b> | Gamma Delta T Cells                           |
| <b>μL</b>         | Microliter                                    |
| <b>% CV</b>       | Percent Coefficient of Variation              |

# **Chapter 1. Introduction.**

## **1.1. Amyotrophic Lateral Sclerosis – a fatal motor neuron disorder.**

Amyotrophic lateral sclerosis (ALS), first described around 150 years ago by Jean Martin Charcot, is a degenerative motor neuron disease (MND), with no cure (Kumar *et al.*, 2011). The progressive loss of motor neurons leads to muscle weakness, muscle atrophy, paralysis and death, typically due to respiratory failure (Barbeito *et al.*, 2010). The events that trigger the death of motor neurons in ALS are not fully understood but some genetic and environmental risk factors have been described (Bozzoni *et al.*, 2016). The environmental risk factors include smoking, occupation, exposure to heavy metals and physical activity. In most cases, it is hard to link these to ALS, because these studies are not done frequently as they are expensive, depend on patient recall, and are affected by geographical location (Martin *et al.*, 2017). The genes that harbour disease-associated variants will be discussed later. The median incidence of ALS worldwide is 1.68 cases per 100,000 persons per year while the median prevalence is 4.48 cases per 100,000 persons per year, this varies based on factors such as geographical location where higher incidence is reported in Europe than the US or Asia, age and sex (Logroscino *et al.*, 2018; Longinetti and Fang, 2019). The low prevalence and incidence are confounding factors causing difficulty in research where large cohorts of ALS patients are needed (and large cohorts are needed to show efficacy in clinical trials or in biomarker discovery) as they are very low when compared to the prevalence of Multiple Sclerosis (MS) of 30.1 cases per 100,000 persons worldwide (Wallin *et al.*, 2019). Another factor is the short survival time from diagnosis which in itself varies depending on the publication but it is generally a median of 2 to 5 years (Saudagar and Garge,

2019; Trojsi *et al.*, 2019). Although technically ALS onset can occur at any age, typically the age of diagnosis ranges from 50 to 60 years, and the incidence is more common in men than women, 1 in 350 and 1 in 400 respectively (Saudagar and Garge, 2019). Recent statistics show that at any given time, the number of individuals living with ALS is around 5000 in the United Kingdom, and at least 16,000 in the United States, however projections based on meta-analysis from 10 major regions across the globe suggest that there will be an increase of around 69% of ALS diagnosis by the year 2040 (Arthur *et al.*, 2016). ALS cases are on the rise, the low incidence, prevalence and short survival time makes clinical trials or longitudinal studies very difficult, and to confound the problem even more, the events that trigger ALS are largely unknown nor can ALS be diagnosed early (Paganoni *et al.*, 2014).

### **1.1.1. Clinical presentation and diagnosis.**

There is no ALS-specific diagnostic test and early symptoms may not be disabling enough to cause concern to the patients, resulting in an average delay of 10-16 months from first symptom to diagnosis (Richards *et al.*, 2020). Around 70% of all ALS cases are limb-onset, with symptoms such as fasciculations or muscle cramps in the arm or leg, and the remaining cases are grouped into either bulbar onset (25%), affecting speech and swallowing, and the remaining 5% are rarer forms affecting the trunk or respiratory system, with the latter two associated with poorer prognosis (Kiernan *et al.*, 2011; Wales *et al.*, 2011). The disease is diagnosed based on physicians assessment of symptom progression combined with electromyography to investigate upper and lower motor neuron involvement, and to disregard other potential causes of symptoms, such as reversible diseases

resembling ALS, known as mimics (Brown and Al-Chalabi, 2017). If the patient's symptoms are indicative of ALS, they are assigned a level of diagnostic certainty, either suspected, possible, laboratory-supported probable, probable or definitive ALS based on a set of established diagnostic criteria known as the El Escorial, developed in 1990 and revised in 1998 to improve diagnostic sensitivity (Traynor *et al.*, 2000). ALS staging systems have also been proposed, namely the King's clinical staging system, where patients are classed based on the number of bodily regions affected by neuronal decline; stages 1-3 are based on the number of regions with functional decline, stage 4 is when there is respiratory or nutritional failure and stage 5 is sadly death (Martin *et al.*, 2017). Following diagnosis, the progression of ALS is monitored using the ALS functional rating scale-revised (ALSFRS-R), this is a points system based on the patient's ability to perform daily functions, which will be discussed in more detail later (Bakker *et al.*, 2017).

### **1.1.2. Genetic association with ALS.**

Between 5-10% of all cases are familial (fALS), passed down as both autosomal dominant and autosomal recessive traits, while the remaining 90-95% are sporadic (sALS) (Chadi *et al.*, 2017). Since the 1990s, the discovery of genes linked with ALS has rapidly increased, and currently there are over 25 genes associated with ALS onset, associated with both, fALS and sALS cases. These genes are involved in protein homeostasis, altering RNA-binding and cytoskeletal proteins (Brown and Al-Chalabi, 2017). The first of these was reported in 1993 by Rosen and colleagues in the *SOD1* gene, encoding a protein called Superoxide Dismutase 1 (SOD1) (Rosen *et al.*, 1993). The SOD1 protein is involved in the elimination of free radicals that cause oxidative stress by

simultaneous oxidation and reduction (dismutation) of free superoxide radicals into molecular oxygen and hydrogen peroxide (Pansarasa *et al.*, 2018). A mutation in *SOD1* leads to build up of misfolded *SOD1* proteins unable to perform their function resulting in a toxic environment around motor neurones (Forsberg *et al.*, 2019). Other mutations, such as *TARDBP* encoding the trans-activation response element DNA-binding protein 43 (TDP-43), *FUS* encoding the fused in sarcoma RNA-binding protein and most recently, mutations in the *KIF5A* gene encoding kinesin family member 5A (*KIF5A*) have been linked with a risk of ALS in a genome-wide association study (GWAS) of over 20,000 ALS patients and nearly 60,000 healthy controls (Ajroud-Driss and Siddique, 2015; Nicolas *et al.*, 2018). Just like for *SOD1*, there is an overabundance of TDP-43 and *FUS* proteins in ALS patients however the molecular mechanisms by which they cause neuronal death are elusive (Guerrero *et al.*, 2016). Finally, a mutation described as the repeat expansion in the non-coding region of chromosome 9 open reading frame 72 (*C9orf72*) gene affects 40-50% of patients with fALS and 5-10% of sALS patients, a mutation that overlaps highly with frontotemporal dementia (FTD) (DeJesus-Hernandez *et al.*, 2011). In terms of disease burden, patients with the *C9orf72* expansion have a significantly shorter survival time, earlier age of onset and an increased prevalence of bulbar onset compared to those without but once again, the exact mechanisms of the *C9orf72* in ALS pathology are elusive (Van Blitterswijk *et al.*, 2012; Umoh *et al.*, 2016). Genetic mutations account for a small proportion of all ALS cases and even the ones that have been identified do not provide a direct link with mechanisms of motor neuron death, and this is one of the key confounding factors in the lack of efficacious therapy in ALS patients

(Katyal and Govindarajan, 2017). To date, few, if any, polymorphisms that might affect the immune system have been identified in ALS GWAS studies.

## **1.2. Currently approved treatment in ALS.**

Currently, the disease modifying therapies approved for use in ALS, riluzole and edaravone, only marginally slow ALS progression, the former at a specific stage of the disease and the latter in a specific subgroup of patients (Khairoalsindi and Abuzinadah, 2018).

### **1.2.1. Riluzole.**

Riluzole was the first Food and Drug Administration (FDA) approved drug in the United States for ALS, and is the only ALS drug approved in Europe to date (Bhandari *et al.*, 2018). Studies in the late 1980s and early 1990s on rodent brains showed that riluzole contributes to neuroprotection by controlling the release of glutamate, and given that one of the hypotheses of neuronal death in ALS is the toxic build of glutamate, it was trialled in ALS patients (Mizoule *et al.*, 1985; Martin *et al.*, 1993). The first placebo-controlled trial of riluzole in ALS patients followed shortly and reported that 100mg of riluzole a day for 12 months reduced the mortality rate by 38.6% at the end of that period when compared to the placebo group (Bensimon *et al.*, 1994). The reductions in mortality rate vary between studies but this is largely due to cohort size (Traynor *et al.*, 2003). A riluzole dose-ranging trial of 50mg, 100mg, 200mg or placebo a day for 18 months soon followed in a cohort of 959 ALS patients and reported a 35% reduction in mortality in patients receiving the 100mg dose (Lacomblez *et al.*, 1996). It was also shown

at which stage of disease does riluzole extend survival in a post-hoc analysis of the dose-ranging study, final stage of disease (stage 4) was prolonged in patients receiving the 100mg dose when compared to the other doses (Fang *et al.*, 2018). The results of these analysis contradicted the findings of a 1998 published study which concluded that riluzole is more effective at earlier stages of disease (Riviere *et al.*, 1998). A common theme across these studies is that riluzole appears to improve survival more in those with bulbar disease onset (Bensimon *et al.*, 1994; Traynor *et al.*, 2003). Since its approval in 1995 riluzole has been extensively used as a disease-modifying drug for patients with ALS, but it is not without limitations (Dharmadasa and Kiernan, 2018). Riluzole only prolongs survival by 2-3 months, it has never shown to have an effect on the functional rating scale, although this is commonly due to patients with severe disability dropping out of the studies (Dharmadasa and Kiernan, 2018; Fang *et al.*, 2018). Furthermore, the exact mechanisms by which riluzole exerts its effects in ALS patients are not fully understood, and there are also a plethora of side effects such as asthenia, breathing difficulty, nausea and gastrointestinal discomfort (Grant *et al.*, 2010; Bellingham, 2011). However, since 2017 it is no longer the only FDA approved drug for treatment of ALS in the US.

### **1.2.2. Edaravone.**

Edaravone, a free radical scavenger, was developed as a therapy for acute ischaemic stroke and has been used for that purpose in Japan since 2003 but work in an ALS mouse model showed significant decline in motor neuron loss in all injected mice, it was trialled in ALS patients (Ito *et al.*, 2008; Breiner *et al.*, 2020). A subsequent open-label trial of 20 ALS patients receiving either 30mg (5

participants) and 60mg (15 participants) a day for two weeks, followed by a two week observation period, repeated for a total of six times showed a reduction in the ALSFRS-R score over the six months on treatment (60mg edaravone) when compared to the ALSFRS-R score in the six months leading up to the start of treatment (Yoshino and Kimura, 2006). A confirmatory, double-blind, placebo-controlled study of 102 patients receiving edaravone and 104 receiving placebo carried out afterwards did not produce similar results, in fact the decline in ALSFRS-R was greater in the edaravone group than in the placebo group, albeit very slightly, over the 24-week treatment period (Abe *et al.*, 2014). Data analysed post-hoc showed that edaravone maybe efficacious in a specific group of patients, those in the very early stage with definite or probable ALS and as a result of this, a third trial was carried out with recruitment based on these stringent criteria (Abe *et al.*, 2017). The published data from this study reported lower decline in ALSFRS-R in ALS patients receiving edaravone (n=68) versus placebo (n=66) with a mean difference of 2.49 points between the groups over the same 24-week treatment period as before (Abe *et al.*, 2017). This led to edaravone being approved by the US FDA for the treatment of ALS in May 2017, but there are several limitations to still consider (Khairoalsindi and Abuzinadah, 2018). First the strict inclusion criteria for the most recent trial showing efficacy, second is the fact that a 24-week treatment period is short especially if it includes a 12-week observation period, third is the fact that it is possible to subgroup patients in several diseases, in ALS it is difficult to identify patients with early stage ALS as there are no reliable markers to identify them (Hardiman and van den Berg, 2017). Neither riluzole nor edaravone are a cure and with ALS incidence projected to increase, there is a desperately growing need for new ALS therapies.

### **1.3. ALS Research.**

The current knowledge surrounding ALS, and the vast number of research projects that are ongoing around the world, are the combined work of cohorts of ALS patients and animal models. The animal models are necessary for analysis of the pathogenic properties of the mechanisms that are responsible for the degeneration of motor neurons, and also for the development of ALS therapies (Morrice *et al.*, 2018).

#### **1.3.1. ALS Mouse model(s).**

There are several genetic mouse models that researchers use to try to understand the mechanisms of disease in ALS (De Giorgio *et al.*, 2019). The discovery of the afore mentioned mutation in *SOD1*, led to a breakthrough development of the first transgenic ALS mouse model, which expresses 20-24 copies of the human coding sequence and has a mutation in the G93A region, otherwise known as the *SOD1*<sup>G93A</sup> or the mutant *SOD1* (m*SOD1*) ALS mouse model (McGoldrick *et al.*, 2013). Using the m*SOD1* mice, scientists were able to show that ALS is a non-cell autonomous disease, and induction of *SOD1* mutations in neurons, motor neurons, astrocytes, microglia or Schwann cells alone was not enough to induce the typical pathologies associated with ALS (Philips and Rothstein, 2015). The *SOD1*<sup>G93A</sup> is the most robust rodent model of ALS, showing characteristics of misfolded *SOD1* aggregates, motor neuron loss and degradation, and weakness, in fact much of the current knowledge surrounding ALS pathology is thanks to this rodent model (Stephenson and Amor, 2017; Van Damme *et al.*, 2017). Other than the m*SOD1*, rodent models with the afore mentioned mutations in *C9ORF72*, *FUS* and *TARDBP* led to the

generation of their corresponding rodent models, which are robust in assessing the role of these mutation on biological processes and cellular dysfunction in the brain (Alrafiah, 2018) These mouse models have been useful but the heterogeneity of ALS extends beyond these mutations, and ALS mouse models cannot be used to represent all cases of ALS, much like the mouse models of other diseases (Stephenson and Amor, 2017). As a result, these rodent models may not aid in areas of research such as biomarker discovery, where a standardised and robust measure of diagnosis and prognosis is not only necessary but, is currently lacking in ALS (Turner *et al.*, 2013).

### **1.3.2. Biomarkers in ALS diagnosis and prognosis.**

Motor neuron loss in ALS is largely a result of the delay in diagnosis as well as a lack of reliable diagnostic and prognostic biomarkers (Gagliardi *et al.*, 2019). The ALSFRS-R score is a test for monitoring the rate of disability of someone suffering from ALS (Cedarbaum *et al.*, 1999). It is called the revised scale as the initial ALSFRS only minimally assessed respiratory function which was rectified for the revised scale (Maier *et al.*, 2012). It is still the most widely used measure of progression in clinical practice, and response to therapy in clinical trials (Bakker *et al.*, 2017). The ALSFRS-R is a clinician administered, 12 item, multiple choice questionnaire to determine the functional impairment of ALS patients, with each question describing a physical activity, such as ‘HANDWRITTING’, and each answer carrying a score between 0 and 4, where 4 corresponds to no loss of function and 0 to total loss of function (Bakker *et al.*, 2017). As death in ALS is normally a result of respiratory failure, the ALSFRS score is accompanied by measurements of forced vital capacity (FVC) which aids in the prediction of

survival and progression of disability (Proudfoot *et al.*, 2016). Calculating the change in ALSFRS ( $\delta$ ALSFRS) has been shown to predict survival in some studies however, this relies on the patient's own recall of the date when they noticed the first symptoms of ALS, which has been shown to underestimate the rate of disability (Proudfoot *et al.*, 2016). It is also quick and easy to complete and can even be carried out by phone or online without the need to attend clinic, which can be difficult for some patients however, the ALSFRS-R is not without limitation (Rutkove, 2015). As it is a subjective test, it can be affected by factors such as mood, depression and the level of emotional and physical support the patient has (Ilse *et al.*, 2014). Furthermore, it is not very sensitive to patients who are progressing very slowly meaning it could take several months to notice and report a decline in motor function, and the FVC is only focussed on one specific body part (Rutkove, 2015). Therefore, there needs to be a more direct way to determine neuronal death in ALS, with biomarker discovery efforts focussing on cerebrospinal fluid (CSF), serum, plasma and saliva (Vu and Bowser, 2017).

### **1.3.2.1. Neurofilaments.**

Neurofilaments are neuron-specific, cytoskeletal proteins present in cell bodies and axons, and are essential for axonal structural support and nerve conduction (Khalil *et al.*, 2018). Neurofilaments are potential biomarkers in various pathologies as their levels in bodily fluids are increased proportionally to axonal damage (figure 1-1), under both homeostatic and pathological conditions (Gagliardi *et al.*, 2019).

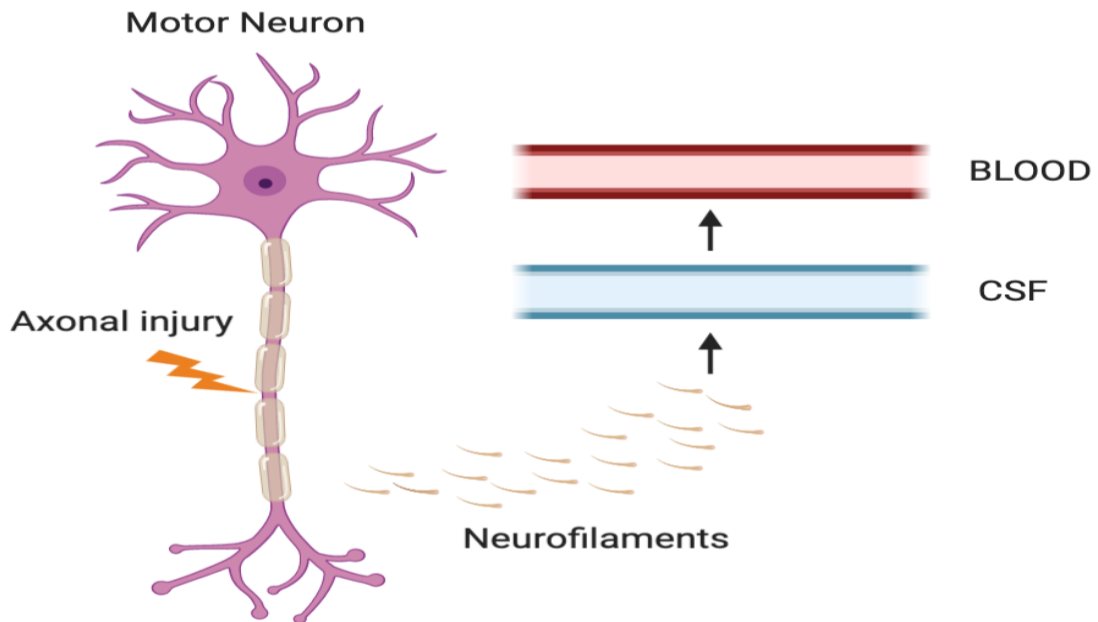


**Figure 1-1 Neurofilament release into bodily fluids.** Neurofilament proteins are released as a result of motor neuron damage into the CSF, from here they can get into the blood stream. CSF: Cerebrospinal fluid.  
Adapted from (Gagliardi et al., 2019).

Neurofilaments are composed of 4 subunits, an alpha-internexin subunit and the neurofilament light (NF-L), medium (NF-M) and heavy (NF-H) chains (Kušnierová *et al.*, 2019). Several studies have shown that ALS patients have elevated levels of NF-L and phosphorylated NF-H (pNF-H) chains in their cerebrospinal fluid (CSF), serum and plasma (Reijn *et al.*, 2009; Boylan *et al.*, 2013; Steinacker *et al.*, 2016). Neurofilament proteins can also discriminate ALS from other neurologic disorders and MND mimicking diseases as shown by a few studies with a combined cohort of over 300 ALS patients, over 300 neurologic disease controls and over 100 genuine MND disease mimics where elevated levels of serum neurofilament light chain (NF-L), CSF NF-L and phosphorylated neurofilament heavy chain (pNF-H) were detected in early and late symptomatic

phases of ALS, and that these proteins could distinguish patients at early ALS symptom onset from the other patient cohorts with high specificity (over 85%) and sensitivity (over 90%) (Poesen *et al.*, 2017; Feneberg *et al.*, 2018). Neurofilament levels also correlate with disease progression as lower CSF pNF-H were present in those progressing slower as determined by the ALSFRS-R score (De Schaeppdryver *et al.*, 2018). pNF-H CSF levels also negatively correlated with disease duration as lower levels were detected in early disease but decreased with time in a Chinese ALS cohort (Li *et al.*, 2018). NF-L and pNF-H appear reliable biomarkers in detecting ALS and even correlate with disease progression however, as outlined in all these studies, neurofilaments are not ALS specific, and are associated with neurological conditions such as Alzheimer's disease (AD), Parkinson's disease (PD) and Polyneuropathy (Khalil *et al.*, 2018). Furthermore, most neurofilament comparisons are done between relatively small cohorts of ALS patients and healthy individuals (other than the afore mentioned studies) and of course, there will be a significant difference in NF-L and pNF-H in someone with a progressive MND versus someone without one (Poesen and Van Damme, 2019). So neurofilaments may be promising, but they are not the gold standard, and a large portion of the ALS research field is focused on exactly that, finding a reliable, robust, prognostic and diagnostic biomarker that is abundant and easily obtainable, such as the components of the immune system in blood.

#### **1.4. ALS and the immune system.**

The mammalian immune system is a well organised group of cells, functions and chemicals that work together to protect its host from foreign antigens such as bacteria, viruses and cancer cells (Marshall *et al.*, 2018). The immune system

can be subdivided into two lines of defence, the innate and adaptive (Chaplin, 2010). Human and animal studies have provided insight into the role of both arms of the immune system in ALS, how some of the immune components are deleterious to motor neurons while others may be neuroprotective and how these immune signatures may act as indicators of disease progression (Phani *et al.*, 2012; Lyon *et al.*, 2019).

#### **1.4.1. The immunogenetics of ALS.**

In autoimmune conditions such as type 1 diabetes (T1D), rheumatoid arthritis (RA), multiple sclerosis (MS) and systemic lupus erythematosus (SLE) there are known associations between disease susceptibility and the human leukocyte antigen (HLA) gene region on chromosome 6, which encodes for several molecules of the immune system, in ALS however, it is still unknown whether immune genes play a role in susceptibility to disease (Gough and Simmonds, 2009). A recent metanalysis, taking into account data from 14 observational studies, reported evidence of a significant association between the C282Y polymorphism on the haemochromatosis (HFE) locus, important in iron homeostasis, and ALS risk (Li *et al.*, 2014). This could provide a potential link with the HLA locus and ALS, as HFE is also found on chromosome 6 but at this time this is only a theory. The role of immunogenetics in ALS certainly raises the need for further investigation, as it might be important to independently assess the immunogenetics of disease versus non-disease states as well as in ALS patients progressing fast versus slow. This could account for the following immune findings in ALS patients, as well as the heterogeneity in the immune responses between ALS patients (McCombe *et al.*, 2020).

#### **1.4.2. The innate immune system in ALS.**

The innate immune system is the first line of defence against a foreign pathogen, it is rapid, it is not dependent on antigen (but is able to discriminate self from non-self) nor does it retain memory of the previous encounter with the pathogen (Smith *et al.*, 2019). This part of the immune system consists of several components, these include cells such as macrophages, dendritic cells (DCs), mast cells, monocytes, natural killer (NK) cells and eosinophils (Turvey and Broide, 2010). It is also comprised of barriers such as the skin and the epithelial cell linings in the respiratory and gastrointestinal tracts, as well as components of humoral immunity such as the complement proteins (Dunkelberger and Song, 2010; Matejuk, 2018). A virus or a bacterium is identified by a component of innate immunity when its pattern recognition receptor (PRR), such as the Toll-like receptor, detects structures on said pathogen called pathogen-associated molecular patterns (PAMPs) (Mogensen, 2009). The elimination of the pathogen is then initiated through pathways such as killing of infected host cells by NK cells, phagocytosis by macrophages or the activation of adaptive immune system by antigen presenting cells (APCs) (Brubaker *et al.*, 2015). There are several reports showing altered innate immune parameters in the periphery and brain of ALS patients when compared to healthy individuals. These include differences in monocyte and NK cell frequencies, an abundance of inflammatory cytokines and activation of brain macrophages.

##### **1.4.2.1. Monocytes and microglia.**

Monocytes are circulating blood cells comprising ~10% of all leukocytes in the periphery, thought to arise in the bone marrow (Guilliams *et al.*, 2018). Human

monocytes can be divided into three distinct populations based on their expression surface CD14 and CD16 (Ginhoux and Jung, 2014). Around 85-90% of circulating monocytes are classical monocytes, defined as CD14<sup>+</sup>CD16<sup>-</sup>, while the remaining 10-15% are further subdivided into the intermediate monocytes (CD14<sup>+</sup>CD16<sup>+</sup>) and the non-classical monocytes (CD14<sup>dim</sup>CD16<sup>+</sup>) (Patel *et al.*, 2017; Kapellos *et al.*, 2019). Monocytes are of a plastic nature, possessing the ability to adapt and carry out several roles in homeostasis and under inflammatory conditions such as pro- and anti-tumoral responses, pathogen clearance, antigen presentation, wound healing and cytokine production (Canè *et al.*, 2019). Specifically, classical monocytes are well characterised as having an inflammatory role during injury or infection, whereby after homing to the site of injury via a chemokine gradient, they secret cytokines that attract other immune cells, phagocytose pathogens and present antigen via MHC class II (Chiu and Bharat, 2016). The intermediate monocytes share similar properties to classical in their cytokine production and antigen presentation (Ziegler-Heitbrock, 2007). The role of non-classical monocytes is less well characterised but they do display patrolling properties and are thought to have a role in innate tissue surveillance and even give rise to wound healing macrophages after homing to skin tissue following injury (Idzkowska *et al.*, 2015; Olingy *et al.*, 2017). Although peripheral monocytes are well characterised, the relationship(s) between these subsets, and how long these subsets persist in the blood is still being investigated. Recent findings indicate a tightly regulated process whereby monocyte precursors differentiate into classical monocytes, are retained in the bone marrow, and are released into circulation following the onset of inflammation (Patel *et al.*, 2017). Fate-mapping of these cells in humans and rodent models has shown, with great

consistency, that the majority of these classical monocytes exit the circulation after ~1 day, while a small number mature into intermediate monocytes and these further convert to non-classical monocytes (Patel *et al.*, 2017). Studies of monocytic cell ontogeny and kinetics have shown minimal monocyte contribution to the maintenance of several tissue macrophage populations such as liver Kupffer cells, lung alveolar macrophages and microglia in the brain, which are embryonically derived and are able to self-renew (Mass *et al.*, 2016; Soucie *et al.*, 2016).

Macrophages are specialised myeloid immune cells, not present in the periphery, but are distributed throughout tissue. In the CNS, these macrophages are known as microglia and account for 5 – 10% of the total cells in the brain (Li and Barres, 2018). Microglia are embryonically derived and have the ability to self-renew (Song and Colonna, 2018). Human studies have shown that microglia gain entry and are distributed throughout the human CNS from 4.5 weeks of gestation, as characterised by microglial markers such as CD68, CD45 and MHC class II antigens (Rezaie *et al.*, 2005; Monier *et al.*, 2007). While studies in mouse models showed that microglia can regenerate and repopulate the brain to normal density levels within a week and, this replenishment is the result of proliferation of surviving microglia, which can be as low as 1% in number (Ajami *et al.*, 2007; Huang *et al.*, 2018). Microglia have several functions and are involved in CNS development and homeostasis, synaptogenesis, removal of less active synapses and post-traumatic neuronal regeneration (Lannes *et al.*, 2017; Wolf *et al.*, 2017). They also help mount immune responses against infections, phagocytose apoptotic cells in the developing brain, cause neuroinflammation and have been

found to contribute to neurodegeneration as a result of mutations in their genes (Bachiller *et al.*, 2018; Song and Colonna, 2018). With regards to immunity in the CNS, microglia can act as either pro-inflammatory cells associated with cytotoxicity, secreting cytokines such as IL-6, or as anti-inflammatory cells promoting tissue repair and remodelling, characterised by the release of cytokines such as IL-4 and IL-10 (Da Pozzo *et al.*, 2019). Their activation state is dependent on the milieu in which they become activated, and in many cases microglial responses are beneficial and subside after the pathogen or damage has been cleared. However, prolonged, chronic inflammation can induce a semi-permanent pro-inflammatory microglial state, leading to permanent tissue damage (Cherry *et al.*, 2014).

Research in ALS patients and mouse models have identified changes in monocytes and microglia. Studies have shown significant increases in the number (per  $\mu$ L/blood) of CD14 $^{+}$ CD16 $^{+}$  monocytes and with no change in the number or frequency of CD16 $^{+}$  monocytes in ALS patients when compared to healthy controls (Murdock *et al.*, 2016, 2017). Small cohorts of sALS, fALS and pre-symptomatic ALS mutation carriers not only had greater frequency of classical monocytes (CD14 $^{+}$ ), expressed as a ratio of CD14 $^{+}$ /CD16 $^{+}$ , but also CD14 $^{+}$  monocytes of the sALS patients differentially expressed 420 genes, 46 of which were immune system related (Zondler *et al.*, 2016). While the expression of CX3CR1, a chemokine responsible for migration, on ALS monocytes is found to correlate with slower disease progression (Murdock *et al.*, 2017). Immunohistochemical analysis of lumbar spinal cord tissue sections of sALS patients also showed CNS infiltration of peripheral cells of monocytic lineage

(Zondler *et al.*, 2016). There are also reports suggesting a skewing of peripheral blood ALS monocytes towards a proinflammatory phenotype through differential expression of *IL1B*, *IL8*, *CXCL1* and *CXCL2* when compared to healthy controls (Zhao *et al.*, 2017). The same report indicated that monocytes of ALS patients progressing faster expressed greater numbers of proinflammatory genes than monocytes of slow progressing patients (Zhao *et al.*, 2017). With regards to microglia, there is a change of microglial phenotype from neuroprotective, M2, to neurotoxic, M1, as the disease progresses. Transgenic mSDO1 mice developing ALS around 11 weeks of age, show significant upregulation of Ym1, CD206 and CX3CR1, a group of proteins associated with alternatively activated (M2) microglia, at 14-16 weeks of age (Beers *et al.*, 2011). Whereas factors associated with pro-inflammatory (M1) microglia such as NOX2 and IL-1 $\beta$  were significantly upregulated from 18 weeks onwards (Beers *et al.*, 2011). Whether this change in M1/M2 balance is present in ALS patients is unknown as diagnosis of disease occurs ~1 year after onset of symptoms. Compared to healthy controls, the presence of activated microglia has been shown in a small group ALS patients using positron emission topography following an intravenous injection of a ligand, specifically binding activated, but not resting, microglia (Turner *et al.*, 2004). Post-mortem analysis of ALS patient corticospinal tract also show microglial activation determined by CD68 expression (Brettschneider *et al.*, 2012).

#### 1.4.2.2. NK Cells.

NK cells, comprising of two main classes, the CD56<sup>dim</sup> and CD56<sup>bright</sup>, are a subset of innate lymphocytes mediating responses against virally infected and tumour cells (Abel *et al.*, 2018). The CD56<sup>dim</sup> subsets exerts its effects through

secretion of perforin and inflammatory cytokines such as IFN- $\gamma$ , while the CD56<sup>bright</sup> subsets is thought to possess both, immunoregulatory and cytotoxic properties (Martin *et al.*, 2020). The importance of NK subsets in ALS is unknown, but studies have shown that total NK cell number (per  $\mu\text{L}$  blood) is increased in ALS patients compared to healthy controls (Gustafson *et al.*, 2017; Murdock *et al.*, 2017). NK numbers have not been identified to correlate with disease progression however, their inflammatory potential to shift the immune system towards a destructive state suggests that these cells may play a part in ALS progression (Murdock *et al.*, 2017). NK target cells lacking MHC I, a recently published study found motor neurones from ALS mice and patients to lack this protein, potentially increasing susceptibility to NK targeting killing (Song *et al.*, 2016).

#### **1.4.2.3. Cytokines.**

Cytokines are soluble proteins within the immune system, secreted by immune cells of both the innate and adaptive arms, which function to provide instructions to, and mediate the communication between immune and non-immune cells (Duque and Descoteaux, 2014). Immune cytokines are comprised of two major subsets, the proinflammatory and anti-inflammatory (Su *et al.*, 2012). Proinflammatory cytokines such as IL-6, TNF- $\alpha$  and interleukin-1 $\beta$  (IL-1 $\beta$ ) are involved in the upregulation of inflammatory processes (Zhang and An, 2007). While the role of the anti-inflammatory cytokines, such as IL-4, interleukin-10 (IL-10) and interleukin-1 (IL-1) receptor agonist, is to control the response of proinflammatory cytokines (Opal and DePalo, 2000). Although the evidence may not be as clear as in other disease settings including autoimmunity and infection

associated immunopathology, there is some evidence to suggest a shift towards inflammation in the periphery and in the brain of ALS patients (Moudgil and Choubey, 2011). A meta-analysis of published data in literature carried out by Hu and colleagues in 2017 identified 25 eligible articles comparing inflammatory cytokines in blood between 812 ALS patients and 639 control subjects found significantly elevated pro-inflammatory cytokines such as IL-6, interleukin-8 (IL-8), IL-1 $\beta$  and TNF- $\alpha$  in blood of ALS patients when compared to healthy controls (Hu *et al.*, 2017). A year later, a similar meta-analysis of published data gathered from 71 articles compared inflammatory cytokines in CSF of ALS versus healthy controls reported significantly greater concentrations of pro-inflammatory proteins such as granulocyte colony-stimulating factor (G-CSF), interleukin-17 (IL-17), interleukin-15 (IL-15), macrophage inflammatory protein-1 $\alpha$  (MIP-1 $\alpha$ ) and monocyte chemoattractant protein-1 (MCP-1) in CSF of ALS patients when compared to healthy controls (Chen *et al.*, 2018). Moreover, some proteins such as MCP-1 and chemokine (C-X3-C motif) ligand 1 (CX3CL1) may have a dual roles in ALS and could potentially serve as prognostic/disease modifying proteins (Moreno-Martinez *et al.*, 2019).

#### **1.4.2.3.1. MCP-1.**

MCP-1, otherwise known as the chemokine (C-C motif) ligand 2 (CCL2), is a chemokine (a type of cytokine) that functions to attract immune cells to sites of inflammation (Yadav *et al.*, 2010). It is expressed by several types of cells within the CNS such as neurones, microglia and astrocytes (Yao and Tsirka, 2014). MCP-1 exerts its effects by binding to its high affinity C-C chemokine receptor type 2 (CCR2), which is expressed on a limited number of cells such as

monocytes, macrophages, T lymphocytes, NK cells and DCs (Bianconi *et al.*, 2018). ALS patients have been found to have significantly greater levels of plasma, serum and CSF MCP-1, and MCP-1 mRNA, compared to healthy or individuals with other neurological conditions (Henkel *et al.*, 2004; Baron *et al.*, 2005; Zhang *et al.*, 2006; Nagata *et al.*, 2013). While CCR2 expression on CD14<sup>+</sup> monocytes were significantly lower in a cohort of slow progressing sALS patients (Zhang *et al.*, 2006). The potential role of MCP-1 as a predictor of disease progression emerged when stratification of ALS patients into either low, mid or high tertiles based on the amount of MCP-1 detected in the CSF, revealed that patients in the low tertile group had 85% probability of survival to 25 months, while probability to survive to 25 months in the other two tertile groups was only 40% (Gille *et al.*, 2019).

#### 1.4.2.3.2. CX3CL1.

CX3CL1, otherwise known as fractalkine, is a chemokine which can act as an attractant and as an adhesion molecule for immune cells (Wojdasiewicz *et al.*, 2014). CX3CL1 promotes chemotaxis and adhesion through its sole receptor known as the chemokine (C-X3-C motif) receptor 1 (CX3CR1) which in the immune system is expressed on B cells, effector and cytotoxic T cells, NK cells and some monocyte subsets (Ferretti *et al.*, 2014). Within the CNS, neurones express CX3CL1 while its corresponding receptor, CX3CR1, is solely expressed on microglia (Finneran and Nash, 2019). Changes in the balance of surface and mRNA CX3CL1/CX3CR1 levels may contribute to inflammation in the CNS of ALS mice (Zhang *et al.*, 2018). Specifically, in motor neurones of transgenic SOD1<sup>G93A</sup> mice, high expression of CX3CL1 was observed at the age of 40 days

(asymptomatic stage) but as motor neurones died, a decline in CX3CL1 expression was observed at the ages of 90 (symptomatic stage) and 120 days (terminal stage), while the expression of CX3CR1 on microglia increased at the ages of 90 and 120 days in line with microglial proliferation (Zhang *et al.*, 2018). Moreover, these changes in CX3CL1/CX3CR1 were accompanied by an imbalance in activated microglia, with increases in M1 phenotype observed at the ages of 90 and 120 days and decreases in M2 microglia seen at 120 days of age (Zhang *et al.*, 2018). Currently these findings are not supported by data obtained from ALS patients however, human studies have indicated that polymorphisms in the CX3CR1 gene may influence the survival time of ALS patients (Lopez-Lopez *et al.*, 2014; Moglia *et al.*, 2017). Analysis of genotypes and haplotypes of the two CX3CR1 variants, V249I and T280M, in a Spanish cohort of 187 ALS patients found that sALS patients with CX3CR1 249<sup>I/I</sup> or 249<sup>V/I</sup> survived an average of  $42.27 \pm 4.90$  months compared to the  $67.65 \pm 7.42$  months sALS patients with 249<sup>V/V</sup> genotype survive (Lopez-Lopez *et al.*, 2014). On the contrary, a subsequent larger study of 755 ALS patients diagnosed between 2007 and 2012 in Italy found that it's those with a 249<sup>V/V</sup> genotype on average survived 6 months longer than patients with 249<sup>I/I</sup> or 249<sup>V/I</sup> genotypes (Moglia *et al.*, 2017). The innate immune findings in ALS (summarised in figure 1-2) present with novel insights and potential therapeutic approaches in patients with a condition previously thought to be localised in the CNS.

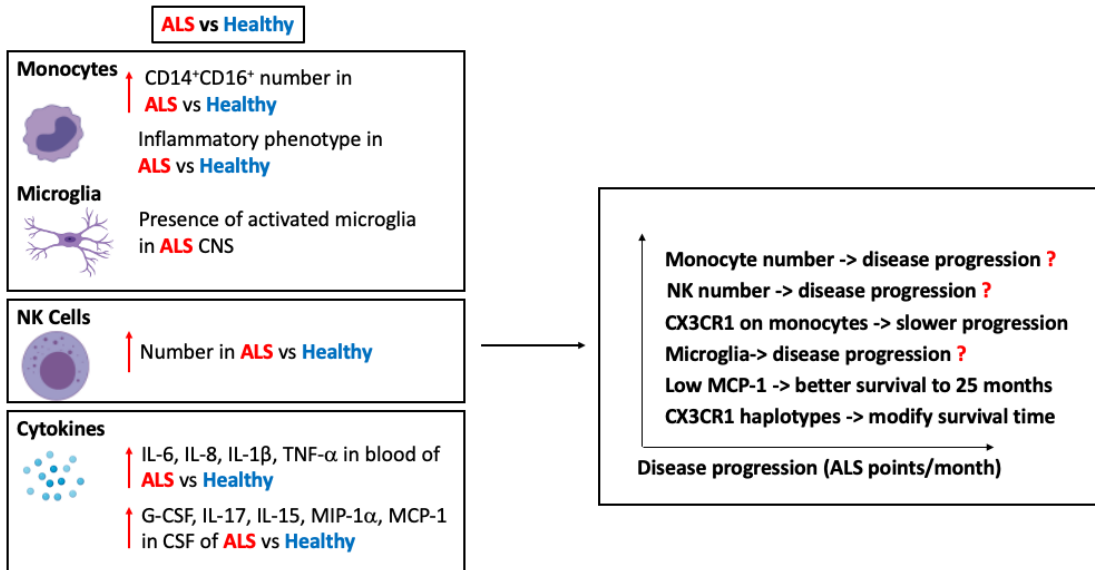


**Figure 1-2 Summary of innate immunity findings in ALS.** Greater numbers of monocytes and NK cells are found in ALS patients versus healthy individuals. There is also the presence of activated microglia in the CNS of ALS patients. In blood, greater levels of proinflammatory cytokines such as IL-6, IL-8, IL-1 and TNF- $\alpha$  are found in ALS patients versus healthy individuals. In the CSF there are greater levels of G-CSF, IL-17, IL-15, MIP-1 $\alpha$  and MCP-1 in ALS versus healthy individuals. CX3CR1 expression on monocytes and their genetic haplotypes, along with MCP-1 are found to correlate with disease progression.

#### 1.4.3. ALS and the adaptive immune system.

The adaptive immune system, unlike the innate, is antigen specific, can take several days to respond to pathogen, able to distinguish self from non-self-antigens and retains memory of encountered pathogens (Marshall *et al.*, 2018). Two major lymphocyte populations make up the adaptive immune system, these are called T (maturing in the thymus) and B (arising in the bone marrow) cells (Cooper and Alder, 2006). The adaptive immune response is initiated when antigen presenting cells (APCs) of the innate immune system, such as dendritic cells (DCs), process antigens into smaller fragments called peptides, package these peptides into major histocompatibility complex (MHC) proteins and present them to T cells (Yatim and Lakkis, 2015). T cells are activated when their surface

T cell receptor (TCR) binds the antigenic peptide on the MHC complex, this combined with co-stimulatory signalling and secretion of chemokines by the APC, or the T cell itself, causes the differentiation of T lymphocytes into specialised populations (Hwang *et al.*, 2020). There are several populations of T cells, cytotoxic T cells expressing surface cluster of differentiation (CD) 8 as well as cells expressing surface CD4, which can be subdivided into helper/effector and regulatory T (Treg) cells (Laidlaw *et al.*, 2016). The helper populations, collectively known as effector T cells (Teff), include T helper 1 ( $T_{H1}$ ), T helper 2 ( $T_{H2}$ ), T helper 17 ( $T_{H17}$ ) and T follicular helper ( $T_{FH}$ ) (Flajnik, 2018). Each T cell subset has a different role to play,  $CD8^+$  cytotoxic T cells secrete apoptosis inducing proteins such as perforin and granzymes,  $T_{H1}$  cells help protect against intracellular infections,  $T_{H2}$  produce cytokines that recruit B cells,  $T_{H17}$  produces IL-17A, an inflammatory cytokine recruiting immune cells to tissue, Treg suppress immune responses and the memory T cell populations help protect against future encounters with the same antigen (Kaiko *et al.*, 2008; MacLeod *et al.*, 2009; Marwaha *et al.*, 2012; Martin and Badovinac, 2018; Cortez *et al.*, 2020). B cells are also activated by co-engagement of their surface receptor, called the B cell receptor (Iwasaki and Medzhitov, 2010). Once activated they participate in the immune response by either the production of antibody to neutralise or opsonise pathogens, or act as APCs by capturing and presenting antigen to T cells (Li *et al.*, 2019). Just like T lymphocytes, B cells can differentiate specific cell types such as antibody secreting plasma cells and also memory B cells (Yam-Puc *et al.*, 2018).

#### **1.4.3.1. CD8<sup>+</sup> T cells.**

CD8<sup>+</sup> T cells are antigen specific secretors of apoptotic cytokines such as perforin and granzyme, which results in the killing of infected cells (Zhang and Bevan, 2011). There are conflicting reports of CD8<sup>+</sup> T cells in ALS. Studies published between 2009 and 2017 have reported a reduction, no difference, and significant increases in CD8<sup>+</sup> T cell number in ALS patients when compared to healthy controls, with no correlation with disease progression (Mantovani *et al.*, 2009; Rentzos *et al.*, 2012; Chen *et al.*, 2014; Gustafson *et al.*, 2017; Murdock *et al.*, 2017). These findings could be a result of individual variability and cohort size. Whereas in conditions such as MS, where CD8<sup>+</sup> T cells can be found in MS lesions, in ALS this is simply not the case and there is no evidence to ascertain whether these cells are detrimental (Ghasemi *et al.*, 2017).

#### **1.4.3.2. Treg.**

Treg are a heterogeneous subset of T lymphocytes, enforcing tolerance through suppression or regulation of various immune responses (Zhao *et al.*, 2017). There are several types of Treg, including those that exit the thymus programmed for regulatory function, and those that gain regulatory function in the periphery. The best characterised Treg and the main subject of this thesis are FoxP3<sup>+</sup> Treg. These are identified based on the expression of surface CD4, high constitutive expression of surface CD25 and low expression of surface CD127. Their development and regulatory function is dependent on the expression of intracellular forkhead box protein 3 (FoxP3) (Liu *et al.*, 2006; Li *et al.*, 2015). For simplicity, FoxP3<sup>+</sup> Treg will be referred to as Treg for the remainder of this thesis.

Like all lymphocytes, the majority of Treg are generated in the cortex of the thymus, and are known as thymic Treg (tTreg), during a process called positive selection, however it is yet unclear what percentage of Treg are tTreg in an adult (Maggi *et al.*, 2005). This is a process where a thymocyte TCR is engaged by a self-peptide-MHC complex presented by thymic stromal cells which leads to a high affinity interaction, resulting in the now self-reactive thymocytes maturation into a FoxP3 expressing Treg (Sakaguchi *et al.*, 2010). The TCR engagement is only one step of the Treg maturation process, Treg development has been described to involve cytokines such as interleukin-2 (IL-2), this will be discussed in more detail in the following section (Nelson, 2004). Other than the thymus, Treg can also acquire the expression of FoxP3 and gain regulatory function in the periphery (pTreg), by differentiating from naïve CD4+ T cells when they are activated via their TCR and co-stimulatory molecules in the presence of cytokines like IL-2 (Sakaguchi *et al.*, 2008).

Treg can suppress a wide range of immune cells such as CD4+ T cells, CD8+ T cells, NKT cells, B cells, NK cells, monocytes and DC (Schmidt *et al.*, 2012). The mechanisms by which Treg assert their suppressive function within the immune system can be classified into two main categories, cell-contact-dependent and cell-contact-independent (figure 1-3) (Meng *et al.*, 2016). The cell-contact-dependent mechanisms involve Treg interaction with DCs through binding of surface lymphocyte-activation gene 3 (LAG3) to MHCII inhibiting DC maturation and thus their antigen presenting capabilities (figure 1-3) (Arce-Sillas *et al.*, 2016). Treg can also outcompete Teff by binding their surface cytotoxic T-lymphocyte-associated protein 4 (CTLA-4) to DC surface CD80/CD86, leading to

DC production of indoleamine 2,3-dioxygenase (IDO), an immunosuppressive molecule. This removes the ability of CD80/CD86 to provide co-stimulation to Teff via CD28 (Vignali *et al.*, 2008). The cell-contact-independent mechanisms involve the release of immunosuppressive cytokines such as TGF- $\beta$  and IL-10, inhibiting the activities of cells such as Teff, DCs and macrophages (figure 1-3) (Sojka *et al.*, 2008). A recently reported Treg mode of action with regards to DCs is trogocytosis, whereby Treg bind to DCs resulting in the removal of MHCII from DC surface, leading to DC capacity to present antigen (Akkaya *et al.*, 2019). Cytolysis is another cell-contact-independent mechanism by which Treg suppress, this involves the secretion of granzymes A and B leading to perforin pore mediated apoptosis of Teff, CD8 $^{+}$  T cells and several other cells (figure 1-3) (Liberal *et al.*, 2015). Treg can also exert their suppressive function via their surface receptors CD25, capturing IL-2 and thus depriving Teff of this cytokine, which is needed for their effector function (figure 1-3) (Meng *et al.*, 2016). Finally, Treg can also generate adenosine diphosphate (ADP) and adenosine monophosphate (AMP) via their surface CD73 and CD39 receptors, in Teff the ADP will enhance intracellular cyclic AMP (cAMP) suppressing their function, and in DC the AMP will disrupt their maturation (figure 1-3) (Zhao *et al.*, 2017). Moreover, Treg have been described to modulate monocytes to secrete anti-inflammatory cytokines *in vitro* (Taams *et al.*, 2005).

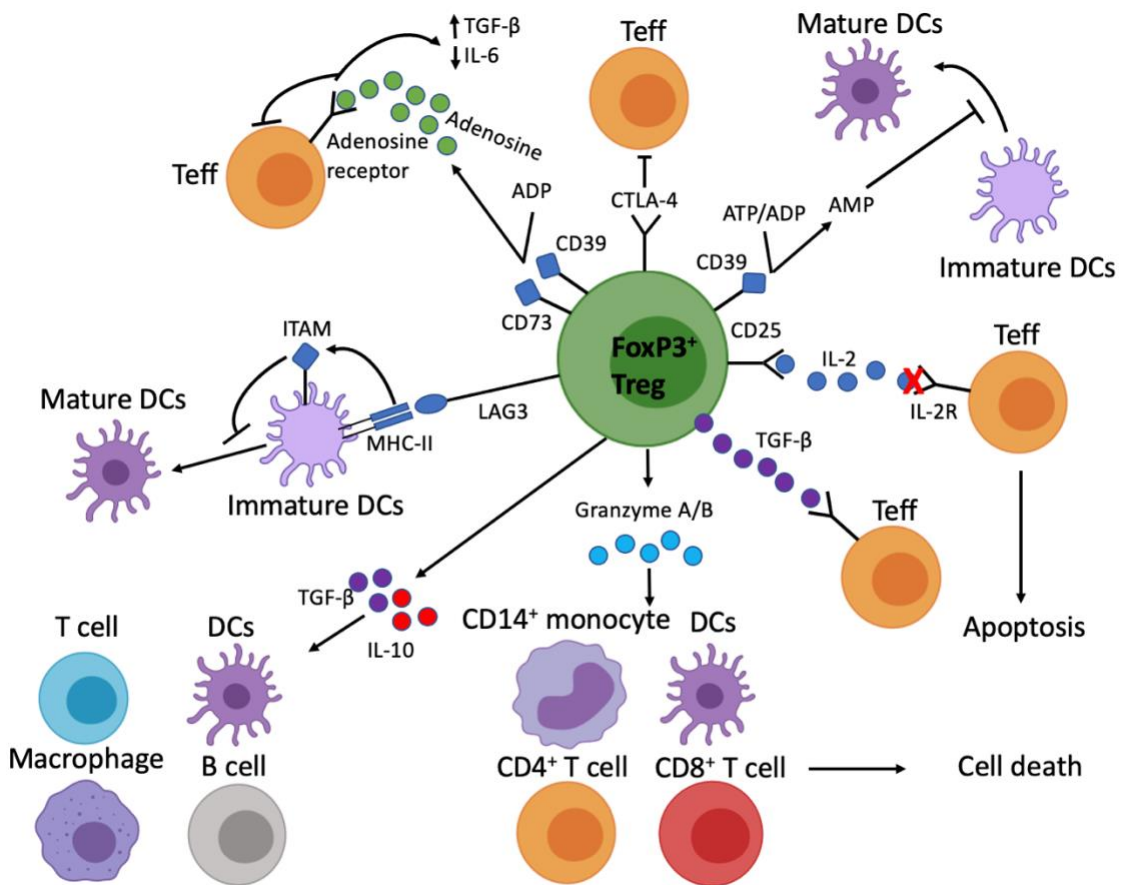


**Figure 1-3 Mechanisms of Treg mediated suppression.** Treg exert their suppressive function in two major ways, cell-contact dependent such as through the use of surface receptors such as CTLA-4 and LAG 3, or through cell-contact independent mechanisms such as the secretion of granzymes and IL-10 cytokines. Adapted from (Meng *et al.*, 2016).

Certain Treg functions or properties may be attributed to their phenotype, as research has shown that Treg are comprised of several distinct subpopulations (Mason *et al.*, 2015). For example, Treg expressing surface Sialyl Lewis x (CD15s) are thought to be most suppressive, while those expressing high levels of CD39 are most stable under inflammatory conditions, and Treg expressing Helios, a member of the Ikaros family of transcription factors, are in a highly activated state with enhanced suppressive capabilities (Zabransky *et al.*, 2012; Miyara *et al.*, 2015; Gu *et al.*, 2017). Breakdowns in Treg-mediated immune tolerance have been implicated in several autoimmune diseases such as type 1

diabetes (T1D) and MS, while their accumulation in tumour microenvironments are associated with metastasis and poorer prognosis (Wang *et al.*, 2012; Bluestone *et al.*, 2015; Danikowski, Jayaraman and Prabhakar, 2017; Kimura, 2020).

In ALS, Treg frequency and suppressive ability correlate with disease progression (Henkel *et al.*, 2013; Beers *et al.*, 2017). Before Treg, CD4<sup>+</sup> T cell presence was discovered at all stages of disease in the spinal cords of mSOD1 mice, and breeding of these with CD4<sup>+/−</sup> mice resulted in delayed onset, significantly longer survival and slower progression of disease compared to mSDO1/CD4<sup>−/−</sup> littermates, suggesting a neuroprotective role for CD4<sup>+</sup> T cells (Beers *et al.*, 2008). Subsequently, a study of disease progression in mSOD1 mice (8 to 16 weeks – early, stable disease phase; 18 weeks onwards – late, accelerated disease phase) revealed significant increases of both, blood and lymph node CD4<sup>+</sup>CD25<sup>+</sup>FoxP3<sup>+</sup> cells and FoxP3<sup>+</sup> fluorescence intensity at 16 weeks, all of which steadily declined from 18 weeks of age onwards (Beers *et al.*, 2011). The contribution of Treg to ALS progression in humans was first addressed in 2013, where assessment of T cells by flow cytometry revealed no significant difference in frequencies of blood Treg between ALS and healthy control individuals, but when ALS patients were categorised into either slow or rapidly progressing, the latter group had lower frequencies of CD4<sup>+</sup>FoxP3<sup>+</sup> cells and significantly lower expression of FoxP3 than the control group, and the slowly progressing ALS patients (Henkel *et al.*, 2013). The most compelling data from this study comes from the stratification of 102 ALS patients based on leukocyte mRNA expression of FoxP3, data gathered every three months for three and a

half years shows that those with high levels of FoxP3 mRNA had significantly slower progression rates and significantly lower death rates indicating that greater FoxP3 expression may be a precursor for better prognosis in ALS patients (Henkel *et al.*, 2013). These findings are further supported by recent, and more comprehensive flow cytometry analysis where inverse correlations between total FoxP3<sup>+</sup> Treg, CD45RO<sup>+</sup>FoxP3<sup>+</sup> (memory) Treg and ALS progression rate (ALSFRS points/month) were reported in 33 ALS patients (Sheean *et al.*, 2018). Furthermore, *in vitro* co-cultures of Tregs from ALS patients with autologous effector T (Teff) cells found ALS Tregs were significantly less effective at suppressing Teff proliferation when compared to Treg:Teff co-cultures of healthy controls. Similarly, Tregs from rapidly progressing ALS patients were significantly less suppressive than Tregs of slowly progressing ALS patients, with Treg suppression of Teff proliferation found to be inversely correlated with ALS progression (Beers *et al.*, 2017). As a result of these findings (summarised in figure 1-4), Treg have emerged as a potential therapeutic target in ALS (Rajabinejad *et al.*, 2020).

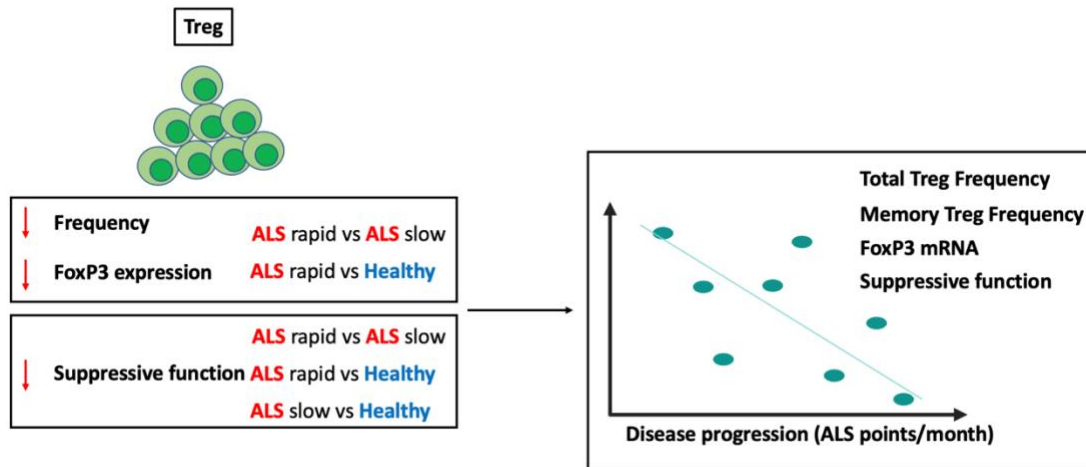


**Figure 1-4 Summary of Treg findings in ALS.** Treg frequency, FoxP3 expression and suppressive function are lower in rapidly progressing versus slow progressing ALS patients. FoxP3 expression and suppressive function is also significantly between rapid ALS versus healthy controls. Suppressive function is significantly reduced in slow ALS versus healthy controls. Total and memory Treg frequencies, FoxP3 mRNA and suppressive function negatively correlate with disease progression.

### 1.5. The role of IL-2 in Treg generation and function.

Interleukin-2 (IL-2), through its receptor subunits, is largely involved in the generation, differentiation and activation of white blood cells of the adaptive immune system, it can also mediate functions of some innate cells. In this section, I will discuss the discovery of immunoregulatory properties of IL-2, production of IL-2, IL-2 receptor subunits and signalling downstream, the effects of IL-2 on immune cells with particular focus on Treg reliance on IL-2 and ways to strengthen Treg using low-dose IL-2 (LD-IL-2) therapy *in vivo*.

### **1.5.1. Origins of IL-2.**

IL-2 is a 15.5 kilodalton (kDa) cytokine bundle made up of four  $\alpha$ -helices, first discovered over 40 years ago in T cell culture supernatants (Liao *et al.*, 2013). IL-2 was first named as the T cell growth factor (TCGF) as in the original report it was concluded that the protein present in the supernatants of T cells, activated by plant lectins such as phytohemagglutinin (PHA), could induce and support the proliferation and differentiation of antigen-activated T cells (Ross and Cantrell, 2018). IL-2 was the first TCGF to be purified and cloned establishing there is a single copy of the IL-2 gene in the human genome (Malek, 2008). The IL-2 paradox then came around when the role of IL-2 as a TCGF was challenged by research utilising IL-2 allele knockout (KO) mouse models which showed accumulations of activated lymphocytes, lymphadenopathy and severe autoimmune reactions in the IL-2KO mice, indicating that IL-2 also has immunoregulatory properties (Chastagner *et al.*, 2002). Similar phenotypes were observed in mice lacking CD25 alleles, which is a subunit of the IL-2 receptor (IL-2R), indicating that IL-2 facilitates its immunoregulatory actions through the IL-2R (Boyman and Sprent, 2012; Ross and Cantrell, 2018).

### **1.5.2. Production of IL-2.**

CD4 $^{+}$  T cells, when activated via the TCR and costimulatory signalling, are the main producers of endogenous IL-2 in the body (Nelson, 2004). Although Treg are part of the CD4 $^{+}$  T cell family, they do not produce IL-2 but rely on it for many processes (Moon *et al.*, 2015). It has been shown that activated DCs, naïve CD8 $^{+}$ , thymic cells and NK T cells also contribute to production of IL-2, but to a lesser extent than CD4 $^{+}$  T cells (Nelson, 2004; Zelante *et al.*, 2012). IL-2 production is

a result of the transcription of the *IL2* gene in the cell's nucleus, which is a process facilitated by several factors such as activator protein-1 (AP-1), octamer transcription factor (OCT-1), nuclear factor of activated T cells (NFAT) and nuclear factor κ-light-chain-enhancer of activated B cells (NF-κB) (figure 1-5) to name a few (Liao *et al.*, 2013).

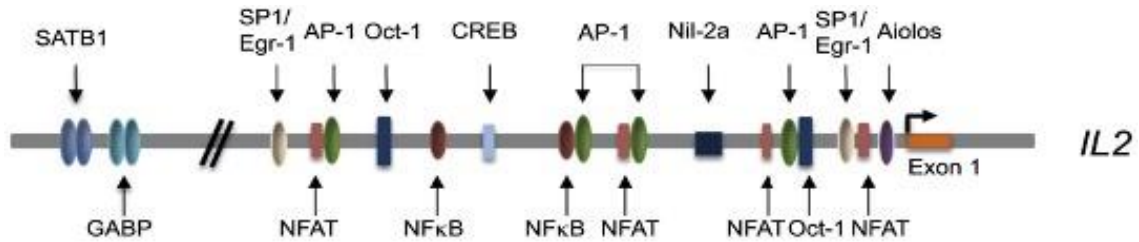


**Figure 1-5 Transcription factors that regulate the expression *IL2* gene.** The production of IL-2 is a result of the transcription of the *IL2* promoter region is mediated by transcription factors such as AP-1, OCT-1 and NFAT. Taken from (Liao *et al.*, 2013).

Once synthesised, IL-2 is released into the extracellular environment, this is rapidly followed by the expression of surface IL-2R (Gaffen and Liu, 2004). *In vitro* studies have shown that the binding of the newly synthesised IL-2 to IL-2R initiates two feedback loops, a negative feedback loop that silences the *IL2* gene, and a positive feedback loop that enhances the expression of IL-2R indicating that IL-2 can regulate its own production (Malek, 2008; Waysbort *et al.*, 2013).

### 1.5.3. The IL-2R.

The IL-2R is made up of three subunits, the α-chain (IL-2R $\alpha$ ) otherwise known as (and previously mentioned) CD25, the β-chain (IL-2R $\beta$ ) otherwise known as CD122 and the common gamma chain (IL-2γc) otherwise known as CD132

(Malek, 2008). All three subunits are needed to form the high affinity IL-2R (figure 1-6) (Morris and Waldmann, 2000).

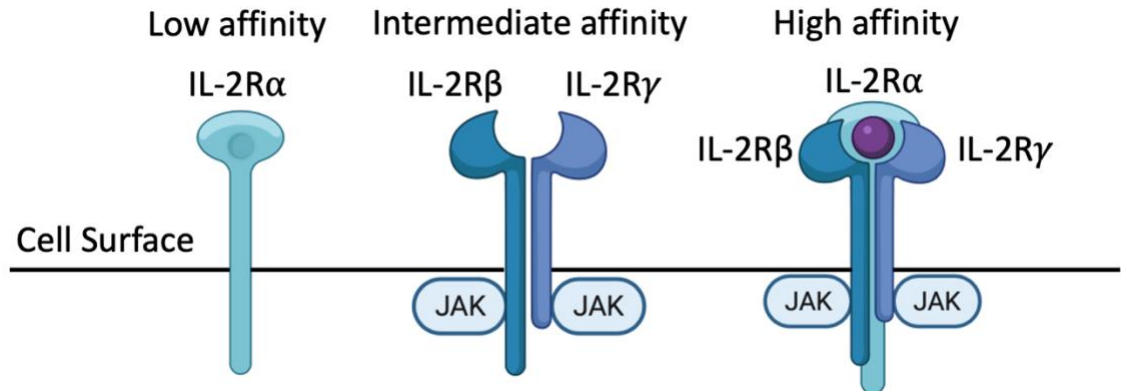


**Figure 1-6 IL-2R subunits on the cell surface.** IL-2R is made up of three subunits IL-2R $\alpha$ , IL-2R $\beta$  and IL-2 $\gamma$ c. IL-2 binds IL-2R $\alpha$  with low affinity (left), IL-2R $\beta$  and IL-2 $\gamma$ c with medium affinity (middle) and all three subunits with high affinity (right). Adapted from (Spolski *et al.*, 2018).

Research suggests that the three IL-2R subunits are not pre-formed as stable heterodimers, instead results from IL-2 crystal structure experiments suggest that the binding of IL-2 to IL-2R drives the trimeric assembly of the high affinity IL-2R (Stauber *et al.*, 2006). IL-2 is captured by IL-2R $\alpha$  on its hydrophobic binding surface leading to a conformational change in the IL-2 molecule, thus promoting an association with IL-2R $\beta$ , this IL-2R $\alpha$ -IL-2R $\beta$ -IL-2 complex then recruits the IL-2 $\gamma$ c to produce a stable, high affinity IL-2R (Malek and Castro, 2010; Bayer *et al.*, 2013).

#### 1.5.4. Expression of IL-2R.

The expression of each IL-2 subunit is dependent on the transcription of different promoter regions (figure 1-7) within the cell's nucleus and therefore the expression of surface IL-2R $\alpha$ , IL-2R $\beta$  or IL-2 $\gamma$ c can be regulated independently

of one another (Yu *et al.*, 2000). The IL-2R $\alpha$  sub-unit is constitutively expressed at high levels on Treg, naïve Teff do not express this sub-unit, however, antigen experienced (memory) Teff constitutively express low levels of IL-2R $\alpha$  (Spolski *et al.*, 2018). IL-2R $\alpha$  is also constitutively expressed on the CD56<sup>bright</sup> NK cell subset but at lower levels than Treg, while the CD56<sup>dim</sup>CD16 $^{+}$  NK cells express IL-2R $\alpha$  upon activation (Caldirola *et al.*, 2018). The transcription of the IL-2R $\alpha$  promoter gene in the nucleus of immune cells depends on several mediators such as the E74-like factor 1 (ELF1), signal transducer and activator of transcription 5 (STAT5), specificity protein 1 (SP1), AP-1, NFAT and NF- $\kappa$ B located in the positive regulatory regions (PRRs) such as the PRRIV, PRRIII and PRRI/II (figure 1-7 A) of the *IL2RA* gene (Kim *et al.*, 2001).

The IL-2R $\beta$  sub-unit is expressed on NK cells, resting T cells including CD8 $^{+}$  cells and Treg, monocytes and neutrophils while the IL-2 $\gamma$ c is constitutively expressed on all cells of the lymphoid lineage (Malek and Castro, 2010; Liao *et al.*, 2013). The *IL2RB* gene is transcribed by several transcription factors such early growth response protein 1 (EGR1), a fused, chimeric transcription factor of the Ewing sarcoma gene (EWS) and Wilms tumour suppressor gene (WT1), EWS-WT1, erythroblast transformation specific protein 1 (ETS1), GA-binding protein (GABP), SP1 and STAT5 (figure 1-7 B) (Kim *et al.*, 2006). Much less is known about the promoter of IL-2 $\gamma$ c subunit, some studies have shown the *IL2RG* gene to contain several ETS sites which interact with ELF1 and GABP which in turn may regulate the expression of surface IL-2 $\gamma$ c (figure 1-7 C) (Spolski *et al.*, 2018).

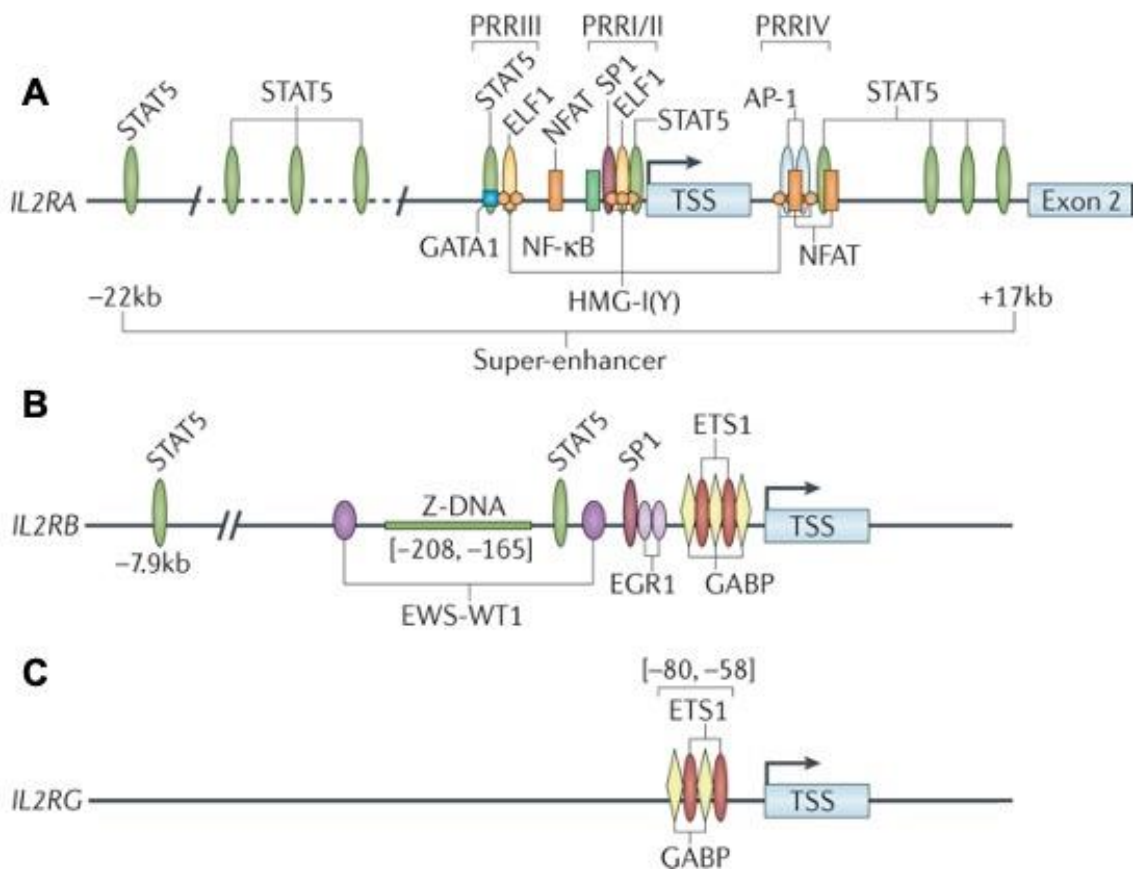


**Figure 1-7 Transcription factors that regulate the expression of *IL2RA*, *IL2RB* and *IL2RG* genes.** The expression of the IL-2R subunits is the result of the transcription of their respective promoter regions within their genes. The IL-2R subunit expression is mediated by several transcription factors such as STAT5 and SP1 for *IL2RA* and *IL2RB*, and GABP for *IL2RG* (Spolski *et al.*, 2018).

The binding of an IL-2 molecule to the IL-2R complex initiates several signaling pathways downstream (Ye *et al.*, 2018).

### 1.5.5. Signaling downstream of the IL-2R.

There is more than one signalling pathway downstream of the IL-2R (figure 1-8). The intracellular IL-2 signalling cascade is initiated when the binding of IL-2 to IL-2R complex causes the phosphorylation of the IL-2R $\beta$  and IL-2R $\gamma$ c cytoplasmic tails by binding to tyrosine kinase family molecules Janus kinase 1 and 3 (JAK1 and JAK3) respectively (Yu *et al.*, 2000). This can then result in the recruitment

and phosphorylation of STAT1, STAT3, STAT5a and STAT5b molecules (Villarino *et al.*, 2015). Following phosphorylation, STAT5a and STAT5b are dimerized and translocated to the nucleus where they bind to their target DNA sequences and regulate expression of genes (figure 1-8) (Ye *et al.*, 2018). The JAK-STAT signaling pathway is more active in Treg than other immune cells and it regulates expression of genes such as *FOXP3* and *IL2RA*, essential for Treg survival, proliferation and immunoregulatory activities (Hulme *et al.*, 2012). Other IL-2 signaling pathways such as the phosphoinositol 3-kinase (PI3-K) or the mitogen activated protein kinase/extracellular signal-related kinase (MAPK/ERK) can also be activated (figure 1-8) (Fung *et al.*, 2003). The PI3-K pathway leads to the phosphorylation of transcription factors such as the ribosomal protein S6 kinase (P70 S6K) (figure 1-8), regulating processes such as cell growth and survival (Harada *et al.*, 2001). While the MAPK/ERK signaling pathway results in ERK translocation to the nucleus (figure 1-8) and subsequent phosphorylation of transcription factors such as AP-1, responsible for proliferation, differentiation and apoptosis of a cell (Gazon *et al.*, 2018). The MAPK/ERK and PI3-K signaling pathways are more active in Teff and in these cells can regulate the expression of the *IL2* gene leading to the production of IL-2 (Hulme *et al.*, 2012). IL-2, once released into the extracellular environment, has the ability to affect the activity of multiple cell types (Valle-Mendiola *et al.*, 2016).

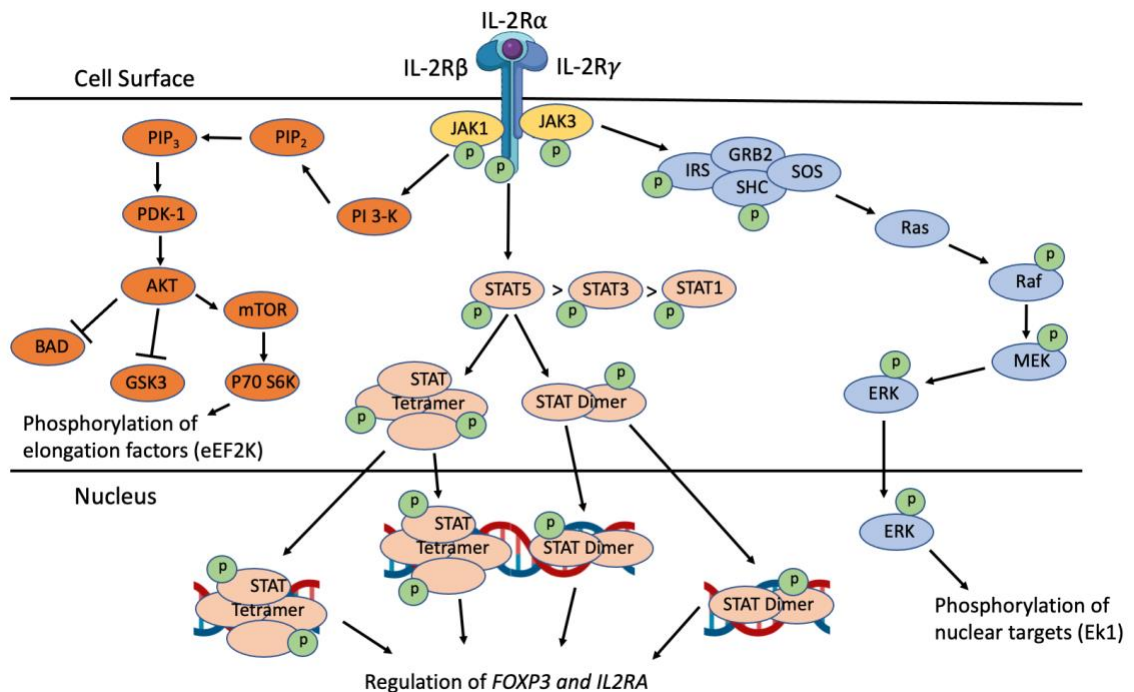


**Figure 1-8 Signaling pathways downstream of the IL-2R.** The engagement of the IL-2R can lead to the activation of intracellular signaling pathways like JAK-STAT, MAPK/ERK and PI-3K via the phosphorylation of proteins such as JAK1 and JAK3. Adapted from (Liao *et al.*, 2013).

### 1.5.6. Pleiotropic effects of IL-2.

The majority of IL-2 target cells belong to the adaptive immune system (figure 1-9) however, NK cells, type 2 innate lymphoid cells (ILC2) and gamma delta ( $\gamma\delta$ ) T can also be activated (Klatzmann and Abbas, 2015). Activation of NK cells by IL-2 results in increased cytotoxic activity and production of cytokines such as interferon gamma (IFN $\gamma$ ), with similar activation profiles observed in  $\gamma\delta$  T cells (Grimm Tse-Kuan Yu *et al.*, 2000; Klatzmann and Abbas, 2015). IL-2 can also activate peripheral monocytes as they constitutively express the IL-2R $\beta$  and IL-2 $\gamma$ c. Furthermore, the expression of IL-2R $\alpha$  (CD25) can be induced on monocytes when stimulated with IFN- $\gamma$  (Bosco *et al.*, 2000).

In cells of the adaptive immune system, IL-2 has been shown to aid the differentiation of naïve CD4<sup>+</sup> T cells into specialised subsets such as T<sub>H</sub>1, T<sub>H</sub>2, T<sub>H</sub>17 and T<sub>FH</sub> which contribute to inflammation and autoantibody production (figure 1-9) in tissue (Kalia and Sarkar, 2018). Similarly, IL-2 signalling pathways drive the differentiation of naïve CD8<sup>+</sup> T cells into memory subsets (figure 1-9) which participate in T cell mediated autoimmunity in tissue (Kalia and Sarkar, 2018).

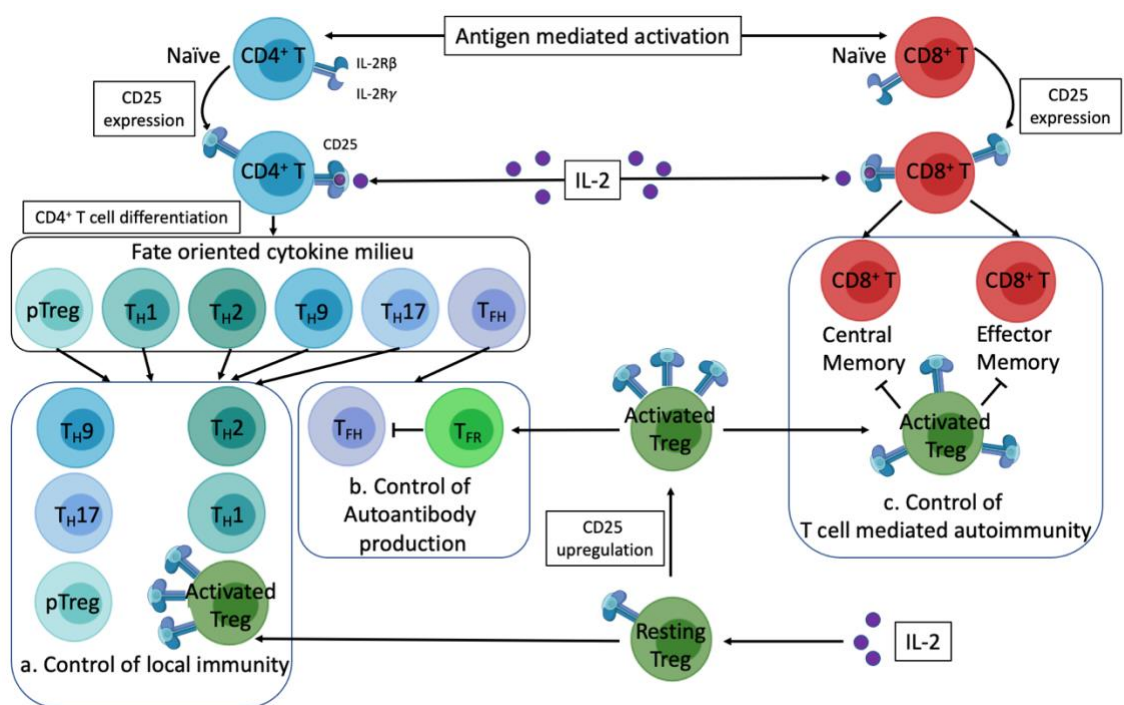


**Figure 1-9 The pleiotropic effects of IL-2 within the mammalian immune system.** The majority of effects that IL-2 exerts is within the adaptive immune system. It is involved in processes such as the activation of circulating memory and naïve Treg and the differentiation of naïve CD4<sup>+</sup> and CD8<sup>+</sup> T cells into specialized subsets. Adapted from (Klatzmann and Abbas, 2015).

Treg are the most affected population of cells by IL-2 throughout their life cycle, beginning in the thymus, where TCR signals during selection cause expression of CD25 on developing thymocytes and IL-2, stored at low levels within the thymic microenvironment, provides a signal for FoxP3 and CD25 upregulation, causing

these thymocytes to develop into Treg (Cheng *et al.*, 2013). In the periphery, pTreg differentiation from naïve CD4<sup>+</sup> T cell precursors is driven by IL-2, while IL-2 activation of circulating memory Treg results in Treg-mediated control of local inflammation, autoantibody production and T cell mediated autoimmunity (figure 1-9) in tissue (Klatzmann and Abbas, 2015). Moreover, IL-2 is essential for Treg survival in secondary lymphoid organs (SLOs) where they outcompete Teff and NK for IL-2, and also regulation of Treg homeostasis, suppressive function, as well as growth, differentiation and expansion through selective upregulation of *FOXP3* gene via the aforementioned JAK-STAT signalling pathway (Zorn *et al.*, 2006; Cheng, Yu and Malek, 2011; Hayes *et al.*, 2019). The constitutively high level of IL-2R $\alpha$  expression, as well as the constitutive expression of IL-2R $\beta$  and IL-2 $\gamma$ C, combined with the selective activation of the JAK-STAT pathway intracellularly, provides Treg with enhanced sensitivity to IL-2 when compared to NK or Teff, which is the basis for many intervention trials utilising low-dose IL-2 (LD-IL-2) (Ghelani *et al.*, 2020). Furthermore, research has shown that certain genetic polymorphisms in the IL-2/IL-2R signaling pathway, such as the *IL2RArs2104286*, may be associated with the development of autoimmune diseases such as T1D and MS, suggesting a key role for IL-2 and potentially Treg in disease development (Long *et al.*, 2010; Garg *et al.*, 2012; Cerosaletti *et al.*, 2013).

#### **1.5.7. Clinical trials utilising low-dose IL-2.**

Interleukin-2 (IL-2) was first approved by the FDA as treatment for metastatic renal carcinoma in 1992 followed by metastatic melanoma in 1997 and has since been utilised as a potential therapeutic approach to expand or invigorate Treg, in

conditions such as systemic lupus erythematosus (SLE), graft versus host disease (GVHD) and T1D (Koreth *et al.*, 2011; Hartemann *et al.*, 2013; Jiang, Zhou and Ren, 2016; He *et al.*, 2020). In fact, a search for the phrase “IL-2” on [ClinicalTrials.gov](#) (19-05-2021) produces results for 1843 studies, while the phrase “Low Dose IL-2” gives results for 188 studies (no filters applied) in a wide range of conditions, from cancers such as Acute Lymphoblastic Leukaemia (ALL), to autoimmune diseases such as Relapsing Remitting Multiple Sclerosis (RRMS), to infections such as Cytomegalovirus (CMV). Generally, a LD-IL-2 trial utilises doses of 1-3 million international units (MIU) injected subcutaneously (most often self-administered) to selectively expand the Treg population with minimal or no effect on Teff and NK. One of the first placebo-controlled studies to show that LD-IL-2 is safe and well tolerated was carried out by Hartemann and colleagues and used doses of 0.33, 1, 3 MIU/day or placebo for 5 consecutive days with a follow-up visit 60 days post final injection in patients with T1D (Hartemann *et al.*, 2013). It reported no serious adverse events and no deleterious changes in glucose metabolism, only influenza-like syndrome and injection site reaction in some participants. It also reported a dose dependent increase in Treg proportion which was significant at all doses when compared with placebo, and treatment associated increases in Teff and NK however these were not significantly different between any of the IL-2 doses and placebo treated (Hartemann *et al.*, 2013). Subsequent intervention studies/trials of LD-IL-2 have shown similar safety profiles along with efficacy and clinical responses. In individuals suffering from severe Alopecia Areata (AA), 4 out of the 5 patients had partial regrowth of scalp hair and a decrease in the median Severity of Alopecia Tool (SALT) from 82 to 69 after a course of 1.5MIU/day followed by 3 courses of

3MIU/day every three weeks (Castela *et al.*, 2014). Clinical responses were also reported in a 2016 publication where 20 out of 33 chronic GVHD patients taking part showed improved liver and lung function tests, and reduced skin erythema after receiving IL-2 at 1 MIU/m<sup>2</sup> of body surface area a day for 12 weeks (Koreth *et al.*, 2016). A study published in 2016 reported clinical responses in all 38 SLE patients taking part as measured by the SLE responder index following 3 cycles of every other day subcutaneous injections of 1MIU IL-2 (He *et al.*, 2016). Other than the safety and efficacy aspect, all of these studies also reported LD-IL-2 associated increases in Treg, and in some cases NK cells (Castela *et al.*, 2014; He *et al.*, 2016; Koreth *et al.*, 2016). These studies show the variety of conditions in which LD-IL-2 is a possible therapeutic mean however, the data from these studies confer to two common themes:

1. Highly variable Treg increases among trial participants
2. Variable clinical responses among trial participants

Nevertheless, it is clear that IL-2 is safe and well tolerated in adults and, was also reported to be safe in children, recently diagnosed with T1D, although at doses below 1MIU/day (Rosenzwajg *et al.*, 2020).

### **1.6. Clinical trials in ALS.**

Intervention trials in ALS are challenging due to short survival time, delay from neuronal damage to disease diagnosis, genetic association with disease onset and rapid deterioration of mobility, which could be problematic if the patients are self-administering (Katyal and Govindarajan, 2017). Nevertheless, since the approval of riluzole, over 60 disease modifying agents have been tested as potential treatments for ALS, unfortunately they failed to show clinical efficacy in

randomised, placebo controlled clinical trials and did not get approval (Petrov *et al.*, 2017). Numerous molecular agents tested exert their effects on the immune system (McCombe *et al.*, 2020). Some of the first immune therapy trials attempted in ALS throughout the 1990s utilised agents such as prednisolone, azathioprine, cyclophosphamide and intravenous immunoglobulins, none of which were deemed to alter the course of ALS progression (Werdelin *et al.*, 1990; Smith *et al.*, 1994; Meucci *et al.*, 1996). Anti-inflammatories such as celecoxib and minocycline both failed to slow the decline in muscle strength, vital capacity or the ALSFRS-R, in fact the ALSFRS-R decline was greater in those taking minocycline versus placebo (Cudkowicz *et al.*, 2006; Gordon *et al.*, 2007). Recently, Masitinib, which targets microglia and macrophage activity within the nervous system to provide a neuroprotective effect, as an add-on to riluzole has shown a decline in the ALSFRS-R and vital capacity but only in a subgroup of patients termed “Normal Progressors” (Mora *et al.*, 2020). There is also Ravulizumab-cwvz, which blocks terminal complement C5 activation and is designed to reduce neuroinflammation, but the results of its effectiveness are still outstanding (Chen, 2020). Immunomodulatory trials pose another challenge in ALS, this is because the risk of infection increases as ALS progresses, therefore a medicine deemed safe in an autoimmune disorder or cancer, may result in harmful cytotoxicity in ALS patients (Khalid *et al.*, 2017). IL-2 at low doses however, has been shown to selectively expand Treg and promote suppression of immune responses (Hartemann *et al.*, 2013). Clinical trial data also shows that at low doses, IL-2 is safe and well tolerated without detrimental effects brought on by the activation of NK and CD8 T cells (Mahmoudpour *et al.*, 2019; He *et al.*, 2020). This, combined with the Treg association with ALS progression, lays down

the groundwork for assessing the role of LD-IL-2 in ALS (Camu, Mickunas *et al.*, 2020).

### **1.7. Immuno-modulation in ALS (IMODALS) clinical trial.**

The work in this thesis is based on samples obtained from the trial of LD-IL-2 in ALS (IMODALS). The trial design and some of the data presented in chapters 2 and 3 are published by Camu, W., Mickunas, M., Veyrune, J.L., Payane, C., Garlanda, C., Locati, M., Juntas-Morales, R., Pageot, N., Malaspina, A., Andreasson, U., Kirby, J., Suehs, C., Saker, S., Masseguin, C., De Vos, J., Zetterberg, H., Shaw, P.J., Al-Chalabi, A., Leigh, P.N., Tree, T., Bensimon, G. (2020) 'Repeated 5-day cycles of low dose aldesleukin in amyotrophic lateral sclerosis (IMODALS): A phase 2a randomised, double-blind, placebo-controlled trial', EBioMedicine. Elsevier B.V., 59. doi: 10.1016/j.ebiom.2020.102844.

Extensive detail regarding the IMODALS clinical trial can also be found on ClinicalTrials.gov using the identifier NCT02059759. Briefly, IMODALS was a randomised (1:1:1), parallel group, double-blind, single-centre, placebo-controlled phase II study of safety and activity of LD-IL-2 in patients with ALS, carried out between September 2015 and May 2016 at the CHRU de Montpellier – Hospital Gui de Chauliac Montpellier, France, 34295. The study utilised 1 million international units (MIU) and 2MIU doses of IL-2 to determine the best for ALS, which will subsequently be used in a phase II/III trial. The primary outcome was to assess the activity of LD-IL-2 on Treg and immune inflammatory markers in ALS patients treated for 3 months (5 doses of IL-2 per day for 5 consecutive days, every 4 weeks, repeated 3 times). The secondary objectives of this study were:

1. To evaluate whether T cell responses are maintained 4 weeks after each 5-day course and 12 weeks after the 3<sup>rd</sup> course.
2. To evaluate the safety of LD-IL-2 in ALS patients with 6-month follow-up after the final sub-cutaneous injection.
3. To evaluate functional changes throughout the study
4. To evaluate changes in other pre-defined blood cytology parameters, and an axonal damage biomarker in blood.

A total of 39 patients between the ages of 18 and 75 were enrolled, but following examination by a physician, 3 were excluded having not met the inclusion criteria which is briefly summarised in table 1-1.

| Inclusion Criteria  | Exclusion Criteria  |
|---|---|
| Patient informed and signed consent   | Cancer within the past 5 years  |
| Disease duration less than 5 years  | Severe cardiac or pulmonary disease   |
| On riluzole treatment for 3 months  | Respiratory or feeding assistance   |
| Vital capacity of ≥ 70% of normal   | Autoimmune disorders  |
| Ability to swallow  | Adult patient is under guardianship   |
| Probable, laboratory supported probable or definite ALS defined by El Escorial Revised ALS criteria | Evidence of recent infection based on positive serology for IgM (e.g., cytomegalovirus, Epstein-Barr virus) |

**Table 1-1 Brief summary of the main inclusion and exclusion criteria used for patient randomisation in IMODALS.** HIV: Human Immunodeficiency Virus; EBV: Epstein-Barr Virus; CMV: Cytomegalovirus.

The remaining 36 participants, whose demographic and baseline characteristics are presented in table 1-2, were allocated their treatment group using a web-based inclusion and randomisation (with blocking) application (Camu *et al.*, 2020).

|                                    | Placebo (n=12)         | IL-2 at 1MIU/d (n=12)                          | IL-2 at 2MIU/d (n=12)  |
|------------------------------------|------------------------|--|------------------------|
| <u>Sex (female)</u>                | 3 (25%)                | 5 (41.7%)                                      | 3 (25%)                |
| <u>Familial form</u>               | 0 (0%)                 | 2 (16.7%)                                      | 2 (16.7%)              |
|                                    |                        | <u>Age</u>                                     |                        |
| Mean (SD)                          | 56.45 (9.57)           | 54.98 (10.99)                                  | 57.68 (12.91)          |
| Median (Range)                     | 56.20 (42.2 to 69.7)   | 54.80 (40.2 to 75.4)                           | 61.25 (36.5 to 76.6.)  |
|                                    |                        | <u>BMI</u>                                     |                        |
| Mean (SD)                          | 26.80 (5.6)            | 25.34 (2.53)                                   | 24.39 (1.71)           |
| Median (Range)                     | 25.10 (22.2 to 43.4)   | 24.90 (21.90 to 28.7)                          | 24.35 (21.6 to 26.7)   |
|                                    |                        | <u>Age at onset</u>                            |                        |
| Mean (SD)                          | 54.27 (9.85)           | 52.43 (11.02)                                  | 55.80 (12.86)          |
| Median (Range)                     | 55.30 (38.1 to 68.0)   | 52.20 (37.4 to 72.6)                           | 58.25 (35.1 to 76.0)   |
|                                    |                        | <u>Disease duration (years)</u>                |                        |
| Mean (SD)                          | 2.2 (1.44)             | 2.60 (1.33)                                    | 1.96 (1.44)            |
| Median (Range)                     | 1.75 (0.5 to 5.0)      | 2.85 (0.9 to 4.6)                              | 1.45 (0.6 to 4.6)      |
|                                    |                        | <u>Duration of riluzole treatment (months)</u> |                        |
| Mean (SD)                          | 16.58 (12.49)          | 20.70 (14.90)                                  | 14.18 (11.47)          |
| Median (Range)                     | 12.35 (4.6 to 39.8)    | 17.45 (5.0 to 45.1)                            | 11.10 (3.1 to 34.0)    |
|                                    |                        | <u>Diagnosis</u>                               |                        |
| Definite                           | 5 (41.7%)              | 6 (50%)  | 4 (33.3%)              |
| Probable                           | 5 (41.7%)              | 6 (50%)  | 3 (25%)                |
| Probable<br>(laboratory supported) | 2 (16.7%)              | 0 (0%)   | 5 (41.7%)              |
|                                    |                        | <u>Site of onset</u>                           |                        |
| Limb                               | 11 (92%)               | 11 (92%)                                       | 9 (75%)                |
| Bulbar                             | 1 (8%)                 | 1 (8%)   | 3 (25%)                |
|                                    |                        | <u>Slow vital capacity (percent predicted)</u> |                        |
| Mean (SD)                          | 94.4 (12.4)            | 101.5 (18.1)                                   | 93.6 (16.3)            |
| Median (Range)                     | 96.5 (77.00 to 119.00) | 101.0 (79.00 to 132.00)                        | 94.5 (72.00 to 118.00) |
|                                    |                        | <u>ALSFRS-R score</u>                          |                        |
| Mean (SD)                          | 38.8 (3.4)             | 38.0 (4.8)                                     | 37.8 (5.3)             |
| Median (Range)                     | 38.5 (34.00 to 45.00)  | 38.0 (30.00 to 44.00)                          | 39.5 (26.00 to 44.00)  |
|                                    |                        | <u>NFL-MSD (pg/ml)</u>                         |                        |
| Mean (SD)                          | 127.84 (89.90)         | 135.55 (76.80)                                 | 178.19 (94.84)         |
| Median (Range)                     | 116.6 (6.7 – 349.2)    | 103.4 (46.2 – 245.5)                           | 144.2 (109.1 – 460.0)  |

**Table 1-2 Demographic and baseline characteristics of IMODALS trial participants.** BMI: Body Mass

Index; SD: Standard Deviation; NFL-MSD: Neurofilament Light Chain Proteins – Electroluminescent Detection Method (Meso Scale Discovery); ALSFRS-R: Amyotrophic Lateral Sclerosis Functional Rating Score – Revised (Camu *et al.*, 2020).

Following randomisation, the participants underwent 3 cycles of 5-daily doses of placebo, 1MIU IL-2 or 2MIU IL-2 at the beginning of 3 consecutive months, followed by two follow-up visits after the final sub-cutaneous injection, as detailed in figure 1-10.

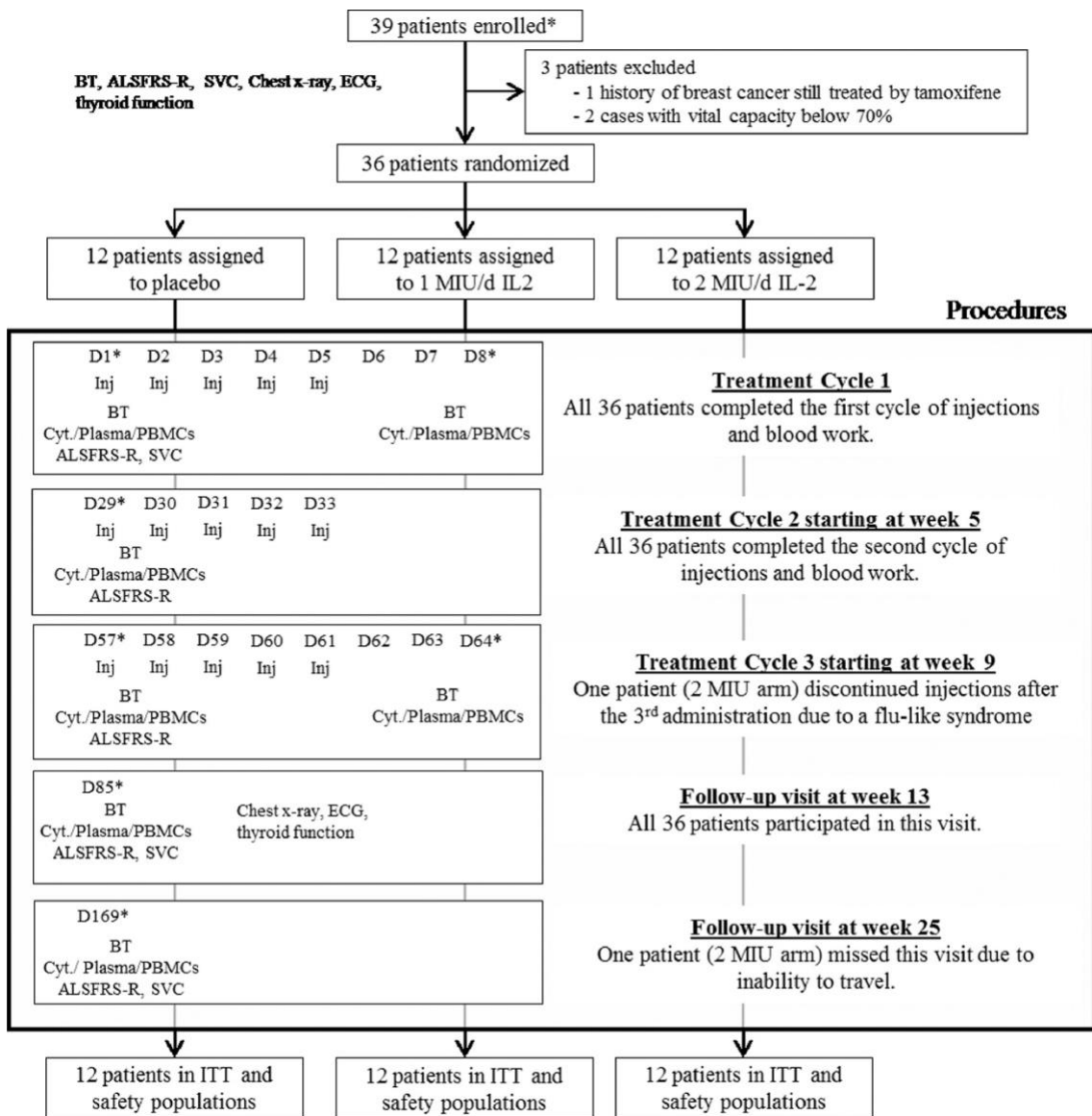


**Figure 1-10 IMODALS clinical trial profile.** ALSFRS-R: Amyotrophic Lateral Sclerosis Functional Rating Score – Revised; BT: Blood Test; Cyt: Fresh Blood Flow Cytometry; SVC: Slow Vital Capacity; PBMCs: Peripheral Blood Mononuclear Cells; Inj: Sub-cutaneous Injection; D: Day; ECG: Electrocardiogram; ITT: Intention-to-treat. \*Patients visits attended in hospital (Camu *et al.*, 2020).

During the trial all work was conducted in a fully blinded manner without knowledge of patient ID, visit or treatment group. However, work carried out by the PhD candidate for this thesis required the unblinding of patient ID and visit in order for all timepoints per patient to be assayed on the same day.

### **1.8. Aims of this thesis.**

The experimental work in this thesis will utilise data from fresh blood flow cytometry and cryopreserved PBMC samples from IMODALS trial participants to test the following hypotheses:

1. In addition to being safe and well tolerated, IL-2 will preferentially expand Treg in ALS patients receiving either the 1MIU or 2MIU dose. Non-Treg cells bearing the IL-2R subunits will also be expanded.
2. In addition to increase in Treg number, IL-2 therapy will also increase Treg function and any effect on Treg function, may persist after the therapy has stopped.
3. Treg and non-Treg IL-2 signalling at baseline will correlate with observed expansion in response to therapy and, continued IL-2 therapy may affect IL-2 signalling.
4. IL-2 therapy will selectively expand specific subpopulations of Treg and non-Treg cells and, any effect of treatment on these subpopulations may persist after the therapy has stopped.

## **Chapter 2. Investigating the effects of IL-2 therapy on immune cells in peripheral blood of ALS patients.**

### **2.1. Introduction.**

As discussed in chapter 1, neuroinflammation and alterations of innate and adaptive immune components in peripheral blood are common pathological features in ALS patients when compared to healthy controls. These include increased frequencies of proinflammatory monocytes and NK cells, as well as reduced Treg numbers. (McCombe and Henderson, 2011; Heneka *et al.*, 2015). Lower Treg frequency, FoxP3 expression and suppressive function inversely correlate with ALS progression. Treg are responsible for maintaining immune tolerance by suppressing the actions of inflammatory cells. Studies have shown that Treg numbers can be improved *in vivo* through selective expansion by LD-IL-2 (Koreth *et al.*, 2011; Hartemann *et al.*, 2013). As a result, we carried out the first study of LD-IL-2 in ALS called IMODALS. The primary outcome of this trial was to assess the safety and activity of three cycles of 5-daily doses of LD-IL-2 on Treg and other immune inflammatory markers in ALS. To investigate the effects of IL-2 on immune cells in peripheral blood, we used flow cytometry to assess the number and frequency of Treg, Teff, B cells, CD8<sup>+</sup> T and NK cells. We will also assess any effects of IL-2 on monocyte subsets. Reports show a skewing of ALS monocytes towards the inflammatory phenotype and IL-2 may activate monocytes as they constitutively express the IL-2R $\beta$  and IL-2yc. When activated *in vitro*, monocytes also upregulate CD25 (Bosco *et al.*, 2000). Furthermore, when cocultured with Tregs, monocytes increase expression of markers such as CD163 a scavenger protein (Taams *et al.*, 2005). It has also

been shown that Tregs expanded with IL-2 *in vitro*, are better at modulating monocytes to secrete anti-inflammatory cytokines than non-expanded Tregs (Romano *et al.*, 2018). Therefore, we wanted to assess whether there was a change in monocyte balance in blood as a result of IL-2 therapy. To assess this, in addition to using CD14 and CD16, we will also incorporate other monocyte markers associated such as CCR2 and CD163.

The experimental work will test the following hypotheses:

1. In addition to being safe and well tolerated, IL-2 will selectively expand Treg in peripheral blood of ALS patients.
2. Non-Treg cells bearing the IL-2R subunits will also be expanded.
3. IL-2 therapy will alter the balance of monocytes.

To test these hypotheses in this chapter, the gating strategy, analysis templates and the data analysis itself were designed and carried out by the PhD candidate as part of this thesis at the Department of Immunobiology, Faculty of Life Sciences and Medicine, King's College London, United Kingdom. While the wet laboratory experiments in this chapter were carried out by a collaborator at the Department for Cell and Tissue Engineering of the Montpellier University Hospital, France, where the IMODALS clinical trial was conducted.

## **2.2. Materials and methods.**

### **Flow cytometry:**

Peripheral blood was collected into EDTA blood collection tubes and stained with four panels of monoclonal antibodies within two hours of draw as detailed in tables 2-1 and 2-2. For panel 1, 50µL of blood was mixed with the surface antibodies followed by fixation and permeabilization with PerFix-nc buffer set (Beckman Coulter). The cells were then stained with FoxP3 AF647 antibody. For panel 2, 100µL of blood was added to a tube containing Flow-Count Flurosphere microbeads (Beckman Coulter) and stained with cell surface antibodies. The red blood cells were then lysed using 1ml of Versalyse (Beckman Coulter). Prior to analysis, the sample was diluted with 1ml PBS. For panels 3 and 4, 100µL of blood was stained with cell surface antibodies. The red blood cells were then lysed just as in panel 2. All samples were acquired on a CyAn flow cytometer (Beckman Coulter) (Camu *et al.*, 2020).

| Fresh Blood Flow Cytometry – Panel 1 |              |             |        |                 |
|--------------------------------------|--------------|-------------|--------|-----------------|
| Target                               | Conjugate    | Clone       | Origin | Manufacturer    |
| CD3                                  | FITC         | UCHT1       | Mouse  | Beckman Coulter |
| CD4                                  | ECD          | SFCI12T4D11 | Mouse  | Beckman Coulter |
| CD25                                 | PE           | B1.49.9     | Mouse  | Beckman Coulter |
| CD127                                | PE-Cy7       | R34.34      | Mouse  | Beckman Coulter |
| FOXP3                                | AF647        | 259D        | Mouse  | Beckman Coulter |
| Fresh Blood Flow Cytometry – Panel 2 |              |             |        |                 |
| CD3                                  | FITC         | UCHT1       | Mouse  | Beckman Coulter |
| CD4                                  | ECD          | SFCI12T4D11 | Mouse  | Beckman Coulter |
| CD8                                  | PE-Cy5.5     | B9.11       | Mouse  | Beckman Coulter |
| CD56                                 | PE           | N901        | Mouse  | Beckman Coulter |
| CD16                                 | PE-Cy7       | 3G8         | Mouse  | Beckman Coulter |
| CD14                                 | APC          | RMO52       | Mouse  | Beckman Coulter |
| CD19                                 | APC-AF750    | J3-119      | Mouse  | Beckman Coulter |
| CD45                                 | Krome Orange | J33         | Mouse  | Beckman Coulter |

**Table 2-1 Details of flow cytometry antibodies used in fresh blood immunophenotyping panels 1 and 2.**

| Fresh Blood Flow Cytometry – Panel 3 |              |          |        |                 |
|--------------------------------------|--------------|----------|--------|-----------------|
| Target                               | Conjugate    | Clone    | Origin | Manufacturer    |
| CD8                                  | PE-Cy5.5     | B9.11    | Mouse  | Beckman Coulter |
| CD14                                 | APC          | RMO52    | Mouse  | Beckman Coulter |
| CD16                                 | PE-Cy7       | 3G8      | Mouse  | Beckman Coulter |
| CD45                                 | Krome Orange | J33      | Mouse  | Beckman Coulter |
| HLA-DR                               | APC-AF750    | Imm-357  | Mouse  | Beckman Coulter |
| CCR2                                 | FITC         | SA203G11 | Mouse  | Beckman Coulter |
| CD163                                | ECD          | GHI/61   | Mouse  | Beckman Coulter |
| Fresh Blood Flow Cytometry – Panel 4 |              |          |        |                 |
| CD8                                  | PE-Cy5.5     | B9.11    | Mouse  | Beckman Coulter |
| CD14                                 | APC          | RMO52    | Mouse  | Beckman Coulter |
| CD16                                 | PE-Cy7       | 3G8      | Mouse  | Beckman Coulter |
| CD45                                 | Krome Orange | J33      | Mouse  | Beckman Coulter |
| HLA-DR                               | APC-AF750    | Imm-357  | Mouse  | Beckman Coulter |

Table 2-2 Details of flow cytometry antibodies used in fresh blood immunophenotyping panels 3 and 4.

### Data Analysis:

Changes in immune cell absolute number and frequency from baseline in each treatment arm were assessed using GraphPad Prism version 8. First, column statistics were performed using D'Agostino & Pearson normality and lognormality. If the data was normally distributed then a matched, repeated measures one-way ANOVA with Geisser-Greenhouse correction and Bonferroni's multiple comparisons test was used. If the data was not normally distributed then a matched, Friedman test with Dunn's multiple comparisons test was used. To assess any changes in absolute number or relative frequency in relation to either dose of IL-2, the reported values at each visit for each patient were compared to that of day 1 (baseline visit), significant changes are reported as having a p value of 0.05 or less.

## **2.3. Results.**

### **2.3.1. Designing analysis templates to identify the major leukocyte populations in whole blood.**

FlowJo version 9 (Tree Star) was used to create the analysis templates. For staining panel 1, Treg and Tconv cell subsets were identified as CD4<sup>+</sup>CD25<sup>hi/+</sup>CD127<sup>lo/-</sup>FoxP3<sup>+</sup> and CD4<sup>+</sup>CD25<sup>+</sup>CD127<sup>+</sup>FoxP3<sup>-</sup> respectively (figure 2-1). Staining panel 2 was analysed to identify CD3<sup>+</sup>, CD4<sup>+</sup>, CD8<sup>+</sup>, CD19<sup>+</sup>, CD56<sup>+</sup> NK cells, monocytes and their classical, intermediate and alternative subsets (figure 2-2). Staining panel 3 was designed to investigate specific subsets of monocytes, also incorporating CD163 and CCR2 (figure 2-3). Staining panel 4 was identical to staining panel 3 except it did not contain monoclonal antibodies for CD163 and CCR2. This panel would act as a negative control and used as a guide for gating monocytes expressing CD163 and CCR2 (figure 2-4). From each staining panel, the relative frequencies and the absolute numbers were reported for each of the afore mentioned leukocyte populations. For relative frequencies, CD3 T cells, CD19 B lymphocytes, CD56 NK cells and total monocytes were expressed as percentages of CD45<sup>+</sup> cells. CD4 and CD8 T cells as percentages of CD3<sup>+</sup> cells while Treg and Teff as percentages of CD4<sup>+</sup> cells. The classical, intermediate and non-classical monocyte subsets as percentages of total monocytes and the NK subsets, CD56<sup>bright</sup> and CD56<sup>dim</sup>CD16<sup>+</sup>, as percentages of total NK cells. The absolute counts of immune cell populations were calculated using routine blood tests and frequencies from flow cytometry and reported as number per µL of blood.

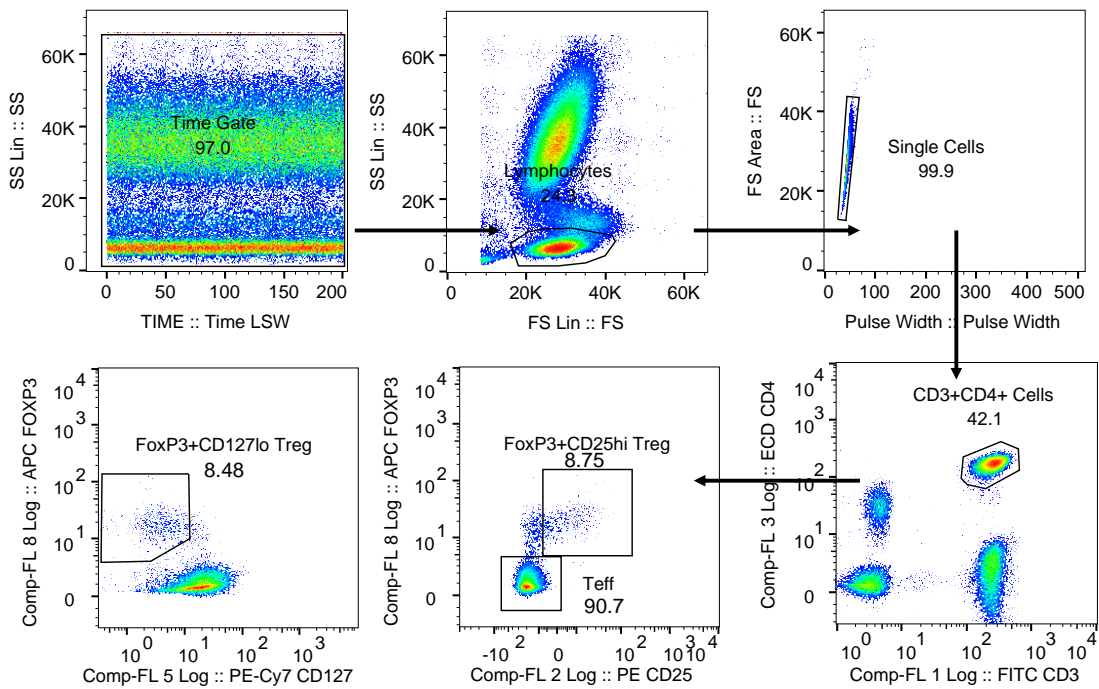


**Figure 2-1 Gating scheme for staining panel 1.** 50 $\mu$ L of blood was stained to identify Treg and Tconv.

The assay was analysed by gating on all cells across time, then isolating lymphocytes based on their FS Lin/SS Lin profile and by gating on single cells to exclude any doubles and debris. Treg and Tconv were then identified as CD4<sup>+</sup>CD25<sup>hi/+</sup>CD127<sup>lo/-</sup>FoxP3<sup>+</sup> and CD4<sup>+</sup>CD25<sup>+</sup>CD127<sup>+</sup>FoxP3<sup>-</sup> respectively.

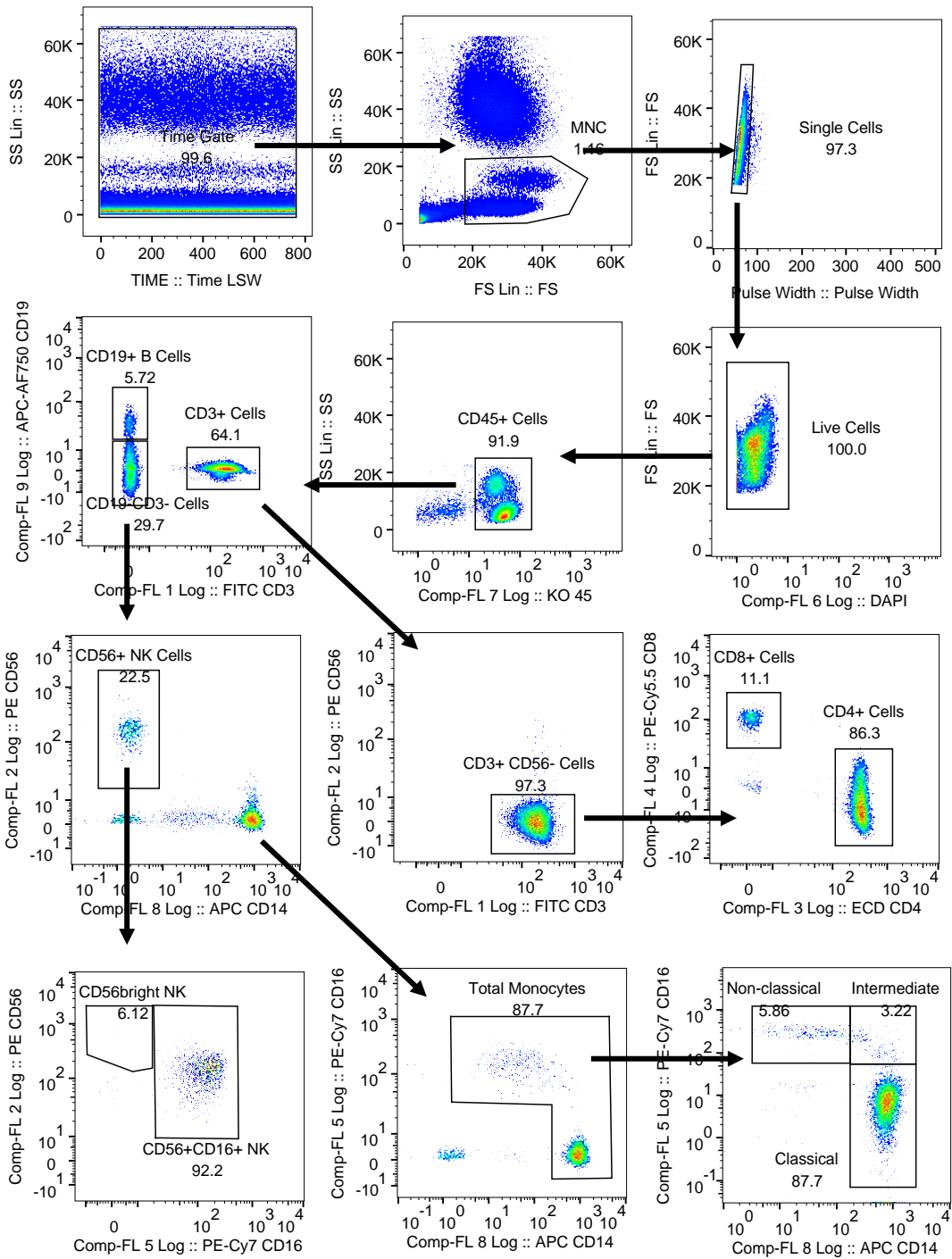


**Figure 2-2 Gating scheme for panel 2.** 100 $\mu$ L of blood was stained to characterise the major immune cell subsets. The experiment was analysed by gating on all cells across time, then isolating all mononuclear cells based on their FS Lin/SS Lin profile followed by gating on single and live cells to exclude doublets and dead cells. Expression of CD45, CD3 and CD19 was used to identify CD3 T and CD19 B lymphocytes. Expression of the former was then used to isolate CD4 and CD8 T cells while CD56 NK cells were identified as neither CD3 nor CD19 positive. Finally, to identify total monocytes and their non-classical, intermediate and classical subsets the ‘not gate’ function was used on all non-CD56 NK cells.

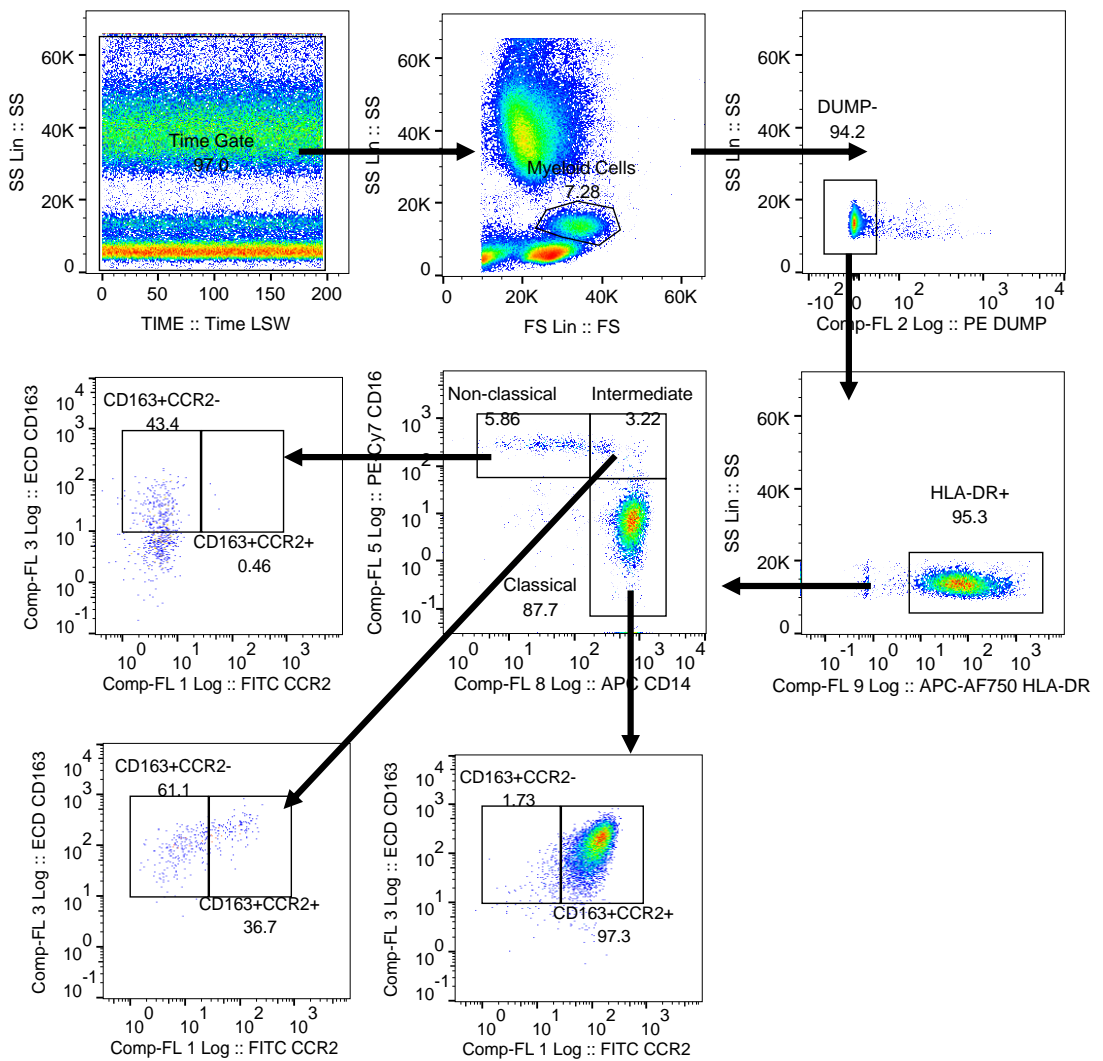


**Figure 2-3 Gating scheme for monocyte phenotypes in panel 3.** 100 $\mu$ L of blood was stained to characterise monocytes subsets. The experiment was analysed by gating on all cells across time, then isolating all myeloid cells based on their FS Lin/SS Lin profile followed by the gating out of all cells in the DUMP channel (CD3, CD19 B and CD56 NK cells). All HLA-DR+ cells were then gated to identify the classical, intermediate and non-classical monocyte subsets. The expression of CD163 and/or CCR2 was used to further categorise the three monocyte subsets.

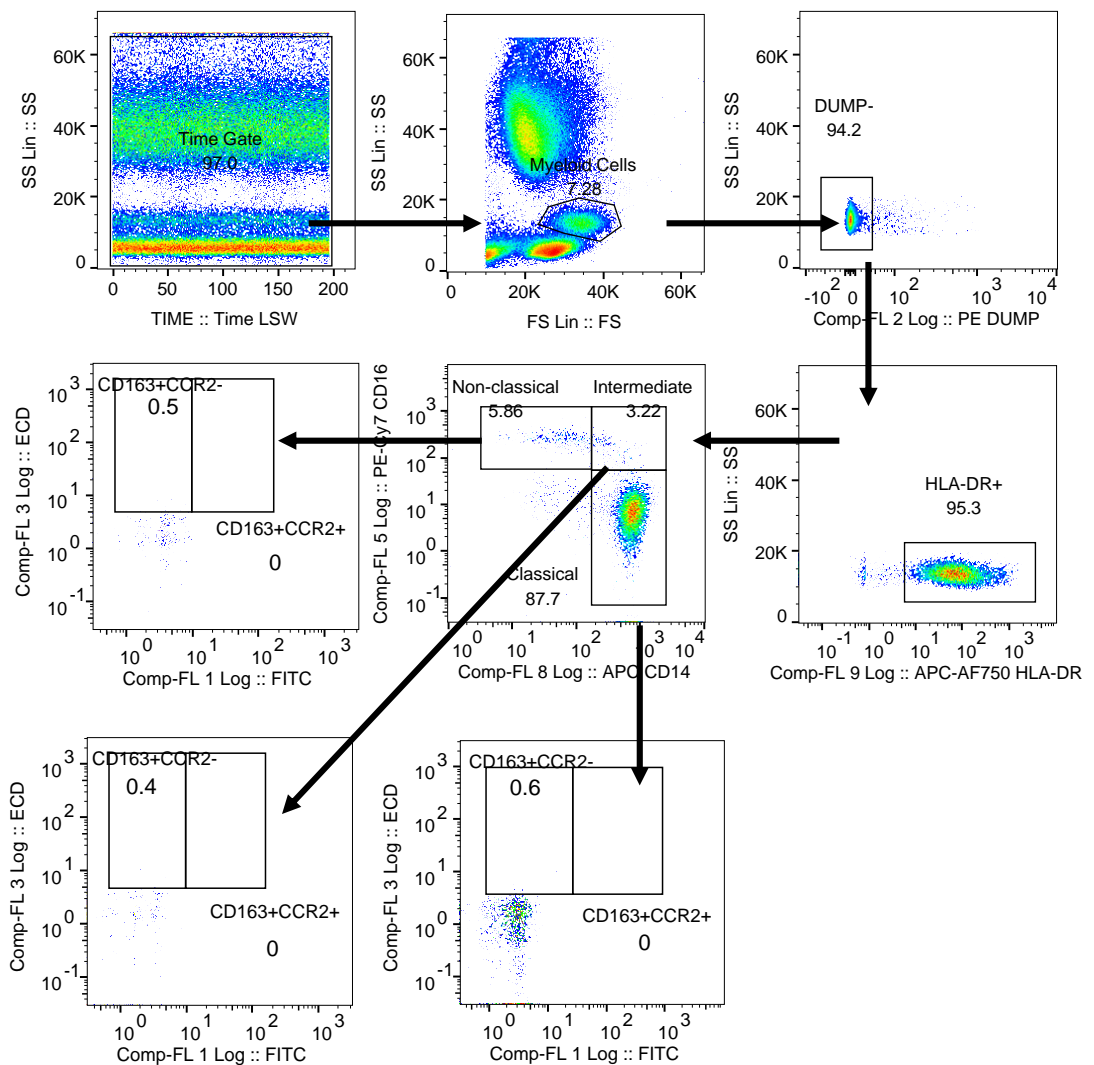


**Figure 2-4 Gating scheme for monocyte phenotypes in panel 4.** 100 $\mu$ L of blood was stained to characterise monocytes subsets. The experiment was analysed by gating on all cells across time, then isolating all myeloid cells based on their FS Lin/SS Lin profile followed by the gating out of all cells in the DUMP channel (CD3, CD19 B and CD56 NK cells). All HLA-DR+ cells were then gated to identify the classical, intermediate and non-classical monocyte subsets. The isotype control monoclonal antibodies were then used to set the gates for the CD163+CCR2- and CD163+CCR2+ cells.

### **2.3.2. Data concordance between analysts.**

Following the creation of analysis templates, all patient samples were analysed, and the relative frequencies and absolute numbers reported by two independent analysts, the PhD candidate (analyst 1) and a scientist at the Department for Cell and Tissue Engineering of the Montpellier University Hospital, France (analyst 2). To exclude bias, each analyst was blinded to the trial participants treatment arm and visit number. To assess gating accuracy, two-tailed Pearson correlation coefficients were computed for the frequency and absolute number values obtained by analyst 1 versus analyst 2. Discordant values were investigated, and consensus reached. In most cases, discordant values were either due to an error when transferring values between data analysis programmes or a misplaced gate in FlowJo. Once rectified, the resultant data showed good concordance for CD3, CD4, CD8+ T cell, Treg, Teff and NK cell frequency and number with significant correlations ( $p<0.0001$ ) observed between the two analysts as well as an  $R^2$  of >0.9 for all cell populations (figure 2-5 and 2-6).

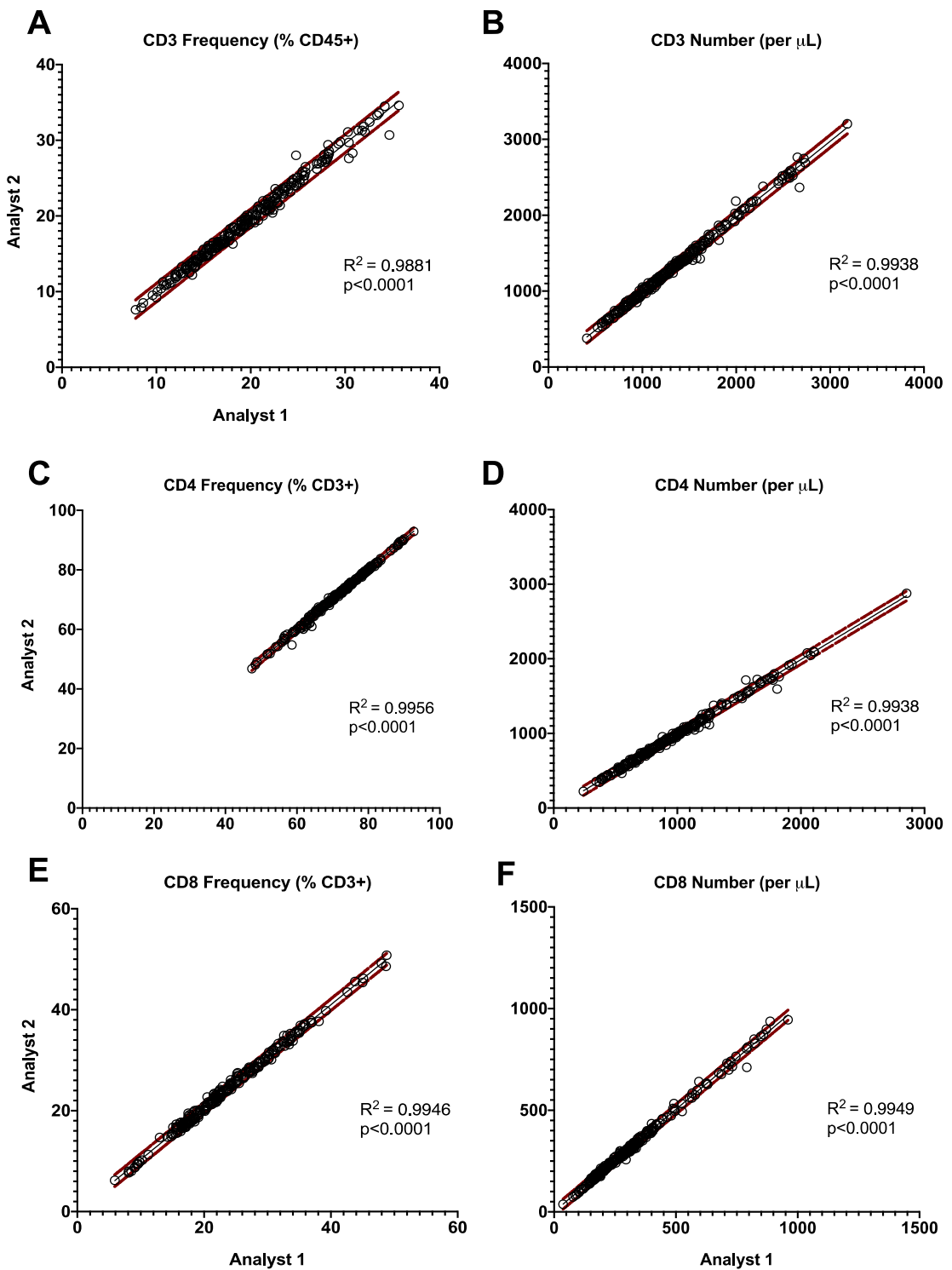


**Figure 2-5 Pearson correlation coefficient for CD3, CD4 and CD8 T cells between analyst 1 and 2.**

Panels A and B: relative frequency and absolute number of CD3 T cells. Panels C and D: relative frequency and absolute number of CD4 T cells. Panels E and F: relative frequency and absolute number of CD8 T cells. x-axis – analyst 1; y-axis – analyst 2. Brown dotted line – 95% prediction bands.

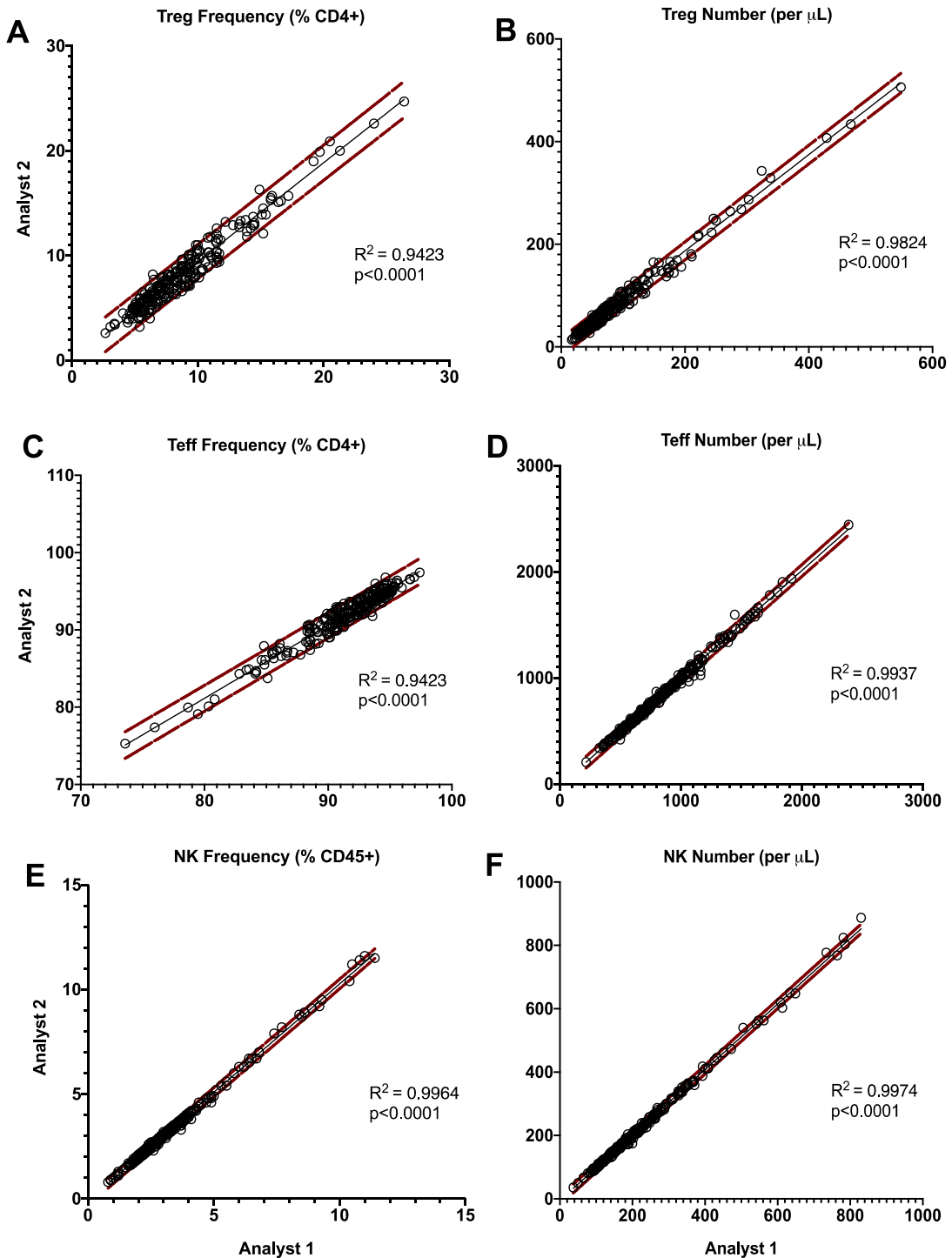


**Figure 2-6 Pearson correlation coefficient for Treg, Teff and NK cells between analyst 1 and 2.** Panels A and B: relative frequency and absolute number of Treg. Panels C and D: relative frequency and absolute number of Teff. Panels E and F: relative frequency and absolute number of NK cells. x-axis – analyst 1; y-axis – analyst 2. Brown dotted line – 95% prediction bands.

### 2.3.3. Significant increases in total lymphocytes, CD3<sup>+</sup> and CD4<sup>+</sup> T cells as a result of IL-2 therapy.

To analyse the flow cytometry results, we employed two analysis methods:

1. We used paired analysis to look at change in frequency or number in time within each treatment group, when compared to day 1 (figure 2-7 A).
2. We used unpaired statistics to compare the mean frequency or number between the three treatment groups, allowing us to not only assess whether the changes we see in treated are significantly different from those on placebo, but also to investigate any dose-dependent increases (figure 2-7 B).

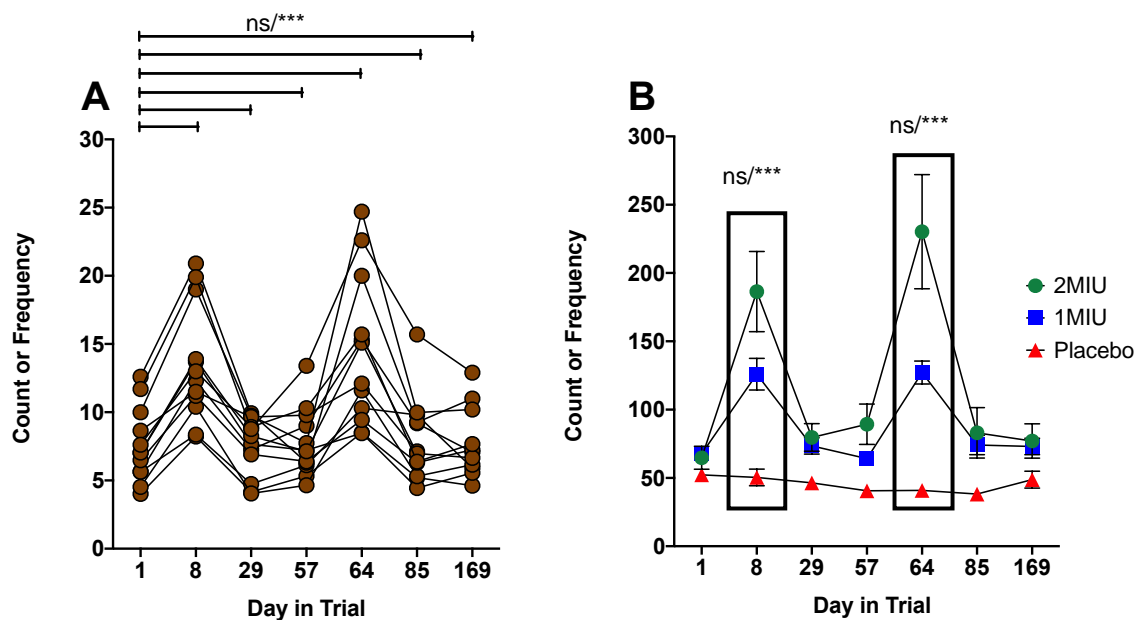


**Figure 2-7 Analysis methods used to investigate changes in immune cells after IL-2 therapy.** Panel A: Paired statistics were used to compare the frequency or number at each timepoint to day 1 within each treatment group. Panel B: Unpaired stats were used to assess whether the mean frequency or number was significantly different between groups at timepoints of interest. The significance levels in panel B are shown as an example, in the results section they are reported in the text and not shown on the graph.

Before addressing the main hypotheses of this chapter, we looked at whether IL-2 therapy had an effect on total lymphocytes, CD3<sup>+</sup> and CD4<sup>+</sup> T cells. As we expected IL-2 to expand Treg and non-Treg cells, we wanted to assess whether this resulted in greater numbers of their parent populations. Furthermore, we also wanted to confirm that any changes we see are a result of IL-2, therefore we also assessed the frequency and number of CD19<sup>+</sup> B cells across all timepoints, as we did not expect these cells to be expanded by IL-2.

There were significant increases in the total lymphocyte number at days 8 (2MIU p=0.0002; 1MIU p=0.0060) and 64 (2MIU p<0.0001; 1MIU p=0.0044) in patients receiving either dose of IL-2. At 2MIU IL-2, the number of total lymphocytes was also significantly greater at day 57 (p=0.0133) (figure 2-8 A-C). Group analysis shows that these increases are significantly different in placebo vs 2MIU (day 8 p=0.0031; day 57 p=0.0167; day 64 p=0.0006) and placebo vs 1MIU (day 8 p=0.0346). This analysis also showed that the number of totally lymphocytes was significantly greater at day 29 (p=0.0296), but not days 85 or 169 at 2MIU when compared to placebo (figure 2-8 D). These data show that IL-2 therapy led to an increase in the number of circulating lymphocytes in ALS patients and, this number remained greater three weeks after cycles 1 (day 29) and 2 (day 57) in those on 2MIU versus those on placebo.

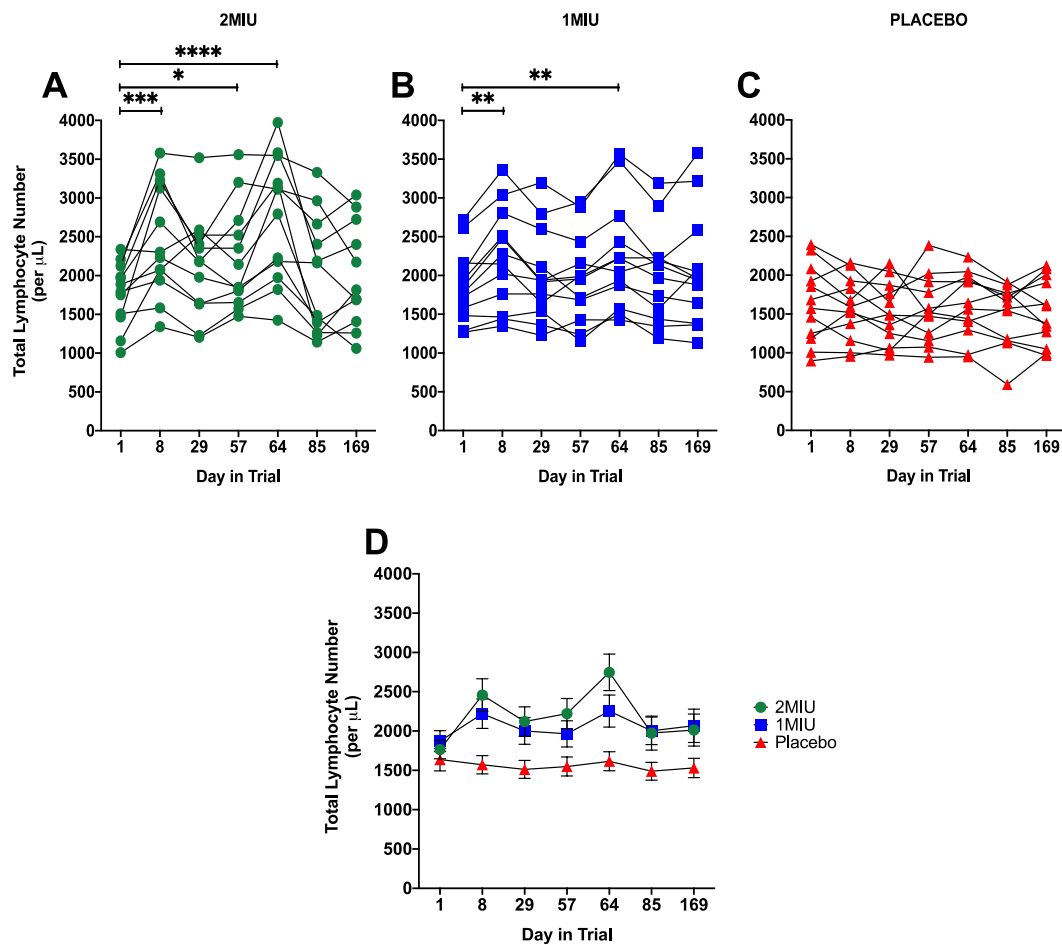


**Figure 2-8 the effects of LD-IL-2 on total lymphocyte number.** Panels A-C: total lymphocyte number (per  $\mu\text{L}$  of blood) for each individual participant at every trial visit. The lymphocyte number at each trial visit is compared to Day 1. Panel D: change in total lymphocyte number throughout the trial for all three treatment arms with data points indicating mean value and error bars indicating SEM. \*\*\*\*p<0.0001, \*\*\*p<0.001, \*\*p<0.01, \*p<0.05, by matched Friedman test with Dunn's multiple comparisons (A) or by matched repeated measures one-way ANOVA with Bonferroni's multiple comparisons test (B and C). Green circles – 2MIU; blue squares – 1MIU; red triangles – Placebo.

As expected, no significant changes were observed in B cell number or frequency in patients receiving either dose of IL-2. Interestingly, a reduction in the absolute number and the relative frequency of CD19 B cells was observed at day 85 in the placebo treated group (B cell frequency  $p=0.0109$ ; B cell number  $p=0.0020$ ) (figure 2-9 A-F). Group analysis shows no significant differences in B cell number between groups at any timepoint (figure 2-9 G and H).

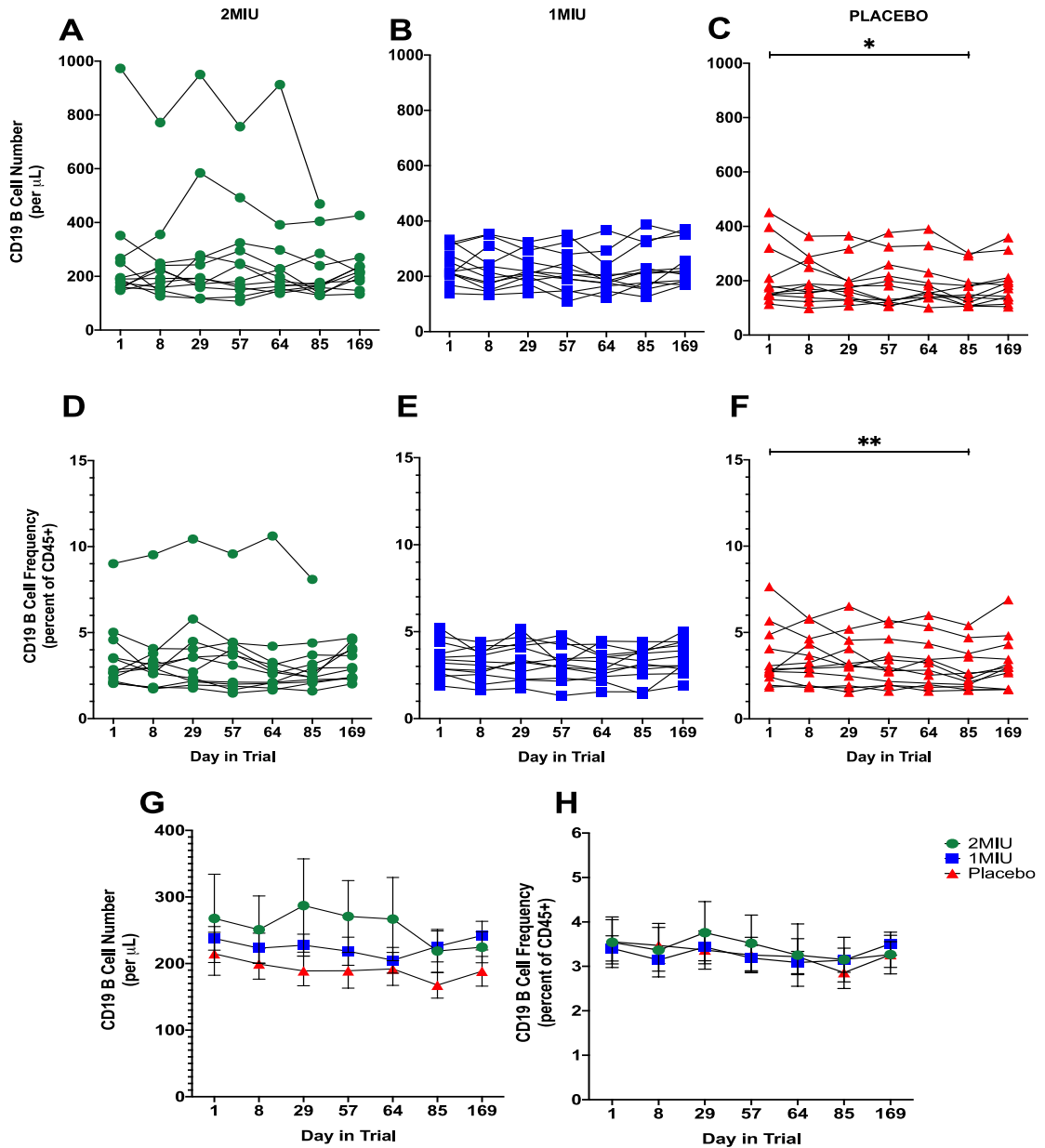


**Figure 2-9 the effects of LD-IL-2 on B cell number and frequency.** Panels A-F: B cell number (per  $\mu$ L of blood – A, B, C) and frequency (as percent of CD45+ cells – D, E, F) for each individual participant at every trial visit. B cell number and frequency at each trial visit is compared to Day 1. Panels G and H: change in B cell number (G) and frequency (H) throughout the trial for all three treatment arms with data points indicating mean value and error bars indicating SEM. \*\*p<0.01, \*p<0.05, by matched Friedman test with Dunn's multiple comparisons (A, B, C, F) or by matched repeated measures one-way ANOVA with Bonferroni's multiple comparisons test (D, E). Green circles – 2MIU; blue squares – 1MIU; red triangles – Placebo.

Within the total lymphocyte compartment, we observed significant increase in CD3<sup>+</sup>, and their daughter population, CD4<sup>+</sup> T cells (figure 2-10 and 2-11). For CD3<sup>+</sup> T cells, there were significant increases in number (day 8 2MIU p=0.0064 and 1MIU p=0.0042; day 64 2MIU p=0.0014 and 1MIU p=0.0038) and relative frequency (day 8 2MIU p=0.0003 and 1MIU p=0.0001; day 64 2MIU p=0.0077 and 1MIU p<0.0001) in both IL-2 treated groups. The frequency of CD3 T cells was also greater at day 29 (p=0.0420) at 2MIU IL-2. No significant changes were observed in the placebo treated individuals (figure 2-10 A-F). Group analysis showed that the increase in CD3 T cell number days 8 and 64 is significantly different in patients receiving 2MIU (p=0.0034 and p=0.0016) and 1MIU (p=0.0439 and p=0.0299) when compared to placebo but isn't significantly different between 2MIU and 1MIU. As with total lymphocytes, we also observed that the number of CD3<sup>+</sup> T cells remained significantly greater at days 29 (p=0.0250) and 57 (p=0.0215) in the 2MIU group when compared to placebo. While the increase in CD3 T cell frequency is only differs significantly between patients receiving 2MIU versus placebo (day 8 p=0.0218 and day 64 p=0.0291) (figure 2-10 G-H).

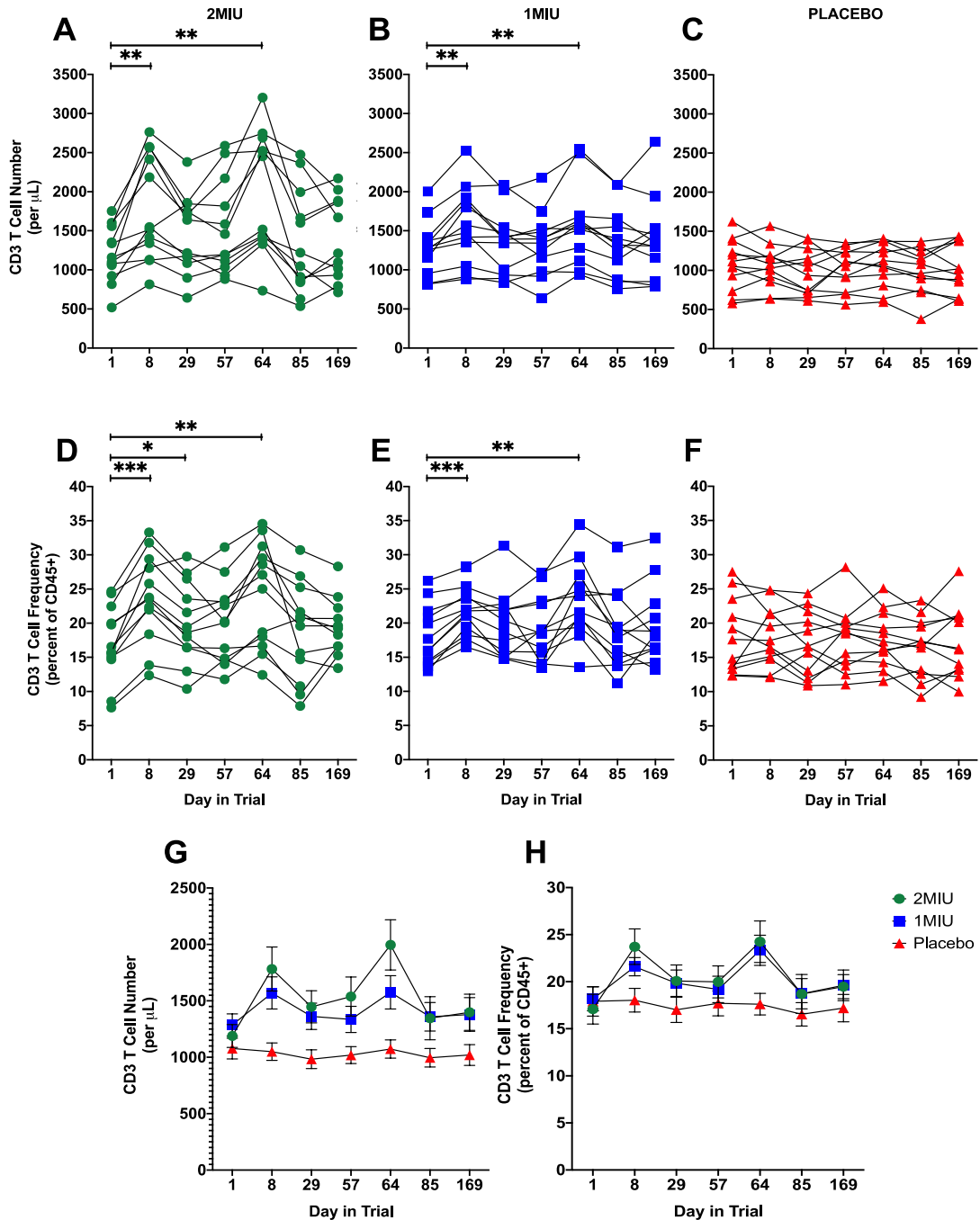


**Figure 2-10 the effects of LD-IL-2 on CD3 T cell number and frequency.** Panels A-F: CD3 T cell number (per  $\mu$ L of blood – A, B, C) and frequency (as percent of CD45+ cells – D, E, F) for each individual participant at every trial visit. CD3 T cell number and frequency at each trial visit is compared to Day 1. Panels G and H: change in CD3 T cell number (G) and frequency (H) throughout the trial for all three treatment arms with data points indicating mean value and error bars indicating SEM. \*\*\*p<0.001, \*\*p<0.01, \*p<0.05, by matched repeated measures one-way ANOVA with Bonferroni's multiple comparisons test. Green circles – 2MIU; blue squares – 1MIU; red triangles – Placebo.

Within the CD3<sup>+</sup> T cell compartment, there were significant increases in CD4<sup>+</sup> T cell number at days 8 (2MIU p=0.0028; 1MIU p=0.0009) and 64 (2MIU p=0.0015; 1MIU p<0.0001), and in frequency (day 8 2MIU p=0.0003 and 1MIU p=0.0017; day 64 2MIU p=<0.0001 and 1MIU p=0.0009). The frequency of CD4<sup>+</sup> T cells was also elevated at day 85 (p=0.0461) in the 1MIU group. There were no significant changes in CD4<sup>+</sup> T cell number or frequency in the placebo group (figure 2-11 A-F). The increase in CD4<sup>+</sup> T cell number at days 8 and 64 is significantly greater in 2MIU (p=0.0018 and p=0.0018) and 1MIU (p=0.0321 and p=0.0225) when compared to individuals in the placebo group, with no significant difference was observed between 2MIU and 1MIU groups. Once again, the number of CD4+ T cells remained significantly greater at days 29 (p=0.0203) and 57 (p=0.0166) in those on 2MIU when compared to those on placebo (figure 2-11 G). This shows that those treated with 2MIU had significantly greater numbers of CD4<sup>+</sup> T cells three weeks after the first and second cycle. There were no significant differences in the mean frequency of CD4<sup>+</sup> T cells between groups at any timepoint (figure 2-11 H).

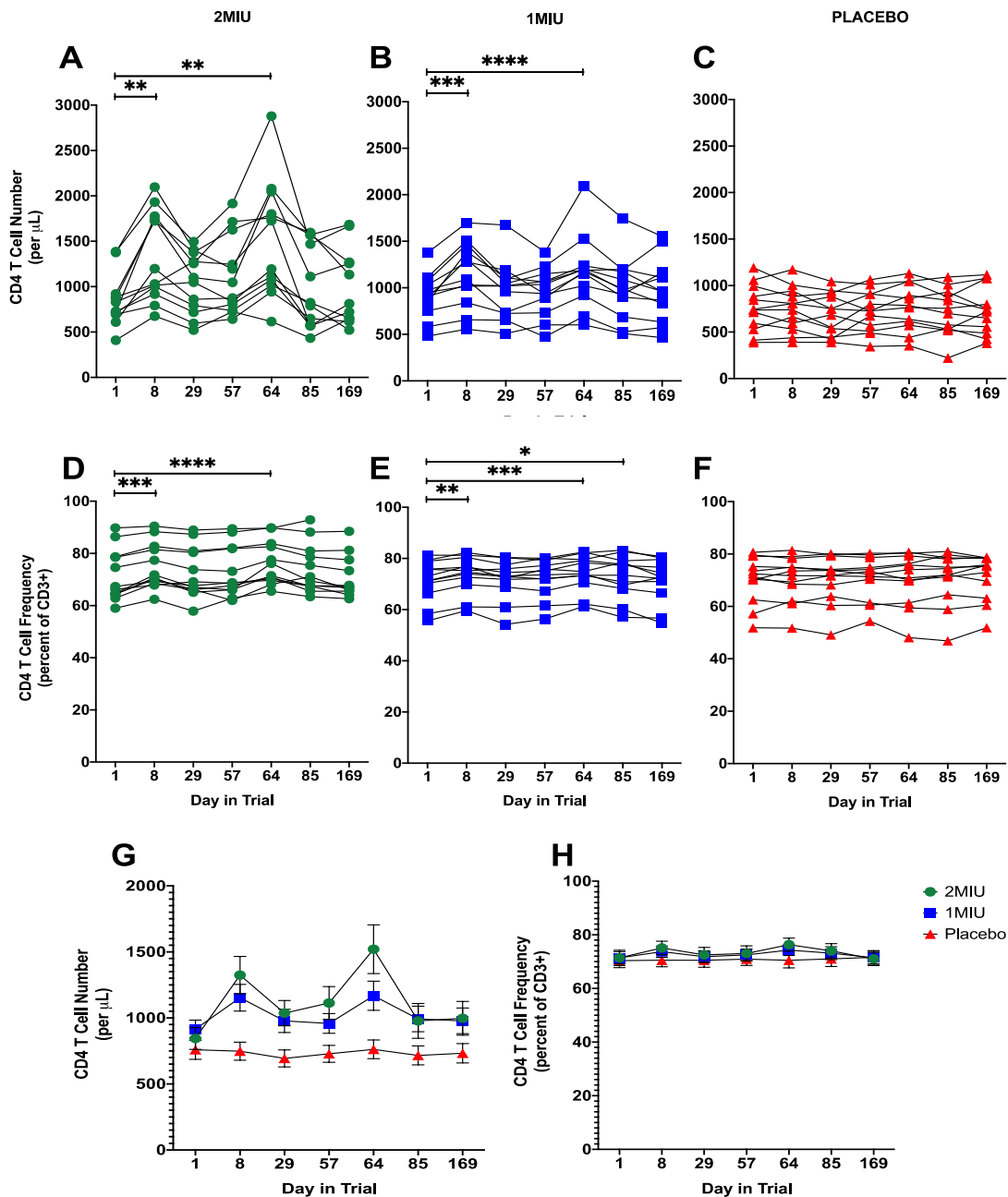


**Figure 2-11 the effects of LD-IL-2 on CD4 T cell number and frequency.** Panels A-F: CD4 T cell number (per  $\mu$ L of blood – A, B, C) and frequency (as percent of CD45+ cells – D, E, F) for each individual participant at every trial visit. CD4 T cell number and frequency at each trial visit is compared to Day 1. Panels G and H: change in CD4 T cell number (G) and frequency (H) throughout the trial for all three treatment arms with data points indicating mean value and error bars indicating SEM. \*\*\*\*p<0.0001, \*\*\*p<0.001, \*\*p<0.01, \*p<0.05, by matched Friedman test with Dunn's multiple comparisons (B, D, F) or by matched repeated measures one-way ANOVA with Bonferroni's multiple comparisons test (A, C, E). Green circles – 2MIU; blue squares – 1MIU; red triangles – Placebo.

### **2.3.4. Significant expansion of Treg by IL-2 in ALS patients.**

To address the first hypothesis of this chapter, we assessed changes in Treg number and frequency in all participants. The number of Treg was significantly greater at days 8 and 64 than day 1 in patients receiving either dose of IL-2 (2MIU day8 p=0.0001 and day 64 p<0.0001; 1MIU day 8 p=0.0004 and day 64 p=0.0002) (figure 2-12 A and B). Interestingly, Treg number at days 57 and 85 were significantly lower than day 1 in the placebo group (p=0.0053 and p=0.0135) (figure 2-11 C). Concurrently, relative Treg frequency was also greater at days 8 and 64 in the IL-2 treated groups (2MIU day 8 p=0.005 and day 64 p<0.0001; 1MIU day 8 p=0.0020 and day 64 p=0.0014) and lower at days 57, 64 and 85 (p=0.0057, p=0.0109 and p=0.0079) in the placebo group (figure 2-12 D, E and F). Group comparisons show the mean increase in Treg number at day 8 is significantly different at 2MIU (p<0.0001) and 1MIU (p=0.0186) when compared to placebo treated. Analysis of mean Treg number at day 64 show significantly greater number of Treg in the 2MIU when compared to placebo (p<0.0001) and also, a dose-dependent increase in 2MIU versus 1MIU (p=0.0176). Furthermore, the number of Treg is significantly greater at days 29, 57 and 85 in 1MIU vs placebo (p=0.0397; p=0.0252; p=0.0036) and 2MIU vs placebo (p=0.0087; p=0.0024; p=0.0353) (figure 2-12 G). Analysis of Treg frequency showed significant differences at days 8 and 64 between placebo and 2MIU (p<0.0001 and p<0.0001) and placebo and 1MIU (p=0.0035 and p=0.0010) (figure 2-12 H). These data indicate that IL-2 therapy significantly expanded Treg in both treated groups, this expansion was dose-dependent at day 64 and Treg of those on IL-2 remain at greater levels between cycles than those on placebo. We also observe that the mean Treg number is greater at day 64 (230.3 cells/ $\mu$ l) than day 8 (188.4

cells/ $\mu$ l), showing that the expansion increases with repeated cycles however, paired analysis did not show any significant difference in Treg number between these two timepoints.

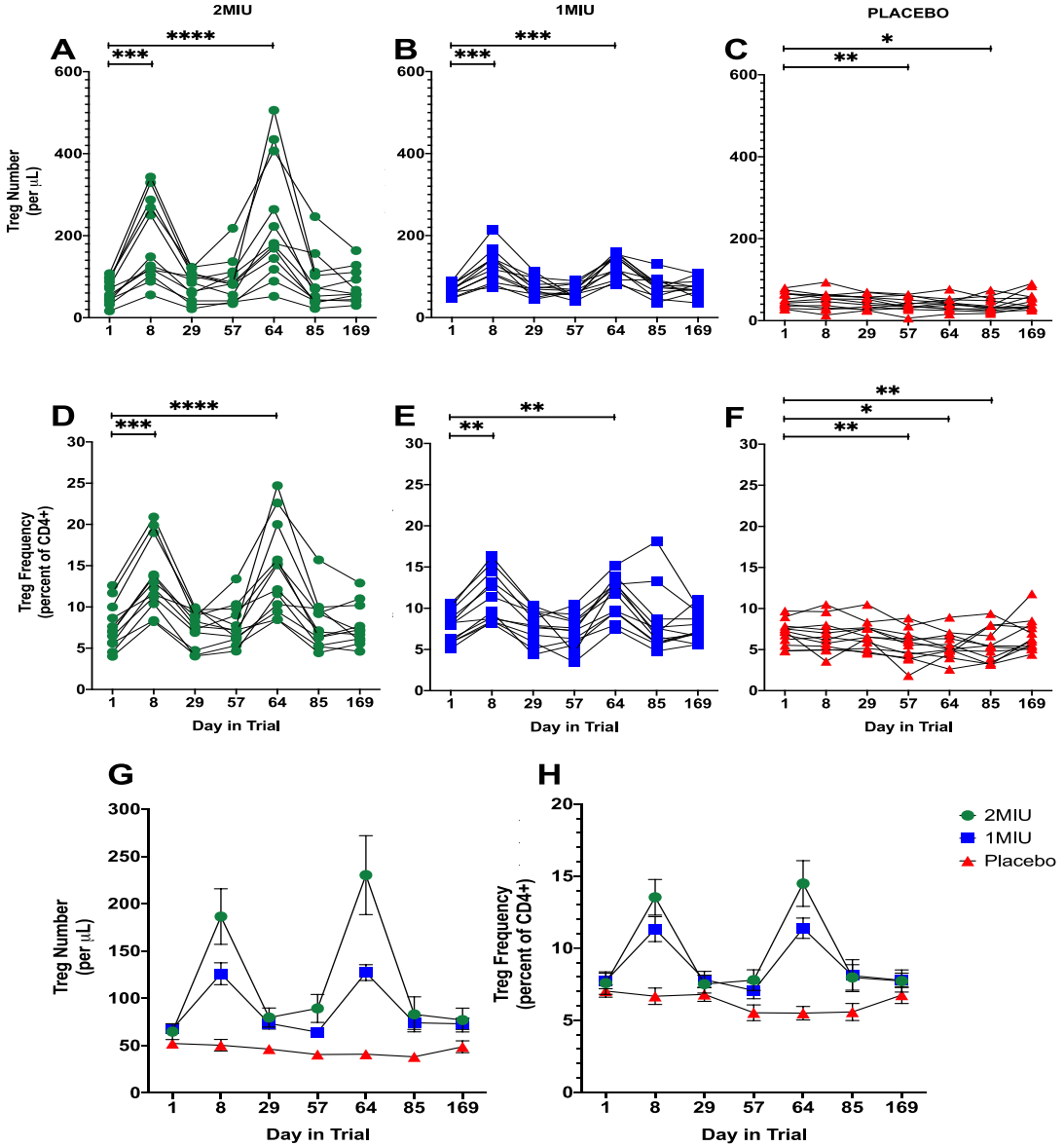


**Figure 2-12 the effects of LD-IL-2 on Treg cell number and frequency.** Panels A-F: Treg cell number (per  $\mu$ L of blood – A, B, C) and frequency (as percent of CD4+ cells – D, E, F) for each individual participant at every trial visit. Treg cell number and frequency at each trial visit is compared to Day 1. Panels G and H: change in Treg cell number (G) and frequency (H) throughout the trial for all three treatment arms with data points indicating mean value and error bars indicating SEM. \*\*\*\* $p<0.0001$ , \*\*\* $p<0.001$ , \*\* $p<0.01$ , \* $p<0.05$ , by matched Friedman test with Dunn's multiple comparisons (A, D, E, F) or by matched repeated measures one-way ANOVA with Bonferroni's multiple comparisons test (B and C). Green circles – 2MIU; blue squares – 1MIU; red triangles – Placebo.

### **2.3.5. IL-2 therapy expanded non-Treg cells bearing the IL-2R subunits.**

The second hypothesis of this chapter was to assess the effects of IL-2 therapy on non-Treg cells in ALS. We observe expansion of Teff, CD8<sup>+</sup> T cells, NK cells and their subsets. The expansion of CD8 and NK cells has been reported to be associated with increased cytotoxicity in other trials and we also wanted to investigate these as part of our safety assessment. We observed significant increases in Teff number in both IL-2 treated groups (2MIU day 8 p=0.0038 and day 64 p=0.0001; 1MIU day 8 p=0.0095 and day 64 p=0.0007). There were no significant changes observed in Teff number in the placebo group (figure 2-13 A to C). The observed changes in Teff number at days 8 and 64 are significantly different in the 2MIU (p=0.0140 and p=0.066) and only at day 8 in 1MIU (p=0.0416) when compared to the placebo group (figure 2-13 D). There was also a significant increase in CD8<sup>+</sup> T cell number at 2MIU IL-2 at days 8 and 64 (p=0.0095 and p=0.0343). Conversely, a reduction in CD8<sup>+</sup> T cell frequency was observed at days 8, 29, 64 and 85 in patients receiving 2MIU IL-2 (p=0.0002, p=0.477, p=0.0003 and p=0.0113 respectively) and at days 8, 64 and 85 in those receiving 1MIU IL-2 (p=0.0009, p=0.0002 and p=0.0262 respectively). There were no significant changes in the number of CD8<sup>+</sup> T cells in the 1MIU group nor in the number or frequency in the placebo group (figure 2-14 A-F). There were also no significant differences between groups (figure 2-14 G and H).

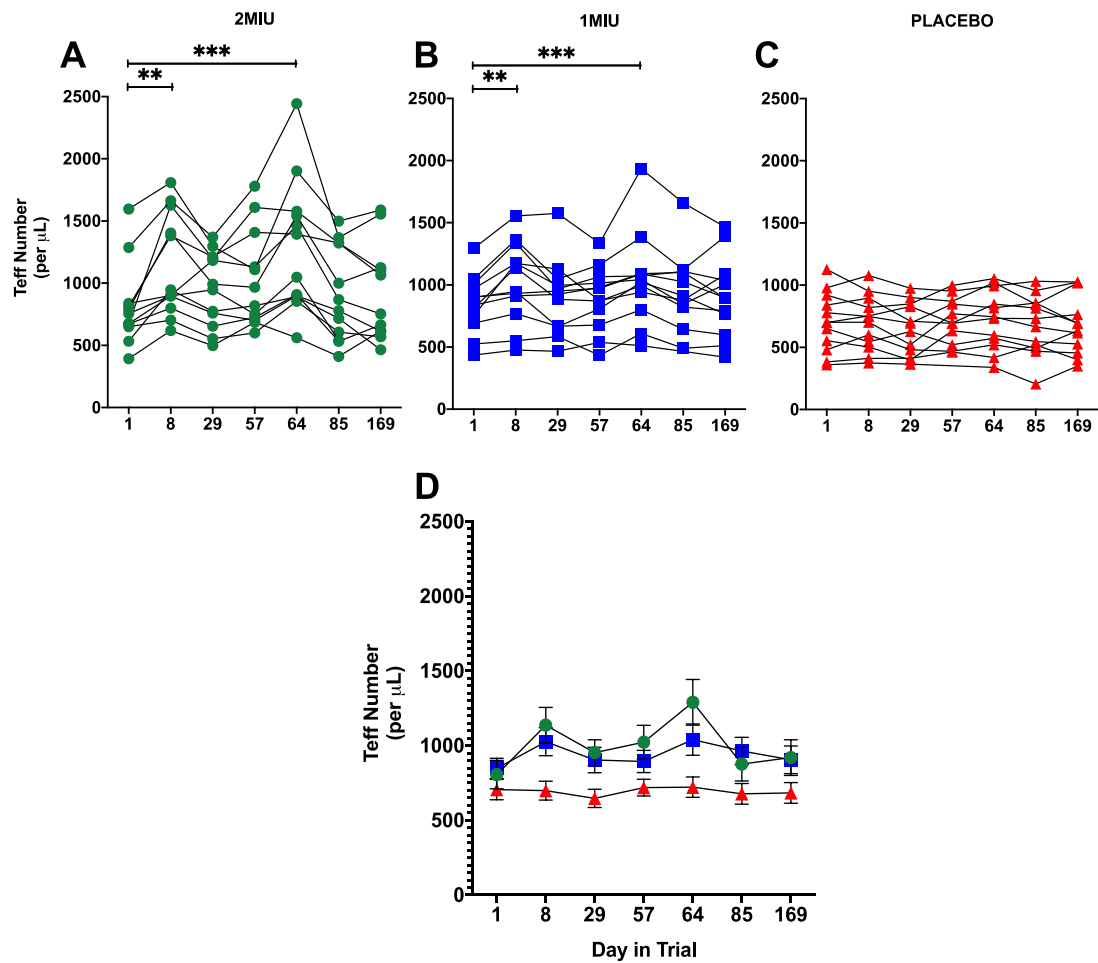


**Figure 2-13 the effects of LD-IL-2 on Teff cell number and frequency.** Panels A-F: Teff cell number (per  $\mu\text{L}$  of blood – A, B, C) and frequency (as percent of CD4+ cells – D, E, F) for each individual participant at every trial visit. Teff cell number and frequency at each trial visit is compared to Day 1. Panels G and H: change in Teff cell number (G) and frequency (H) throughout the trial for all three treatment arms with data points indicating mean value and error bars indicating SEM. \*\*\*\*p<0.0001, \*\*\*p<0.001, \*\*p<0.01, \*p<0.05, by matched Friedman test with Dunn's multiple comparisons (A, B, E) or by matched repeated measures one-way ANOVA with Bonferroni's multiple comparisons test (C, E, F). Green circles – 2MIU; blue squares – 1MIU; red triangles – Placebo.

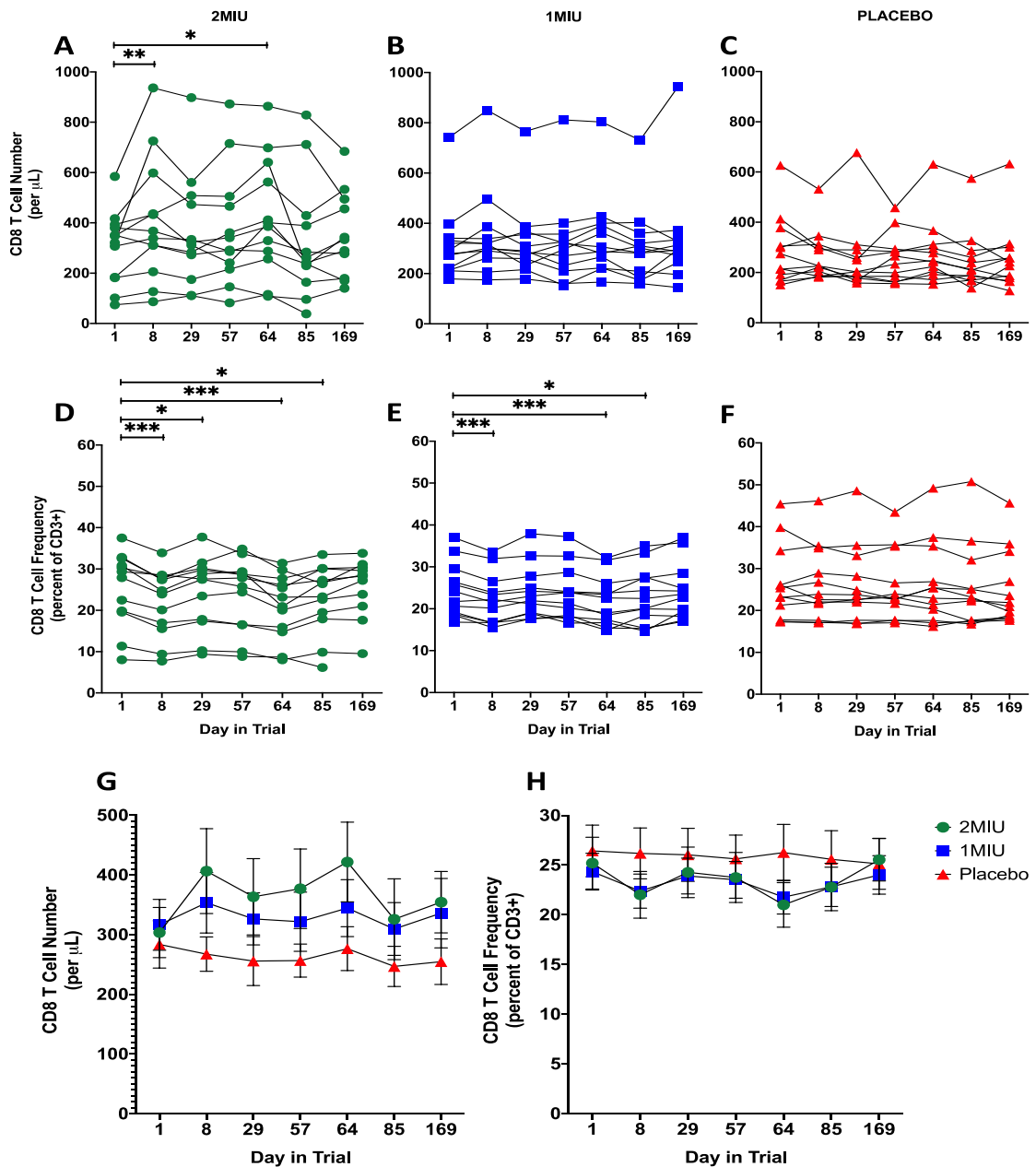


**Figure 2-14 the effects of LD-IL-2 on CD8 T cell number and frequency.** Panels A-F: CD8 T cell number (per  $\mu$ L of blood – A, B, C) and frequency (as percent of CD4+ cells – D, E, F) for each individual participant at every trial visit. CD8 T cell number and frequency at each trial visit is compared to Day 1. Panels G and H: change in CD8 T cell number (G) and frequency (H) throughout the trial for all three treatment arms with data points indicating mean value and error bars indicating SEM. \*\*\* $p < 0.001$ , \*\* $p < 0.01$ , \* $p < 0.05$ , by matched Friedman test with Dunn's multiple comparisons (A, B, C, F) or by matched repeated measures one-way ANOVA with Bonferroni's multiple comparisons test (D, E). Green circles – 2MIU; blue squares – 1MIU; red triangles – Placebo.

There was also an expansion in total CD56<sup>+</sup> NK cells. Significant increases were observed at days 8 and 64 in the number (2MIU p=0.0001 and p=0.0002; 1MIU p=0.0204 and p=0.0275) and frequency (2MIU p=0.0023 and p=0.0051; 1MIU p=0.0040 and p=0.0014) of CD56<sup>+</sup> NK cells. The number of CD56<sup>+</sup> NK cells was also significantly greater at days 29 (p=0.0296) and 57 (p=0.0080) in the 2MIU IL-2 group. No significant changes in number or frequency were seen in the placebo group (figure 2-15 A-F). The observed changes are significantly different between 2MIU and placebo (count at day8 p=0.0097 and day 64 p=0.0178) and 1MIU and placebo (count at day8 p=0.0149 and day 64 p=0.0463; frequency at day 64 p=0.0316) but not between 2MIU and 1MIU groups (figure 2-15 G and H).

As for NK subsets, significant increases from day 1 were observed in the CD56<sup>bright</sup> NK cell number at days 8 and 64 in both treated groups (2MIU day 8 p=0.0003 and day 64 p=0.0095; 1MIU day 8 p=0.0275 and day 64 p=0.0079). The relative frequency of CD56<sup>bright</sup> NK cells was only significantly greater at days 8 and 64 (p=0.0057, p=0.0028) in the 1MIU group, with no significant changes seen in the 2MIU or placebo group (figure 2-16 A-F). Group analysis shows that these increases are significantly different between 2MIU and placebo (counts at day8 p<0.0001 and day 64 p=0.0008; frequencies at day 8 p=0.0028 and day 64 p=0.0225) and 1MIU and placebo (counts at day8 p=0.0003; day 29 p=0.0267 and day 64 p=0.0001; frequency at day8 p=0.0267 and day 64 p=0.0051) but not between 2MIU and 1MIU groups (figure 2-16 G and H).

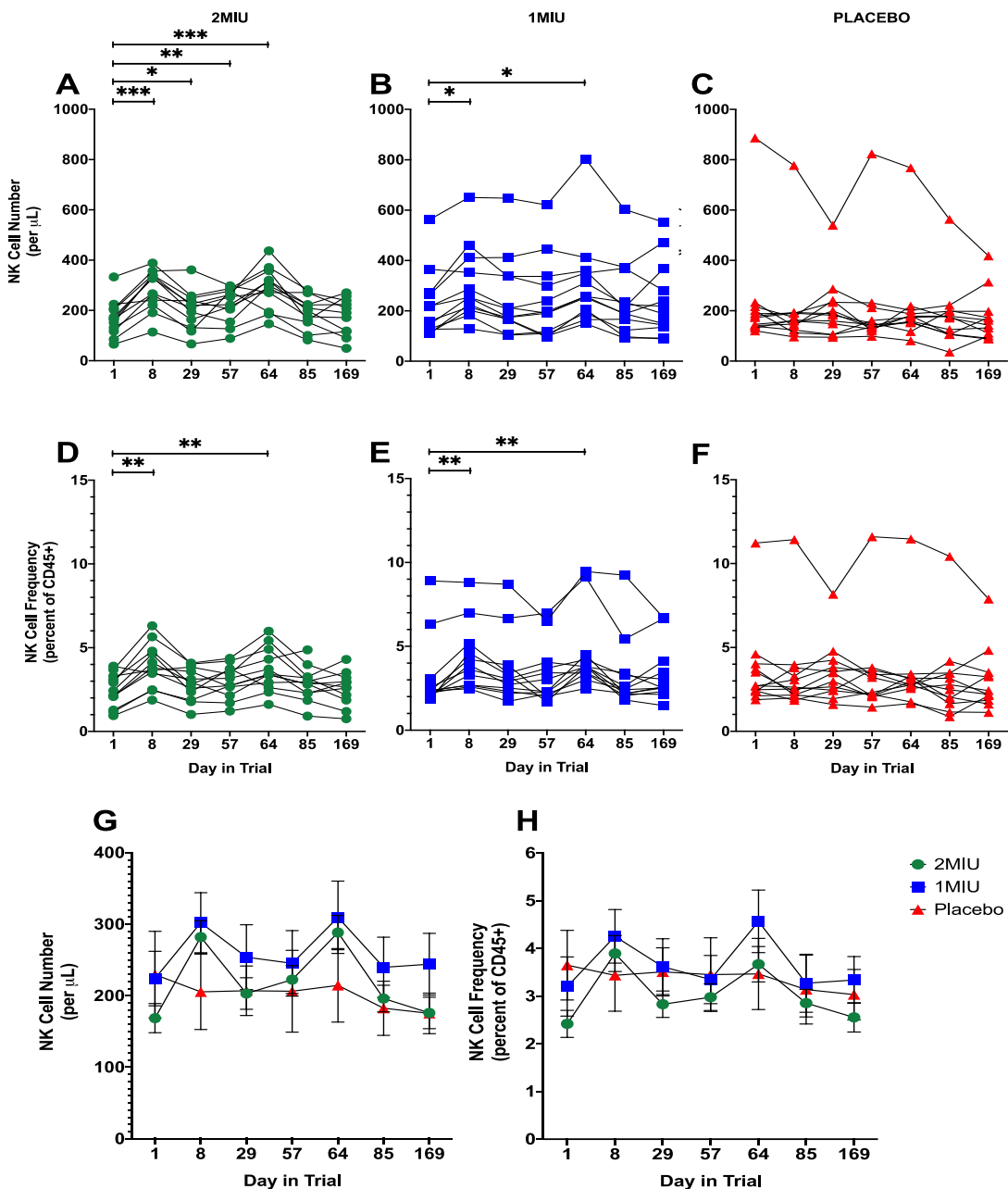


**Figure 2-15 the effects of LD-IL-2 on NK cell number and frequency.** Panels A-F: NK cell number (per  $\mu$ L of blood – A, B, C) and frequency (as percent of CD45+ cells – D, E, F) for each individual participant at every trial visit. NK cell number and frequency at each trial visit is compared to Day 1. Panels G and H: change in NK cell number (G) and frequency (H) throughout the trial for all three treatment arms with data points indicating mean value and error bars indicating SEM. \*\*\* $p<0.001$ , \*\* $p<0.01$ , \* $p<0.05$ , by matched Friedman test with Dunn's multiple comparisons (B, C, E, F) or by matched repeated measures one-way ANOVA with Bonferroni's multiple comparisons test (A, D). Green circles – 2MIU; blue squares – 1MIU; red triangles – Placebo.

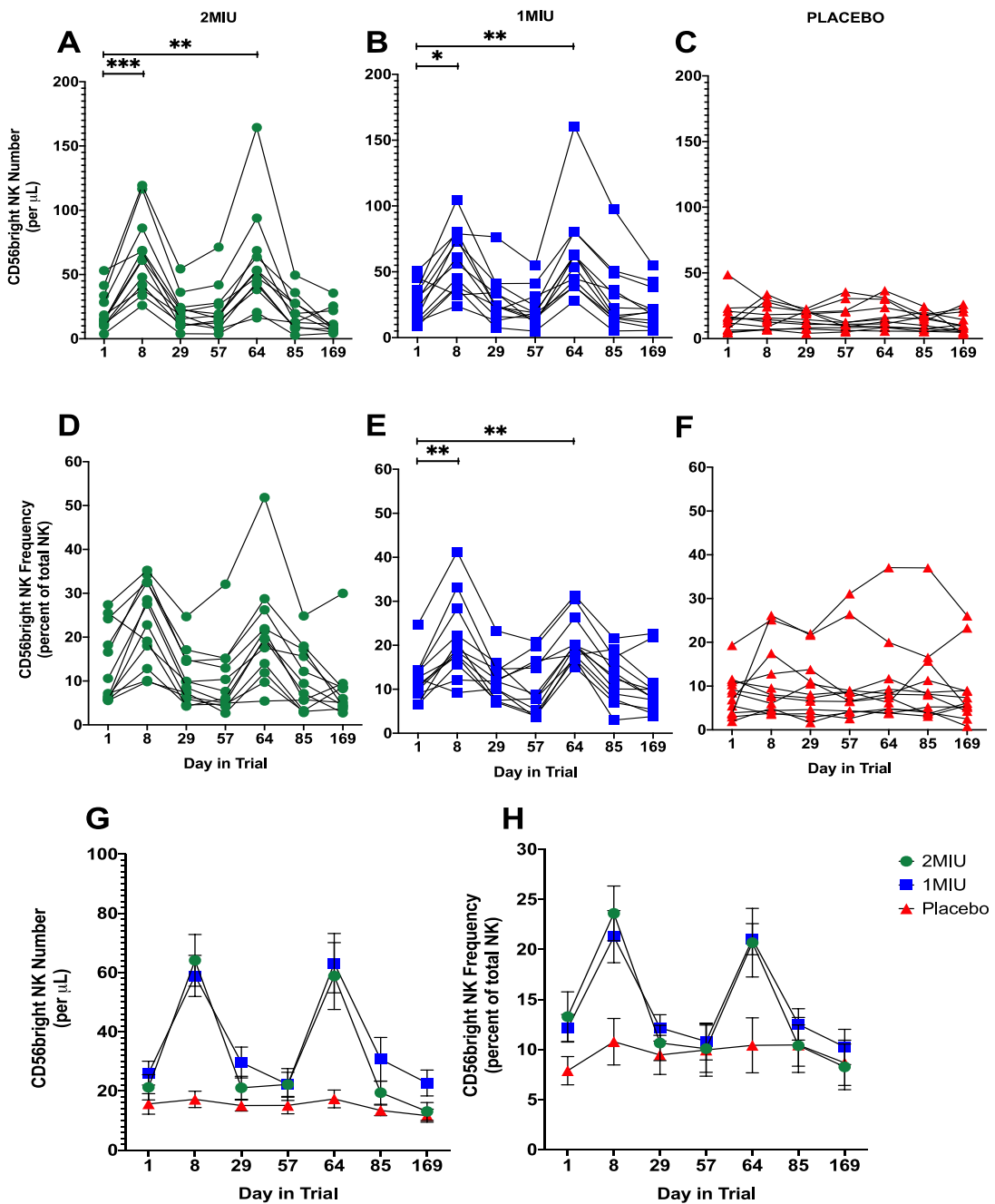


**Figure 2-16 the effects of LD-IL-2 on CD56bright NK cell number and frequency.** Panels A-F: CD56bright NK cell number (per  $\mu$ L of blood – A, B, C) and frequency (as percent of all NK cells – D, E, F) for each individual participant at every trial visit. CD56bright NK cell number and frequency at each trial visit is compared to Day 1. Panels G and H: change in CD56bright NK cell number (G) and frequency (H) throughout the trial for all three treatment arms with data points indicating mean value and error bars indicating SEM. \*\*\* $p$ <0.001, \*\* $p$ <0.01, \* $p$ <0.05, by matched Friedman test with Dunn's multiple comparisons. Green circles – 2MIU; blue squares – 1MIU; red triangles – Placebo.

When investigating the CD56<sup>dim</sup>CD16<sup>+</sup> subset of NK cells, only at 2MIU was there a significant increase in the absolute number at days 8 (p=0.007), 64 (p=0.0027) and 57 (p=0.0148) (figure 2-17 A-C). No significant differences are observed at these timepoints when compared to the other two treatment groups (figure 2-17 D).

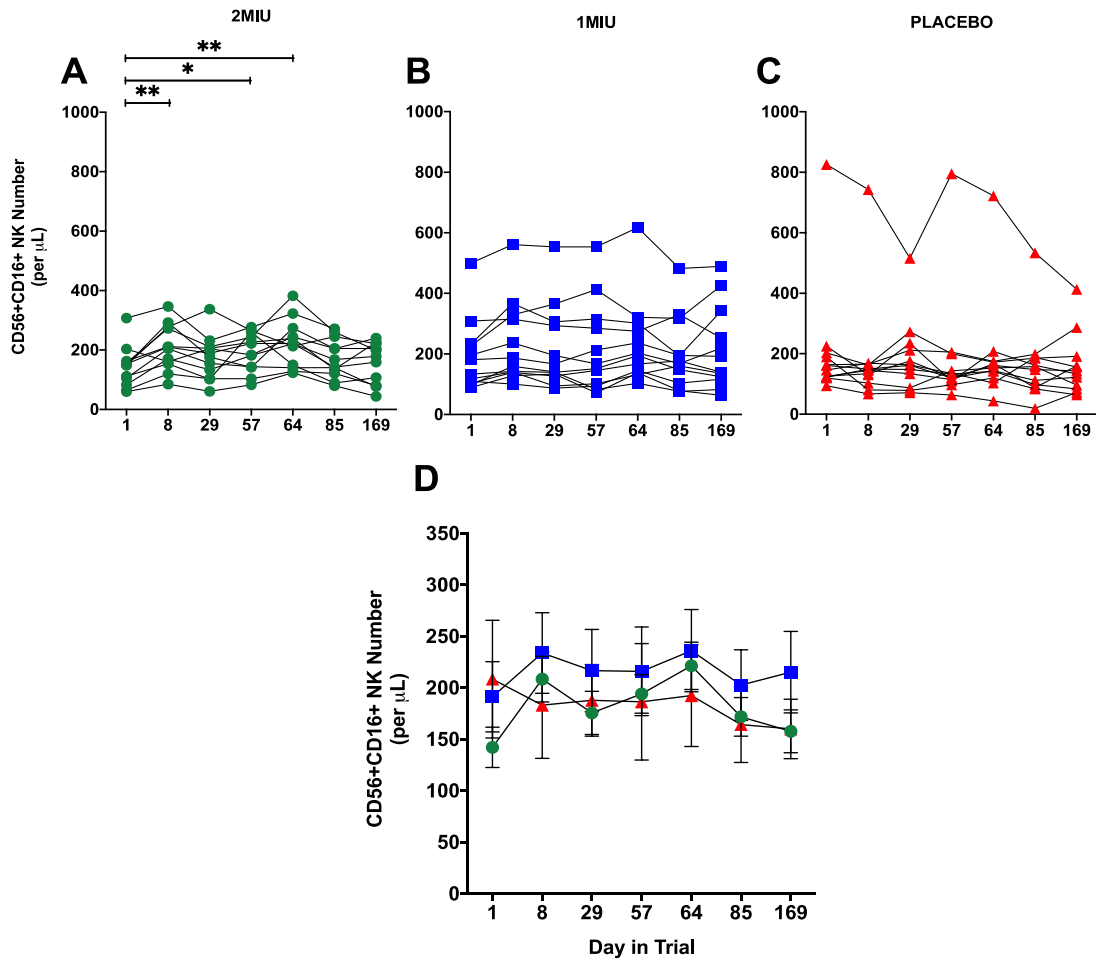


**Figure 2-17 the effects of LD-IL-2 on CD56+CD16+ NK cell number and frequency.** Panels A-C: CD56+CD16+ NK cell number (per  $\mu$ L of blood) for each individual participant at every trial visit. CD56+CD16+ NK cell number and frequency at each trial visit is compared to Day 1. Panel D: change in CD56+CD16+ NK cell number throughout the trial for all three treatment arms with data points indicating mean value and error bars indicating SEM. \*\*p<0.01, \*p<0.05, by matched Friedman test with Dunn's multiple comparisons (B, C) or by matched repeated measures one way ANOVA with Bonferroni's multiple comparisons test (A). Green circles – 2MIU; blue squares – 1MIU; red triangles – Placebo.

### **2.3.6. Reduced numbers and frequencies of monocyte subsets at the height of IL-2 therapy.**

The final hypothesis of this chapter was to assess the effects of IL-2 therapy on monocyte subsets. There were no significant changes in total monocyte number in any of the groups. There was, however, a significant decrease in the total monocyte frequency at day 64 ( $p=0.0399$ ) in 2MIU IL-2, while in the 1MIU IL-2 group a significant increase was observed at day 8 ( $p=0.0113$ ) when compared to day 1, and no change significant changes in the frequencies of placebo participants (figure 2-18 A-H). We observed a small but significant increase in the frequency of classical monocytes at days 29, 57 and 64 ( $p=0.0133$ ,  $p=0.0295$ ,  $p=0.0003$ ) in the 2MIU IL-2 group, with no other significant change in number or frequency in the other two groups (figure 2-19 A-H). As for the intermediate monocytes, there was a significant reduction in the absolute number at day 64 ( $p=0.0003$ ) in the 2MIU group when compared to day 1. No significant changes were observed in the 1MIU or placebo groups. Group analysis shows the reduction in the 2MIU group was significantly different from placebo at this day ( $p=0.0334$ ) (figure 2-20 A-H). Having observed this decrease in those treated with IL-2, we went on to assess whether there was a change CCR2<sup>+</sup> or CD163<sup>+</sup> subsets, as detailed in figure 2-3. However, we did not observe any significant changes in the number or frequency of CCR2<sup>+</sup> or CD163<sup>+</sup> intermediate monocytes (data not shown).

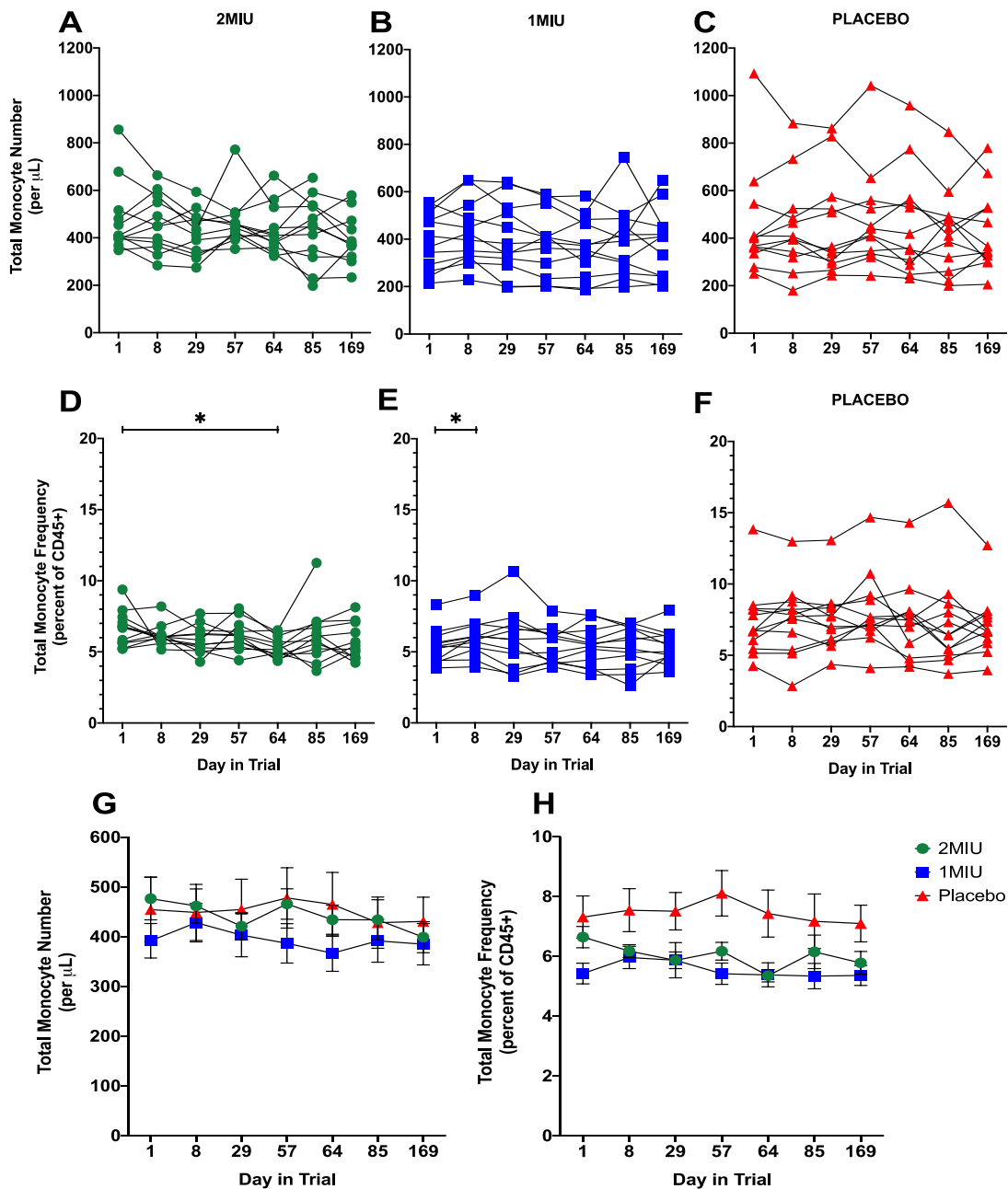


**Figure 2-18 The effects of LD-IL-2 on total monocyte cell number and frequency.** Panels A-F: total monocyte number (per  $\mu\text{L}$  of blood – A, B, C) and frequency (as percent of CD45+ cells – D, E, F) for each individual participant at every trial visit. Total monocyte cell number and frequency at each trial visit is compared to Day 1. Panels G and H: change in total monocyte cell number (G) and frequency (H) throughout the trial for all three treatment arms with data points indicating mean value and error bars indicating SEM. \* $p<0.05$ , by matched Friedman test with Dunn's multiple comparisons (A, C, F) or by matched repeated measures one-way ANOVA with Bonferroni's multiple comparisons test (B, D, E). Green circles – 2MIU; blue squares – 1MIU; red triangles – Placebo.

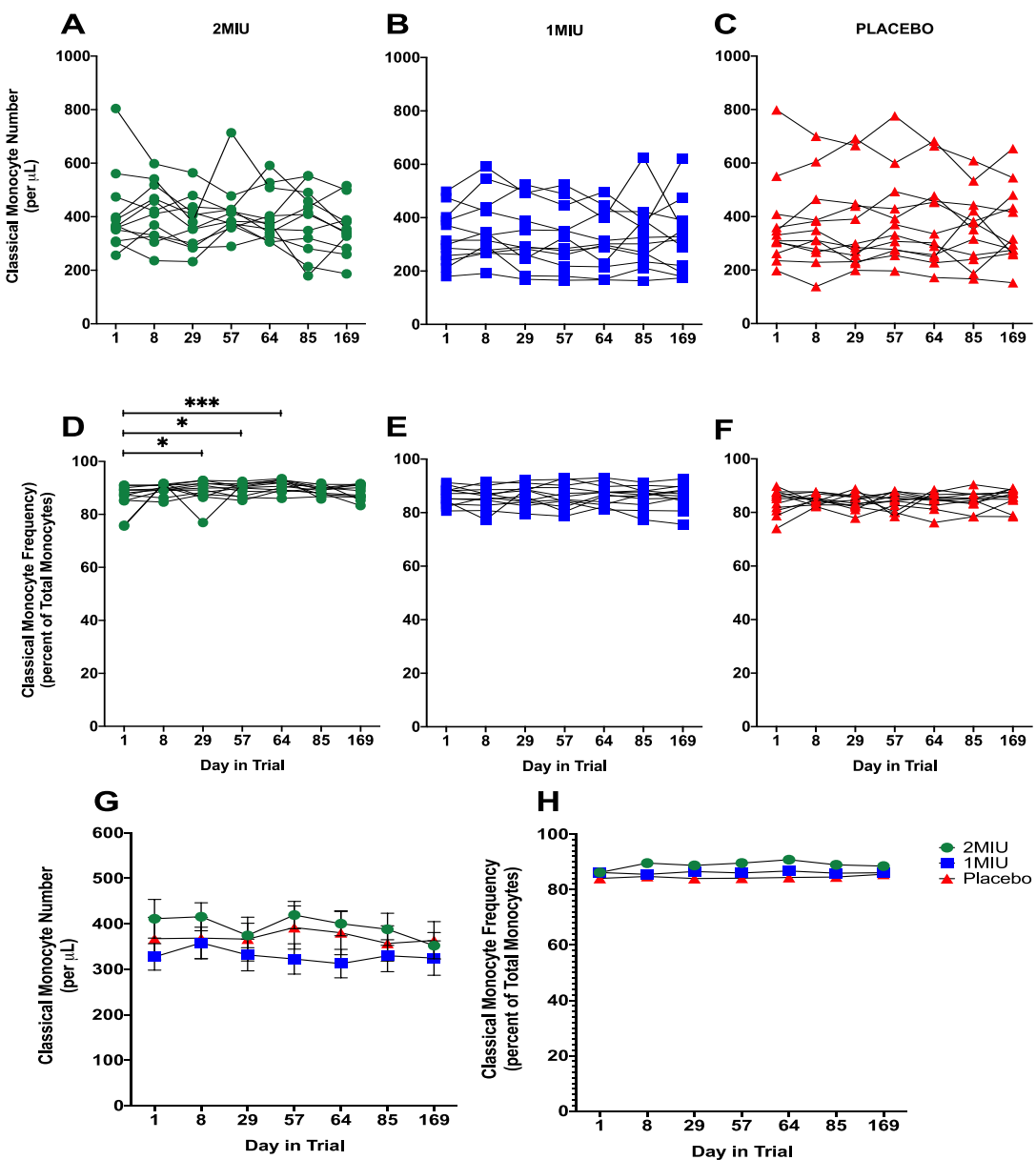


**Figure 2-19 the effects of LD-IL-2 on classical monocyte cell number and frequency.** Panels A-F: classical monocyte number (per  $\mu$ L of blood – A, B, C) and frequency (as percent of all monocytes – D, E, F) for each individual participant at every trial visit. Classical monocyte cell number and frequency at each trial visit is compared to Day 1. Panels G and H: change in classical monocyte cell number (G) and frequency (H) throughout the trial for all three treatment arms with data points indicating mean value and error bars indicating SEM. \*\*\* $p$ <0.001, \*\* $p$ <0.01, \* $p$ <0.05, by matched Friedman test with Dunn's multiple comparisons (A, C, D, F) or by matched repeated measures one-way ANOVA with Bonferroni's multiple comparisons test (B, E). Green circles – 2MIU; blue squares – 1MIU; red triangles – Placebo.

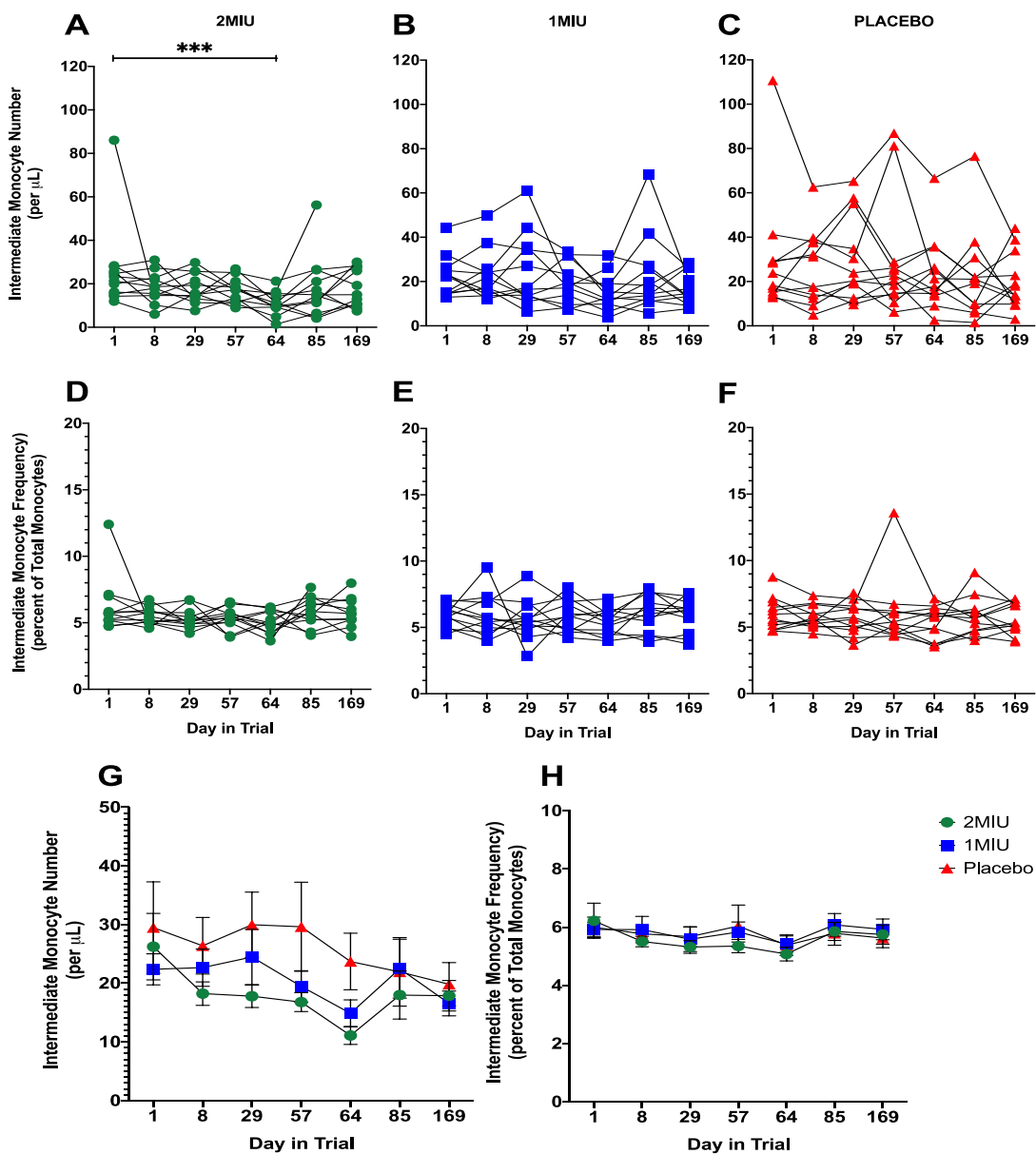


**Figure 2-20 the effects of LD-IL-2 on intermediate monocyte cell number and frequency.** Panels A-F: intermediate monocyte number (per  $\mu$ L of blood – A, B, C) and frequency (as percent of all monocytes – D, E, F) for each individual participant at every trial visit. Intermediate monocyte cell number and frequency at each trial visit is compared to Day 1. Panels G and H: change in intermediate monocyte cell number (G) and frequency (H) throughout the trial for all three treatment arms with data points indicating mean value and error bars indicating SEM. \*\*\* $p<0.001$ , by matched Friedman test with Dunn's multiple comparisons (A, B, C, D, F) or by matched repeated measures one-way ANOVA with Bonferroni's multiple comparisons test (E). Green circles – 2MIU; blue squares – 1MIU; red triangles – Placebo.

As for non-classical monocytes, there was a significant reduction in the absolute number in participants in the 2MIU IL-2 group at day 64 ( $p=0.0133$ ). While the relative frequency is significantly lower at days 29 ( $p=0.0216$ ), 57 ( $p=0.0253$ ), 64 ( $p=0.0007$ ) and 85 ( $p=0.0113$ ) in this group when compared to day 1. There were no significant changes in the number or frequency of these cells in the 1MIU or placebo groups (figure 2-21 A-F). Group analysis shows that in the 2MIU IL-2 group, the reductions in number of non-classical monocytes are significantly lower when compared to placebo at days 8 ( $p=0.0275$ ), 29 ( $p=0.0245$ ) and 64 ( $p=0.0005$ ) (figure 2-21 G). This is also reflected when the mean frequencies are compared between groups. In 2MIU, when compared to placebo, the frequency of non-classical monocytes is significantly lower at days 8 ( $p=0.0014$ ), 29 ( $p=0.0026$ ), 57 ( $p=0.0017$ ), 64 ( $p=0.0005$ ) and 85 ( $p=0.0015$ ). Group analysis also showed a dose-dependent decrease in this subset's frequency at 2MIU when compared to 1MIU at days 8 ( $p=0.0200$ ) and 64 ( $p=0.0373$ ) (figure 2-21 H). Having observed a significant effect of IL-2 therapy on alternative monocytes, as was done on intermediate monocytes, we assessed whether there was a change in subsets expressing CD163 and/or CCR2.

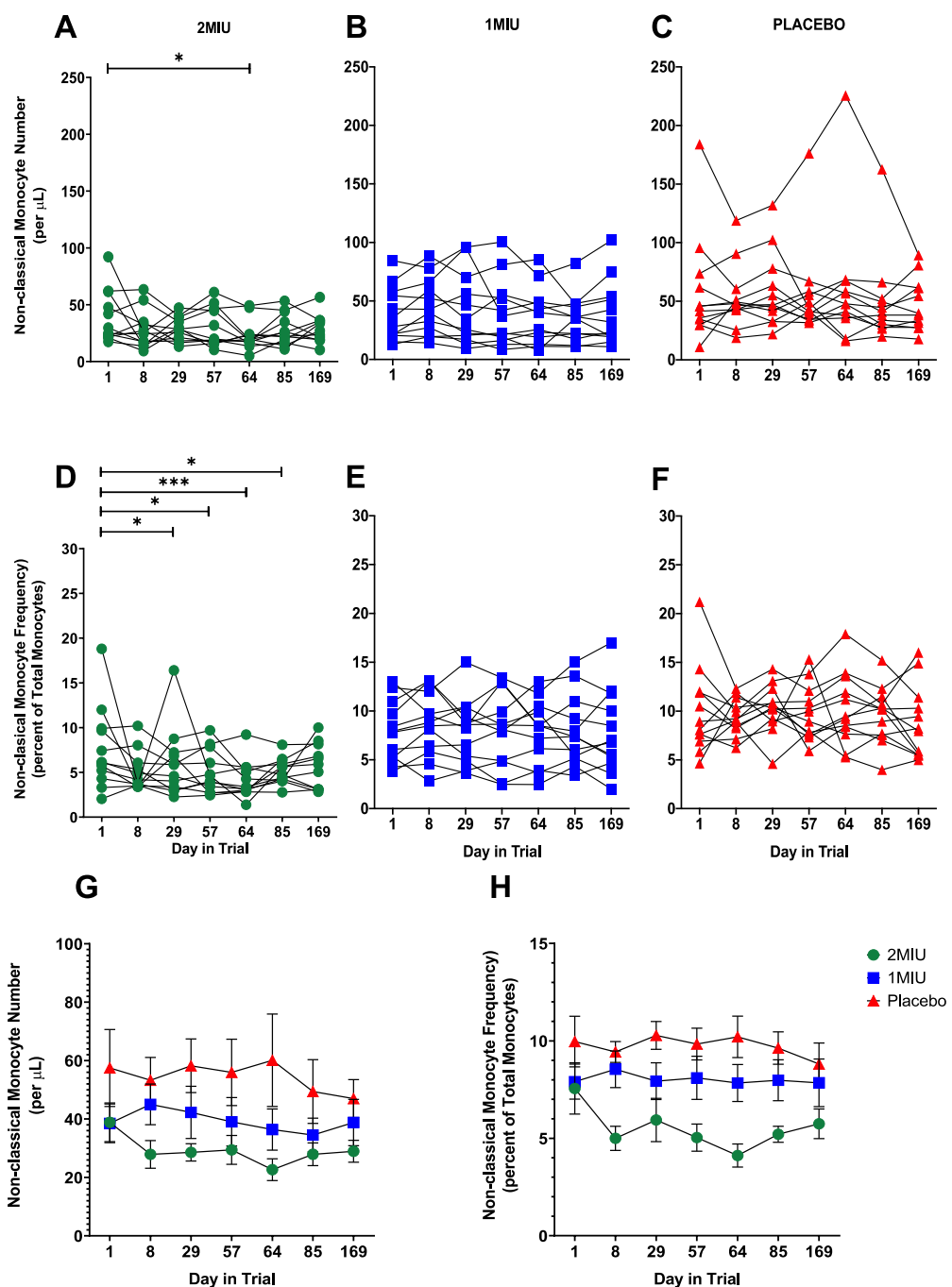


**Figure 2-21 the effects of LD-IL-2 on non-classical monocyte cell number and frequency. Panels A-F:**

alternative monocyte number (per  $\mu$ L of blood – A, B, C) and frequency (as percent of all monocytes – D, E, F) for each individual participant at every trial visit. Alternative monocyte cell number and frequency at each trial visit is compared to Day 1. **Panels G and H:** change in alternative monocyte cell number (G) and frequency (H) throughout the trial for all three treatment arms with data points indicating mean value and error bars indicating SEM. \*\*\*p<0.001, \*p<0.05, by matched Friedman test with Dunn's multiple comparisons (A, C, D, F) or by matched repeated measures one-way ANOVA with Bonferroni's multiple comparisons test (B, E). Green circles – 2MIU; blue squares – 1MIU; red triangles – Placebo.

There was a significant reduction in the CD163<sup>+</sup>CCR2<sup>-</sup> non-classical monocyte number days 8 and 64 in the 2MIU group ( $p<0.0001$  and  $p<0.0001$ ) and day 64 in the 1MIU group ( $p=0.0204$ ). There were also reductions in the frequency of these monocytes in both IL-2 treated groups at days 8 (2MIU  $p<0.0001$ ; 1MIU  $p=0.0040$ ) and 64 (2MIU  $p=0.0005$ ; 1MIU  $p=0.0034$ ). No significant changes were observed in the count or frequency in the placebo group (figure 2-22 A-F). Group analysis shows the reduced number at day 8, is significantly different between 2MIU and placebo ( $p=0.0004$ ) and 2MIU and 1MIU ( $p=0.0323$ ). The decrease at day 64 in the 2MIU is significantly lower when compared to placebo ( $p=0.0003$ ). Finally, comparisons of mean frequency between groups at each timepoint only show significant differences at day 8 ( $p=0.0085$ ) between 2MIU and placebo (figure 2-22 G and H). Collectively these monocyte data show:

1. No effect of IL-2 therapy on total monocyte number or frequency.
2. Small but significant increases in the frequency of classical monocytes.
3. A significant reduction in intermediate and non-classical monocytes in those receiving 2MIU IL-2.
4. A significant reduction in CD163<sup>+</sup>CCR2<sup>-</sup> non-classical monocytes in those receiving 2MIU IL-2.

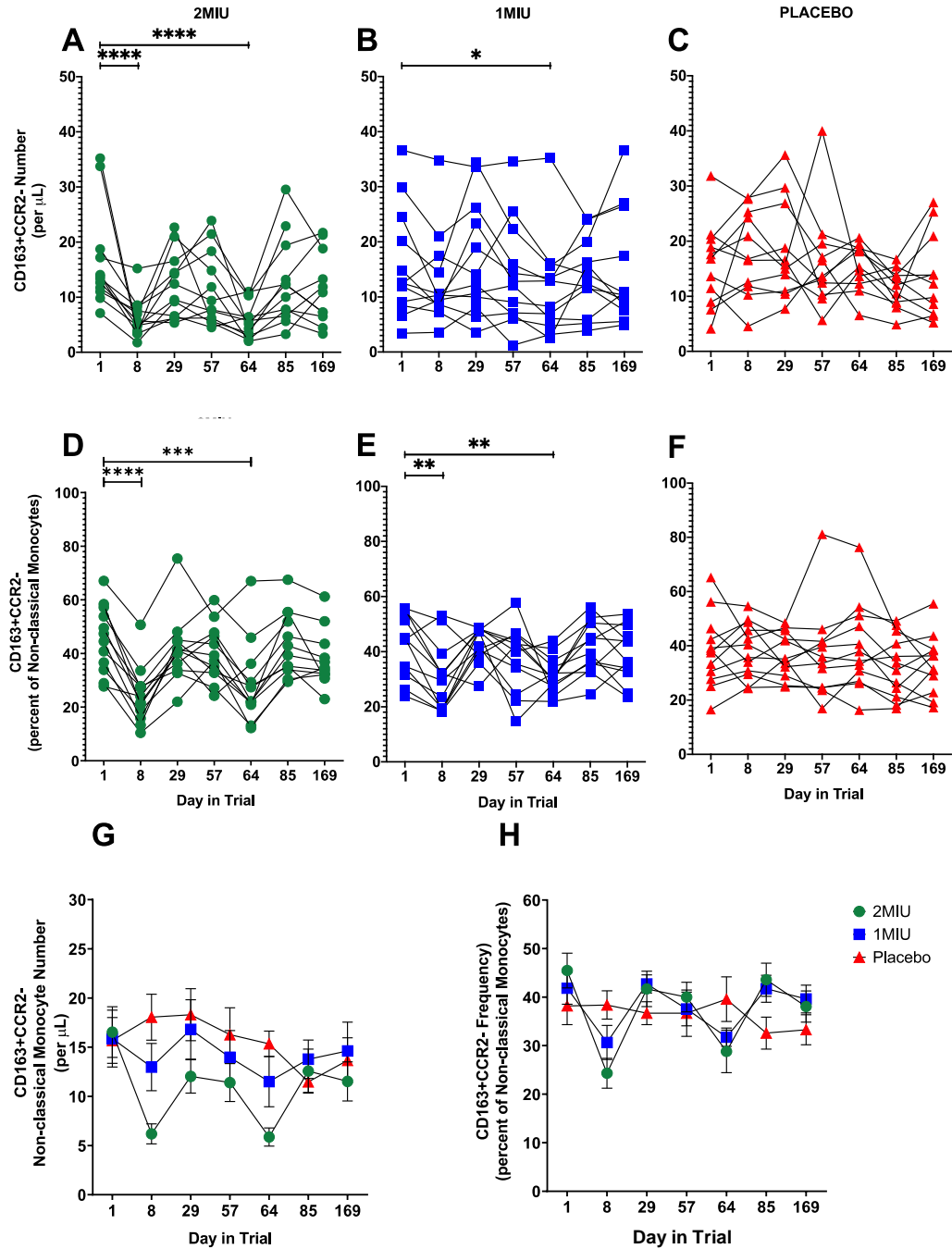


**Figure 2-22 the effects of LD-IL-2 on CD163+CCR2- non-classical monocyte cell number and frequency.** Panels A-F: CD163+CCR2- alternative monocyte number (per  $\mu$ L of blood – A, B, C) and frequency (as percent of alternative monocytes – D, E, F) for each individual participant at every trial visit. CD163+CCR2- alternative monocyte cell number and frequency at each trial visit is compared to Day 1. Panels G and H: change in CD163+CCR2- alternative monocyte cell number (G) and frequency (H) throughout the trial for all three treatment arms with data points indicating mean value and error bars indicating SEM. \*\*\*\* $p<0.0001$ , \*\*\* $p<0.001$ , \*\* $p<0.01$ , \* $p<0.05$ , by matched Friedman test with Dunn's multiple comparisons. Green circles – 2MIU; blue squares – 1MIU; red triangles – Placebo.

## **2.4. Discussion.**

The primary outcome of the IMODALS trial was to assess the safety and activity of three cycles of 5-daily doses of LD-IL-2 on Treg and other immune inflammatory markers in ALS. To address the safety aspect, and in line with previous findings (Koreth *et al.*, 2011; Hartemann *et al.*, 2013), we report that at both doses, IL-2 was safe and clinically well tolerated in all trial participants, with no further safety issues detected following cessation of IL-2 injections. Furthermore, patient compliance was good throughout the study (Camu *et al.*, 2020). To address the IL-2 activity on Treg and other immune inflammatory markers aspect, we first report significant increases in total lymphocyte number, which is largely attributed to the increases in Treg and Teff within the CD3<sup>+</sup>CD4<sup>+</sup> cell compartment. As expected, no IL-2 induced changes were observed in CD19<sup>+</sup> B cells. IL-2 may play a role in activated B cell differentiation into plasma cells however, direct effects of IL-2 on B cells are still debated (Le Gallou *et al.*, 2012). Interestingly, there were also significant increases in eosinophil frequency at day 8 in 2MIU and day 64 in both IL-2 treated groups (data not shown) (Camu *et al.*, 2020). When stimulated with IL-2 *in vitro*, eosinophils have been shown to release excess amounts of eosinophil peroxide (EPO) and IL-6 (Hoenstein *et al.*, 2001), but when measured, we observed no increase in EPO in response to IL-2 in this study.

To test the first hypothesis in this chapter, we assessed changes in Treg number and relative frequency (as a percentage of CD4<sup>+</sup> cells) in peripheral blood of ALS patients. It was important to address this as others have indicated that this therapy in ALS may not work as their Treg responsiveness to IL-2 is impaired

therefore, *ex vivo* expansion of Treg may be required (Thonhoff *et al.*, 2018). We observe significant increases in Treg number and frequency at days 8 (post cycle 1) and 64 (post cycle 3) in both IL-2 treated groups. These findings are in line with previous reports where, increases in Treg number and frequency have been shown in patients with GVHD, SLE, AA and T1D after subcutaneous IL-2 administration (Koreth *et al.*, 2011; Hartemann *et al.*, 2013; Castela *et al.*, 2014; Von Spee-Mayer *et al.*, 2016). Direct comparisons between our findings and published reports are difficult, as no two trials employ the same IL-2 concentration or dosing regimen. Data most comparable to the present study comes from a recent, randomised, placebo-controlled study where individuals with T1D were administered 5 daily doses of either placebo, 0.33MIU, 1MIU or 3MIU (n=6 per group), which showed significant increases from baseline in Treg number and frequency, as percent of CD4<sup>+</sup> cells, in all doses. (Hartemann *et al.*, 2013). A comparison of Treg frequency increases between the 1MIU IL-2 T1D and ALS cohorts, shows a similar magnitude in response of around 1.5-fold. This suggests that 1MIU IL-2 *in vivo* resulted in a similar Treg expansion between two different pathological conditions, which could be important when IL-2 concentrations are selected in future clinical trials. We also observe that those on IL-2 maintain significantly greater numbers of Treg up to three weeks post each cycle. Thus, if approved, the best IL-2 dosing regimen may be one that raised Tregs and maintained them at steady level, but this is yet unknown, especially in ALS. Furthermore, our data also shows that repeated cycles of 2MIU IL-2 increase Treg expansion, as we observed a greater increase in Treg number at day 64 than day 8. This was previously observed by Koreth and colleagues in 2016, where GVHD patients receiving 1MIU IL-2 /m<sup>2</sup>/day for 12 weeks, show a peak

increase in Treg number at 4 weeks. This dosing regimen also resulted in a steady increase in Teff number over the course of therapy, thus reducing the Treg:Teff ratio, while continued therapy did not result in greater Treg expansion (Koreth *et al.*, 2016). The IMODALS trial only consisted of three cycles, thus it is not possible to assess whether Treg expansion at day 64 is at its peak but given the published data its unwise to assume that a similar phenomenon would not occur had IMODALS continued to a fourth or a fifth cycle. If this is the case, then IL-2 dose or frequency may need to be adjusted to maintain Treg expansion.

Aside from Treg, expansions of non-Treg cells such as Teff, CD8<sup>+</sup> T and NK cells were also observed, mainly in the highest dose group. There were increases at days 8 and 64 in the number of Teff in patients treated with either dose of IL-2. Studies of LD-IL-2 are largely focussed on Treg and NK therefore direct comparisons between the Teff data in IMODALS and other studies are difficult, however data from the previously mentioned T1D LD-IL-2 trial reported minimal effects of Teff at 0.33 MIU and 1MIU, but a significant expansion of Teff at 3MIU/day for 5 days (Hartemann *et al.*, 2013). Our data shows that in larger cohorts, 1MIU and 2MIU IL-2 effectively expand Teff, which may be significant in conditions where Teff activation may contribute to disease pathology. We also showed that at the highest dose, there was significant expansion of CD8<sup>+</sup> T cells. This is in line with published findings as it has been reported that doses of 1MIU and below do not appear to significantly expand CD8<sup>+</sup> T cells as shown in a follow-up publication of the same study where T1D patients were receiving 5 daily doses of 0.33, 1MIU or 3MIU IL-2 (Rosenzwaig *et al.*, 2015). Whether Teff and CD8<sup>+</sup> T cells are detrimental in ALS is unknown, as there is no data to suggest

their contribution to neuroinflammation unlike in autoimmune diseases such as T1D, where autoreactive Teff and CD8<sup>+</sup> T cells are established to participate in the destruction of insulin-producing cells. Whereas in T1D, the expansion of these cells is unwanted, in ALS we simply cannot say the same (Tsaim *et al.*, 2008; Pugliese, 2017).

As for NK cells, there were increases in the number and frequency of total NK cells at both doses of IL-2 at days 8 and 64, and the number of NK cells at 2MIU remained greater than day 1 three weeks post cycles 1 and 2. These increases are largely driven by the expansion of CD56<sup>bright</sup> NK subset in both IL-2 treated groups. This NK subset, like Treg, appear to be highly sensitive to IL-2, as both subsets have shown an ~3-fold increase in number at day 8 and 64 at 2MIU and, ~1.5-fold increase in number at these timepoints in the 1MIU group. Other than our own findings in this chapter, research has shown that in T1D patients, a single dose of IL-2 (<1MIU), can sustain increased frequencies of this NK subsets for up to three days after subcutaneous injection (Todd *et al.*, 2016). Other IL-2 therapy trials have also shown a preferential expansion of CD56<sup>bright</sup> NK by three cycles of 1MIU IL-2 in SLE patients (He *et al.*, 2020). Total NK cells are significantly elevated in ALS patients when compared to healthy individuals however, their role in ALS progression and contribution to neuroinflammation is still debated and therefore, as with Teff and CD8<sup>+</sup> T cells, we do not know whether their expansion is detrimental in ALS. With regards to CD56<sup>bright</sup> NK, trials of daclizumab and IFN-β in MS patients have shown that the expansion of these cells were associated with better response to therapy (Bielekova *et al.*, 2011;

Martínez-Rodríguez *et al.*, 2011). Furthermore, given their immunoregulatory properties, the expansion of these cells may be of some benefit in ALS.

To test the final hypothesis of this chapter, we assessed changes in monocyte subsets as a result of IL-2 therapy. Our attention was initially drawn to monocyte changes in blood by plasma chemokine data from IMODALS participants, published by Camu and colleagues 2020. The analysis showed a significant and dose-dependent reduction in CCL2, a molecule recruiting leukocytes to sites of inflammation. This supports the notion that there may be less activated monocytes in the IL-2 treated as CCL2 levels of ALS patients and are associated with infiltration and activation macrophages and microglia in neural tissue (Camu *et al.*, 2020). Other published findings discussed previously, would suggest that an increase in Treg could potentially promote the anti-inflammatory cytokine secretion by monocytes. Interestingly the myeloid cell results in this chapter suggest otherwise. First, we assessed the frequency and number of total monocytes as well as their main subsets, the classical, intermediate and non-classical monocytes, observing a number of statistically significant changes but these were not particularly consistent or large, in terms of relative change. However, a striking change was observed within the non-classical monocyte compartment. The number and frequency of non-classical monocytes expressing CD163, was significantly lower after IL-2 cycles 1 and 3 in both 2MIU and 1MIU patient groups. There is no data relating changes in monocytes or their subsets in the field of IL-2 immunotherapy therefore these findings add a new perspective into the effects of IL-2 therapy *in vivo*. It could be hypothesised that this CD163<sup>+</sup> non-classical monocyte subset is recruited to tissue, to play an anti-inflammatory

role. It could also be argued that as this subset does not express CCR2, a CCL2 ligand responsible for recruiting monocytes to tissue, it may not be possible for these cells to migrate. However, CD163<sup>+</sup> non-classical monocytes generally do not express CCR2, but they have been reported to express high levels of CX3CR1, which can mediate their migration (Deshmane *et al.*, 2009; Lee *et al.*, 2018). To address this, more comprehensive analyses of these subsets is required.

Finally, with respect to clinical efficacy, there were no significant differences in the ALSFRS-R score, slow vital capacity or plasma neurofilament levels between the three treatment groups (Camu *et al.*, 2020). Deeper analysis of plasma neurofilaments did show a 20% increase in the placebo group by day 85, which is consistent with disease progression, which is not seen in the two IL-2 treated groups (5% increase at 2MIU, 1% decrease at 1MIU), but these were not significantly different when compared to the placebo. Clinical efficacy of IL-2 therapy has been shown in conditions such as GVHD and AA, where reduced erythema and partial hair regrowth were visible in some of the treated patients (Koreth *et al.*, 2011; Castela *et al.*, 2014). Furthermore, our measures may not be sensitive enough over the short duration of this study, as there was no significant change in these variables from day 1 in any of the treatment groups. Therefore, we can conclude that IL-2 did not show clinical efficacy in 24 ALS patients, treated with 2 different doses of IL-2 and clinical efficacy could be better assessed with a larger cohort of ALS patients, treated for a longer period. This notwithstanding, the data presented here raises the following questions, which are relevant to both ALS, and IL-2 immunotherapy trials in general:

1. Given the importance of Treg function in ALS, did IL-2 therapy result in an increase in Treg suppressive function?
2. Given the variability in Treg and non-Treg cell expansion in our and other studies as a result of IL-2, can we predict the responses of these cells by assessing IL-2 signalling before the start of therapy?
3. Given that we are continuously expanding Treg *in vivo* with IL-2, does this affect Treg IL-2 signalling?
4. Given the heterogeneity of Treg and non-Treg cells, what are the effects of IL-2 therapy on the subpopulations of these cells?

## **Chapter 3. Evaluating the effects of LD-IL-2 on Treg suppressive function *in vitro*.**

### **3.1. Introduction.**

Having observed an increase in Treg number, the purpose of this chapter was to assess whether LD-IL-2 immunotherapy altered Treg suppressive function *in vitro*, as number is not necessarily an indicator of function. Conventionally, Treg ability to suppress an autologous immune response, most commonly CD4<sup>+</sup> Teff, is determined by titrating the number of Treg and coculturing these with a constant number of Teff in the presence of accessory cells and a stimulus such as anti-CD3/CD28 beads or phytohaemagglutinin (PHA). Proliferation is then assessed by flow cytometry using cell proliferation-based dyes such as carboxyfluorescein succinimidyl ester (CFSE) or by incorporation of [<sup>3</sup>H] thymidine and subsequent scintillation counting (Lindley *et al.*, 2005; Koreth *et al.*, 2011). The published data shows that both techniques are a robust way of assessing Treg function.

Studies in various diseases have shown an impairment in Treg suppressive function without a significant change in Treg number. For an example, in diseases such as T1D, MS and myasthenia gravis (MG) reports show that there is no significant difference between the frequency of Treg in patients with these conditions versus healthy controls. However, when assessing Treg function, it was found that patient Treg were significantly less effective at suppressing autologous Teff *in vitro* when compared to healthy controls (Viglietta *et al.*, 2004; Balandina *et al.*, 2005; Brusko *et al.*, 2005; Lindley *et al.*, 2005; Lawson *et al.*,

2008). In ALS there are also no significant differences in Treg frequencies between patients and healthy controls, significant differences are only evident when stratifying patients into fast and slow progressors. Whereas in cocultures of Treg and Teff, ALS patient Treg are less able to suppress the proliferation of autologous Teff when compared to Treg and Teff of healthy controls. Furthermore, this Treg dysfunction negatively correlates with disease progression (Henkel *et al.*, 2013; Beers *et al.*, 2017).

There is also evidence from immunotherapy studies showing that an increase in Treg number does not always lead to an increase in suppressive function. A combination of rapamycin and IL-2 in T1D patients resulted in an increase in Treg number however, each participant also presented with a decline in  $\beta$ -cell function leading the authors to hypothesise that one of the factors causing this could be a decline in Treg function (Long *et al.*, 2012). Furthermore, data published in 2016 where T1D patients received a single dose of IL-2 ranging from  $0.04 \times 10^6$  –  $1.5 \times 10^6$  IU/m<sup>2</sup> showed a significant change in Treg number in blood but, there was no significant change in Treg ability to suppress autologous Teff *in vitro* (Todd *et al.*, 2016). Conversely, there are also examples of when IL-2 immunotherapy has had a positive effect on Treg function. Treg isolated from patients with GVHD after *in vivo* expansion via administration of IL-2, effectively suppressed the proliferation of autologous Teff (Koreth *et al.*, 2011). A recently published study of SLE patients showed that Treg isolated from patients after 2 weeks of every other day subcutaneous injections of 1MIU of IL-2, are better at suppressing Teff obtained from healthy individuals than Treg isolated before therapy (He *et al.*, 2016). There is also some data with regards to this in ALS.

The afore mentioned study linking Treg function with ALS progression reported that expansion of ALS patient Treg with exogenous IL-2 *in vitro* led to an improvement in Treg function (Beers *et al.*, 2017). Furthermore, Thonhoff and colleagues treated three ALS patients with expanded autologous Treg infusions in combination with subcutaneous IL-2 injections which resulted in an increase in Treg frequency and greater Treg suppression of autologous Teff proliferation (Thonhoff *et al.*, 2018). Moreover, having shown a significant increase in Teff number as a result of IL-2 therapy in the previous chapter, as these cells also express the IL-2R, it is possible that IL-2 therapy might have an effect on Teff proliferation.

The findings in individuals with ALS suggest that Treg function plays a role in disease progression however, the effects of *in vivo* LD-IL-2 immunotherapy on Treg function in ALS are not known. Therefore, we decided to utilise the Treg micro-suppression assay to test the following hypotheses:

1. In addition to the increase in Treg number, LD-IL-2 therapy will increase Treg function.
2. Any effect on Treg function may persist after treatment has been stopped.

We selected cryopreserved PBMC samples of IMODALS participants from the following timepoints:

- Day 1 – the baseline visit that will be used to compare the other timepoints against.
- Day 64 – this is where we observed the greatest change in Treg number and frequency in chapter 2.
- Day 85 and 169 – these visits were needed to address the second part of the hypothesis, investigating long-lasting effects of LD-IL-2 on Treg suppressive function.

The Treg micro-suppression assay, outlined in figure 3-1, was previously developed and validated to a high level of accuracy and precision in the laboratory for use in clinical trials. The PhD candidate underwent full training and competence assessment prior to patient sample analysis.

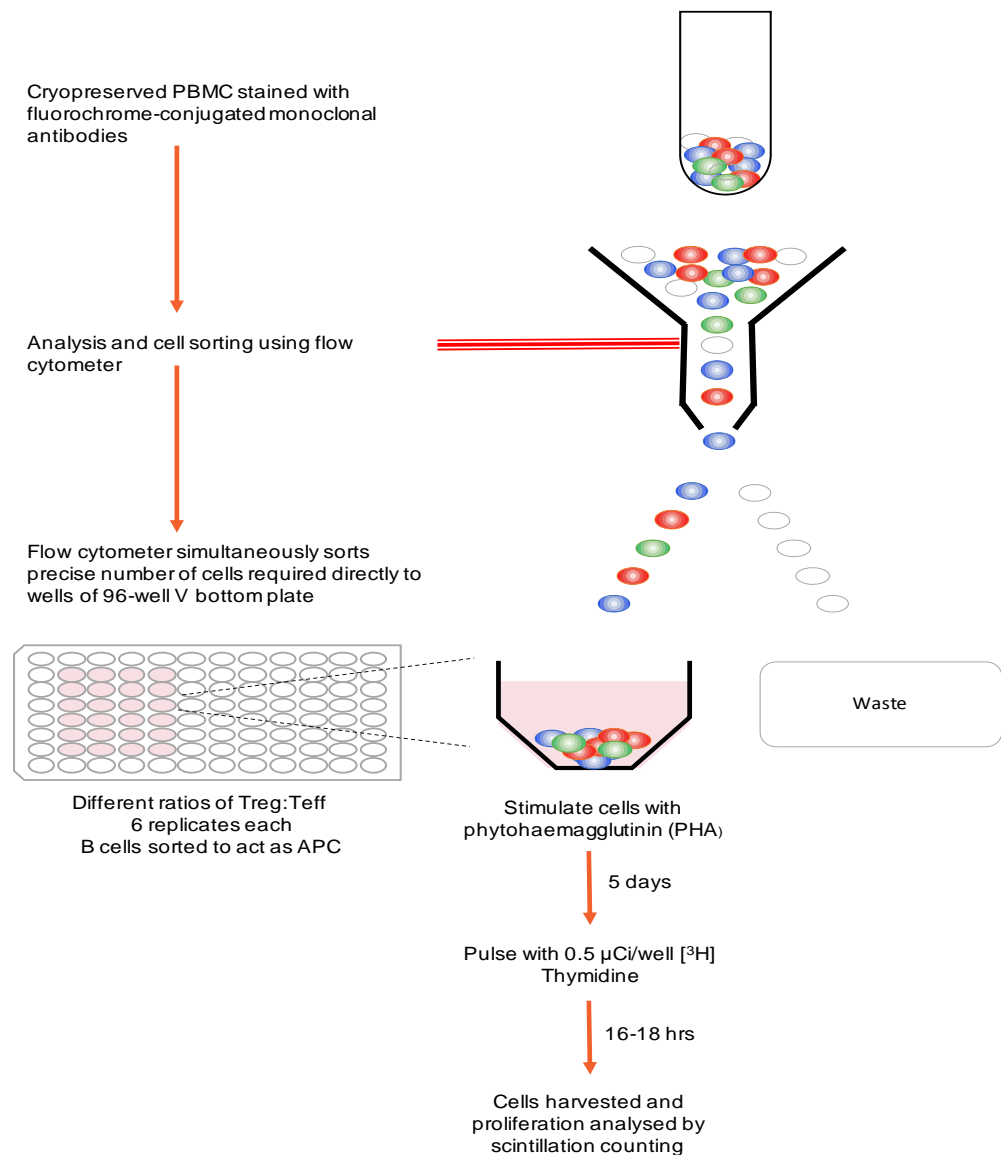


**Figure 3-1 Treg micro-suppression assay protocol.** Cryopreserved cells are thawed and stained with fluorochrome-conjugated monoclonal antibodies. The cells are analysed using a flow cytometer and Treg and Teff are subsequently sorted, along with B cells to act as APC, directly into wells of a 96-well V bottom plate containing coculture media supplemented with PHA. The plates are incubated for 5 days at 37°C and 5% CO<sub>2</sub>. The contents of each well are then pulsed with 0.5 μCi of [<sup>3</sup>H] thymidine, incubated for a further 16-18 hours following which the contents of each well are harvested and proliferation assessed by scintillation counting.

This was the preferred method to assess Treg suppressive function as there were a limited number of PBMC available per patient sample, and this technique has been optimised to utilise cell numbers at or below  $1 \times 10^3$  per population per well, providing a robust, sample sparing platform. Furthermore, all future analysis of IMODALS samples as part of this thesis will be carried out using cryopreserved PBMC and this technique was optimised specifically for, but not limited to, analysis of this type of samples.

### **3.2. Materials and methods.**

#### **Preparation of assay media**

##### Thawing media:

X-VIVO (Lonza) supplemented with PSF (Thermo Fisher) and 10% FBS (Thermo Fisher), filtered using  $0.45\mu\text{m}$  microfilter and pre-warmed to  $37^\circ\text{C}$  prior to thawing of PBMC.

##### Staining buffer:

PBS (Thermo Fisher) supplemented with 2mM EDTA (Sigma) and 1% AB (Sigma), filtered using  $0.45\mu\text{m}$  microfilter.

##### Co-culture media:

X-VIVO supplemented with PSF and 10% AB, filtered using  $0.45\mu\text{m}$  microfilter.

#### **Preparation of PBMC for FACS**

Cryovials containing ALS patient PBMC corresponding to days 1, 64, 85, 169 timepoints in the IMODALS trial were removed from liquid nitrogen and placed into a water bath set at  $37^\circ\text{C}$ . Prior to fully thawing, cryovials were transferred to a tissue culture hood and gently agitated while thawing media was dropwise

added using a pasteur pipette. The contents of each cryovial were transferred to a new 15mL falcon tube, topped up to 10mL with thawing media and the PBMC washed and pelleted by centrifugation at 400g for 10 minutes. The supernatant was removed, PBMC were resuspended in 5mL of staining buffer and viability assessed at a 1:1 ratio of trypan blue using a haemocytometer and microscope. The PBMC were then pelleted at 400g for 5 minutes, supernatant removed, and a master mix of fluorescently labelled antibodies (table 3-1) added to PBMC in residual staining buffer. The PBMC were stained on ice for 30 minutes in the dark and washed in 3mL of cold staining buffer at 400g for 5 minutes. The supernatant was removed and the PBMC resuspended in 1mL of staining buffer by gently pipetting the pellet up and down using a P1000 pipette (Gilson). The PBMC were passed through a cell strainer cap into a new polypropylene tube and placed on ice until FACS.

| Target | Conjugate       | Clone      | Origin | Volume / Test ( $\mu\text{L}$ ) | Manufacturer |
|--------|-----------------|------------|--------|---------------------------------|--------------|
| CD4    | APC-Cy7         | RPA-T4     | Mouse  | 1                               | BD           |
| CD14   | PerCP-Cy5.5     | HCD14      | Mouse  | 1                               | BL           |
| CD19   | Pacific Blue    | HIB19      | Mouse  | 2                               | BL           |
| CD25   | PE              | 2A3        | Mouse  | 10                              | BD           |
| CD25   | PE              | M-A251     | Mouse  | 10                              | BD           |
| CD127  | Alexa Fluor 647 | HIL-7R-M21 | Mouse  | 18                              | BD           |

**Table 3-1 Fluorescently labelled antibodies used for preparing the master mix for surface staining of PBMC.** BL = BioLegend; BD = Becton Dickinson.

## PBMC sorting by FACS

The PBMC were acquired using a FACS Aria II (BD) and a gating strategy was set using FACSDiva software (BD) (figure 3-2). Teff (CD4<sup>+</sup>CD25<sup>-/lo</sup>CD127<sup>+</sup>), Treg (CD4<sup>+</sup>CD25<sup>high</sup>CD127<sup>lo</sup>) and B cells (CD19<sup>+</sup>) were sorted through a 70 $\mu$ m nozzle into wells of 96-well V-bottom plates (Greiner bio-one) containing previously prepared co-culture media. Cells from each timepoint of each trial participant were sorted onto a single plate. Three co-culture conditions were set-up in sextuplicate; 0 Treg and 500 Teff (0:1); 125 Treg and 500 Teff (1:4); 250 Treg and 500 Teff (1:2) with  $1 \times 10^3$  CD19<sup>+</sup> B cells acting as accessory cells in each condition. Lymphocytes were stimulated with 4  $\mu$ g/ml PHA (Alere) or anti-CD3/CD28 Dynabeads. The plates were centrifuged at 400g for 5mins and incubated at 37°C and 5% CO<sub>2</sub> for 5 days.

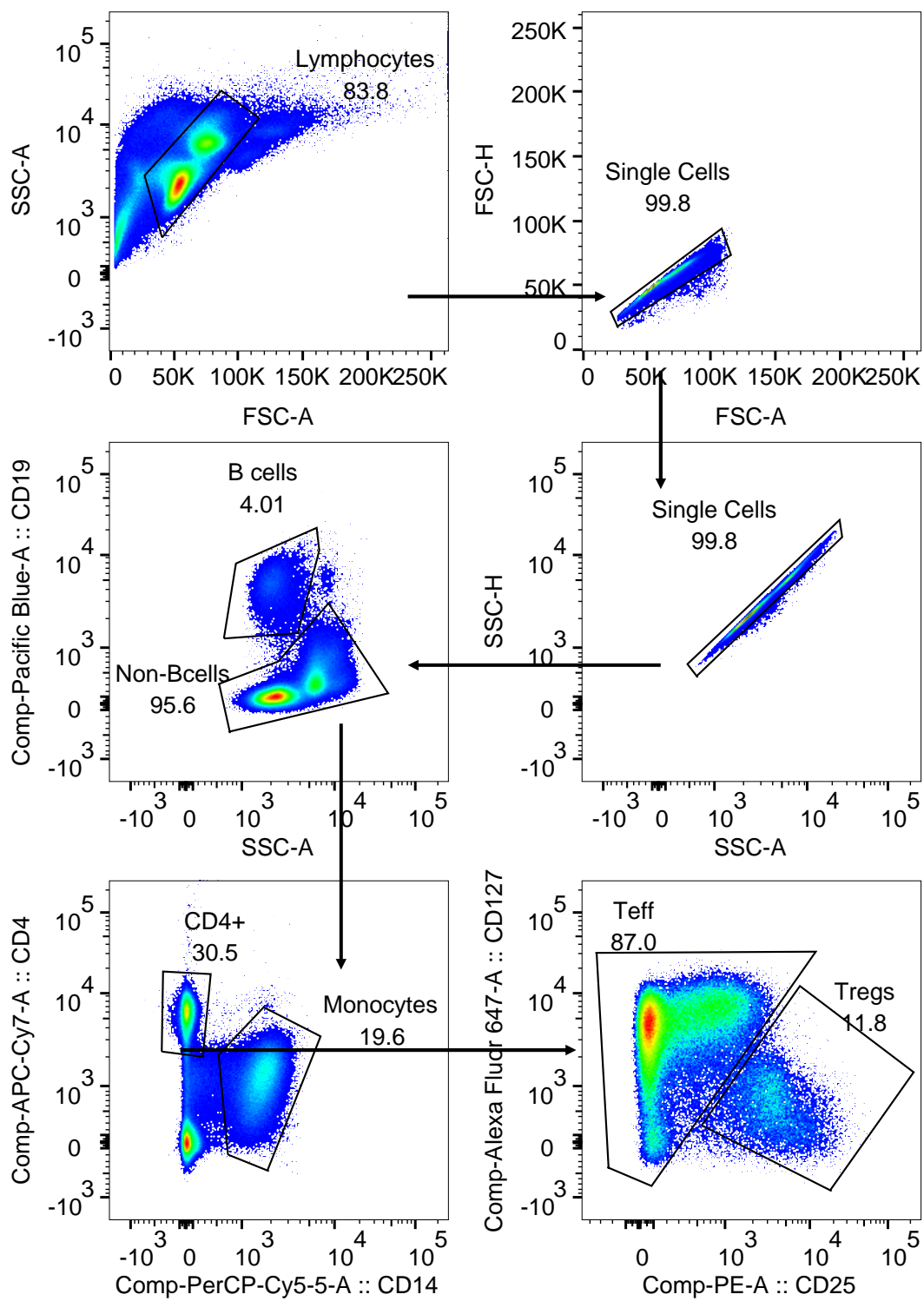


**Figure 3-2 Gating strategy for sorting Tregs, Teff and B cells.** First, PBMC were gated based on size and granularity in FSC-A and SSC-A (log scale). Then aggregated cells and debris were excluded by gating on single cells. Following this, B cells were isolated based on CD19 expression and cells negative for CD19 were used to isolate CD4+ T cells and exclude CD14+ Monocytes. Treg and Teff were then gated based on being CD25<sup>hi</sup>CD127<sup>lo</sup> and CD25<sup>+/-</sup>CD127<sup>+/-</sup> respectively.

### **Assessment of proliferation and percentage suppression**

To assess proliferation, 75 $\mu$ L of co-culture supernatant was harvested from each well, replaced with 75 $\mu$ L of pre-warmed co-culture media containing 0.5  $\mu$ Ci of [ $^3$ H] thymidine (PerkinElmer) and the plates incubated for a further 18 hours at 37°C and 5% CO<sub>2</sub>. The contents of each plate were harvested onto ‘Printed Filtermat A’ filter paper (PerkinElmer) using a ‘Filtermate’ plate harvester (Packard) and proliferation recorded as counts per minute (CPM) using a Microbeta Trilux liquid scintillator and luminescence counter (PerkinElmer). Proliferation readings of less than 3,000 CPM from the Teff wells alone were excluded. The percentage suppression in each co-culture was calculated, as previously reported by Lindley and colleagues 2005, using the following formula:

**percent suppression = 100 – [(CPM in the presence of Tregs ÷ CPM in the absence of Tregs) × 100]** (Lindley *et al.*, 2005).

### **Data Analysis**

The CPM and percent suppression (% suppression) were analysed using Microsoft Excel while statistical analysis was performed using GraphPad Prism 9. For paired analysis of changes between timepoints per treatment group, a D’Agostino & Pearson normality and lognormality test was performed. Depending on whether the data was normally distributed, either a paired t-test or a Wilcoxon matched-pairs sign rank test was used. To assess changes between treatment groups, the same normality test was used followed by an ordinary one-way ANOVA with Bonferroni’s multiple comparisons test or Kruskal-Wallis test with Dunn’s multiple comparisons test.

### **3.3. Results.**

#### **3.3.1. Quality control.**

As there was a large number of samples to analyse, experiments were carried out in 10 batches. Several steps were taken to control for any confounding effects of batch-to-batch variation in assay performance:

1. All timepoints for an individual were analysed on the same day.
2. Each batch contained a random allocation of individuals.
3. The PhD candidate was unblinded to participant ID and day in trial, not treatment group.
4. Replicate vials of PBMC isolated from a single, large blood draw from a control individual were analysed at each assay day alongside trial samples.

The results of control individual PBMC were used as an internal quality control (QC) to assess any day-to-day variation in assay performance, allowing to detect any systematic drift in results. Data collected for the frequencies of Treg and Teff, % suppression (1:2 ratio), Teff CPM, Treg and Teff CD25 median fluorescence intensity (MFI) for the QC sample show the percentage coefficient of variation (% CV) of <20% (table 3-2). When assay precision was assessed during method validation, the %CV value between replicates of the same sample were =<25% for % suppression, thus our %CV value of 17.06 for % suppression indicates excellent day-to-day assay reproducibility and suggest that the 1:2 suppression data from IMODALS participants is best to use for assessment of Treg function. Data for % suppression at 1:4 ratio showed greater variation between batches with % CV of 25.18% which is borderline with the =<25% CV value from method validation and will also be reported (table 3-2).

| Batch       | Treg<br>(%CD4) | Teff<br>(%CD4+) | %<br>Suppression<br>(1:2) | %<br>Suppression<br>(1:4) | Teff<br>CPM    | Treg<br>CD25<br>MFI | Teff<br>CD25<br>MFI |
|-------------|----------------|-----------------|---------------------------|---------------------------|----------------|---------------------|---------------------|
| 1           | 6.39           | 93.1            | 68.57                     | 68.71                     | 6359.5         | 3967                | 117                 |
| 2           | 6.36           | 93.2            | 73.41                     | 59.76                     | 6954.6         | 3656                | 107                 |
| 3           | 6.37           | 93.2            | 39.17                     | 20.11                     | 5453.5         | 4108                | 113                 |
| 4           | 6.51           | 93.2            | 77.38                     | 54.25                     | 8166           | 4537                | 118                 |
| 5           | 6.36           | 93.1            | 80.09                     | 60.25                     | 6063.2         | 3839                | 123                 |
| 6           | 6.85           | 92.7            | 78.34                     | 55.19                     | 9818.4         | 3863                | 130                 |
| 7           | 6.47           | 93.1            | 77.09                     | 66.79                     | 8267.2         | 4116                | 121                 |
| 8           | 6.38           | 93.2            | 64.17                     | 57.94                     | 5774.25        | 3792                | 111                 |
| 9           | 6.47           | 93.2            | 73.83                     | 65.17                     | 7983           | 3448                | 108                 |
| 10          | 6.03           | 93.6            | 75.2                      | 73.78                     | 8669.4         | 2877                | 92.5                |
| <b>Mean</b> | <b>6.42</b>    | <b>93.16</b>    | <b>70.73</b>              | <b>57.99</b>              | <b>7224.91</b> | <b>3820.3</b>       | <b>114.05</b>       |
| <b>SD</b>   | <b>0.2</b>     | <b>0.22</b>     | <b>12.07</b>              | <b>14.6</b>               | <b>1301.20</b> | <b>442.69</b>       | <b>10.37</b>        |
| <b>% CV</b> | <b>3.13</b>    | <b>0.23</b>     | <b>17.06</b>              | <b>25.18</b>              | <b>18.01</b>   | <b>11.59</b>        | <b>9.09</b>         |

**Table 3-2 Analysis of QC PBMC variables across the 11 experimental repeats of IMODALS PBMC suppression assays.**

### **3.3.2. Significant correlations between Treg frequencies in fresh blood and cryopreserved PBMC.**

For analysis of Treg function, we utilised cryopreserved participant PBMC, as such it was important to assess whether the Treg frequencies we obtained from whole blood are in line with those in cryopreserved samples. Cryopreservation has been shown to affect cell viability, phenotype and function, due to factors such as freezing protocol and operator competence (Perdomo-Celis *et al.*, 2016).

With regards to Treg, a significant effect of cryopreservation on Treg frequency when compared to fresh blood Treg has been shown. This was caused by changes in CD25 expression, with the authors concluding that activated Treg, expressing greater levels of CD25, are more susceptible to apoptosis (Seale *et al.*, 2008). Because in IMODALS we sought to activate Treg with LD-IL-2 and then assess their function, we investigated any confounding effect of cryopreservation on Treg, by correlating frequencies obtained in fresh blood,

versus those obtained in cryopreserved PBMC based on the expression of CD4, CD25 and CD127. Using simple linear regression, we observe significant correlations ( $p < 0.0001$ ) in Treg frequency in blood and cryopreserved PBMC at every timepoint, with the strongest correlations at days 1, 64 and 85 with  $r^2$  squared values  $> 0.8$  (figure 3-3 A, B and C), and a good correlation at day 169 with an  $r^2$  squared value  $> 0.6$  (figure 3-3 D).

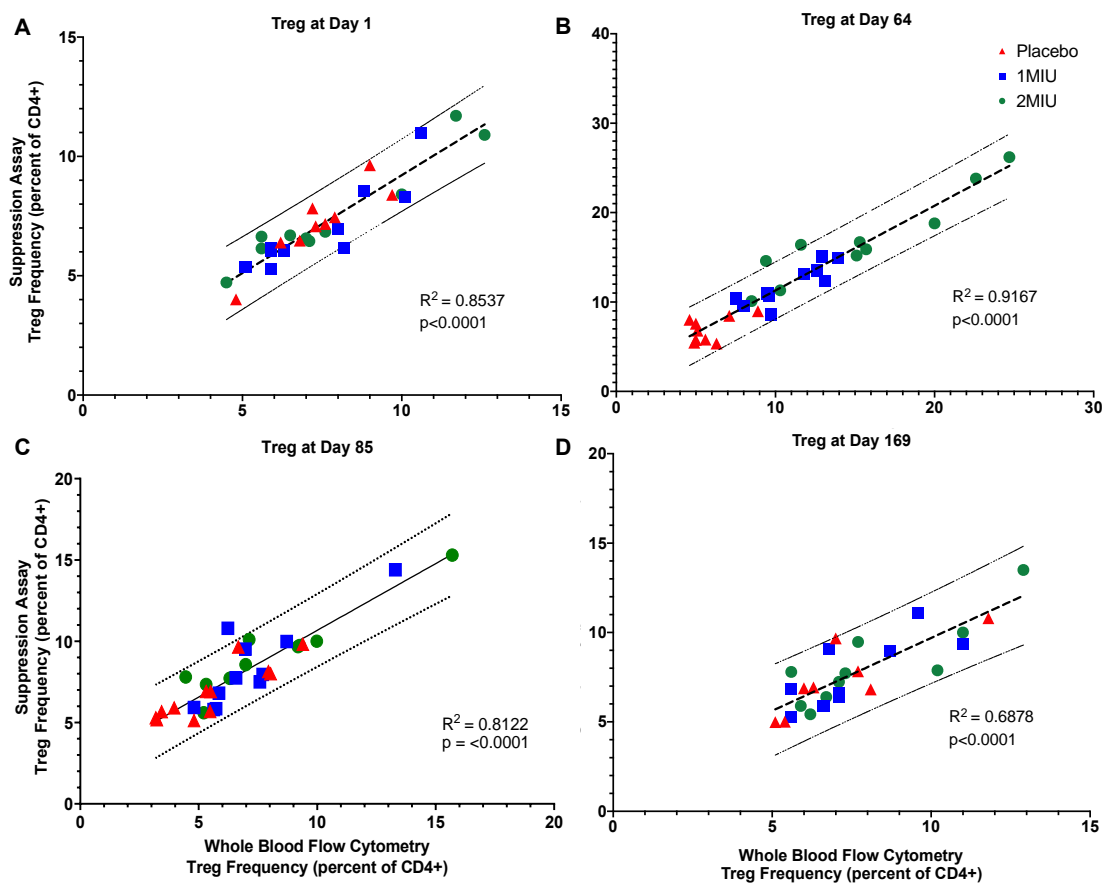


**Figure 3-3 Simple linear regression analysis of Treg frequency in whole blood and cryopreserved PBMC.** Panel A: Treg frequencies at day 1. Panel B: Treg frequency at day 64. Panel C: Treg frequency at day 85. Panel D: Treg frequency at day 169. Outer dotted lines are 95% prediction bands. Red triangle – placebo, blue square – 1MIU, green circle – 2MIU.

### **3.3.3. Improvement in Treg suppressive function after IL-2.**

The first question we sought to answer was whether Teff proliferation was affected by IL-2 therapy. It is well known that Teff are activated by IL-2 and any change in Teff proliferation might affect Treg suppressive function and therefore, we could not claim that an improvement in Treg function was solely due to administration of IL-2 but also a result of Teff becoming more proliferative. Having assessed proliferation of Teff in conditions where they were cultured without Treg, we did not observe any significant changes at day 64 in Teff proliferation in individual treatment groups (figure 3-4 A to C) nor between treatment groups (3-4 D to E).

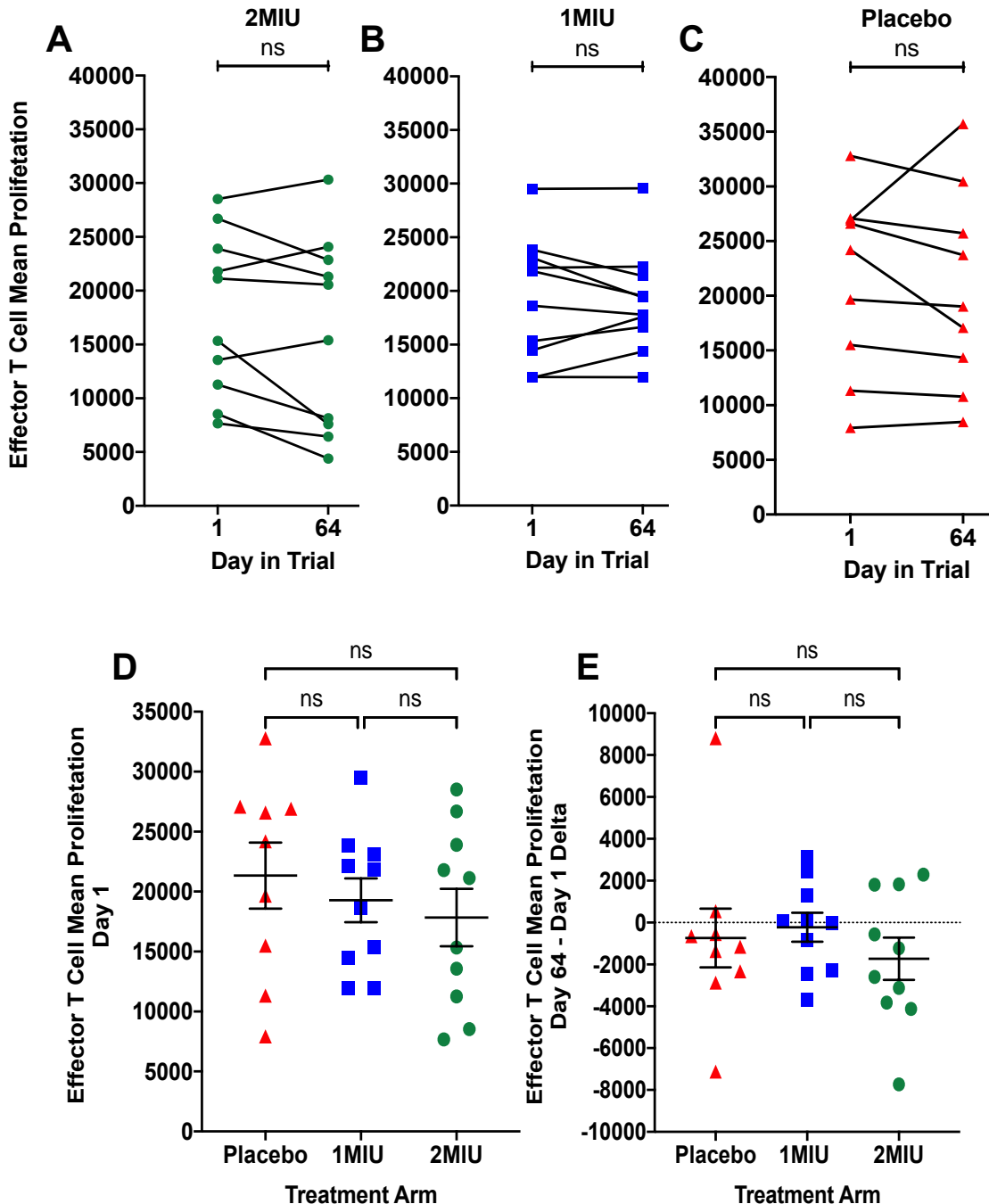


**Figure 3-4 Assessment of mean Teff proliferation at day 1 and day 64 in IMODALS treatment groups.**

Panels A to C: Analysis of mean Teff proliferation in each treatment group at day 1 and day 64. Panel D: Analysis of mean Teff proliferation at day 1 between placebo and 1MIU, placebo and 2MIU, and 1MIU and 2MIU. Panel E: Analysis of change in mean Teff proliferation at day 64 between placebo and 1MIU, placebo and 2MIU, and 1MIU and 2MIU. Error bars indicate mean with SEM. ns – not significant. Panels A to C – paired t test; Panels D – ordinary one-way ANOVA; Panel E – Kruskal-Wallis test. Red triangles – placebo; blue squares – 1MIU; green circles – 2MIU.

Having observed no change in Teff proliferation, we then addressed the first hypothesis of this chapter, that IL-2 immunotherapy will improve Treg function. At Treg:Teff ratio of 1:2, we observed a significant increase in % suppression at day 64 in the 1MIU group ( $p=0.0020$ ) and interestingly, a significant decrease in the placebo group ( $p=0.0464$ ). There was also an increase in % suppression in the 2MIU group however, significance between the two timepoints was not reached ( $p=0.0642$ ) (figure 3-5 A to C). As there was a dose-dependent increase in Treg number and frequency reported in chapter 2, we went on to assess whether the same is true for % suppression. To assess dose-dependency, we calculated the change (delta) in % suppression between day 64 and day 1 and compared these between the 3 treatment groups. Participants receiving 2MIU IL-2 had a mean increase of 11.6% in % suppression while those on 1MIU IL-2 had a 13.7% increase. These were significantly different between placebo and 1MIU ( $p=0.0084$ ), placebo and 2MIU ( $p=0.0099$ ) but not between 1MIU and 2MIU showing treatment induced but not dose-dependent changes in Treg suppressive function. This analysis did show a caveat in the data, the % suppression values at day 1 in the 2MIU group are significantly different to those in the placebo group ( $p=0.0373$ ) (figure 3-5 D and E). At Treg:Teff ratio of 1:4, there is also an increase in % suppression in both IL-2 treated groups, but this is only significant in the 1MIU group ( $p=0.0273$ ). The average increase in % suppression was 6.90% and 10.31% for 2MIU and 1MIU groups respectively, and this was significantly different between the 1MIU and placebo ( $p=0.0347$ ). There were no significant differences in day 1 % suppression values between any of the groups (figure 3-6 A to E).

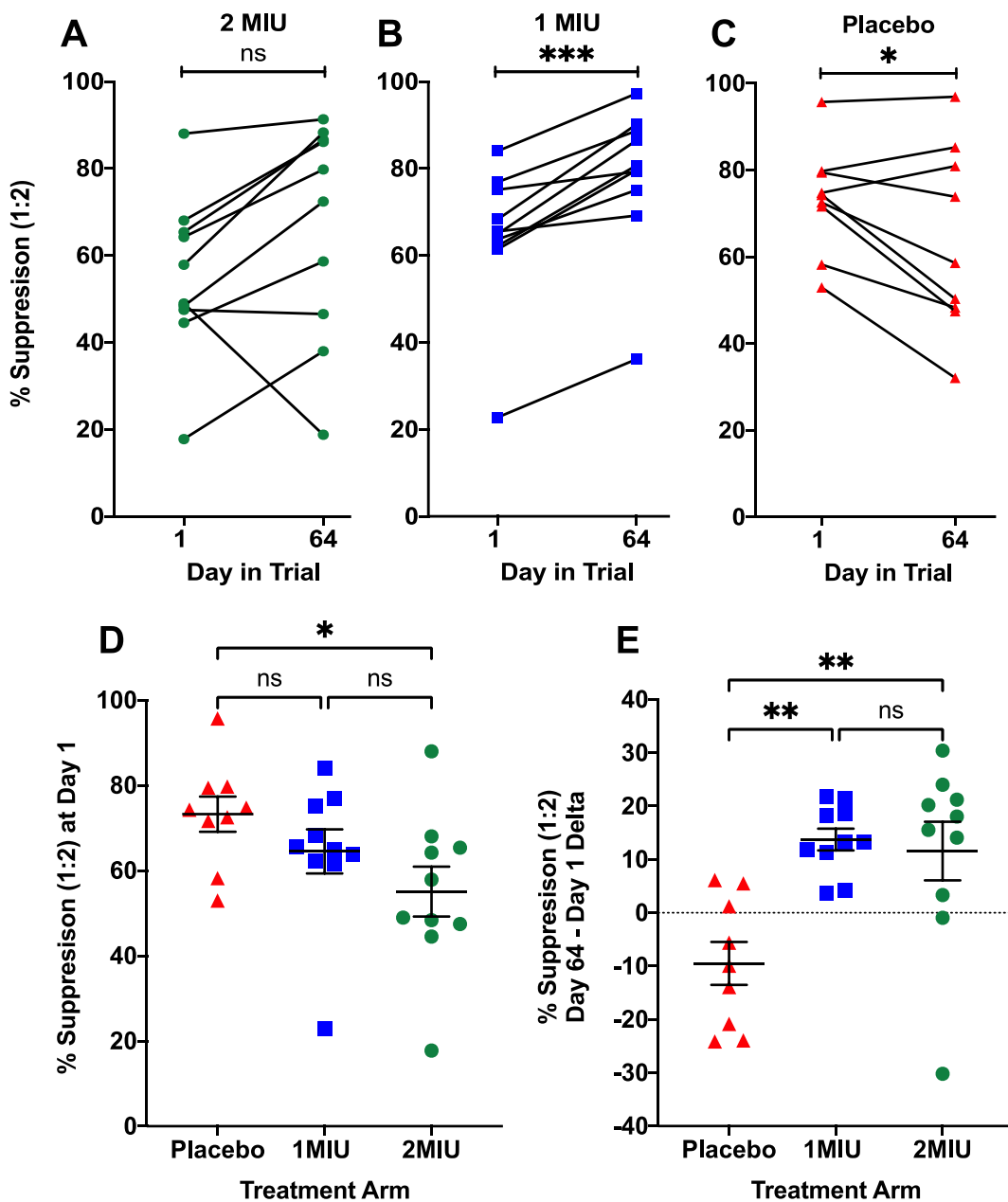


**Figure 3-5 Assessment of % suppression at Treg:Teff ratio of 1:2 at day 1 and day 64 in IMODALS treatment groups.** Panels A to C: Analysis of % suppression in each treatment group at day 1 and day 64. Panel D: Analysis of % suppression at day 1 between placebo and 1MIU, placebo and 2MIU, and 1MIU and 2MIU. Panel E: Analysis of change in % suppression at day 64 between placebo and 1MIU, placebo and 2MIU, and 1MIU and 2MIU. Error bars indicate mean with SEM. \*\*\* $p<0.001$ , \*\* $p<0.01$ , \* $p<0.05$ , ns – not significant. Panels A and C – paired t test; Panel B – Wilcoxon test; Panels D and E – Kruskal-Wallis test. Red triangles – placebo; blue squares – 1MIU; green circles – 2MIU.

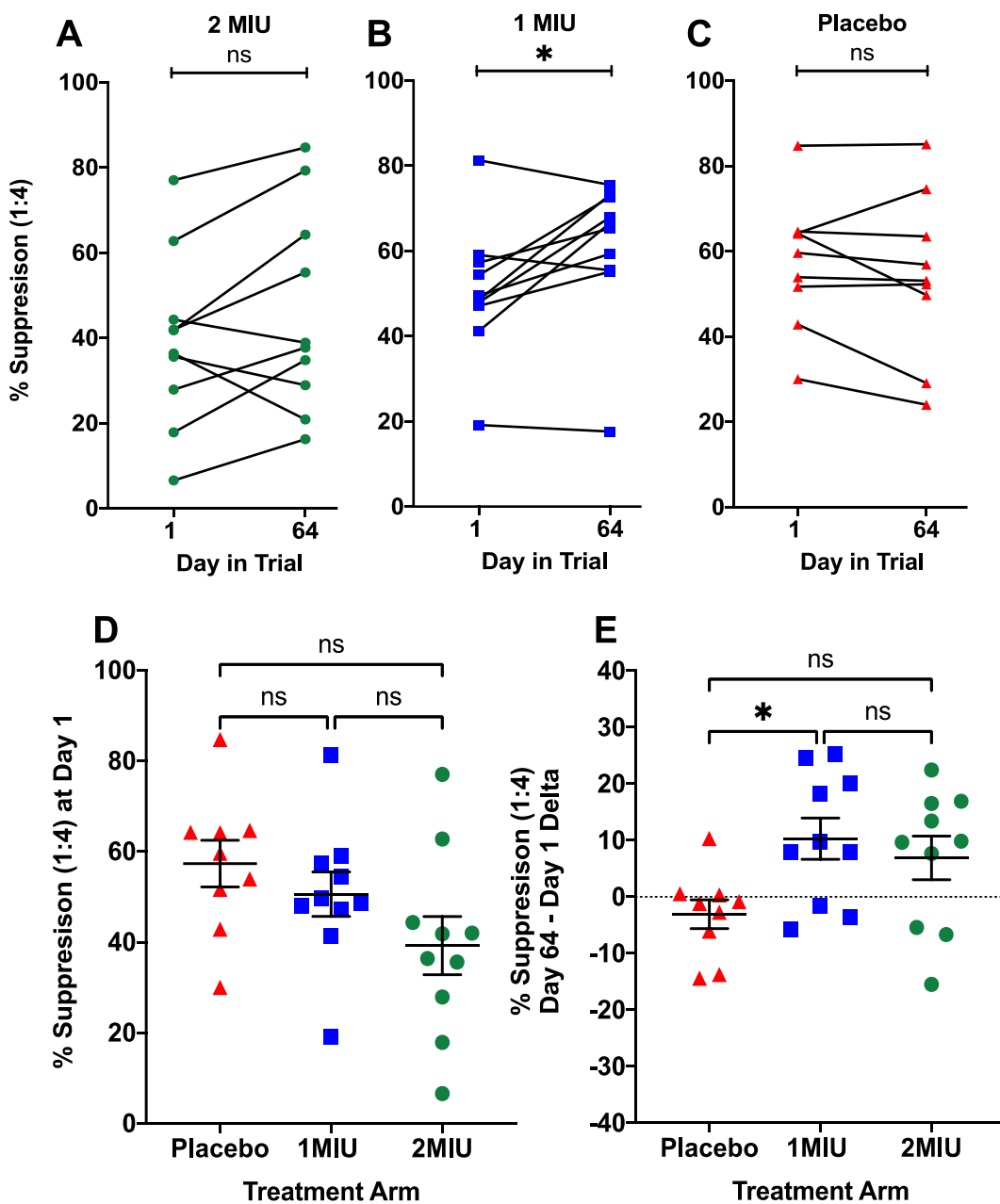


**Figure 3-6 Assessment of % suppression at Treg:Teff ratio of 1:4 at day 1 and day 64 in IMODALS treatment groups.** Panels A to C: Analysis of % suppression in each treatment group at day 1 and day 64. Panel D: Analysis of % suppression at day 1 between placebo and 1MIU, placebo and 2MIU, and 1MIU and 2MIU. Panel E: Analysis of change in % suppression at day 64 between placebo and 1MIU, placebo and 2MIU, and 1MIU and 2MIU. Error bars indicate mean with SEM. \* $p<0.05$ , ns – not significant. Panels A and C – paired t test; Panel B – Wilcoxon test; Panels D and E – Ordinary one-way ANOVA. Red triangles – placebo; blue squares – 1MIU; green circles – 2MIU.

### **3.3.4. Sustained increase in Treg function three weeks after IL-2.**

Having addressed the first hypothesis, we moved on to the second, which was that any effects of LD-IL-2 immunotherapy on Treg function will persist after the treatment has ceased. Once again, we started by assessing Teff proliferation. Analysis at days 85 and 169 showed an overall reduction in Teff proliferation in all treatment groups, with the greatest decline observed in those on placebo. This decrease in CPM was significant at day 85 (2MIU p=0.0148; 1MIU p=0.0031; placebo p=0.0002) and was further observed at day 169 in the 1MIU (p=0.0114) and placebo (p=0.0171) group when compared to day 1 (figure 3-7 A to F). When analysing the change in proliferation between groups, we see an average reduction in Teff proliferation of 4292 CPM in the placebo group at day 85 which further declines by an average of 6362 CPM at day 169. At 1MIU IL-2 this decrease in proliferation remains relatively unchanged between the two timepoints with a mean decrease of 3736 and 3730 CPM at days 85 and 169 respectively. Finally, in the 2MIU group there is an average reduction of 2146 CPM at day 85 but Teff proliferation improves by day 169 to a mean decrease of 983 CPM. Group comparisons of Teff proliferation show that this reduction is significantly different between placebo and 2MIU at day 169 (p=0.0264) (figure 3-7 G and H).

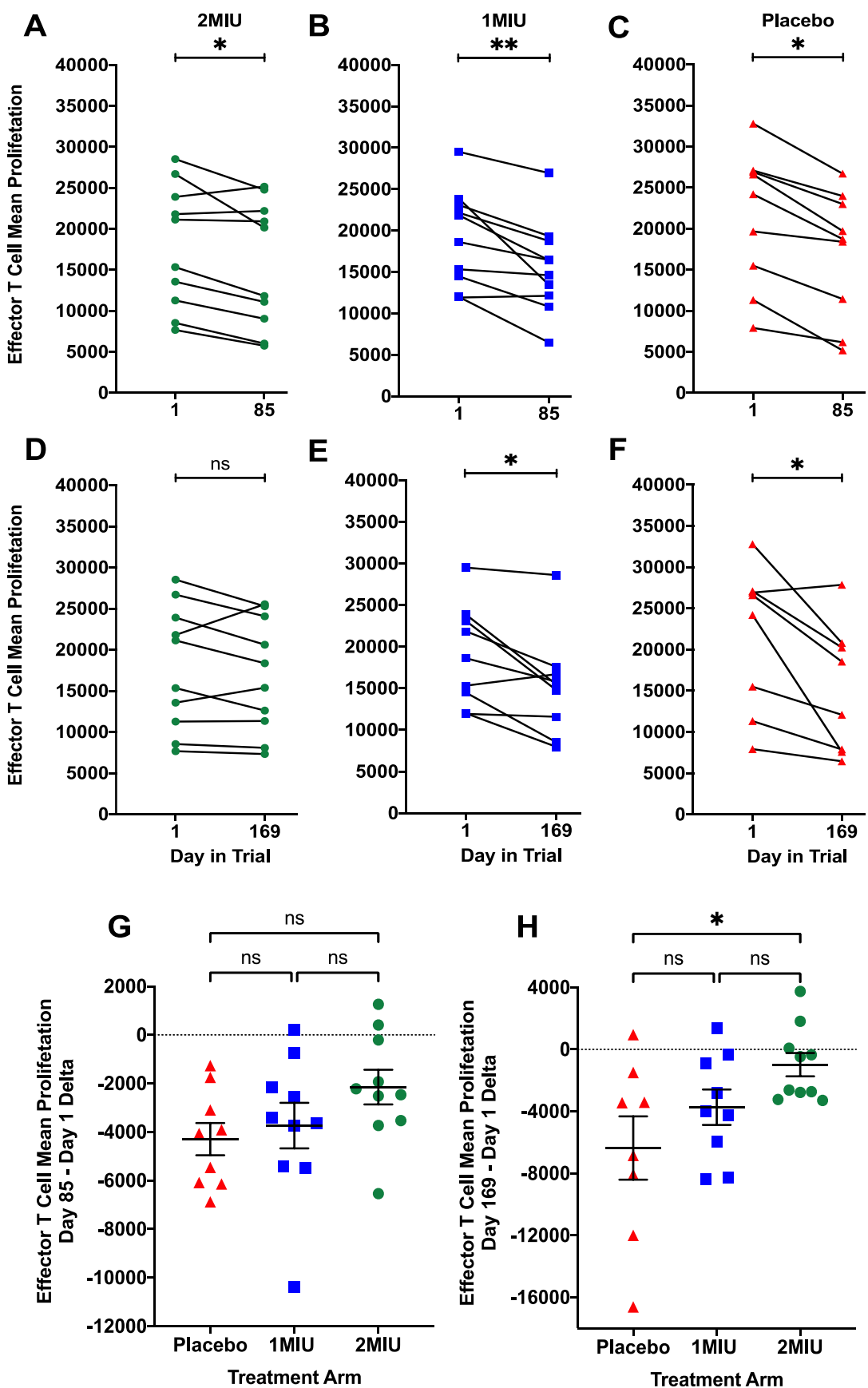


**Figure 3-7 Assessment of mean Teff proliferation at days 85 and 169 versus day 1 in IMODALS treatment groups.** Panels A to C: Analysis of mean Teff proliferation in each treatment group at day 1 and day 85. Panels D to F: Analysis of mean Teff proliferation in each treatment group at day 1 and day 169. Panel G: Analysis of change in mean Teff proliferation at day 85 between placebo and 1MIU, placebo and 2MIU, and 1MIU and 2MIU. Panel H: Analysis of change in mean Teff proliferation at day 169 between placebo and 1MIU, placebo and 2MIU, and 1MIU and 2MIU. Error bars indicate mean with SEM. \*\*p<0.01, \*p<0.05, ns – not significant. Panels A to F – paired t test; Panel B and E – Wilcoxon test; Panels G and H – ordinary one-way ANOVA. Red triangles – placebo; blue squares – 1MIU; green circles – 2MIU.

To address the latter point, we analysed % suppression at Treg:Teff ratio of 1:2 and 1:4 at days 85 and 169. Where Treg and Teff were cocultured at the ratio of 1:2, we do not observe any significant changes in % suppression at these timepoints in either the 2MIU or 1MIU treated groups. There is once again a decrease in % suppression in the placebo group at day 85 and day 169, with the former being significantly lower than day 1 ( $p=0.0319$ ) (figure 3-8 A to F). When we looked at the change in suppression per group, we observed that this decline in function amounted to a mean decrease in % suppression of 11.4% and 21.8% at days 85 and 169 in the placebo group respectively. In the two treated groups however, there is still an average increase of 3.4% in 1MIU and 6.9% 2MIU at day 85. This suggests that there is still an overall effect of IL-2 immunotherapy on Treg function, albeit a small one. By day 169, there is an average decrease in % suppression of 6.5% in the 1MIU group while at 2MIU IL-2 the average % suppression had dropped to 0.6% above baseline. This change in % suppression is significantly different between placebo and 2MIU at day 85 ( $p=0.0163$ ) and day 169 ( $p=0.0071$ ) (figure 3-8 G and H).

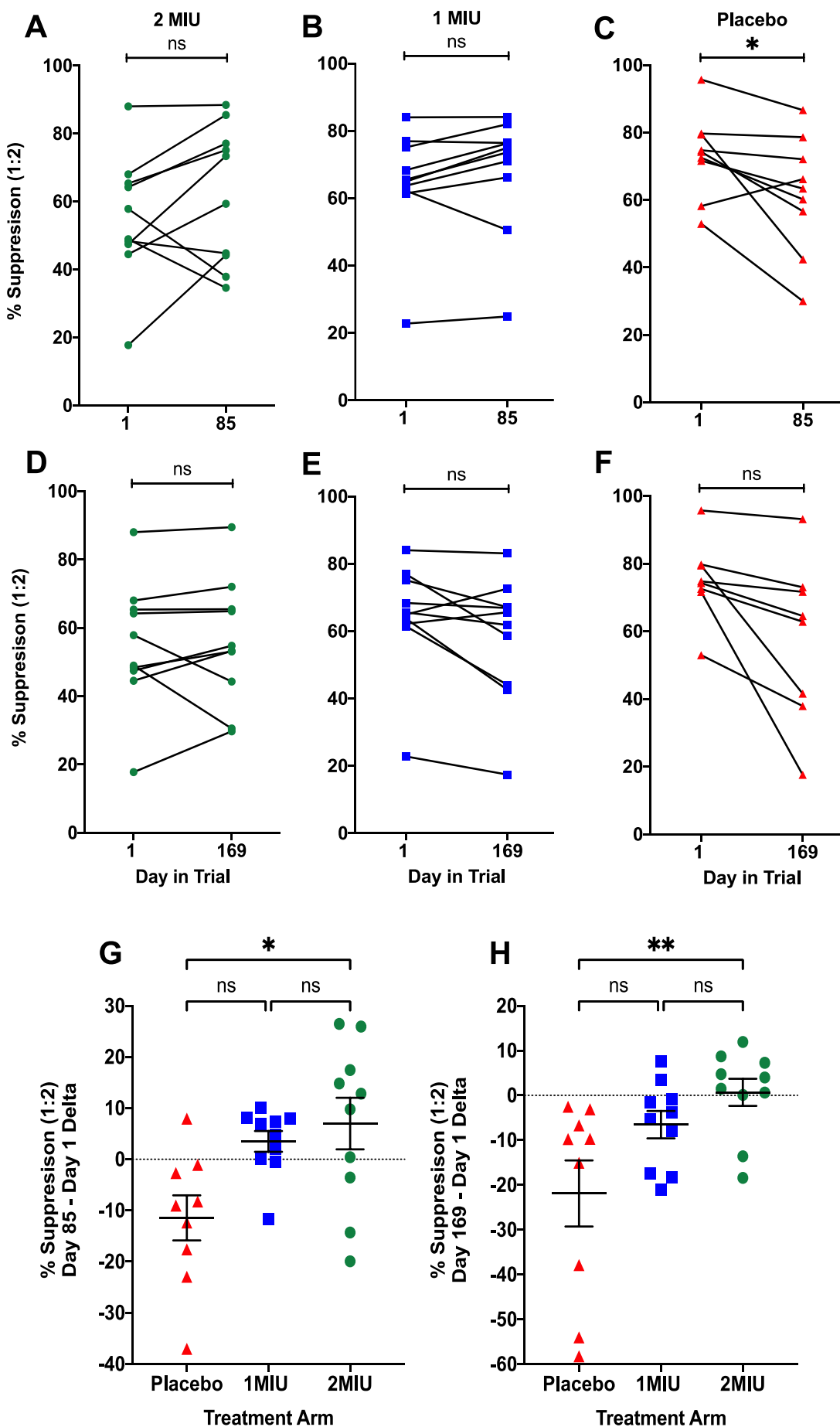


**Figure 3-8 Assessment of % suppression at Treg:Teff ratio of 1:2 at days 85 and 169 versus day 1 in IMODALS treatment groups.** Panels A to C: Analysis of % suppression in each treatment group at day 1 and day 85. Panels D to F: Analysis of % suppression in each treatment group at day 1 and day 169. Panel G: Analysis of change in % suppression at day 85 between placebo and 1MIU, placebo and 2MIU, and 1MIU and 2MIU. Panel H: Analysis of change in % suppression at day 169 between placebo and 1MIU, placebo and 2MIU, and 1MIU and 2MIU. Error bars indicate mean with SEM. \*\*p<0.01, \*p<0.05, ns – not significant. Panels A, C, D, F – paired t test; Panel B and E – Wilcoxon test; Panels G and H – Kruskal-Wallis test. Red triangles – placebo; blue squares – 1MIU; green circles – 2MIU.

At the 1:4 ratio of Treg:Teff, we observe no lasting improvement in Treg ability to suppress autologous Teff. On the contrary, we see an overall decline in % suppression at days 85 (p=0.0002 for 1MIU; p=0.0004 for placebo) and 169 (p=0.0421 for 2MIU; p=0.0015 for 1MIU; p=0.0016 for placebo) in all three groups when compared to day 1 (figure 3-9 A to F). These amount to an average decline of 21.9%, 14.4% and 2.9% at day 85, and 27.3%, 24.7% and 9.7% at day 169 for placebo, 1MIU and 2MIU groups respectively. Group comparisons show this decrease is significantly different at day 85 between placebo and 2MIU (p=0.0195) but not at day 169 as at this visit the % suppression at 2MIU IL-2 has declined further (figure 3-9 G and H). These data show that in IL-2 treated groups, where Treg and Teff are cocultured at a ratio of 1:2, on average, % suppression is maintained at levels above that of day 1, more so at day 85 than 169, indicating a prolonged effect of IL-2 on Treg function. However, altering the ratio to favour Teff, leads to a decline in Treg ability to suppress proliferation.

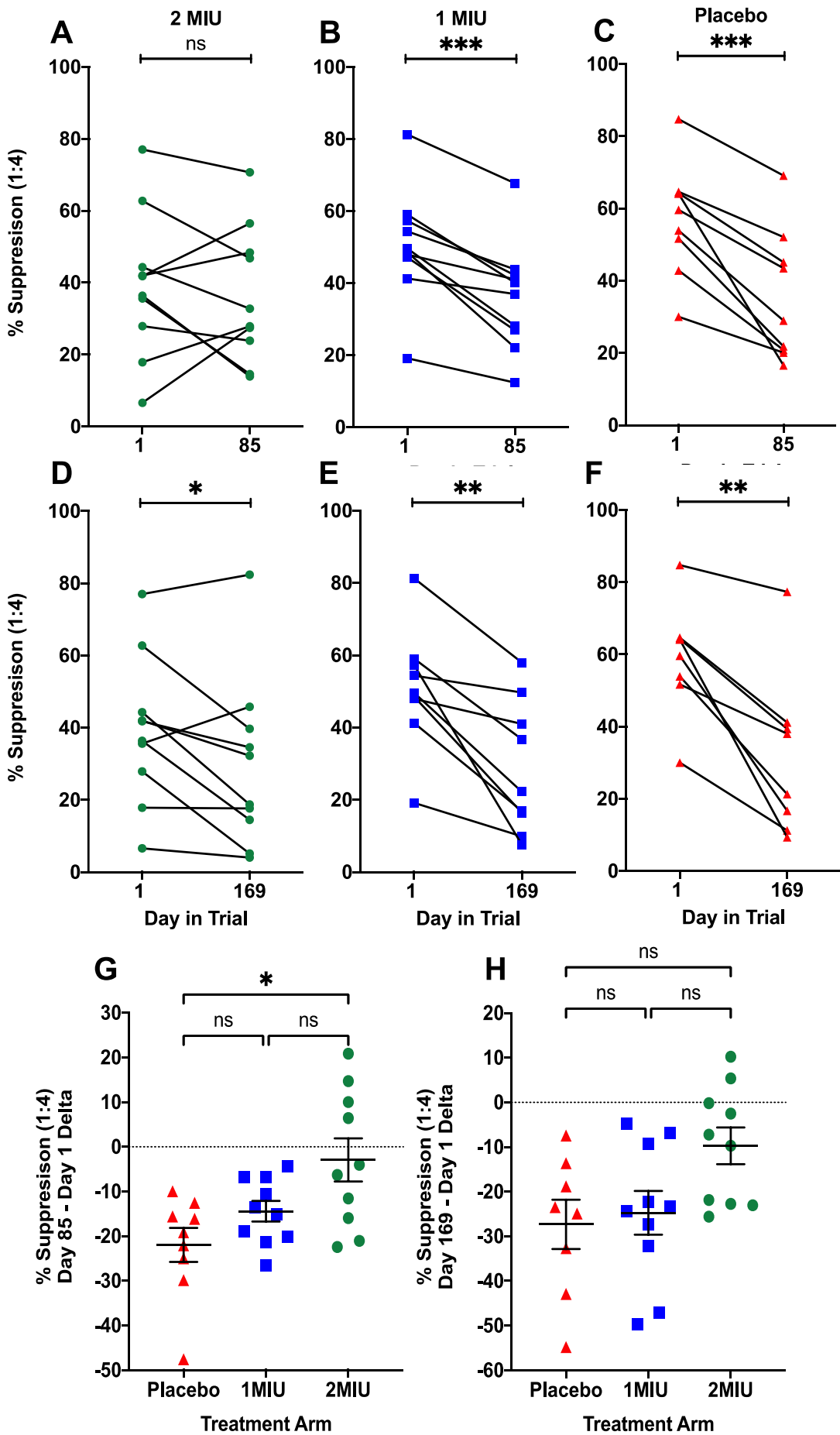


**Figure 3-9 Assessment of % suppression at Treg:Teff ratio of 1:4 at days 85 and 169 versus day 1 in IMODALS treatment groups.** Panels A to C: Analysis of % suppression in each treatment group at day 1 and day 85. Panels D to F: Analysis of % suppression in each treatment group at day 1 and day 169. Panel G: Analysis of change in % suppression at day 85 between placebo and 1MIU, placebo and 2MIU, and 1MIU and 2MIU. Panel H: Analysis of change in % suppression at day 169 between placebo and 1MIU, placebo and 2MIU, and 1MIU and 2MIU. Error bars indicate mean with SEM. \*\*p<0.01, \*p<0.05, ns – not significant. Panels A to F – paired t test; Panel G – Kruskal-Wallis test; Panel H – Ordinary one-way ANOVA. Red triangles – placebo; blue squares – 1MIU; green circles – 2MIU.

### **3.3.5. Is expression of CD25 on Treg associated with increase in Treg suppressive function?**

Although this was not part of the main hypotheses tested in this chapter, we also wanted to assess changes in CD25MFI on Treg and how this relates to Treg suppressive function. Surface CD25 is needed for Treg activation by IL-2, leading to initiation of downstream signalling pathways and subsequent induction of suppressive mechanisms (Lindqvist *et al.*, 2010). Studies in humans and mice have shown that lower CD25 expression can affect some of these Treg suppressive mechanisms, such as decreased IL-10 production and Teff deprivation of IL-2 (Alroqi and Chatila, 2016). IL-2 therapy has been shown to increase CD25 expression levels on Treg and these may be associated with Treg suppressive function (Rosenzwajg *et al.*, 2015; Seelig *et al.*, 2018).

In IMODALS trial participants, we observed significant increases in Treg CD25 MFI at day 64 in 2MIU ( $p=0.0010$ ) and 1MIU ( $p<0.0001$ ) groups only (figure 3-10 A to C). To assess whether these were IL-2 induced and dose-dependent, we once again calculated the change in CD25 MFI between day 64 and day 1 and compared these between groups. At 1MIU IL-2, there was a mean increase of

3295.9 in CD25 MFI while at 2MIU it was 3748.6, these were significantly different when compared to the placebo group ( $p=0.0002$  for 1MIU;  $p<0.0001$  for 2MIU) but not between 1MIU and 2MIU. There were no significant differences in CD25 MFI on Treg at day 1 between treatment groups (figure 3-10 D and E). This shows IL-2 induced but not dose-dependent changes in CD25 MFI on Treg.

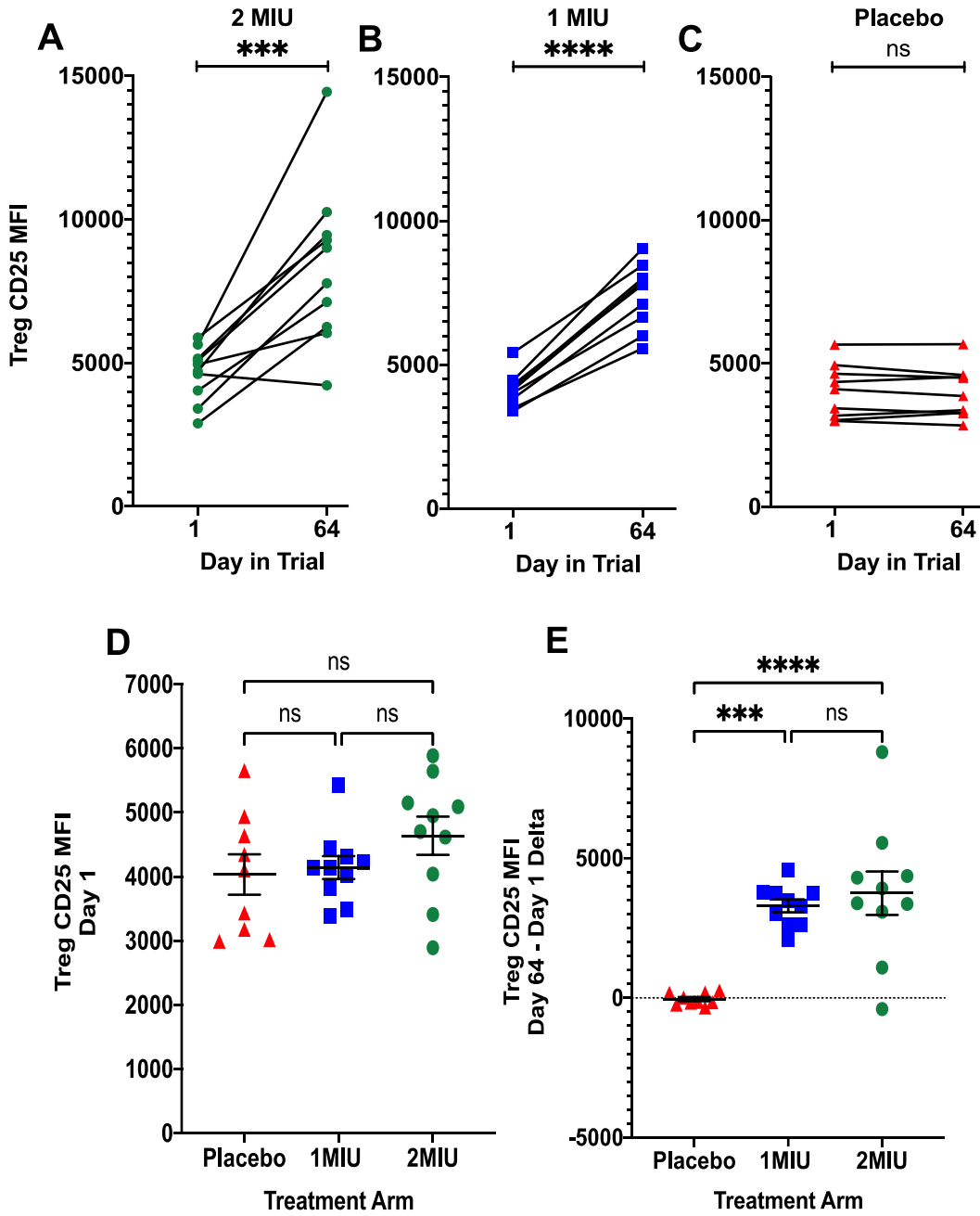


**Figure 3-10 Assessment of CD25 MFI on Treg at day 1 and day 64 in IMODALS treatment groups.**

Panels A to C: Analysis of CD25 MFI on Treg in each treatment group at day 1 and day 64. Panel D: Analysis of CD25 MFI on Treg at day 1 between placebo and 1MIU, placebo and 2MIU, and 1MIU and 2MIU. Panel E: Analysis of change in CD25 MFI on Treg at day 64 between placebo and 1MIU, placebo and 2MIU, and 1MIU and 2MIU. Error bars indicate mean with SEM. \*\*\*\*p<0.0001, \*\*\*p<0.001, ns – not significant. Panels A to C – paired t test; Panels D and E – ordinary one-way ANOVA. Red triangles – placebo; blue squares – 1MIU; green circles – 2MIU.

To assess whether this increase in CD25 MFI on Treg is associated with suppressive function, we calculated percentage change for both variables and performed simple linear regression analysis. We observe a significant correlation ( $p=0.0013$ ) and a positive linear relationship between the two measurements with an  $R^2$  value of 0.3242 (figure 3-11). This data indicates that change in suppression is associated with the change in CD25 MFI on Treg, which in this analysis, is affected by two main factors:

1. Person-to-person variability in response to IL-2 with regards to change in Treg CD25 MFI and suppressive function.
2. Sample size.

There is no way to control, or even predict, how great or small a change in suppressive function or CD25 MFI there will be in a person when given IL-2. However, the fact that this relationship is seen in such a small cohort suggests that having larger patient groups could ameliorate the effects of inter-individual variability on these findings and further improve the  $p$  and  $R^2$  values.

### Change in Treg CD25 MFI vs Change in Suppression

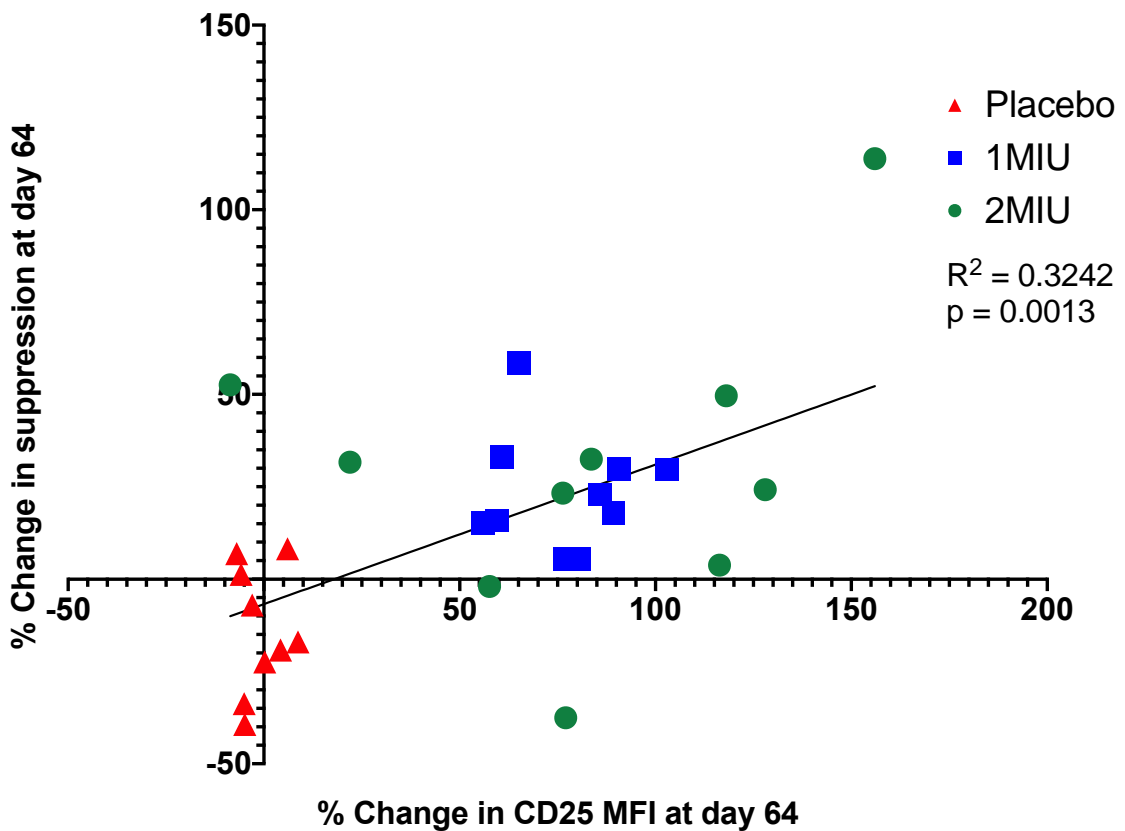


**Figure 3-11 Analysis of percentage change in Treg expression of CD25 and suppressive function.** A percentage change was calculated for Treg CD25 MFI and suppressive function at day 64. The two variables were correlated using simple linear regression.  $R^2 = 0.3242$ ,  $p = 0.0013$ . Red triangles = placebo; blue squares = 1MIU IL-2; green circles = 2MIU IL-2.

As with other analyses in this chapter, we also wanted to assess whether this increase in CD25 expression on Treg persisted after the therapy has stopped. Interestingly, we observed a significant decrease in CD25 MFI on Treg in the 2MIU ( $p=0.0020$  for day 85 and 169) and placebo ( $p=0.0263$  at day 169) groups (figure 3-12 A to F). This decrease amounted to a mean reduction of 634.3 in fluorescence intensity of CD25 at day 85 in the 2MIU group, which was significantly different when compared to placebo ( $p=0.0231$ ) and 1MIU ( $p=0.0076$ ). This decrease persisted up to day 169 in the 2MIU group however it

was no longer significantly different when compared to the other two groups, likely driven by a decline in CD25 expression on Treg in the placebo and 1MIU groups (figure 3-12 G and H). Day 85 would have been the start of treatment cycle four, if the IMODALS study had continued, which raises the question of whether this decline in CD25 MFI would have an effect on Treg response to the next cycle. We will never know the answer to this with regards to this study however, we will assess whether this decrease in CD25 expression has affected IL-2 signalling in Treg in chapter 4.

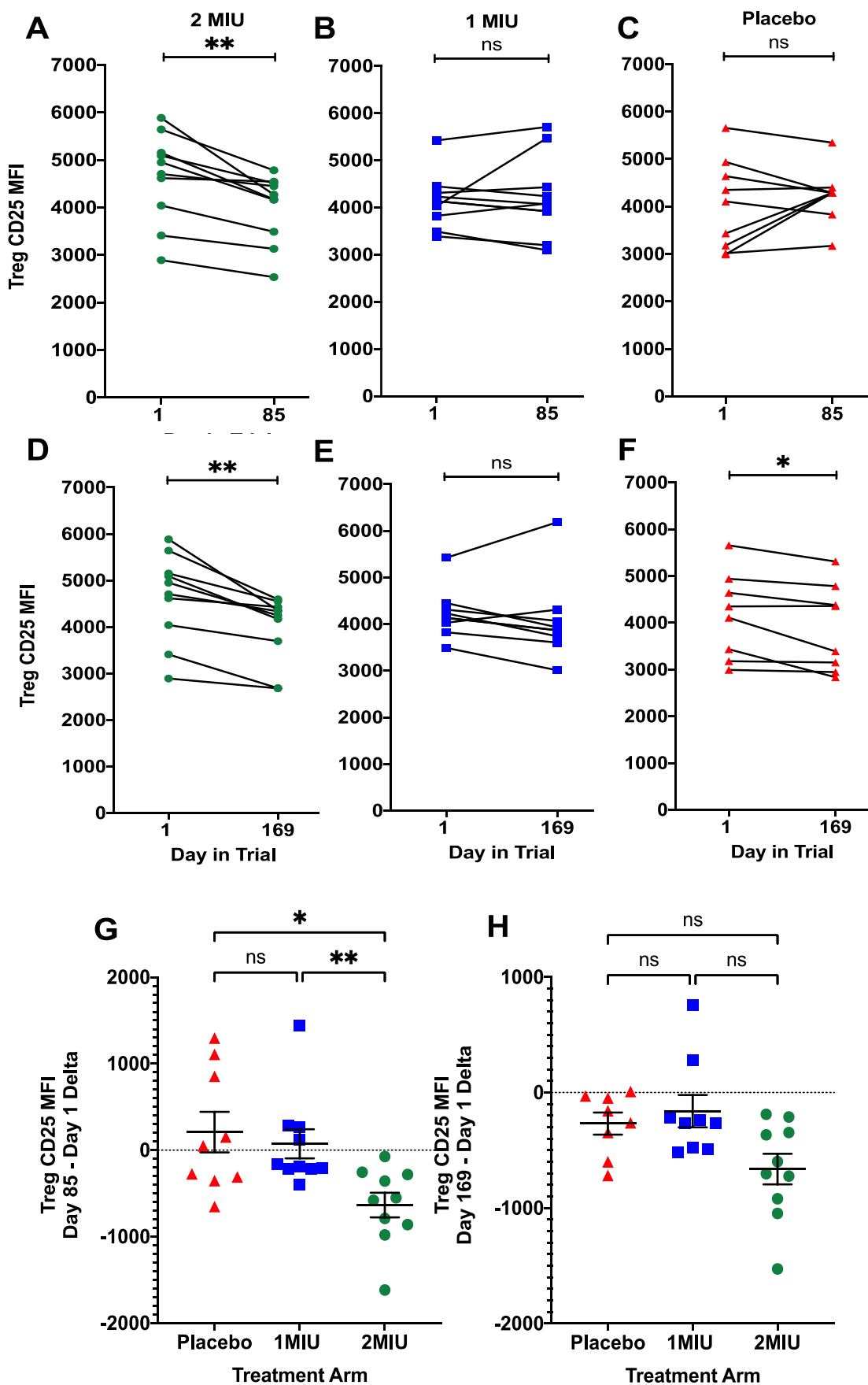


**Figure 3-12 Assessment of CD25 MFI on Treg at days 85 and 169 versus day 1 in IMODALS treatment groups.** Panels A to C: Analysis of CD25 MFI on Treg in each treatment group at day 1 and day 85. Panels D to F: Analysis of CD25 MFI on Treg in each treatment group at day 1 and day 169. Panel G: Analysis of change in CD25 MFI on Treg at day 85 between placebo and 1MIU, placebo and 2MIU, and 1MIU and 2MIU. Panel H: Analysis of change in CD25 MFI on Treg at day 169 between placebo and 1MIU, placebo and 2MIU, and 1MIU and 2MIU. Error bars indicate mean with SEM. \*\*p<0.01, \*p<0.05, ns – not significant. Panels A, B, D, E, F – Wilcoxon test; Panel C – paired t-test; Panels G – Kruskal-Wallis test; Panel H – ordinary one-way ANOVA. Red triangles – placebo; blue squares – 1MIU; green circles – 2MIU.

### 3.4. Discussion.

In this chapter we set out to test the hypothesis that 3 cycles of LD-IL-2 will significantly improve Treg ability to suppress autologous Teff in *in vitro*, and that this increase in suppressive capacity may be sustained for an extended period of time following the cessation of IL-2 injections. To assess this, we used the Treg micro-suppression assay incorporating [<sup>3</sup>H] thymidine, previously designed and optimised in our laboratory. This was the preferred method as it was designed to robustly assess Treg function in cryopreserved PBMC using low cell numbers. Other techniques are available, such as CFSE labelling of Teff and subsequent assessment of cell division following coculture with Treg. Generally, this experimental set up uses Teff and Treg isolated from peripheral blood as the cell numbers needed to accurately assess cell division are in the x10<sup>4</sup> range (Venken *et al.*, 2007; Koreth *et al.*, 2011). To acquire this many Teff may not have been an issue from cryopreserved trial participant PBMC, as they are the most abundant CD4<sup>+</sup> T cell population. However, Treg represent ~5 – 10 % of all CD4<sup>+</sup> T cells (Stelmaszczyk-Emmel *et al.*, 2013) and the mean yield of viable PBMC thawed from IMODALS participants was ~2 x10<sup>6</sup> (data not shown), therefore there may have been a deficit in Treg availability for CFSE based cell division

analysis. Our choice of this method is further supported by other studies in T1D, MS and myasthenia gravis where robust data for Treg suppression using [<sup>3</sup>H] thymidine incorporation has been shown, identifying significant differences in Treg function between healthy control and patient groups (Viglietta *et al.*, 2004; Balandina *et al.*, 2005; Brusko *et al.*, 2005). A caveat of using [<sup>3</sup>H] thymidine method is that in theory the proliferation we are measuring after coculture could be that of Treg, B cells, Teff or a combination of all three, as we have not labelled Teff with CFSE. Data from past studies suggests that PHA is predominantly a T cell activator, with no effect on B cells however, B cell proliferation could be induced by a T cell mitogenic factor as a result of their activation (Phillips and Weisrose, 1974; Miller, 1983; Ceuppens *et al.*, 1988). Our own method validation data (not shown) during assay optimisation suggests that this may not be the case. Combinations of Treg and B cells, Treg and Teff, Teff and B cells and, B cells and Treg cells on their own, showed the resultant proliferation values to be below the acceptable threshold of 3000 CPM per well. Therefore, suppression of proliferation is only visible when Treg and B cells are added to Teff. Furthermore, a study comparing CFSE and [<sup>3</sup>H] thymidine assessment of Treg suppression in MS and healthy controls has shown significant correlations between the proliferation values of the two methods ( $p<0.01$ ,  $R^2>0.9$ ) across all participants, indicating little difference between results of these experimental set ups (Venken *et al.*, 2007). As for [<sup>3</sup>H] thymidine assay robustness, our own performance data show excellent reproducibility across the 10 experimental batches, with a CV of <20% when assessing variables such as Treg and Teff frequency, % suppression, Teff CPM and MFI of CD25 on Treg and Teff in a single QC PBMC sample.

Before addressing the hypotheses, we wanted to investigate whether the Treg frequencies obtained in cryopreserved PBMC in the micro-suppression assay are representative of those in peripheral blood (chapter 2). Viable Treg are needed to assess their suppressive function *in vivo* and cryopreservation has been shown to affect the viability of activated Treg with increased expression of CD25 (Seale *et al.*, 2008). We were particularly concerned about patient Treg from day 64, as this is where we observed the greatest expansion in the previous chapter. However, our analysis shows excellent concordance between peripheral blood and cryopreserved Treg at days 1, 64, 85 and 169 ( $p<0.0001$  for all timepoints).

We used the Treg micro-suppression assay to assess whether IL-2 significantly improved Treg suppressive ability in ALS. Before this, we assessed whether IL-2 therapy resulted in increased Teff proliferation and observed no significant changes. It was important to address this because in chapter 2, we observed significant increases in Teff number in both IL-2 treated groups and, an increase in Teff proliferation may have a direct effect on Treg suppressive function. Therefore, any increase in Treg suppressive function could not be solely attributed to IL-2 therapy. However, we show that this is not the case and the increase in Teff number did not result in increased proliferation as a result of IL-2. As for Treg function, IL-2 induced an increase in Treg suppressive function (1:2 and 1:4 Treg to Teff), which was highly significant in the 1MIU group, while only a trend towards significance is observed in the 2MIU group, largely due to the greater variation in response between individuals. These changes accounted for mean increases of 11.6% and 13.7% in % suppression at 1:2 Treg to Teff ratio and a 6.90% and 10.31% mean increase at 1:4 Treg to Teff in the 2MIU and 1MIU

IL-2 groups respectively. These were significantly greater when compared to the 9.49% and 3.06% mean reductions in % suppression at 1:2 and 1:4 in those on placebo. When performing group comparisons, we observed a caveat in our data, at day 1, the % suppression was significantly lower at 2MIU when compared to placebo. Ideally the day 1 % suppression values would not be significantly different between 2MIU and placebo however this is not something that is always possible to control for, especially as Treg function has been shown to be affected in ALS patients. Whether these Treg suppression findings are in line with published data from other IL-2 immunotherapy trials is unclear, as the aforementioned study of IL-2 in GVHD only report effective Treg suppression of autologous Teff after *in vivo* expansion and not before (Koreth *et al.*, 2011). The SLE study does show a significant increase in Treg suppression by comparison before and after IL-2 therapy however, in this case the SLE patient Treg were suppressing Teff of healthy individuals (He *et al.*, 2016). In that respect, we believe IMODALS is the first, placebo-controlled trial of LD-IL-2 showing a significant improvement in Treg function by Treg suppression of autologous Teff before and after therapy. With regards to ALS, a significant impairment in Treg ability to suppress autologous Teff has been shown in patients when compared to healthy individuals, this impairment negatively correlates with disease progression (Beers *et al.*, 2017). When expanded *in vitro* with IL-2 and rapamycin, suppression of autologous Teff by Treg in these ALS patients was restored to similar levels of healthy controls suggesting that the way to slow disease progression is by *in vitro* expanded autologous Treg infusions (Beers *et al.*, 2017). The effectiveness of these infusions were assessed in three ALS patients, followed for 70 weeks, and did show that Treg function can be improved by

infusion of autologous Treg expanded by recombinant IL-2 (4 infusions at early stage and 4 infusions at late stage of disease), followed by daily injection of subcutaneous IL-2 and, this combination did slow disease progression (Thonhoff *et al.*, 2018). Our study shows that subcutaneous injection of IL-2 alone can significantly improve Treg function in ALS patients and although, IMODALS was not powered to detect clinical changes, as the participants were all at a stable disease phase followed for 22 weeks only these findings do warrant further investigation on whether subcutaneous IL-2 alone can slow disease progression. To that end, clinical efficacy of IL-2 in ALS is now being assessed in a large, phase II clinical trial, with a longer follow-up.

To assess whether increase in Treg function was sustained, we analysed % suppression at days 85 and 169. As before, we assessed Teff proliferation first and interestingly, observed an overall decline in each group, at both day 85 and 169. Given that we did not observe any change in Teff proliferation at day 64 and, this decline is present in the placebo group also, we cannot attribute IL-2 to this. Inadequate PHA stimulation may cause this but, we would have observed greater variation in Teff proliferation of the QC sample. It could be related to disease progression as it is observed in all participants regardless of treatment however, as previously discussed our clinical measures did not show any significant motor neurone decline. But the measures were not sensitive enough to assess a decline in progression in any of the treatment groups over the course of the study. Therefore, it is possible that this is related to disease progression, but we cannot attribute this with certainty. As for % suppression, we observe that at 1:2 Treg to Teff ratio, there is still a mean increase in suppression at 2MIU IL-2 at day 85.

This suggests that 2MIU IL-2 resulted in sustained Treg function, which is important as to achieve clinical efficacy, not only greater number but also increased suppressive capacity of Treg would need to be sustained. The benefit of sustained Treg function by IL-2 is further observed by showing the continued decline in % suppression in participants on placebo.

Finally, we assessed whether the increase in Treg function, is related to the expression of CD25 MFI on Treg. We observe significant increases in CD25 MFI on Treg at both IL-2 doses and, this increase significantly correlates with the increase in % suppression. Although this was not part of the main hypothesis testing, we thought it was important to assess this as, the high affinity IL-2R (CD25) is needed for Treg activation by IL-2, and changes in expression have been shown to affect Treg suppressive mechanisms (Lindqvist *et al.*, 2010; Alroqi and Chatila, 2016). LD-IL-2 trials have shown that the expression of CD25 on Treg increases in response to therapy (Rosenzwaig *et al.*, 2015; Yu *et al.*, 2015; Todd *et al.*, 2016). Furthermore, in ALS it has been suggested that along with Treg dysfunction, there may also be an impairment in Treg responsiveness to IL-2, and this impairment in function may not be restored by LD-IL-2 therapy, but rather *in vitro* expansion and subsequent infusion of autologous Treg (Thonhoff *et al.*, 2018). Our data for increases in CD25 MFI, Treg suppressive function, Treg number, and the relationship between CD25 expression and Treg function suggests no intrinsic impairment in Treg responsiveness to LD-IL-2 *in vivo* in our ALS cohort. Further warranting the need for assessment of clinical efficacy of LD-IL-2 to slow disease progression in ALS. When assessing whether this increase in CD25 expression on Treg was sustained, we observed the opposite, a

significant reduction in CD25 MFI at the highest dose at days 85 and 169. Although we show significant expansion of Treg and an increase in Treg function by IL-2 in ALS, this reduction in CD25 expression would suggest that continuous IL-2 therapy may affect Treg responsiveness to IL-2. Which in turn may affect Treg expansion at the next treatment cycle as other studies have shown that a maximal increase in Treg expansion occurs at 4 weeks after the start of IL-2, but these maximal levels are not reached with continuous therapy (Koreth *et al.*, 2016). We cannot determine whether this is the case as IMODALS consisted of three cycles of IL-2 only. But we can further assess whether Treg responsiveness to IL-2 is affected by way of measuring phosphorylation of STAT5 proteins downstream of the IL-2R. IL-2 signalling may also aid in addressing the variability in Treg and non-Treg responses we see between individuals.

# **Chapter 4. Investigating the effects of LD-IL-2 therapy**

## **on IL-2 signalling in Treg and non-Treg cells.**

### **4.1. Introduction.**

Treg are very responsive to IL-2 stimulation, largely due to their high affinity IL-2 receptor (Matsuoka, 2018). Because of this, we, and several others, have used LD-IL-2 to preferentially expand Treg. Other than IMODALS, clinical trials in pathologies such as SLE, T1D and GVHD have shown the benefits of LD-IL-2 in terms of *in vivo* Treg expansion (Koreth *et al.*, 2011; Hartemann *et al.*, 2013; Von Spee-Mayer *et al.*, 2016). All trials also show a large variation between participants in terms of the observed Treg expansion, this is also true for the IMODALS participants. This could be the result of the level of stimulation that IL-2 gives to Treg. One of the ways this level of stimulation could be determined is by measuring phosphorylated STAT5 (pSTAT5) after *in vitro* exposure to graded doses of IL-2. Using this measure, scientists were able to detect disease associated defects in IL-2 signalling, a link between IL-2 signalling and Treg function and associations between genetic polymorphisms and IL-2 signalling (Garg *et al.*, 2012; Cerosaletti *et al.*, 2013; Yang *et al.*, 2015). For the IMODALS study, we wanted to use this technique and investigate whether IL-2 signalling at day 1, is related to the Treg expansion we saw at day 64, and possibly account for the variable expansions of Treg observed in trial participants. As we observed effects of LD-IL-2 on non-Treg cells (NK, Teff and CD8<sup>+</sup> T cells), we also wanted to assess whether the expansion of these populations at day 64, correlates with IL-2 signalling levels at day 1. Finally, as IMODALS consisted of three cycles of treatment, we also wanted to assess whether this continuous exposure to

subcutaneous IL-2 affected Treg IL-2 signalling. A recent phase 2 study in GVHD patients receiving daily doses of  $1 \times 10^6$  IU/m<sup>2</sup> IL-2 for 12 weeks, showed that the Treg number peaked at week 4, but continued therapy did not result in greater Treg expansion. This could be related to the increase in Treg expressing CD25 and the levels of soluble CD25 in circulation, likely due to shedding by Treg and Teff, which could limit the availability of IL-2 for further expansion of Treg (Koreth *et al.*, 2016). Data presented in chapter 3 showed a reduction in CD25 expression on Treg at 2MIU IL-2 at day 85, whether this is due to shedding is not known. This reduction may not affect IL-2 availability, but it could limit IL-2 binding to CD25 on Treg thus affecting IL-2 signalling downstream of the receptor. In turn, this could affect Treg expansion at the next treatment cycle.

In this chapter we will test the following three hypotheses:

1. Treg IL-2 signalling at baseline correlates with Treg expansion in response to therapy.
2. Effects of LD-IL-2 therapy on non-Treg cells can also be predicted by determining IL-2 signalling at baseline.
3. Continued IL-2 therapy might affect Treg IL-2 signalling.

To test these hypotheses, we selected patient samples corresponding to day 1 and day 85 visits in the study. Conventionally, pSTAT5 is measured by Phosflow to assess IL-2 signalling in Treg, I wanted to refine this assay in a number of ways:

1. Allow for assessment of IL-2 signalling in CD8<sup>+</sup> T cells, NK cells and their subsets, as well as memory and naïve cells.

This required extensive testing of antibody combinations to identify one that was compatible with the fixation and permeabilisation needed for pSTAT5 exposure and FoxP3 staining.

2. The ability to control the assay to a high level of precision to look for subtle differences between individuals as well as the effects of therapy.

To improve experimental reproducibility while at the same time allowing for a greater number of patient samples to be processed in a single experiment, the violet-fluorescent cell barcoding technique was used. This method allows multiple patient samples, stimulated with one concentration of IL-2, to be tagged (barcoded) with covalently bound fluorescent dyes of different concentrations, following which, the samples can be combined into one test tube, stained with a cocktail of monoclonal antibodies, acquired on a flow cytometer and subsequently identified based on the fluorescence profile of the barcode. To assess variability, we used two internal biological control samples. To reveal the subtle differences between individuals or the effects of therapy, we carefully selected doses of IL-2 that led to reproducible but submaximal levels of stimulation in target cell populations.

#### **4.2. Materials and methods.**

##### **Preparation of assay media and reagents:**

###### **Thawing media:**

X-VIVO supplemented with PSF and 10% FBS, filtered using 0.45 $\mu$ m microfilter and pre-warmed to 37°C prior to thawing of PBMC.

Staining buffer:

PBS supplemented with 2mM EDTA and 1% AB, filtered using 0.45µm microfilter.

Culture media:

X-VIVO supplemented with PSF and 1% AB, filtered using 0.45µm microfilter.

Stimulation media:

X-VIVO supplemented with PSF, 1% AB, 0.5 units or 10 units of IL-2, filtered using 0.45µm microfilter and pre-warmed to 37°C prior to use.

Transcription Factor Phospho (TFP) fixation and permeabilisation buffer (BD):

The 4x fixation and permeabilisation concentrate was diluted down to 1x concentration with the diluent provided in the kit. The buffer was kept and used at 4°C throughout the experiment.

TFP permeabilisation wash buffer (BD):

The 5x wash buffer was diluted down to 1x concentration with distilled water. The buffer was kept and used at 4°C throughout the experiment.

Fluorescent cell barcoding wash buffer (BD):

The 4x barcoding wash buffer concentrate was diluted down to 1x concentration with PBS. The buffer was kept and used at 4°C throughout the experiment.

Perm Buffer III (BD):

Perm buffer III was used at stock concentration to expose phosphorylated proteins in cells.

Perm buffer III was diluted to 50% of stock concentration with PBS for cell barcoding (50% perm buffer III).

Violet-fluorescent cell barcoding dyes (BD):

Stock concentrations of cell barcoding dye 450 and 500 (CBD450 and CBD500) were diluted with dimethyl sulfoxide (DMSO) to prepare the CBD450 high,

CBD450 medium, CBD450 low and CBD500 high, CBD500 medium and CBD500 low concentration barcode dyes. First, CBD450 and CBD500 were reconstituted with 1mL of each and mixed thoroughly by vortexing. Following this, the two dyes were transferred to 15mL conical tubes and a further 5.82mL of DMSO was added. This made the CBD450 and CBD500 high barcodes. From these high concentrations of barcode, 1.5mL was removed and added to 15mL conical tubes containing 4.5mL of DMSO and making the CBD450 and CBD500 medium barcode dyes. Finally, from these medium concentration dyes, 1mL was removed and transferred to 15mL conical flasks containing 4mL of DMSO thus making the CBD450 and CBD500 low concentrations of barcode dye. These were aliquoted

into vials of 40 $\mu$ L each and stored at -80°C.

Prior to use, the vials containing CBD450 and CBD500 high, medium and low dyes were thawed and a grid of up to 16 different concentrations of barcode dyes was prepared by mixing 20 $\mu$ L of each CBD450 dye with each of CBD500 concentration of dye as represented in the figure on the right.

| DMSO<br>DMSO<br>Cells  | 450 L<br>DMSO<br>Cells  | 450 M<br>DMSO<br>Cells  | 450 H<br>DMSO<br>Cells  |
|------------------------|-------------------------|-------------------------|-------------------------|
| DMSO<br>500 L<br>Cells | 450 L<br>500 L<br>Cells | 450 M<br>500 L<br>Cells | 450 H<br>500 L<br>Cells |
| DMSO<br>500 M<br>Cells | 450 L<br>500 M<br>Cells | 450 M<br>500 M<br>Cells | 450 H<br>500 M<br>Cells |
| DMSO<br>500 H<br>Cells | 450 L<br>500 H<br>Cells | 450 M<br>500 H<br>Cells | 450 H<br>500 H<br>Cells |

**Preparation of fluorescent barcode dye grid.**

### **PBMC stimulation with IL-2:**

Cryopreserved patient PBMC were thawed and viability assessed using the same technique as in chapter 2. Following which, the PBMC were resuspended at a concentration of  $1 \times 10^6$  cells/100 $\mu$ L of culture media in triplicate. The cells were then stimulated with 0.5, 10 units of IL-2 or left unstimulated for 30 minutes at 37°C.

### **Sample Barcoding:**

Following stimulation, the cells were fixed and permeabilised by adding 2mL of 1x TFP fixation and permeabilisation buffer and incubating at 4°C for 50 minutes in the dark. The cells were then washed twice, first with 1mL of 1x permeabilisation wash buffer at 500g for 15 minutes at 4°C, followed by 2mL of 1x permeabilisation wash buffer and 10 minutes of centrifugation. The supernatant was poured off, cell pellet resuspended using a vortex, and phosphorylated proteins were exposed by gradually adding 1mL of perm buffer III. The samples were incubated for 20 minutes at 4°C. The cells were then pelleted by centrifugation at 500g for 8 minutes at 4°C. The excess perm buffer III was poured off, the cell pellet resuspended using a vortex and then washed and pelleted twice by adding 2mL of 1x permeabilisation wash and centrifuging at 500g for 8 minutes at 4°C. The cell pellet was resuspended in 500µL of 50% perm buffer III, transferred to previously prepared barcode mixtures and incubated for 30 minutes at 4°C in the dark. The cells were then washed by adding 1.5mL of 1x barcoding wash buffer, pelleted by centrifugation, the supernatant poured off and cell pellet resuspended using a vortex. The washing and pelleting steps were repeated for a further two times, but with 2mL of 1x barcoding wash buffer. Following the second wash, the cell pellet was resuspended in 90µL of 1x permeabilisation wash buffer. The cells were ready for staining with surface and intracellular monoclonal antibodies (table 4-1).

### **Flow Cytometry:**

To reduce staining variability, a master mix of all necessary antibodies was made up in brilliant stain buffer plus (Beckton Dickinson) in a FACS tube prior to staining of PBMC. The cells were first stained with a master mix of intracellular target

antibodies FoxP3 AF488 and pSTAT5 AF647 for 15 minutes at 4°C in the dark. Following the 15 minutes, a master mix containing the remaining monoclonal antibodies CD3 BUV395, CD4 BUV661, CD8 BUV737, CD25 PE-Cy7, CD45RA PercP, CD56 BV711 and CD16 PE was added to the cells which were then incubated for a further 45 minutes 4°C in the dark. The cells were then washed with 2mL of 1x permeabilisation wash buffer and pelleted by centrifugation at 500g for 5 minutes at 4°C. The supernatant was then poured off and cell pellet resuspended in 350µL of staining buffer. The samples were acquired on a BD FACSymphony flow cytometer.

| Target | Conjugate | Clone  | Origin | Volume / Test (µL) | Manufacturer |
|--------|-----------|--------|--------|--------------------|--------------|
| CD3    | BUV395    | UCHT1  | Mouse  | 10                 | BD           |
| CD4    | BUV661    | SK3    | Mouse  | 5                  | BD           |
| CD8    | BUV737    | SK1    | Mouse  | 5                  | BD           |
| CD25   | PE-Cy7    | M-A251 | Mouse  | 5                  | BL           |
| CD45RA | PERCP     | HI100  | Mouse  | 5                  | BL           |
| FOXP3  | AF488     | 236A   | Mouse  | 5                  | BD           |
| pSTAT5 | AF647     | pY694  | Mouse  | 20                 | BD           |
| CD56   | BV711     | HCD56  | Mouse  | 5                  | BL           |
| CD16   | PE        | B73.1  | Mouse  | 5                  | BL           |

**Table 4-1. Details of surface and intracellular monoclonal antibodies used to stain the IMODALS**

**PBMC.** BL = BioLegend; BD = Beckton Dickinson.

### Data Analysis:

Frequencies of pSTAT5<sup>+</sup> Treg, Teff, NK and CD8<sup>+</sup> T cells from patient sample data were extracted from the barcoded grids using manual gating in FlowJo version 9 (Tree Star) according to the gating strategy in figure 4-1 A and B. First total lymphocytes for all patient samples analysed in that particular experiment were gated. Then aggregated cells and debris were removed by gating on single cells only. Following this, target cell populations of CD56<sup>+</sup> NK cells, CD3<sup>+</sup>CD4<sup>+</sup>

and CD3<sup>+</sup>CD8<sup>+</sup> T cells were gated. Then, for each of these cell populations, patient samples (S1 D1 = patient sample 1, day 1) were gated on in the barcoded grid. In patient and QC samples, further gating was performed to identify Treg (CD25<sup>hi</sup>FoxP3<sup>+</sup>) and Teff (CD25<sup>+lo</sup>FoxP3<sup>-</sup>) and their CD45RA<sup>+</sup> and CD45RA<sup>-</sup> subsets. These two subsets were also gated on in CD8<sup>+</sup> T cells (figure 4-1 A). Once the lymphocyte populations of interest were identified, we assessed the expression of pSTAT5 by gating on pSTAT5+ cells in the unstimulated samples first, and then applying this gate to the samples stimulated with 0.5U and 10U of IL-2 (figure 4-1 B). The analysis shown in figure 4-1 B is that for Treg, but the same principle was applied to NK, Teff, CD8<sup>+</sup> T cells and their CD45RA<sup>+</sup> and CD45RA<sup>-</sup> subsets.

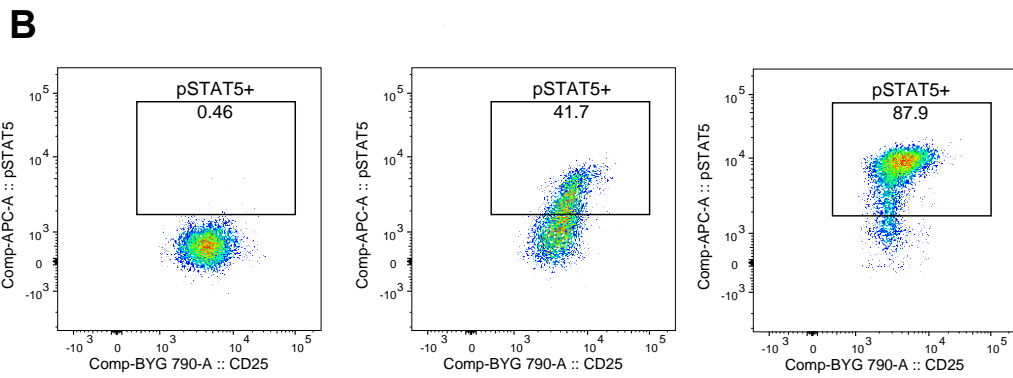
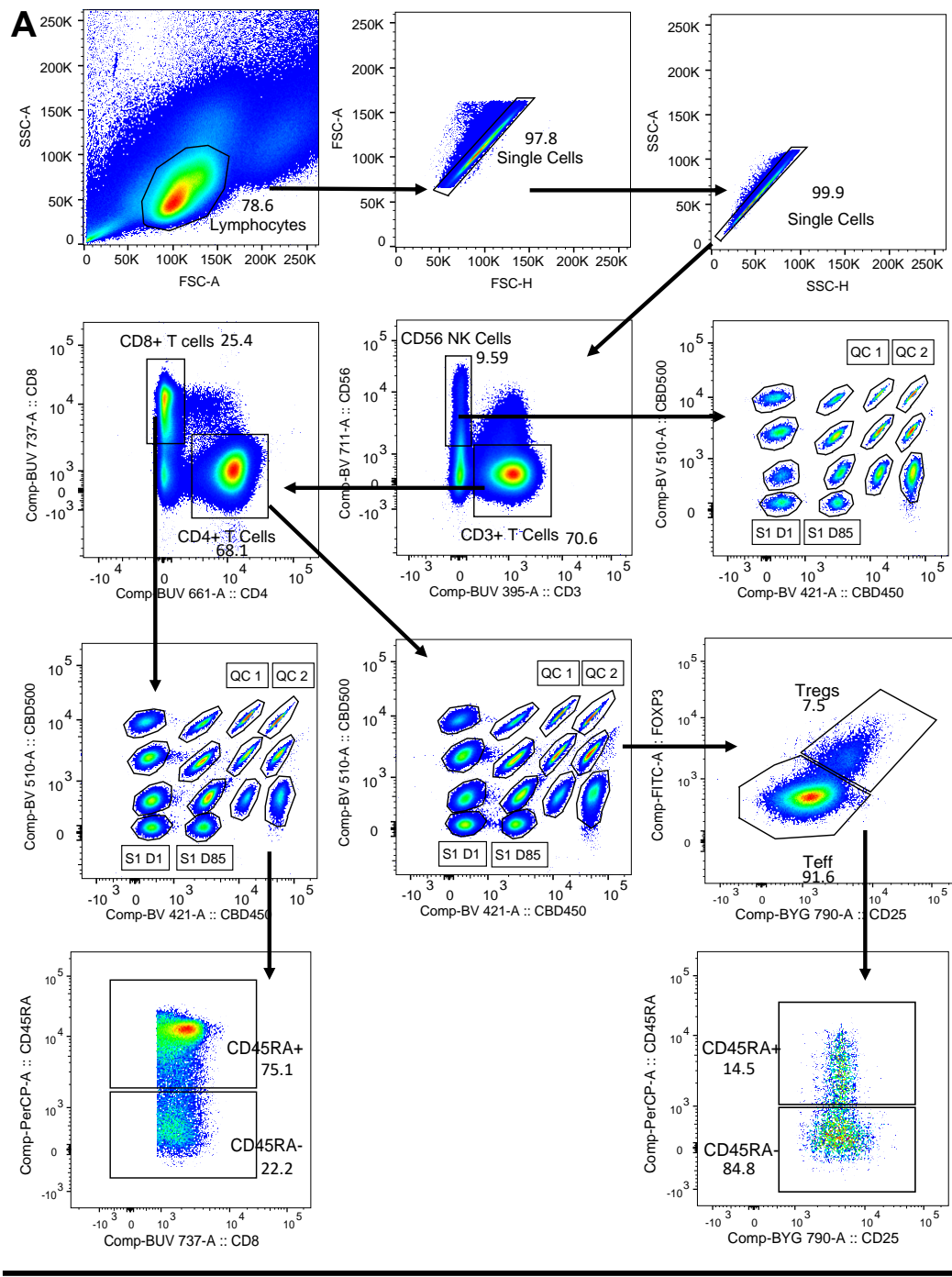


**Figure 4-1 Representative gating scheme for analysis of barcoded IMODALS patient samples.** Panel A: Total lymphocytes were gated based on size and granularity in the FSC-A and SSC-A profile. Then cell aggregates and debris were removed by gating on single cells following which, NK, CD4<sup>+</sup> and CD8<sup>+</sup> T cells were isolated based on their expression of markers of the same name. Once each population was identified, patient samples pertaining to that population were then gated on in the barcoded grids. Further gating was performed to identify CD25<sup>hi</sup>FoxP3<sup>+</sup> Treg, CD25<sup>+/lo</sup>FoxP3<sup>-</sup> Teff and their CD45RA<sup>+</sup> and CD45RA<sup>-</sup> subsets. For CD8<sup>+</sup> T cells, CD45RA<sup>+</sup> and CD45RA<sup>-</sup> subsets were also identified. Panel B: pSTAT5<sup>+</sup> cells were then gated in the unstimulated sample; this was then applied to the stimulated samples. QC 1 and QC 2 = Quality Control 1 and 2; S1 D1 = patient sample day 1; S1 D85 = patient sample day 85.

Statistical analysis was performed using GraphPad Prism 9. We used simple linear regression analysis to assess whether pSTAT5 expression at day 1 correlates with the expansion of Treg and non-Treg at day 64. For paired analysis of changes between timepoints per treatment group, a D'Agostino & Pearson normality and lognormality test was performed. Depending on whether the data was normally distributed, either a paired t-test or a Wilcoxon matched-pairs sign rank test was used. To assess changes between treatment groups, the same normality test was used followed by an ordinary one-way ANOVA with Bonferroni's multiple comparisons test or Kruskal-Wallis test with Dunn's multiple comparisons test.

### 4.3. Results.

#### 4.3.1. Optimisation of experimental protocol.

To assess IL-2 signalling in Treg and non-Treg cells following *in vitro* stimulation with IL-2, we had to design a comprehensive and robust flow cytometry staining panel. In order to expose intracellular pSTAT5, we had to use permeabilisation buffer III, a methanol-based reagent obtained from BD Biosciences. This posed

a problem as cell surface proteins are sensitive to fixation and permeabilisation, particularly to harsh methanol reagents, which can result in loss of recognition by their respective antibodies and thus, result in inadequate staining. This is less of a problem if pSTAT5 is only of interest in Treg, as the staining panel is relatively small and data from previously published reports can aid optimisation. However, the problem arises when the number of target cells where pSTAT5 is of interest increases. Throughout experimental optimisation we observed that several surface proteins to be incompatible with perm buffer III, resulting in poor staining. One example of this is shown in figure 4-2, where poor staining was observed for CD3 and CD8.

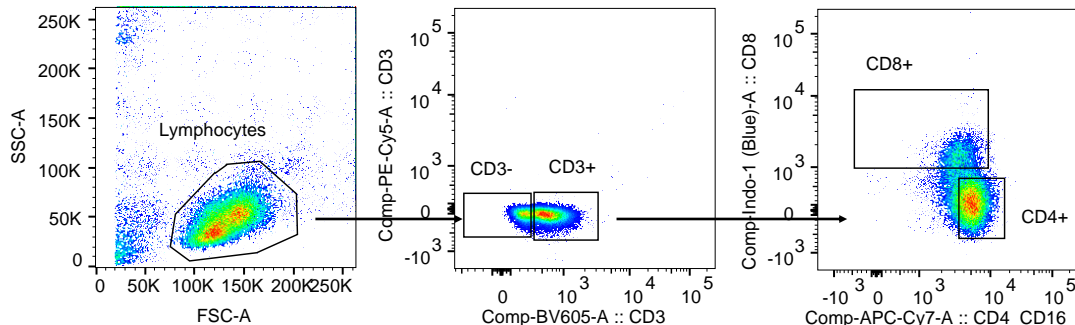


**Figure 4-2 Incompatibility of certain monoclonal antibodies with BD perm buffer III.** Permeabilisation of PBMC with perm buffer III resulted in poor staining for CD3 BV605 and CD8 Indo-1 blue.

To design a comprehensive flow cytometry staining panel, we tested multiple combinations of target-clone-conjugate for compatibility with perm buffer III, (table 4-2). In most cases we found that a certain clone of antibody to be incompatible with this buffer, such as the Hit8a clone of CD8. Whereas in the case of FoxP3, we observed that the conjugate (fluorochrome) itself was incompatible with perm buffer III. Multiple iterations were required before the optimal staining panel was determined, as previously shown in table 4-1.

| Target | Clone    | Conjugate   | Perm Buffer III Compatible |
|--------|----------|-------------|----------------------------|
| CD3    | OKT3     | BV605       | No                         |
|        | UCHT1    | PE-Cy5      | No                         |
|        |          | PerCP-Cy5.5 | No                         |
|        |          | BV650       | No                         |
|        |          | BUV395      | Yes*                       |
| CD4    | RPA-T4   | BV605       | No                         |
|        | SK3      | APC-eF780   | Yes                        |
|        |          | BUV661      | Yes*                       |
| CD8    | Hit8a    | APC-Cy7     | No                         |
|        |          | Pe-Cy7      | No                         |
|        |          | Indo-1 blue | No                         |
|        | SK1      | BUV737      | Yes*                       |
| CD45RA | HI100    | Pe-Cy7      | Yes                        |
|        |          | PERCP       | Yes*                       |
|        |          | PE-CF594    | Yes                        |
| CD25   | M-A251   | Pe-Cy7      | Yes*                       |
| FoxP3  | 236A     | PE-CDF594   | No                         |
|        |          | AF488       | Yes*                       |
| pSTAT5 | pY694    | AF647       | Yes*                       |
| CD16   | B73.1    | APC-eF780   | Yes                        |
|        | eBioCB16 | PE          | Yes*                       |
| CD56   | HCD56    | BV711       | Yes*                       |
| CD14   | M5E2     | Pe-Cy7      | No                         |
|        | HCD14    | AF488       | No                         |

**Table 4-2 Summary of target-clone-conjugate combinations tested for compatibility with perm buffer III during assay optimisation.** \*selected for final staining panel.

Initially we also sought to incorporate monocytes into our IL-2 signalling assessment as in chapter 2 we observed significant reductions in alternative and intermediate monocyte subsets as a result of IL-2 therapy. However, early experimental optimisation showed that CD14 is not compatible with this buffer set, as supported by buffer compatibility data published by BD. Furthermore, STAT5 signalling in response to IL-2 by monocytes has not been reported.

#### 4.3.2. Determining the concentrations of IL-2 needed for stimulation of different lymphocyte subsets.

Prior to analysis of IMODALS samples, we set out to optimise the stimulation conditions by which we could observe a robust, but submaximal expression of pSTAT5 in the lymphocyte subsets of interest. This will allow us to observe the effects of therapy and also, the differences between individuals in IL-2 signalling. To do this we stimulated PBMC from two healthy donors with incremental concentrations of IL-2 *in vitro*. As expected, Treg showed the highest sensitivity to IL-2, with samples from both individuals showing dose dependent induction of pSTAT5 from 0.1U which reached a plateau at 10U. Teff, NK and CD8<sup>+</sup> T cells responded to higher levels of IL-2, with good dose dependency being observed between 10-50U for all populations in both individuals (figure 4-3). We therefore selected the 0.5U and 10U of IL-2 concentrations for stimulation of IMODALS PBMC.

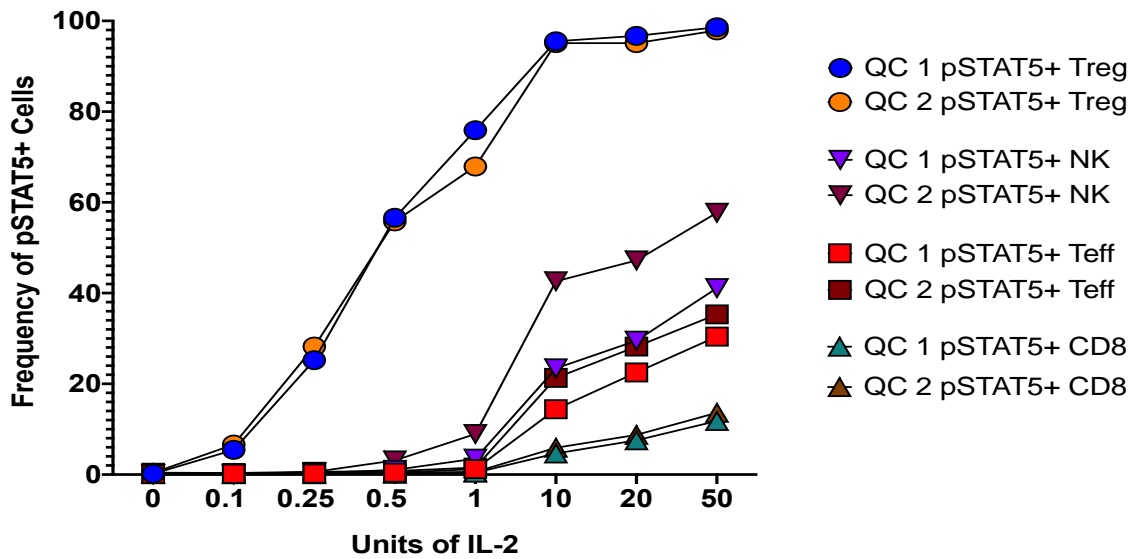


**Figure 4-3 pSTAT5 expression by different populations of white blood cells in response to increasing concentrations of exogenous IL-2.** Treg, NK, Teff and CD8<sup>+</sup> T cell expression of pSTAT5 following 30-minute *in vitro* stimulation with 0, 0.1, 0.25, 0.5, 1, 10, 20 and 50 units of IL-2 in two healthy donors.

### 4.3.3. Experimental quality control.

Due to the number of patient samples to be analysed, the experiments had to be carried out in a number of batches. Similar to the approach in the previous chapter, we mitigated against any influence of day-to-day variation in assay performance by:

1. Assessing all timepoints for an individual on the same day.
2. Assessing a random allocation of individuals in each batch.
3. Two, single blood draw QC samples were used to assess any day-to-day variation in assay performance, allowing to detect any systematic drift in results.

Data collected for the frequencies of Treg, Teff, CD8<sup>+</sup> T cells, NK cells and their levels of pSTAT5 expression, show good day-to-day experimental reproducibility determined by %CV of <20% for all variables, with the exception of NK cell data for QC 1 (tables 4-3 and 4-4). In this instance we observed increased variance in the frequency of NK (%CV 28.81) and pSTAT5<sup>+</sup> NK cells (%CV 27.81). This may be the result of variation in NK cell number we observed in this sample.

| QC 1                      |                        | Batch number |      |      |      |      | Mean         | SD          | %CV          |
|---------------------------|------------------------|--------------|------|------|------|------|--------------|-------------|--------------|
|                           |                        | 1            | 2    | 3    | 4    | 5    |              |             |              |
| Treg<br>(0.5U)            | % CD4 <sup>+</sup>     | 7.82         | 7.98 | 8.11 | 7.81 | 7.16 | <b>7.78</b>  | <b>0.37</b> | <b>4.71</b>  |
|                           | pSTAT5 <sup>+</sup>    | 82.6         | 78.7 | 72.8 | 80.5 | 67   | <b>76.32</b> | <b>6.36</b> | <b>8.33</b>  |
| Teff<br>(10U)             | % CD4 <sup>+</sup>     | 91.4         | 91.5 | 91.3 | 91.4 | 92.3 | <b>91.58</b> | <b>0.41</b> | <b>0.45</b>  |
|                           | pSTAT5 <sup>+</sup>    | 42.8         | 36.2 | 31.6 | 43.7 | 31.4 | <b>37.14</b> | <b>5.91</b> | <b>15.91</b> |
| CD8 <sup>+</sup><br>(10U) | % CD3 <sup>+</sup>     | 30.9         | 31   | 34.3 | 36.4 | 33.5 | <b>33.22</b> | <b>2.33</b> | <b>7.01</b>  |
|                           | pSTAT5 <sup>+</sup>    | 5.65         | 6.18 | 4.11 | 4.4  | 5.02 | <b>5.01</b>  | <b>0.86</b> | <b>16.91</b> |
| NK<br>(10U)               | % of total lymphocytes | 0.3          | 0.24 | 0.23 | 0.19 | 0.39 | <b>0.27</b>  | <b>0.08</b> | <b>28.81</b> |
|                           | pSTAT5 <sup>+</sup>    | 12.6         | 10.5 | 11   | 19.9 | 14   | <b>13.6</b>  | <b>3.78</b> | <b>27.81</b> |

Table 4-3 Analysis of QC 1 variables measured across the experimental batches.

| QC 2                      |                        | Batch number |      |      |      |      |              |             |              |  |
|---------------------------|------------------------|--------------|------|------|------|------|--------------|-------------|--------------|--|
|                           |                        | 1            | 2    | 3    | 4    | 5    | Mean         | SD          | %CV          |  |
| Treg<br>(0.5U)            | % CD4 <sup>+</sup>     | 4.86         | 5.08 | 4.84 | 4.53 | 4.67 | <b>7.78</b>  | <b>0.37</b> | <b>4.71</b>  |  |
|                           | pSTAT5 <sup>+</sup>    | 76.2         | 79.9 | 70.5 | 74.5 | 58.9 | <b>72</b>    | <b>8.06</b> | <b>11.2</b>  |  |
| Teff<br>(10U)             | % CD4 <sup>+</sup>     | 94.6         | 94.5 | 94.8 | 95   | 95.1 | <b>94.8</b>  | <b>0.25</b> | <b>0.27</b>  |  |
|                           | pSTAT5 <sup>+</sup>    | 26.6         | 25.8 | 22.2 | 27.7 | 21.7 | <b>24.8</b>  | <b>2.69</b> | <b>10.86</b> |  |
| CD8 <sup>+</sup><br>(10U) | % CD3 <sup>+</sup>     | 25.6         | 27.6 | 27.8 | 29   | 28.9 | <b>27.78</b> | <b>1.37</b> | <b>4.93</b>  |  |
|                           | pSTAT5 <sup>+</sup>    | 7.11         | 6.89 | 6.44 | 6.65 | 6.2  | <b>6.66</b>  | <b>0.36</b> | <b>5.39</b>  |  |
| NK<br>(10U)               | % of total lymphocytes | 0.38         | 0.37 | 0.33 | 0.34 | 0.44 | <b>0.37</b>  | <b>0.04</b> | <b>11.62</b> |  |
|                           | pSTAT5 <sup>+</sup>    | 27.8         | 25.9 | 29.9 | 39.9 | 30.8 | <b>30.86</b> | <b>5.39</b> | <b>17.49</b> |  |

Table 4-4 Analysis of QC 2 variables measured across the experimental batches.

#### 4.3.4. IL-2 signalling at day 1 in Treg and non-Treg cells did not correlate with the expansions observed at day 64 in these cell types.

To test the first and second hypotheses, we calculated percent change at day 64 for Treg, Teff, NK and CD8<sup>+</sup> T cell number (obtained from chapter 2) and correlated this with pSTAT5 expression at day 1, induced by 0.5U of IL-2 in Treg, and 10U of IL-2 in Teff, NK and CD8<sup>+</sup> T cells. For this analysis we used patient data from the 1MIU and 2MIU IL-2 treated groups only, as this is where the expansions in these cell types were observed. Furthermore, to mitigate for any confounding effects of IL-2 dose, we correlate our findings in each IL-2 treated group separately. We observed no significant correlations between pSTAT5 expression at day 1 and percent change in Treg ( $p=0.4071$ ), Teff ( $p=0.2161$ ), total NK ( $p=0.1493$ ) or CD8<sup>+</sup> T cells ( $p=0.8998$ ) in the 1MIU group (figure 4-4 A to D).

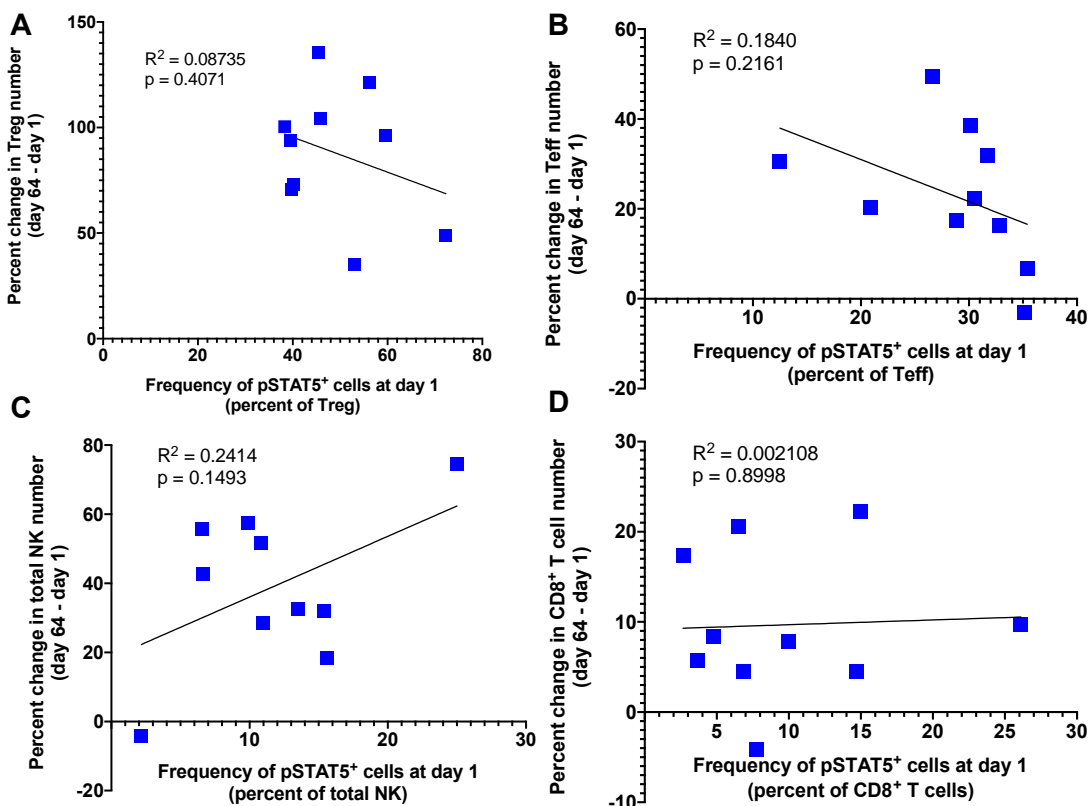


**Figure 4-4 Simple linear regression analysis of Treg and non-Treg cell percent change in number at day 64 and pSTAT5 expression at day 1 in the 1MIU IL-2 group.** Panel A: y-axis – percent change in Treg number; x-axis – frequency of pSTAT5<sup>+</sup> Treg. Panel B: y-axis – percent change in Teff number; x-axis – frequency of pSTAT5<sup>+</sup> Teff. Panel C: y-axis – percent change in total NK number; x-axis – frequency of pSTAT5<sup>+</sup> NK. Panel D: y-axis – percent change in CD8<sup>+</sup> T cell number; x-axis – frequency of pSTAT5<sup>+</sup> CD8<sup>+</sup> T cells.

Similarly, at 2MIU IL-2 there were also no significant correlations between the frequency of pSTAT5<sup>+</sup> cells at day 1 and percent change in the number of Treg ( $p=0.5925$ ), Teff ( $p=0.7576$ ) and total NK ( $p=0.1728$ ) at day 64 (figure 4-5 A to C). There was, however, a significant correlation between pSTAT5 and percent change in CD8<sup>+</sup> T cell number ( $p=0.0295$ ;  $R^2=0.4666$ ) in this group (figure 4-5 D).

The data in figure 4-4 and 4-5 show:

1. IL-2 signalling at day 1, measured by the expression of pSTAT5, does not predict the expansion in Treg and non-Treg cells seen at day 64 in our trial.
2. The data is affected by large person-to-person variation in response in terms of pSTAT5 expression and percentage change in cell number.
3. There are trends towards a positive linear relationship in populations such as total NK cells and CD8<sup>+</sup> T cells, and their levels of significance could benefit from a larger cohort.
4. No significant change in relationships is observed when correlating findings from both IL-2 treated groups together (data not shown).
5. No significant relationship is observed between IL-2 signalling in CD56bright NK and their *in vivo* expansion (data not shown).

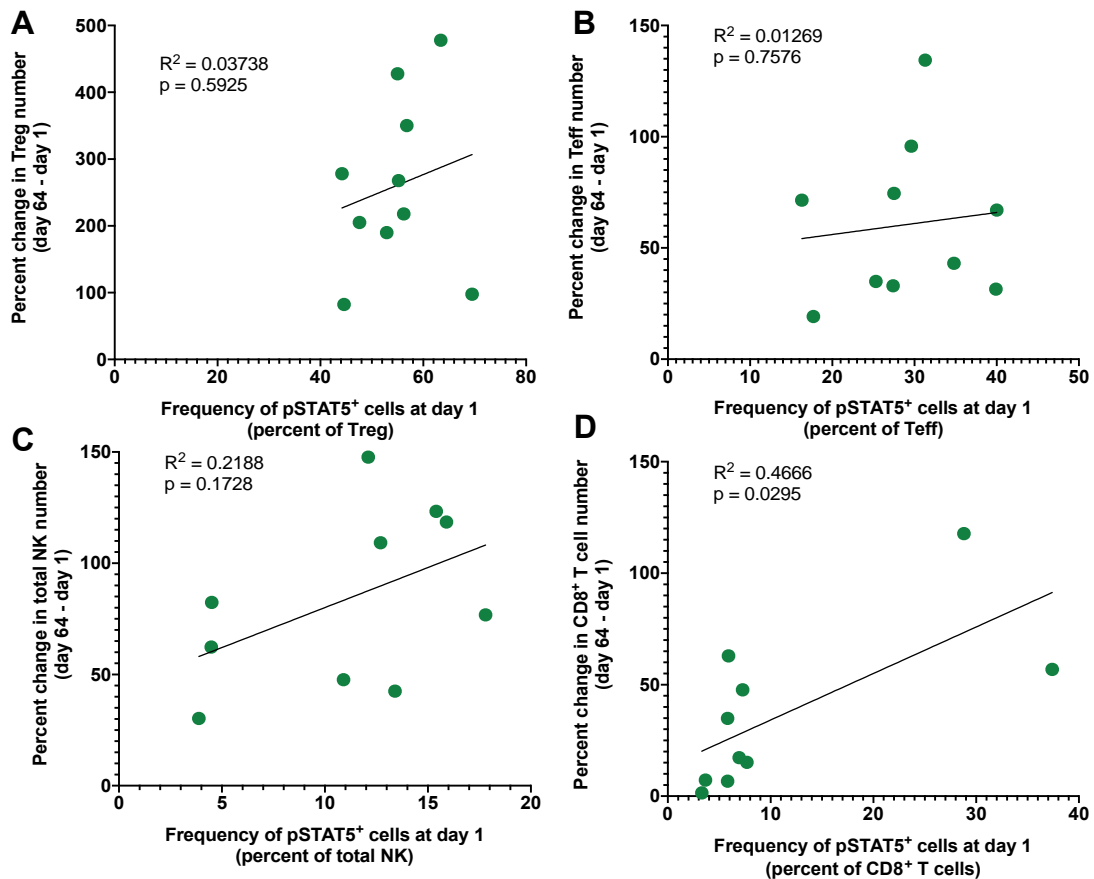


**Figure 4-5 Simple linear regression analysis of Treg and non-Treg cell percent change in number at day 64 and pSTAT5 expression at day 1 in the 2MIU IL-2 group.** Panel A: y-axis – percent change in Treg number; x-axis – frequency of pSTAT5<sup>+</sup> Treg. Panel B: y-axis – percent change in Teff number; x-axis – frequency of pSTAT5<sup>+</sup> Teff. Panel C: y-axis – percent change in total NK number; x-axis – frequency of pSTAT5<sup>+</sup> NK. Panel D: y-axis – percent change in CD8<sup>+</sup> T cell number; x-axis – frequency of pSTAT5<sup>+</sup> CD8<sup>+</sup> T cells.

#### 4.3.5. Reduced IL-2 signalling in Treg following IL-2 therapy.

For the third hypothesis, testing whether IL-2 therapy influenced IL-2 signalling, we analysed pSTAT5 expression at day 1 and compared it to that of day 85 in Treg, Teff, NK and CD8<sup>+</sup> T cells. We did not observe any significant changes in IL-2 signalling at these two timepoints in Teff or NK cells (data not shown). For Treg, we observed a significant decrease ( $p=0.0014$ ) in pSTAT5 at day 85 in all participants on 2MIU IL-2. No significant changes were observed in the 1MIU or

placebo group (figure 4-6 A to C) but the majority of patients on 1MIU do show a declining trend. To assess whether this decrease is treatment-associated and dose-dependent, we calculated and compared the change in pSTAT5 expression between the treatment groups. At 2MIU IL-2 there was a mean decrease of 8.04% in pSTAT5 expression on Treg, while at 1MIU there was a mean decrease of 1.52%. Group comparisons showed this reduction in pSTAT5 to be significantly different between 2MIU and placebo ( $p=0.0009$ ) and 2MIU and 1MIU ( $p=0.0331$ ). There were no significant differences in expression of pSTAT5 on Treg at day 1 between any of the treatment groups (figure 4-6 D and E). These findings show a treatment-associated and dose-dependent decline in pSTAT5 expression on Treg in the 2MIU group.

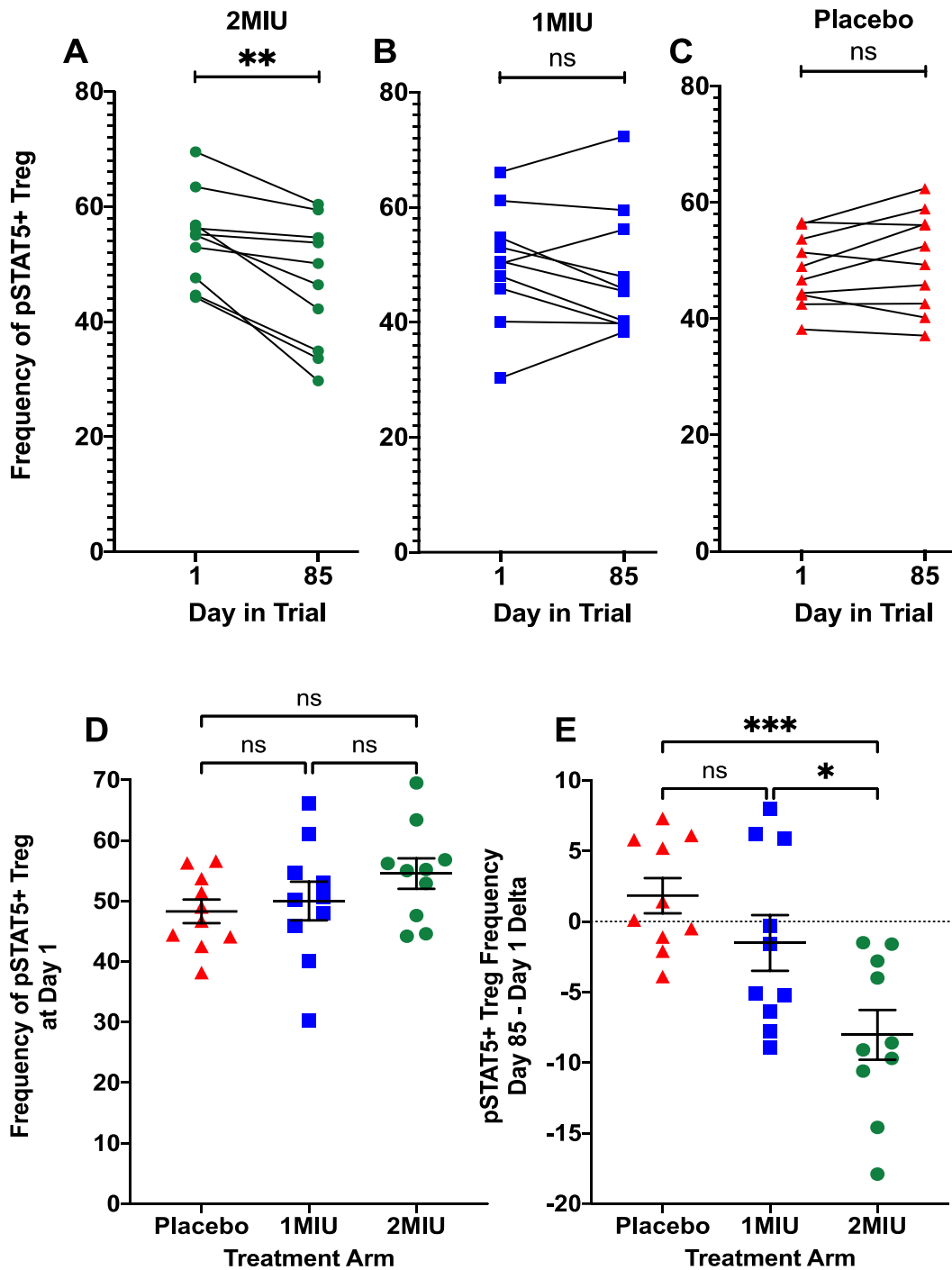


**Figure 4-6 Assessment of pSTAT5<sup>+</sup> Treg at day 1 and day 85 in IMODALS treatment groups.** Panels A to C: Analysis of pSTAT5<sup>+</sup> Treg in each treatment group at day 1 and day 64. Panel D: Analysis of pSTAT5<sup>+</sup> Treg at day 1 between placebo and 1MIU, placebo and 2MIU, and 1MIU and 2MIU. Panel E: Analysis of change in pSTAT5<sup>+</sup> Treg at day 64 between placebo and 1MIU, placebo and 2MIU, and 1MIU and 2MIU. Error bars indicate mean with SEM. \*\*\*p<0.001, \*\*p<0.01, \*p<0.05, ns – not significant. Panels A to C – paired t test; Panels D and E – Ordinary one-way ANOVA. Red triangles – placebo; blue squares – 1MIU; green circles – 2MIU.

Having observed this decrease in pSTAT5 expression on Treg at day 85, we hypothesised that this might be related to the decrease in CD25 MFI on Treg we observed at the same trial visit in the previous chapter. To this end, we calculated percent changes from day 1 to day 85 for both variables for trial participants on 2MIU IL-2. We observe no significant relationship ( $p=0.5619$ ) between the percent changes in pSTAT5 versus percent change in CD25 MFI on Treg (figure 4-7). This indicates that in IMODALS trial participants, receiving 2MIU IL-2, the expression levels of CD25 on Treg, are not associated with IL-2 signalling. However, we do observe a trend towards a relationship, affected by sample size and person-to-person variation in response, therefore a larger cohort is needed to fully investigate this.

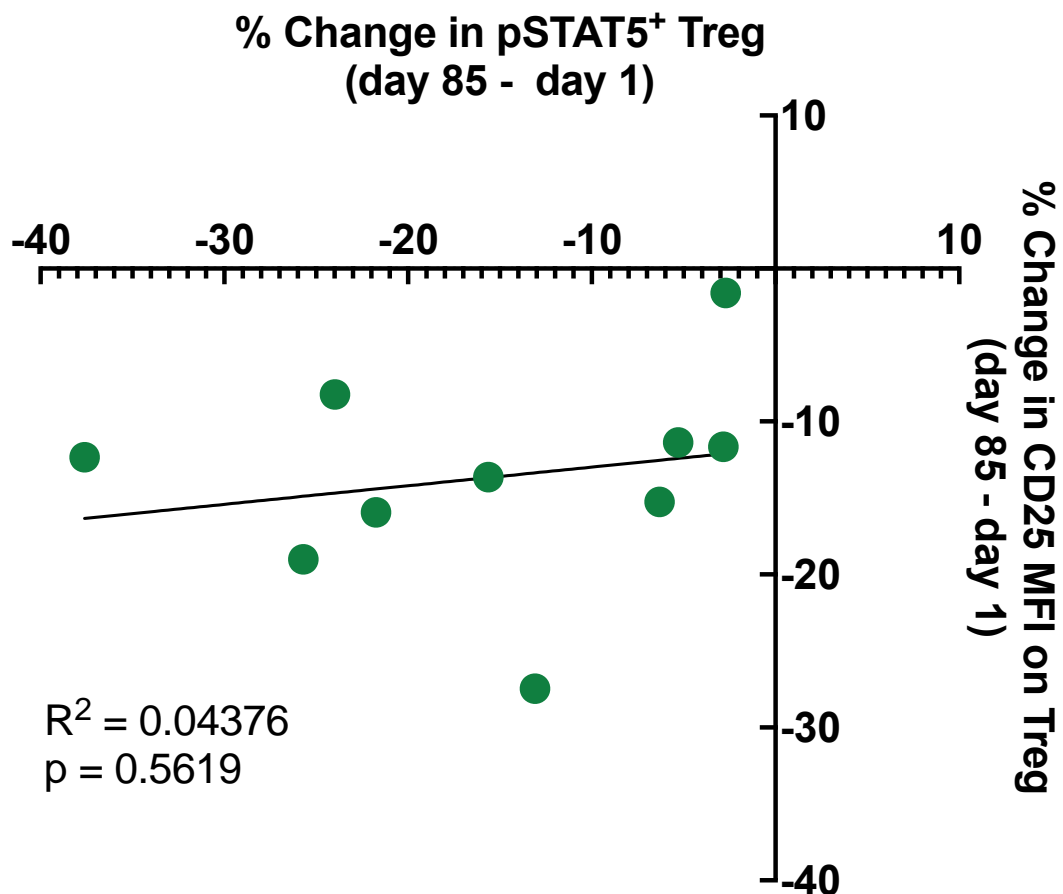
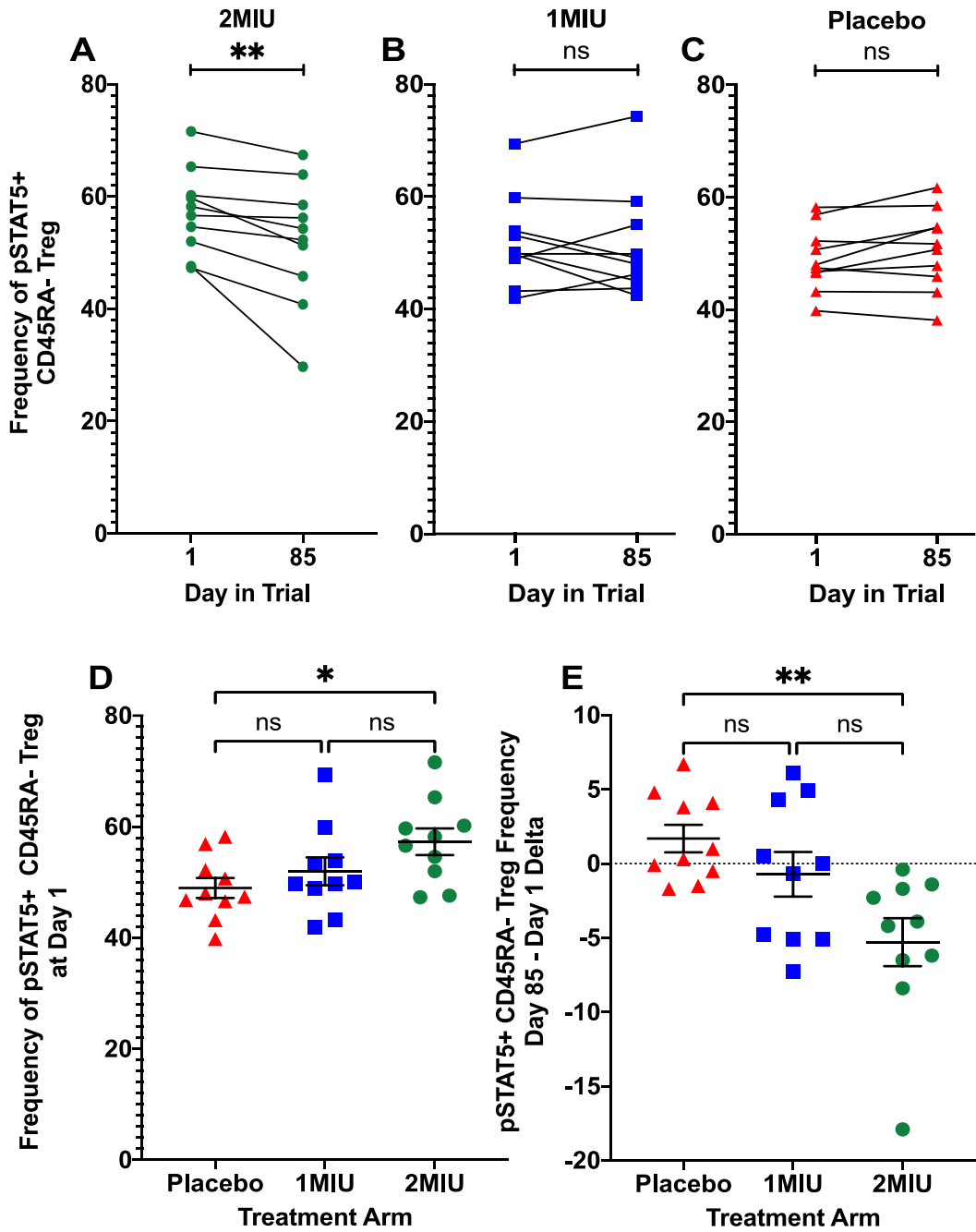


**Figure 4-7 Simple linear regression analysis of percent change in the expression of pSTAT5 and CD25 MFI on Treg in the 2MIU group.** x-axis – percent change in pSTAT5 expression on Treg at day 85; y-axis – percent change in CD25 MFI on Treg.  $p=0.5619$ ;  $R^2=0.04376$ .

We took this analysis further by examining the expression of pSTAT5 in CD45RA<sup>+</sup> (naïve) and CD45RA<sup>-</sup> (memory) Treg. We wanted to address this because studies from other medical conditions have shown that the presence of memory, and not naïve Treg, may be more beneficial. In chronic MS patients, memory Treg regained suppressive function after a decline in early disease while naïve Treg did not (Venken *et al.*, 2008). Following allograft transplantation, those without the need for immunosuppressants had greater levels of memory Treg (Braza *et al.*, 2015). In some SLE patients, memory Treg inversely correlated with disease activity while naïve Treg were found to have impaired suppressive

function in a different SLE cohort (Pan *et al.*, 2012; Silva-Neta *et al.*, 2018). In ALS it has been shown that both memory and naïve Treg numbers inversely correlate with disease progression (Sheean *et al.*, 2018). Furthermore, aging affects the balance of naive and memory Treg, with the latter more prevalent at older age (Booth *et al.*, 2010). As the mean age of trial participants was  $56.4 \pm 11\%$ , it is safe to hypothesise that we will largely be expanding memory Treg using IL-2. We observed no significant change in pSTAT5 expression in naïve Treg at day 85, although there was a trend towards a reduction in signalling (data not shown). However, we did observe a significant decrease in pSTAT5 expression in memory Treg at 2MIU ( $p=0.0096$ ) and not in the other two treatment groups (figure 4-8 A to C). When analysing the change in pSTAT5 expression in memory Treg we observe a mean reduction of 5.29%. This is significantly different when compared to placebo ( $p=0.0045$ ) but not when compared to 1MIU group (figure 4-8 D and E). These data also show that the frequency pSTAT5<sup>+</sup> memory Treg at day 1 differs between the 2MIU group and placebo ( $p=0.0440$ ). These data suggest that three cycles of the highest dose of IL-2 negatively affected IL-2 signalling in Treg.



Panels A to C: Analysis of pSTAT5<sup>+</sup>CD45RA<sup>-</sup> Treg in each treatment group at day 1 and day 64. Panel D: Analysis of pSTAT5<sup>+</sup>CD45RA<sup>-</sup> Treg at day 1 between placebo and 1MIU, placebo and 2MIU, and 1MIU and 2MIU. Panel E: Analysis of change in pSTAT5<sup>+</sup>CD45RA<sup>-</sup> Treg at day 64 between placebo and 1MIU, placebo and 2MIU, and 1MIU and 2MIU. Error bars indicate mean with SEM. \*\*p<0.01, \*p<0.05, ns – not significant. Panels A and C – paired t test; Panel B – Wilcoxon test; Panels D – Ordinary one-way ANOVA; Panel E – Kruskal-Wallis test. Red triangles – placebo; blue squares – 1MIU; green circles – 2MIU.

#### **4.3.6. Increased IL-2 signalling in CD8<sup>+</sup> T cells following IL-2 therapy.**

Our investigation of IL-2 signalling in non-Treg cells showed a significant increase in pSTAT5 expression on CD8<sup>+</sup> T cells from day 1 to day 85 in the 2MIU ( $p=0.0098$ ) and 1MIU ( $p=0.0371$ ) IL-2 treated groups (figure 4-9 A to C). These changes amounted to a mean increase of 3.67% and 2% in pSTAT5<sup>+</sup> CD8<sup>+</sup> T cells in the 2MIU and 1MIU groups respectively. However, group comparisons of change in pSTAT5 expression showed no significant differences between 2MIU and placebo, 1MIU and placebo, 1MIU and 2MIU groups (figure 4-9 D and E). As we did for Treg, we assessed pSTAT5 expression in CD45RA<sup>+</sup> and CD45RA<sup>-</sup> CD8<sup>+</sup> T cells. It is important to note that CD45RA is not an ideal marker for classifying naïve CD8<sup>+</sup> T cells, as there is a subset of effector memory CD8<sup>+</sup> T cells that also expresses CD45RA, known as TEMRA cells (Willinger *et al.*, 2005). We did not observe any significant changes in pSTAT5 expression on CD45RA<sup>+</sup> CD8<sup>+</sup> T cells (data not shown). The increase in pSTAT5 expression is only confined to the CD45RA<sup>-</sup> CD8<sup>+</sup> T cell subset and is observed in both the 2MIU and 1MIU groups. However, it is only significantly different between day 1 and day 85 in the 2MIU IL-2 group ( $p=0.0264$ ), with no significant changes observed in those on placebo (figure 4-10 A to C). Analysis of change in pSTAT5 expression shows a mean increase of 5.67% and 2.54% in the 2MIU and 1MIU groups respectively. These were not significantly different between the two treatment groups, nor when compared to placebo (figure 4-10 D and E). These data show that IL-2 therapy increased IL-2 signalling in CD8<sup>+</sup> T CD45RA<sup>-</sup> subset. IL-2 signalling in CD8<sup>+</sup> T cells is known to contribute to their survival, proliferation and effector subset differentiation (Kalia and Sarkar, 2018). Whether this increase in our study participants is biologically significant, remains unclear.

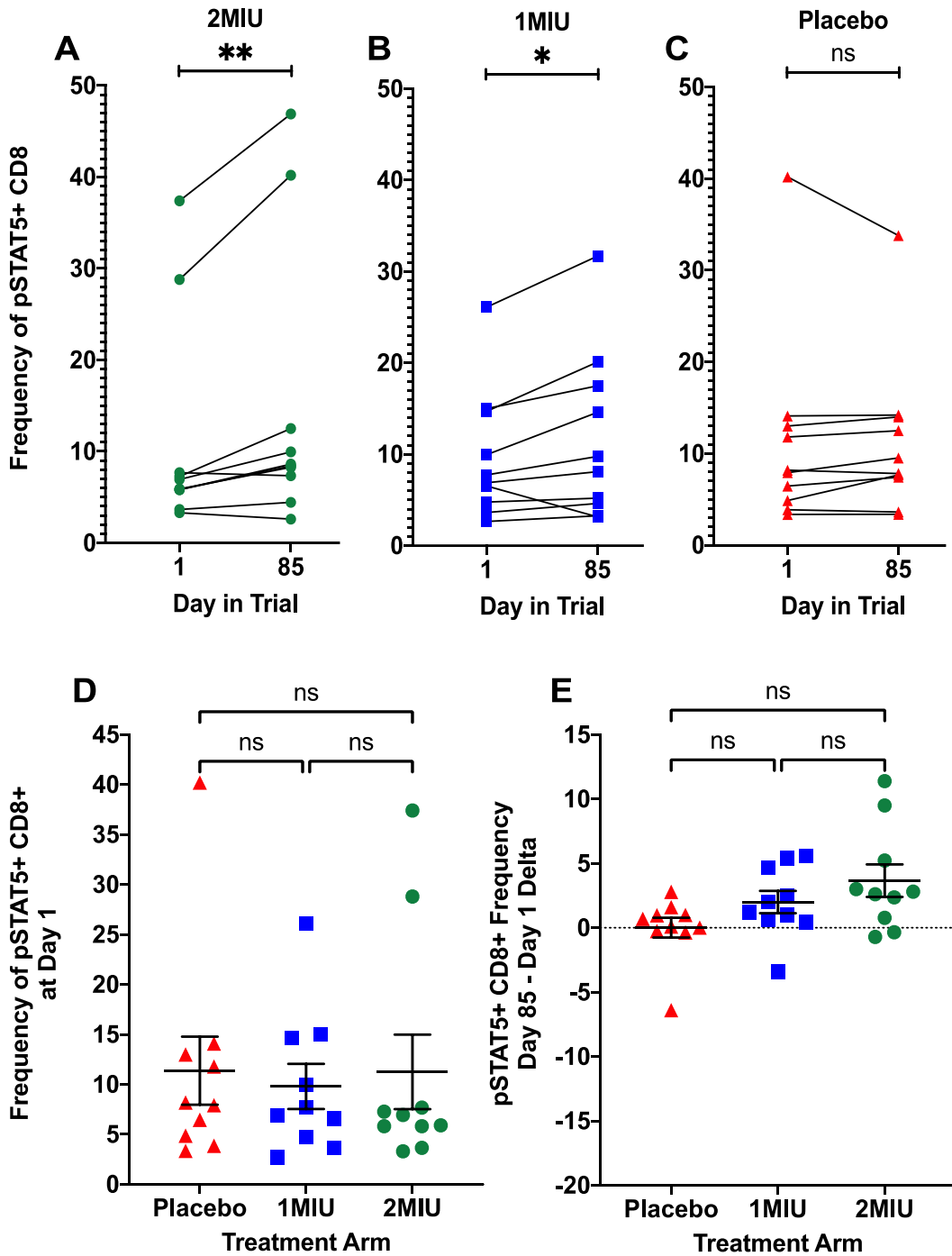


**Figure 4-9 Assessment of pSTAT5<sup>+</sup> CD8<sup>+</sup> T cells at day 1 and day 85 in IMODALS treatment groups.**

Panels A to C: Analysis of pSTAT5<sup>+</sup> CD8<sup>+</sup> T cells in each treatment group at day 1 and day 64. Panel D: Analysis of pSTAT5<sup>+</sup> CD8<sup>+</sup> T cells at day 1 between placebo and 1MIU, placebo and 2MIU, and 1MIU and 2MIU. Panel E: Analysis of change in pSTAT5<sup>+</sup> CD8<sup>+</sup> T cells at day 64 between placebo and 1MIU, placebo and 2MIU, and 1MIU and 2MIU. Error bars indicate mean with SEM. \*\*p<0.01, \*p<0.05, ns – not significant. Panels A to C – Wilcoxon test; Panels D and E – Kruskal-Wallis test. Red triangles – placebo; blue squares – 1MIU; green circles – 2MIU.

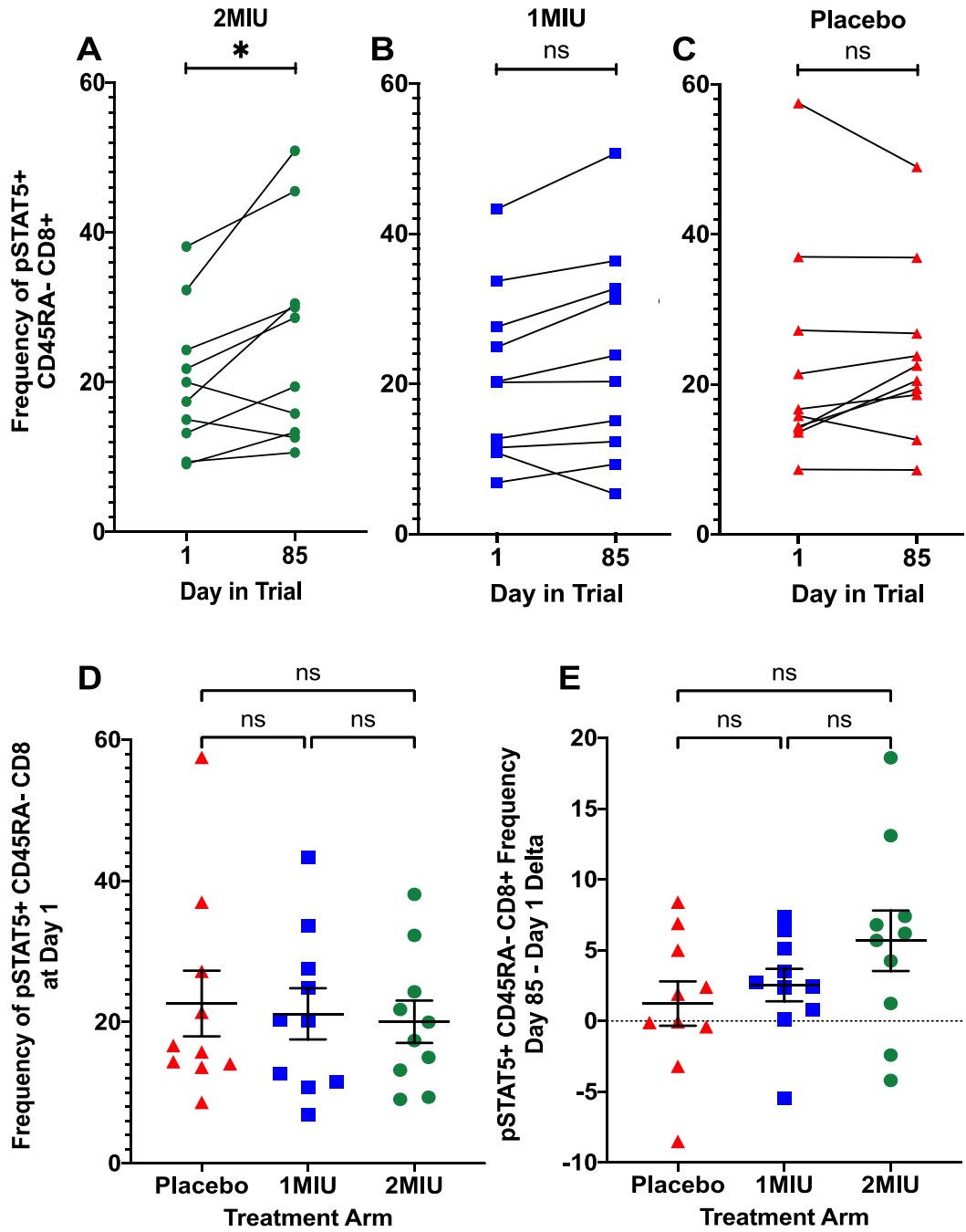


**Figure 4-10 Assessment of pSTAT5<sup>+</sup>CD45RA<sup>-</sup> CD8<sup>+</sup> T cells at day 1 and day 85 in IMODALS treatment groups.** Panels A to C: Analysis of pSTAT5<sup>+</sup>CD45RA<sup>-</sup> CD8<sup>+</sup> T cells in each treatment group at day 1 and day 64. Panel D: Analysis of pSTAT5<sup>+</sup>CD45RA<sup>-</sup> CD8<sup>+</sup> T cells at day 1 between placebo and 1MIU, placebo and 2MIU, and 1MIU and 2MIU. Panel E: Analysis of change in pSTAT5<sup>+</sup>CD45RA<sup>-</sup> CD8<sup>+</sup> T cells at day 64 between placebo and 1MIU, placebo and 2MIU, and 1MIU and 2MIU. Error bars indicate mean with SEM. \*p<0.05, ns – not significant. Panels A and B – paired t test; Panel C – Wilcoxon test; Panels D – Kruskal-Wallis test; Panel E – Ordinary one-way ANOVA. Red triangles – placebo; blue squares – 1MIU; green circles – 2MIU.

#### **4.3.7. Assessment of IL-2 signalling via STAT proteins in whole blood monocytes from healthy donors.**

Although not part of the main hypothesis testing of this chapter, we also sought to assess whether IL-2 signalling in monocytes took place. We observed an effect of IL-2 treatment on the polarisation of monocytes in chapter 2. It is possible that this is a direct influence of Treg on monocyte polarisation, as suggested by others *in vitro* (Taams *et al.*, 2005; Tiemessen *et al.*, 2007). However, it could also be a direct action of IL-2 on monocytes since others have reported that, under certain conditions, monocytes can express all 3 subunits of the high affinity IL-2R (Bosco *et al.*, 2000). Therefore, we hypothesized that:

1. Upregulation of CD25 following activation may permit IL-2 signaling downstream in monocytes.
2. This could result in upregulation of surface proteins associated with migration.

Before committing patient samples to any analysis, we wished to determine whether we could observe IL-2 signalling in monocytes of healthy donors. Literature has shown that monocytes can upregulate CD25 when whole blood is stimulated with granulocyte-macrophage colony-stimulating factor (GM-CSF) and IFN- $\gamma$  (Dendrou *et al.*, 2009). Using this data, we designed an experiment to assess the effect of concentration (20U/mL, 200U/mL and 2000U/mL) of GM-CSF and IFN- $\gamma$  and stimulation time (6 hours and 24 Hours) on CD25 expression on monocytes by stimulating whole blood, from a single healthy donor, collected in EDTA blood collection tubes. Following which the expression of CD25 was assessed by flow cytometry. White blood cells were gated based on size and granularity in the FSC-A and SSC-A profile following which, lymphocytes were

excluded by gating on CD3<sup>-</sup>CD19<sup>-</sup>CD56<sup>-</sup>. Finally, total monocytes were isolated based on HLA-DR, CD14 and CD16 expression (figure 4-11 A). Whole blood stimulation with incremental concentrations of GM-CSF and IFN- $\gamma$  resulted in a dose-dependent upregulation of CD25 on total monocytes (figure 4-11 B). This expression of CD25 was greater following a 24-hour stimulation than a 6-hour stimulation at each concentration of GM-CSF and IFN- $\gamma$  (figure 4-11 C). Therefore, for further analyses we elected to stimulate whole blood with 2000U/mL of GM-CSF and IFN- $\gamma$  for 24 hours.

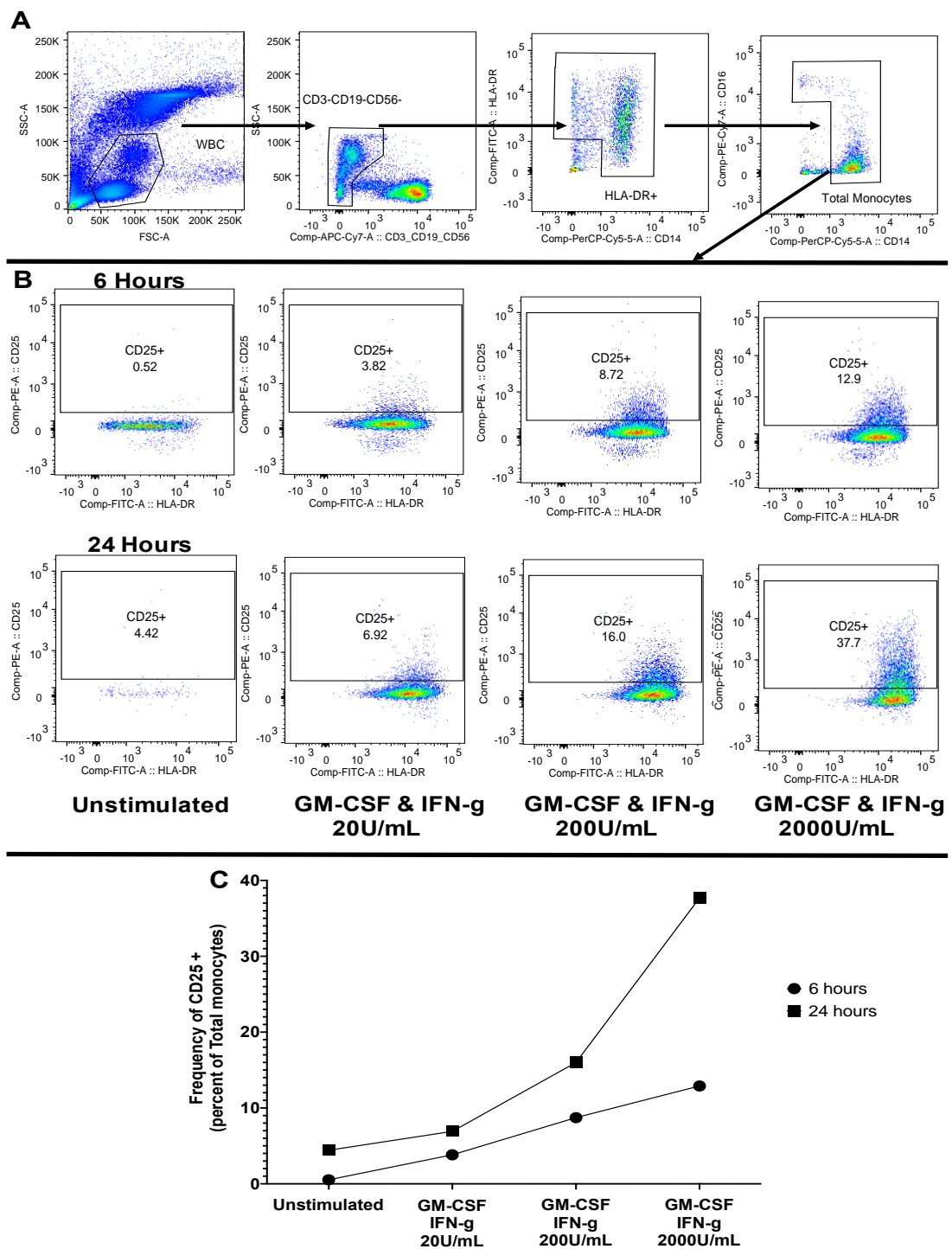


**Figure 4-11 Induction of CD25 expression in whole blood monocytes by GM-CSF and IFN- $\gamma$ . Panel A:**

Following stimulation, monocytes were identified as CD3-CD19-CD56-HLA-DR<sup>+</sup>. Total monocytes were then isolated based on their expression of CD14 and CD16. **Panel B:** The effects of 20U/mL, 200U/mL and 2000U/mL of GM-CSF and IFN- $\gamma$  on CD25 expression in total monocytes following a 6- and 24-hour stimulation. **Panel C:** The frequency of CD25<sup>+</sup> monocytes at each concentration of GM-CSF and IFN-g at 6 hours versus 24 hours.

Having determined that monocytes can be induced to express CD25, we assessed whether the addition of IL-2 to GM-CSF and IFN- $\gamma$  stimulated blood will result in downstream IL-2 signalling in monocytes. To investigate this, we stimulated whole blood with 2000U/mL of GM-CSF and IFN- $\gamma$  while adding IL-2 at incrementally increasing concentrations (1000U/mL, 2000U/mL and 4000U/mL). To look for signalling, we designed a flow cytometry panel where phosphorylation of STAT1, STAT3 and STAT5 proteins could be assessed, as IL-2 engagement by IL-2R leads to the recruitment of all three proteins downstream, with STAT5 being the most abundant (Liao, Lin and Leonard, 2013). When monocytes are stimulated with IL-2 alone, we observed no phosphorylation of STATs 1, 3 or 5 (figure 4-12 A). When monocytes are stimulated with IL-2, GM-CSF and IFN- $\gamma$  we also observe no phosphorylation of STATs 1, 3 or 5 despite the upregulation of CD25 (figure 4-12 B). In both settings, CD3 $^+$  T cells responded as expected with phosphorylation of STAT5 when IL-2 was present (figure 4-12 A and B). There was also an induction of STAT1 and STAT3 in CD3 $^-$ CD56 $^+$ CD16 $^+$  NK cells when stimulated with IL-2, GM-CSF and IFN- $\gamma$ , indicating that the STAT1 and STAT3 antibodies performed as expected (data not shown). These data indicated that once CD25 is upregulated on monocytes, the addition of IL-2 does not induce downstream signaling via STAT1, STAT3 or STAT5.

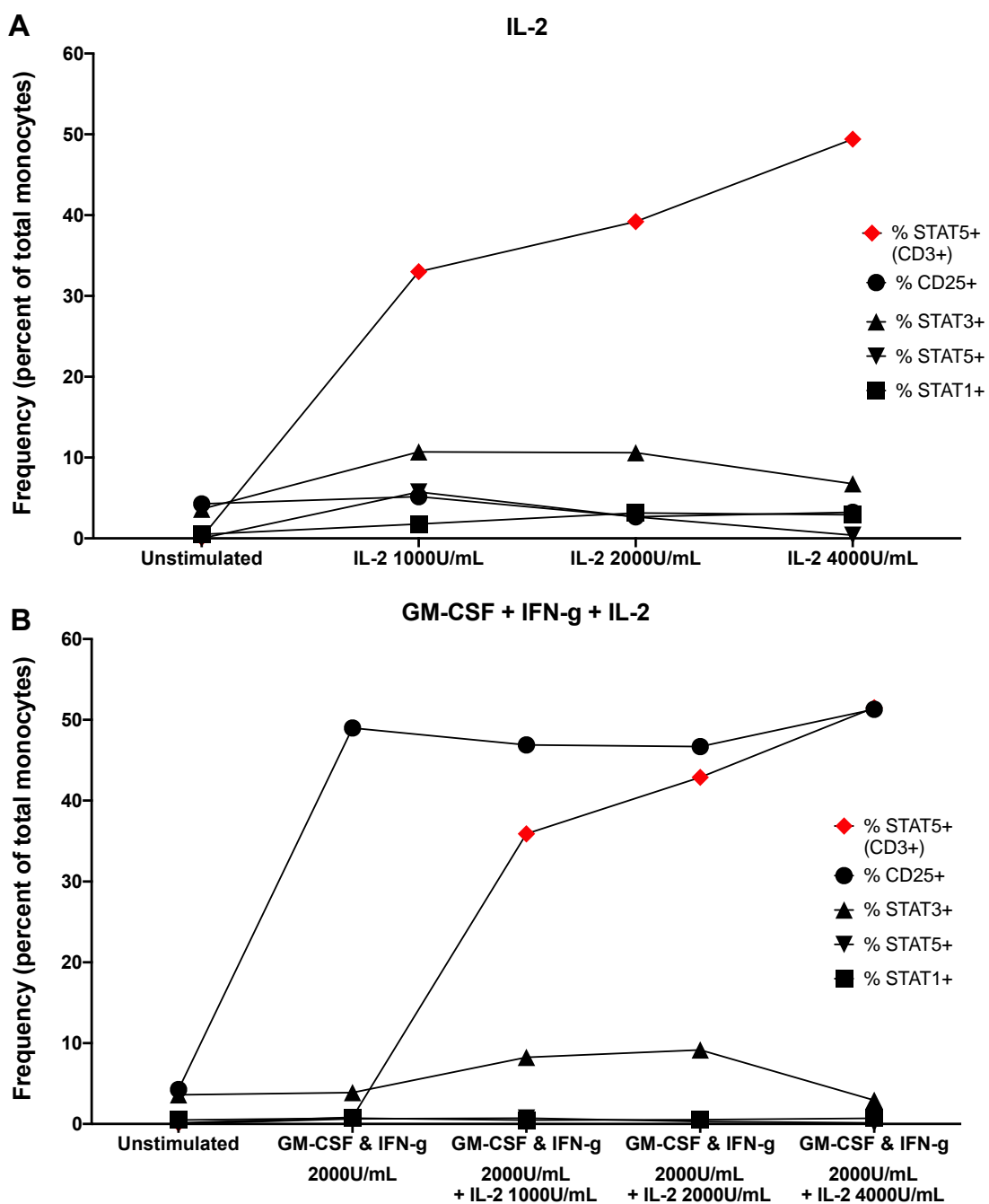


**Figure 4-12 Assessment of IL-2 signalling in whole blood monocytes.** Whole blood was stimulated with 1000U/mL, 2000U/mL or 4000U/mL IL-2 alone (**A**) or in combination with 2000U/mL of GM-CSF and IFN-g (**B**) for 24 hours. In each stimulation condition, the expression of STAT1, STAT3, STAT5 and CD25 was assessed in monocytes by flow cytometry. STAT5 expression on CD3<sup>+</sup> T cells was used as a positive control.

#### **4.4. Discussion.**

We measured IL-2 signalling *in vitro* at day 1, to assesses whether this correlates with expansion *in vivo* at day 64. We thought it was important to assess this as we, and other IL-2 immunotherapy trials have shown that the magnitude of response to IL-2, measured by the increase in Treg number or frequency, varies greatly between individuals. This variability in expansion could be related to clinical efficacy as some IL-2 therapy trials conducted on GVHD and AA patients have shown clinical efficacy with regards to improved liver function and decreased erythema, and partial hair regrowth however, these responses were not observed in all participants on IL-2. Other factors could influence this variability in clinical efficacy such as, the extent of tissue injury, patient characteristics, underlying disease and concomitant immunosuppressive medications but it could also be related to variable Treg expansion and subsequent recruitment to tissue (Koreth *et al.*, 2011; Castela *et al.*, 2014). We hypothesised that this variability in Treg expansion could be related to the level of stimulation IL-2 provides to Treg. If this is the case, then by observing a relationship between IL-2 signalling at baseline and Treg expansion after IL-2 in our cohort, would indicate that we could predict how well a person will respond to therapy. This knowledge could benefit future IL-2 trials as patients could be assigned an optimal dose of IL-2, based on the knowledge of how well their Treg will expand, potentially leading to better clinical efficacy in all participants on active drug. The same rationale is true for non-Treg cells. IL-2 trials in T1D, GVHD, vasculitis as well as our own study, observed IL-2 induced increases in Teff, CD8<sup>+</sup> T cells and NK cells (Saadoun *et al.*, 2011; Hartemann *et al.*, 2013; Todd *et al.*, 2016; Koreth *et al.*, 2016). Whether the expansion of these cells is

detrimental in ALS is unknown, but in autoimmune diseases such as T1D, autoreactive Teff and CD8<sup>+</sup> T cells contribute to the destruction of insulin producing cells (Ahmed *et al.*, 2019). Therefore, *in vivo* Teff and CD8<sup>+</sup> T cell expansion with IL-2 could further contribute to T1D pathogenesis. In researching methods by which we could assess IL-2 signalling, we have found that the level of stimulation provided by IL-2 can be determined by measuring intracellular pSTAT5 after *in vitro* exposure to graded doses of IL-2. In other settings, by assessing IL-2 signalling this way, scientists were able to detect disease associated defects in IL-2 signalling, where significantly lower pSTAT5 expression was observed on Treg of T1D and MS patients when compared to healthy individuals (Cerosaletti *et al.*, 2013). Reports also show associations between genetic polymorphisms and IL-2 signalling, where lower pSTAT5 expression on Treg was observed in individuals bearing *IL-2RA* polymorphisms associated with increased susceptibility to autoimmune diseases, versus those with protective haplotypes (Garg *et al.*, 2012). Finally, a link between IL-2 signalling and Treg function has also been shown, where Treg of T1D patients with high expression of pSTAT5 following *in vitro* stimulation with IL-2, when compared to patients with low pSTAT5 expression, had significantly greater numbers of circulating FoxP3<sup>+</sup> Treg, which were better at suppressing autologous Teff *in vitro* (Yang *et al.*, 2015). As these reports focus on IL-2 signalling in Treg, and for our analyses we were also interested in non-Treg cells, we developed an assay that was accurate and comprehensive, allowing a detailed assessment of IL-2 signalling in Treg, Teff, NK and CD8<sup>+</sup> T cells.

To develop this assay, we had to:

1. Test several combinations of target-clone-conjugate to obtain optimal staining of target cells.
2. Determine the stimulation conditions where we could observe robust, but submaximal expression of pSTAT5 on target cells.

The first part was particularly complicated, as to expose pSTAT5 intracellularly, we had to permeabilise the cells using perm buffer III, a methanol-based reagent. Many cell surface proteins are sensitive to these volatile methanol reagents, resulting in a loss of recognition by their respective antibodies. In turn this leads to no positive staining observed by flow cytometry. This assay has been extensively interrogated Treg, aiding in selection of clone and conjugate for FoxP3. However, for non-Treg cells this is not the case. There is helpful buffer compatibility information provided by BD however, at the time of experimental design, this information had not been updated for at least five years. It took several attempts to find compatible combinations of fluorochrome-antibody-clone that produced robust staining of target cells. Although not part of our hypothesis stated at the beginning of this chapter, initially we wished to also investigate whether there was IL-2 signalling in monocytes using this assay, given that we saw an IL-2 induced decrease in one of the populations in chapter 2. However, compatibility data published by BD indicates that CD14 is not compatible with perm buffer III when conjugated to any of the available fluorochromes, as we discovered during our own optimisation experiments (data not shown). Furthermore, evidence shows that monocytes constitutively express the IL-2R $\beta$  and IL-2 $\gamma$ c, and the expression of IL-2R $\alpha$  can be induced when monocytes are activated *in vitro*, but there is no evidence to indicate that IL-2 signals via the

STAT5 pathway in these cells (Bosco *et al.*, 2000). As for the stimulation conditions, we wished to observe submaximal expression of pSTAT5 on target cells as this would allow us to assess the effects of therapy and also, the differences between individuals in IL-2 signalling. When stimulating QC PBMC with incremental concentrations of IL-2 *in vitro*, we observed that dose-dependent submaximal expression of pSTAT5 was obtained in Treg with 0.5 units of IL-2. While concentrations of 1 unit resulted in near maximal induction of pSTAT5, which reached a plateau at 10 units and greater, indicating that these concentrations are too high for our analyses. For non-Treg cells, which are not as sensitive to IL-2 as Treg, we observed a dose-dependent induction of pSTAT5 at 10 units, which did not significantly change as the concentration increased. Therefore, we selected 0.5 and 10 units of IL-2 as the preferred stimulation conditions for IMODALS participant PBMC. Measuring IL-2 signalling in several white blood cell populations in a single experiment, to our knowledge, has not been reported. As such, to assess day-to-day variation in assay performance, we measured variables such as Treg, Teff, CD8<sup>+</sup> T and NK cell frequency as well as, the percentage expression of pSTAT5 on these cells, in two single blood draw QC samples alongside the IMODALS PBMC samples. We observe good experimental reproducibility with % CV of <20% for all variables, with the exception of frequencies for NK (% CV 28.81%) and pSTAT5<sup>+</sup> NK cells (% CV 27.81%) for QC sample 1. As total NK frequency values are low, a small change in frequency between experimental batches can drive an increase in %CV. Another reason for this could be the result of inaccurate assessment in viability and subsequently, stimulation of QC PBMC cells outside the indented number of 1x10<sup>6</sup>. This increase in variance could be sample specific and it is likely that we

simply cannot enumerate NK cells accurately in this particular QC PBMC sample, as this is not observed in our other QC PBMC sample.

To test the first hypothesis, we assessed whether IL-2 signalling at baseline correlated with the expansion of Treg and non-Treg cells following IL-2 therapy, accounting for the variable expansions we observe. However, we did not observe significant correlations between pSTAT5<sup>+</sup> Treg at day 1 and percent change in Treg number at day 64 in either IL-2 treated group. This indicates that IL-2 signalling is not a strong predictor of Treg expansion in our patient cohorts. Thus, the question still remains as to what influences this variable Treg expansion we and others have observed using IL-2 *in vivo*. Finding the answer may provide the means to predict individuals who may optimally benefit from IL-2 therapy and also may help personalise IL-2 doses. As mentioned previously, other contributing factors such as patient characteristics and disease progression have been hypothesised to, but not implicated in variable Treg expansion in IL-2 trials. However, it has been shown that these factors affect the basal Treg levels circulating in the periphery. Age is one of the patient characteristics that has been shown to affect Treg numbers, with studies in healthy individuals showing that numbers increase with age (Gregg *et al.*, 2005; Hou *et al.*, 2017). In terms of disease progression, in ALS it has been shown that Treg numbers are significantly lower in fast progressors when compared to slow progressors and healthy controls (Henkel *et al.*, 2013). Furthermore, studies assessing Treg levels in healthy graft donors have shown that circulating Treg numbers can vary up to five-fold between individuals (Lamikanra *et al.*, 2020). Therefore, it stands to reason that, when administering IL-2, we are expanding Treg that are already

present at variable levels inter-individually, thus the expansion we see may be proportional to the circulating levels of Treg. However, it is also likely that, given how heterogenous Treg are, the inter-individual variability in expansion is related to specific subpopulation(s) of Treg. To assess this, comprehensive phenotyping of Treg before and after IL-2 therapy is required. For non-Treg cells, we also did not observe significant correlations between pSTAT5 induction at day 1 and the expansion of Teff, NK and CD8<sup>+</sup> T cells at 1MIU, and Teff and NK at 2MIU. There was, however, a significant correlation between pSTAT5 at day 1 and CD8<sup>+</sup> T cell expansion at day 64 at 2MIU IL-2. It appears that the significance is driven by two patients with high responses in CD8<sup>+</sup> T cell number and pSTAT5 expression. Our study would benefit from a larger group of patients receiving 2MIU IL-2 to further confirm the strength of this relationship. If this is the case, then we may not be able to predict Treg expansion by IL-2 signalling but rather, use this technique to predetermine the effects of IL-2 therapy on CD8<sup>+</sup> T cells. As previously discussed, the role of CD8<sup>+</sup> T cells in ALS is unclear, but in autoimmune diseases such as T1D, SLE and MS epigenetic modifications in genes involved in the activation and proliferation of CD8<sup>+</sup> T cells have been shown (Deng *et al.*, 2019). In T1D, autoreactive CD8<sup>+</sup> T cells contribute to destruction of insulin producing cells. Furthermore, CD8<sup>+</sup> T cell infiltrates dominate over CD4<sup>+</sup> T cells in areas of the CNS where demyelination is present in MS patients (Liblau *et al.*, 2002). Therefore, future IL-2 trials would benefit from knowing how CD8<sup>+</sup> T cells will respond to therapy.

To test the second hypothesis, we assessed whether IL-2 therapy had an effect on IL-2 signalling in Treg and non-Treg cells. For this analysis we assessed

pSTAT5<sup>+</sup> cells at days 1 and 85. We did not select day 64 for this assessment as IL-2 therapy trials in GVHD and T1D have shown an IL-2 dose-dependent upregulation of pSTAT5 in trial participants and we expected this to be the case in our participants (Matsuoka *et al.*, 2013; Rosenzwajg *et al.*, 2015; Todd *et al.*, 2016). We did not observe any significant change in induction of pSTAT5 expression on Teff or NK cells in either IL-2 treated group at day 85. However, at 2MIU IL-2, we did observe alterations in induction of pSTAT5 on Treg and CD8<sup>+</sup> T cells between days 1 and 85. There was a significant, dose-dependent decrease in induction of pSTAT5 on Treg and, a significant increase in pSTAT5 on CD8<sup>+</sup> T cells. Further analysis revealed these changes to be confined to the CD45RA<sup>-</sup> subsets of Treg and CD8<sup>+</sup> T cells. Our Treg findings from the 2MIU cohort can be partially compared to a 2013 study by Matsuoka and colleagues. In this study, patients with chronic GVHD (n=14) were administered  $3 \times 10^5$  IU/m<sup>2</sup> IL-2 (n=7) or  $1.0 \times 10^6$  to  $1.5 \times 10^6$  IU/m<sup>2</sup> IL-2 (n=7) daily for 8 weeks. When examining mean pSTAT5 expression on Treg of all participants, the authors show a significant increase one week after the start of therapy, which subsequently declined to levels below baseline. This decreased expression of pSTAT5 was steadily maintained while the patients were on IL-2. Whether this is the case in IMODALS participants is unknown as we did not assess pSTAT5 at every visit and even if we did, it is unlikely that we would have observed a similar effect as our dosing regimen was not continuous but consisted of 5-daily doses of IL-2 at the beginning of three consecutive months. However, similarly to our findings, the authors do show a further decline, below baseline, in pSTAT5 expression on Treg at the 12-week follow-up, three weeks after cessation of IL-2 (Matsuoka *et al.*, 2013). Although this data is similar, it was gathered by two different methods and

therefore direct comparisons cannot be made. The authors assessed the time on IL-2 effect on pSTAT5 expression, by staining participant PBMC at every timepoint without stimulation. Whereas we took a different approach and assessed whether Treg taken from before and three weeks after therapy, when stimulated with the same concentration of IL-2 *in vitro*, would show a difference in IL-2 signalling. Furthermore, the authors elected to show the mean change in pSTAT5 expression in all participants regardless of dose, whereas our approach shows that the reduction in IL-2 signalling in Treg is not only significantly different between 2MIU and placebo but is also dose-dependent. Indicating that higher doses of IL-2 may result in reduced IL-2 signalling. Regardless of how the data was gathered, this reduced Treg sensitivity to IL-2 may have an effect on Treg expansion. Given that the decrease in STAT5 phosphorylation by Treg in our cohort is dose-dependent, and Treg expansion by IL-2 *in vivo* in most cases is also dose-dependent, it stands to reason that these reductions in Treg IL-2 signalling may affect subsequent Treg expansion as a trial continues. Another IL-2 therapy trial carried out on GVHD patients, shows fluctuations in Treg number. Where a peak increase in Treg number is observed early after therapy, subsequently declines but is maintained above baseline with continued IL-2 therapy. However, this peak increase in Treg number is not observed again with continued IL-2 therapy. This may be affected by reduced IL-2 signalling (Koreth *et al.*, 2016). Whether this is the case in IMODALS is unclear as we did not take our participants past the third cycle of IL-2 but the mean increase in Treg number, on average was greater at day 64 than day 8, suggesting that day 64 was our peak. Therefore, we could hypothesise that further cycles of IL-2 in our participants, may not result in greater Treg numbers as decreased IL-2 signalling

may affect expansion. To assess this, a longer duration clinical trial is needed. Nevertheless, if this is the case, for future trials using IL-2 in any pathological condition, scientists may need to consider ways to maintain Treg levels and prevent the loss of CD25 such as giving lower doses more frequently or use of modified IL-2 drugs, which will be addressed in the final discussion. When examining whether changes in IL-2 signalling are confined to either memory or naïve Treg, we observe that in both subsets there is a decrease in pSTAT5 at 2MIU, this is highly significant in memory Treg. There is no data from other IL-2 trials to support this finding. In ALS, all we know so far is that lower numbers of both naïve and memory Treg are associated with faster disease progression, while mechanisms by which these subsets contribute to disease remain unclear (Sheean *et al.*, 2018). Furthermore, memory Treg can be further subdivided into central and effector memory, therefore more comprehensive analysis is needed, both in IL-2 therapy and ALS disease progression to better understand the significance of these data (Shevyrev and Tereshchenko, 2020). Our IL-2 signalling in CD8<sup>+</sup> T cell findings add a level of contradiction to the notion of dose escalation. We report that at both doses, there was a significant increase in pSTAT5 expression on CD8<sup>+</sup> T cells at day 85. Indicating that these cells are potentially more sensitive to IL-2 after therapy, than they were at the beginning of the trial. There are no other reports that show this effect of IL-2 therapy on CD8<sup>+</sup> T cell IL-2 signalling. If we think that IL-2 signalling may affect Treg expansion, then the same logic could be applied to CD8<sup>+</sup> T cells, except in this case we may observe greater expansion of CD8<sup>+</sup> T cells as the trial goes on. As before, this needs further investigation in a clinical trial of longer duration with a larger cohort size. If true, this could be detrimental in conditions where these

cytotoxic T cells contribute to pathological mechanism of disease. Furthermore, it may have a profound effect on life-long IL-2 therapy, as this is thought to be required to maintain elevated Treg levels in order to improve clinical efficacy. As with Treg, we observed that this increase in IL-2 signalling was confined to the CD45RA<sup>-</sup>CD8<sup>+</sup> T cell subset. Again, the significance of this in ALS or in IL-2 therapy trials is still unknown. Furthermore, CD45RA is not an ideal marker to distinguish naïve and memory CD8<sup>+</sup> T cells, as a subset of activated CD8<sup>+</sup> T cells, known as TEMRA, can re-express CD45RA (Willinger *et al.*, 2005). Therefore, more work is needed to assess whether this is truly confined to memory CD8<sup>+</sup> T cells. Regardless of CD45RA, we have shown that at the highest dose, Treg present with a reduction in IL-2 signalling while the opposite is true for CD8<sup>+</sup> T cells. As previously discussed, raising the need for several considerations which not only need to be addressed before the start of IL-2 therapy, but also during.

In this chapter we also sought to assess whether IL-2 signalling took place in monocytes. This was driven by our previous observation where significant reductions in the number of alternative and intermediate monocytes at 2MIU IL-2 was detected. Evidence for direct effects of IL-2 on monocytes are scarce. However, studies have shown that monocytes constitutively express L-2R $\beta$  and IL-2 $\gamma$ c while the expression of IL-2R $\alpha$  (CD25) can be induced by GM-CSF and IFN- $\gamma$  (Bosco *et al.*, 1994, 2000; Dendrou *et al.*, 2009). To that end, we hypothesized that the induction of CD25 on monocytes may permit IL-2 signaling downstream and, having observed a decrease in monocyte subsets following IL-2 therapy, this signaling may result in upregulation of proteins associated with migration. This hypothesis relies heavily on our trial participant monocytes

expressing CD25, which we were not able to determine however, studies have shown that ALS patient monocytes are skewed towards a more activated and inflammatory phenotype when compared to healthy controls (Zhao *et al.*, 2017). If this is the case, then we may be able to utilize patient samples to assess whether:

- a. Upregulation of CD25 on monocytes leads to downstream IL-2 signaling via the classical STAT5, or to the lesser extent STAT1 and STAT3 pathways.
- b. This signaling is associated with increased expression of proteins mediating migration, such as CX3CR1 or CCR2 (Gautier *et al.*, 2009).

For the first part, we elected to assess these STAT proteins as other interleukins, such as IL-10 and IL-27, have been shown to selectively activate STAT3 and STAT1 in human monocytes *in vitro*, while STAT5 is well characterized to be phosphorylated in T cells following IL-2-IL-2R engagement (Nishiki *et al.*, 2004; Kalliolias and Ivashkiv, 2008; Liao *et al.*, 2013). To preserve clinical trial samples, we sought to optimize an assay that could assess this using healthy donor blood first. We successfully induced CD25 expression on monocytes by stimulating whole blood with GM-CSF and IFN- $\gamma$ , however we did not observe any STAT5, STAT1 or STAT3 phosphorylation following the addition of IL-2 to our stimulation cultures. In this setting, we were unable to determine IL-2 signaling in monocytes, hence we did not go on to utilize patient samples for further assessment. Our experimental analysis is limited by the number of signaling proteins we assessed, and it may be the case that IL-2 is mediated by other signaling pathways such as PI-3K or ERK1/2. Both of which are involved in monocyte survival and apoptosis, and are more potent in Teff following activation by IL-2 (Gonzalez-Mejia and

Doseff, 2009; Liao *et al.*, 2013). It may also be the case that there is no IL-2 signaling in monocytes via the IL-2R and the decrease we observe following therapy may be influenced by other cells migrating out of the blood. This may be difficult to assess as studies have showed that *in vitro* Treg and Teff can influence monocytes towards the M2 and M1 phenotype respectively, however data suggesting that this can influence migration is scarce (Tiemessen *et al.*, 2007). One of the ways to investigate this would be to co-culture monocytes and Treg and rather than measuring cytokines, perform flow cytometry and transcriptional profiling of these cells following coculture to investigate whether Treg influence expression of migratory proteins in monocytes. The effects of IL-2 on Treg influence could also be studied this way. Knowing this may shed valuable insight into monocyte-Treg interactions and may be translated to the IL-2 therapy field.

In this chapter we showed that consecutive cycles of IL-2 had a significant effect on IL-2 signalling in Treg and CD8<sup>+</sup> T cells. However, we also showed that when measured at the start of the trial, pSTAT5 expression is not a predictor of Treg and non-Treg cell expansion. Nor can it account for the variable expansion observed between individuals. Several other factors could influence this variability, one of which could be the heterogeneity of Treg and non-Treg cell populations. Furthermore, given this heterogeneity, particularly with regards to Treg, it is relatively unclear how IL-2 therapy affects specific subpopulations of these cells. A question that will be addressed in the subsequent chapter.

## **Chapter 5. Comprehensive phenotyping of Treg and non-Treg cells before and after LD-IL-2.**

### **5.1. Introduction.**

Treg are a heterogenous population of T cells, comprising of multiple subpopulations. A study of just four anonymous individuals identified 22 subpopulations of Treg by mass cytometry, each phenotypically distinct from another (Mason *et al.*, 2015). Studies have also shown that the presence of certain Treg phenotype(s) may be more beneficial than total Treg ( $CD4^+CD127^{lo}FoxP3^+$ ) (Donnelly *et al.*, 2018). For an example, Treg expressing surface Sialyl Lewis x (CD15s) are reported to be the most suppressive and highly differentiated in humans (Miyara *et al.*, 2015). Treg expressing Helios, which is a member of the Ikaros family of transcription factors, are found to be in a highly activated state with enhanced suppressive capabilities. Helios<sup>+</sup> Treg are also more stable, as shown that the fraction of FoxP3<sup>+</sup> Treg that express proinflammatory cytokines usually arise from the Helios<sup>-</sup> fraction (Zabransky *et al.*, 2012). Furthermore, a subset of human Treg expressing high levels of surface ectoenzyme CD39 is reported to maintain stable levels of FoxP3 under inflammatory conditions while CD39<sup>lo</sup> Treg differentiated into Th1 or Th17 cells (Gu *et al.*, 2017). IL-2 therapy has been shown to selectively activate specific Treg subpopulations. A study in GVHD patients on LD-IL-2 therapy, showed that clinical responders had a greater number of memory Treg expressing programmed cell death protein 1 (PD-1) when compared to clinical non-responders (Asano *et al.*, 2017). Another study, also in GVHD patients, showed

selective expansion of Helios<sup>+</sup> naïve and memory Treg subsets *in vivo* in response to 1MIU IL-2/m<sup>2</sup>/day (Hirakawa *et al.*, 2017).

With regards to ALS, the effects of IL-2 on Treg phenotypes are unknown. Data for Treg phenotypes in relation to disease progression is also scarce. This increases the demand for these studies, particularly as the ALS population tend to be older with Treg that are functionally defective, as reported previously. The need is further highlighted by reports showing immune alterations within the ALS population, with Treg cell population as one of the key discriminators. Patients surviving longer tend to be younger, possessing greater numbers (per µL of blood) of several white blood cells, including Treg, than their older counterparts as reported by a 2017 study (Gustafson *et al.*, 2017). Using the published Treg phenotype findings from other diseases, we designed and optimised a flow cytometry-based assay, incorporating several markers of Treg, and by definition Teff, activation and proliferation into a single staining panel, to comprehensively investigate the effects of IL-2 on Treg phenotype in ALS.

As for non-Treg cells, we had to carefully select the populations to investigate based on our own findings in chapter 2, the current knowledge in IL-2 trials, and also their relevance in ALS. In terms of Treg, this was straightforward as Treg numbers correlate with ALS progression and they are selectively expanded by LD-IL-2, which is the foundation of the IMODALS trial (Henkel *et al.*, 2013). As discussed in chapter 1, studies where peripheral immune parameters were assessed in ALS patients alongside healthy controls, have commonly shown

significant differences in monocyte subsets and NK cell numbers between groups.

Published evidence suggests that ALS monocytes are skewed towards a classical (CD14<sup>+</sup>CD16<sup>-</sup>) phenotype, differentially expressing pro-inflammatory genes. While the CD14<sup>+</sup>CD16<sup>+</sup> (intermediate) monocytes may play a protective role in ALS. Furthermore, CX3CR1<sup>+</sup> monocytes are associated with better prognosis (Murdock *et al.*, 2016, 2017; Zhao *et al.*, 2017). To expand upon our chapter 2 monocyte findings, in addition to CD14 and CD16, markers such as CD163, CD206, CD68, CCR2 and CX3CR1 have been used to better assess monocyte phenotypes. Research has shown that high expression of CCR2, CD68 and low CX3CR1, CD163 and CD206 is pertinent to classical and intermediate monocytes, while the opposite is true for the non-classical phenotype where high expression of CX3CR1 in particular, marks the patrolling monocyte phenotype (Italiani and Boraschi, 2014; Fukui *et al.*, 2018; Hou *et al.*, 2018; Trombetta *et al.*, 2018; Canè *et al.*, 2019). Our own findings in chapter 2 show that IL-2 had no effect on classical monocytes but induced a decrease in CD163<sup>+</sup> non-classical monocyte number. Given this, we set out to further investigate the phenotype of the affected monocytes.

Less is known about NK subsets in ALS, other than the consistent reports showing total NK significantly greater in number in ALS when compared to healthy individuals (Gustafson *et al.*, 2017; Murdock *et al.*, 2017). However, NK subsets expressing CD11c or CX3CR1 are found to play disease modifying roles in MS patients and we wanted to assess whether these subsets are affected by

IL-2 therapy in ALS (Aranami *et al.*, 2006; Hamann *et al.*, 2011). Based on these reports, combined with the data in chapter 2 where we observed IL-2 induced changes in NK and monocyte cell subsets, we designed a second, comprehensive immunophenotyping panel to:

1. Assess changes in NK cell subsets following IL-2 therapy.
2. To further assess the phenotype of IL-2 affected monocytes.

The experimental work in this chapter will test the following hypotheses:

1. IL-2 will selectively expand specific Treg and NK subpopulations.
2. Any effect of treatment on these subpopulations will persist after the therapy has stopped.
3. In addition to CD16 and CD163, the reduced non-classical monocytes will show changes in other markers associated with this subset, such as migration.

To test these hypotheses, we selected patient cryopreserved PBMC samples corresponding to day 1, 64, 85 and 169 visits in trial. Flow cytometry is a widely used technique in the immunology research setting. However, the more comprehensive it is, the greater the dimensionality of data obtained, and although it is relatively easy to identify cell populations by manual gating in 2-D space, it cannot be performed in a comprehensive manner, is laborious and biased. Therefore, to assess the effects of IL-2 therapy on subpopulations of Treg, NK and monocytes, we required:

1. Unbiased identification of Treg, NK and monocyte subpopulations in patient samples.
2. The ability to track the frequencies and marker expression of these subpopulations in patient samples over the course of the clinical trial.

There are several algorithms to analyse high dimensional data. From dimensionality reduction techniques such as t-SNE and uniform manifold approximation and projection (UMAP), to unbiased identification of cell subsets based on phenotypic similarities such as SPADE, FlowSOM and Phenograph (Liu *et al.*, 2019; Palit *et al.*, 2019). To reduce the dimensionality of our data set, we elected to use UMAP. Although similar to t-SNE in presenting high dimensional data in 2-D space, it is more sensitive to rare cell populations, such as those in transition, thus allowing a more comprehensive view of all white blood cells (Palit *et al.*, 2019). For unbiased identification and tracking of cell subsets throughout the trial, we selected Phenograph and FlowSOM as analysis algorithms. A recent study comparing several unbiased algorithms on large data sets has determined that Phenograph was a robust algorithm, identifying the highest number of clusters, including rare cells, and is highly stable with increasing sample size. While FlowSOM was deemed to be the most precise algorithm, outperforming other algorithms in accuracy of cell subset identification undergoing cell cycle and in several tissue samples (Liu *et al.*, 2019). Phenograph is an unbiased algorithm that uses k-means clustering to identify and cluster high dimensional, single cell data into cellular networks (subpopulations), based on the phenotypic similarities between cells (DiGiuseppe *et al.*, 2018). FlowSOM employs a self-organising algorithm to group cells into nodes, producing a map

where the distance between nodes represents how similar or different, they are to one another. Using hierarchical clustering, each node is then subsampled several times and assigned to metacluster (subpopulation), based on the how frequently the nodes cluster together. This algorithm can be applied to several samples at once, generating data relating to the frequency and marker expression of each metacluster. However, unlike Phenograph, it requires manual input of the number of metaclusters one wishes to identify prior to analysis (Van Gassen *et al.*, 2015). Therefore, we will use the Phenograph algorithm to identify the number of subpopulations of Treg, NK and monocytes in patient PBMC samples. We will then employ the FlowSOM algorithm to track changes in the frequency and expression profiles in these subpopulations before and after IL-2 therapy. Both algorithms are useful tools for investigating single cell heterogeneity in pathological conditions, that may otherwise be missed using manual gating (Levine *et al.*, 2015; Van Gassen *et al.*, 2015; Araya and Goldszmid, 2020).

## **5.2. Materials and methods.**

### **Preparation of assay media and buffers:**

#### Thawing media:

X-VIVO supplemented with PSF and 10% FBS, filtered using 0.45 $\mu$ m microfilter and pre-warmed to 37°C prior to thawing of PBMC.

#### Staining buffer:

PBS supplemented with 2mM EDTA and 1% AB, filtered using 0.45 $\mu$ m microfilter.

#### FoxP3 fixation and permeabilisation buffer (eBioscience):

The 4x fixation and permeabilisation concentrate was diluted down to 1x concentration with the diluent provided in the kit.

**Permeabilisation wash buffer (eBioscience):**

The 10x wash buffer was diluted down to 1x concentration with distilled water.

**Flow cytometry:**

Trial participant PBMC were thawed, and viability assessed using the same technique as in chapters 3 and 4. Following this, the cells were resuspended at a concentration of  $1 \times 10^6$  cells/mL of PBS. The cells were then incubated with 1 $\mu$ L/mL of LIVE/DEAD fixable blue dead cell stain (ThermoFisher) in 1mL of PBS for 30 minutes at 4°C in the dark. The cells were then washed and pelleted by centrifugation at 400g for 5 minutes at 4°C with 2mL of staining buffer. The supernatant was then poured off and the cell pellet resuspended in 100 $\mu$ L of staining buffer. For panel 1 (table 5-1), the PBMC were first stained with a master mix of PD-1 BV785 and ICOS BV650 antibodies at 37°C for 15 minutes. Following this, the remaining surface antibodies for CD3 PE-Dazzle 594, CD4 BUV395, CD25 PE, CD31 BV421, CD27 BUV737, CD39 BV711, CD15s BV510, CD45RA APC-Cy7, HLA-DR BV605 and CD49d PE-Cy5 were added, and the samples incubated at 4°C in the dark for 30 minutes. Unbound antibody was removed by washing the cells with 2mL of staining buffer and pelleting by centrifugation at 400g for 5 minutes at 4°C, the supernatant was then poured off and the cell pellet resuspended. For staining with intracellular antibodies, the PBMC were fixed and permeabilised by adding 1mL of previously prepared 1x FoxP3 fixation and permeabilisation buffer and incubated for 40 minutes in the dark at room

temperature. The cells were then washed twice with 2mL of 1x permeabilisation wash buffer and pelleted by centrifugation at 400g for 5 minutes at 4°C, the supernatant was poured off and the cell pellet resuspended in residual volume of permeabilisation wash buffer. The master mix of intracellular antibodies for FoxP3 AF647, Ki-67 FITC and Helios PE-Cy7 was added to the PBMC and samples incubated for 40 minutes in the dark at room temperature. Again, the cells were washed twice with 2mL of 1x permeabilisation wash buffer and pelleted by centrifugation at 400g for 5 minutes at 4°C, the supernatant was poured off and the cell pellet resuspended in 200µL of staining buffer.

| Immunophenotyping Panel 1 |              |          |         |         |              |
|---------------------------|--------------|----------|---------|---------|--------------|
| Target                    | Conjugate    | Clone    | Origin  | µL/Test | Manufacturer |
| PD-1                      | BV785        | EH12.2H7 | Mouse   | 5       | BL           |
| ICOS                      | BV650        | DX29     | Mouse   | 5       | BD           |
| CD3                       | PE-Dazzle594 | UCHT1    | Mouse   | 2.5     | BL           |
| CD4                       | BUV395       | SK3      | Mouse   | 2.5     | BD           |
| CD25                      | PE           | 2A3      | Mouse   | 20      | BD           |
| CD25                      | PE           | M-A251   | Mouse   | 20      | BD           |
| CD31                      | BV421        | WM59     | Mouse   | 2.5     | BL           |
| CD27                      | BUV737       | L128     | Mouse   | 5       | BD           |
| CD39                      | BV711        | A1       | Mouse   | 5       | BL           |
| CD15s                     | BV510        | CSLEX1   | Mouse   | 1       | BD           |
| CD45RA                    | APC-Cy7      | HI100    | Mouse   | 0.5     | BL           |
| HLA-DR                    | BV605        | L243     | Mouse   | 5       | BL           |
| CD49d                     | PE-Cy5       | 9F10     | Mouse   | 5       | BL           |
| FOXP3                     | AF647        | 259D/C7  | Mouse   | 20      | BD           |
| FOXP3                     | AF647        | 206D     | Mouse   | 5       | BL           |
| Ki-67                     | FITC         | B56      | Mouse   | 5       | BD           |
| HELIOS                    | PE-Cy7       | 22F6     | Hamster | 5       | BL           |

Table 5-1 Monoclonal antibody details used in immunophenotyping panel 1 to stain IMODALS PBMC.

BL = BioLegend, BD = Beckton Dickinson.

For immunophenotyping panel 2 (table 5-2), the PBMC were first stained with a master mix of CX3CR1 APC, CCR2 BV785, CD163 BV605 and CD206 BV510 antibodies in the water bath set at 37°C for 15 minutes. The PBMC were removed from the water bath, the master mix of remaining surface antibodies for CD3 AF700, TCR $\gamma$  $\delta$  PE-Cy7, CD56 PE, CD14 PercP-Cy5.5 CD16 APC-Cy7, CD19 BUV737, HLA-DR BV650, CD1c BV711, CD11c BV421, CD141 PE-Dazzle 594 and CD123 BUV395 were added, and the cells incubated at 4°C in the dark for 30 minutes. Unbound antibody was removed by washing the cells with 2mL of staining buffer and pelleting by centrifugation at 400g for 5 minutes at 4°C, the supernatant was then poured off and the cell pellet resuspended. For staining with intracellular antibody, the PBMC were first fixed and permeabilised by adding 100 $\mu$ L of 1x fixation and permeabilisation buffer and incubated for 20 minutes in the dark at room temperature. The cells were then washed twice with 2mL of 1x permeabilisation wash buffer and pelleted by centrifugation at 400g for 5 minutes at 4°C, the supernatant was poured off and the cell pellet resuspended in residual volume of permeabilisation wash buffer. The intracellular antibody for CD68 FITC was added to the PBMC and samples incubated for 20 minutes in the dark at room temperature. Again, the cells were washed twice with 2mL of 1x permeabilisation wash buffer and pelleted by centrifugation at 400g for 5 minutes at 4°C, the supernatant was poured off and the cell pellet resuspended in 200 $\mu$ L of staining buffer. The samples were then acquired on a BD LSRFortessa flow cytometer (BD).

| Immunophenotyping Panel 2 |               |         |        |                           |              |
|---------------------------|---------------|---------|--------|---------------------------|--------------|
| Target                    | Conjugate     | Clone   | Origin | $\mu\text{L}/\text{Test}$ | Manufacturer |
| CX3CR1                    | APC           | 2A9-1   | Rat    | 1.5                       | BL           |
| CCR2                      | BV785         | K036C2  | Mouse  | 1.5                       | BL           |
| CD163                     | BV605         | GH1/61  | Mouse  | 5                         | BL           |
| CD206                     | BV510         | 15-2    | Mouse  | 1.5                       | BL           |
| CD3                       | AF700         | UCHT1   | Mouse  | 5                         | BL           |
| TCR $\gamma\delta$        | PE-Cy7        | IMMU510 | Mouse  | 2.5                       | BC           |
| CD56                      | PE            | HCD56   | Mouse  | 5                         | BL           |
| CD14                      | PercP-Cy5.5   | HCD14   | Mouse  | 5                         | BL           |
| CD16                      | APC-Cy7       | B73.1   | Mouse  | 2.5                       | BL           |
| CD19                      | BUV737        | SJ25C1  | Mouse  | 5                         | BD           |
| HLA-DR                    | BV650         | L243    | Mouse  | 5                         | BL           |
| CD1c                      | BV711         | L161    | Mouse  | 2.5                       | BL           |
| CD11c                     | BV421         | Bu15    | Mouse  | 1.5                       | BL           |
| CD141                     | PE-Dazzle 594 | M80     | Mouse  | 5                         | BL           |
| CD123                     | BUV395        | 7G3     | Mouse  | 5                         | BD           |
| CD68                      | FITC          | Y1/82   | Mouse  | 2.5                       | BL           |

**Table 5-2 Monoclonal antibody details used in immunophenotyping panel 2 to stain IMODALS PBMC.**

BL = BioLegend, BC = Beckman Coulter, BD = Beckton Dickinson.

### Data Analysis:

Total Treg ( $\text{CD3}^+\text{CD4}^+\text{CD25}^{\text{hi}}\text{FoxP3}^+$ ), Teff ( $\text{CD3}^+\text{CD4}^+\text{CD25}^{+/\text{lo}}\text{FoxP3}^-$ ), NK ( $\text{CD3}^-\text{CD56}^+$ ) and monocytes ( $\text{CD3}^-\text{CD56}^-\text{HLA-DR}^+$ ) were manually gated as indicated in figures 5-1 and 5-2 using FlowJo version 9. The flow cytometry analysis also permitted us to look into DC and TCR $\gamma\delta^+$  T cells, as we did not observe any changes in these as a result of IL-2, these cell types will not be presented in this chapter. CD19 $^+$  B cells were gated for exclusion purposes only.

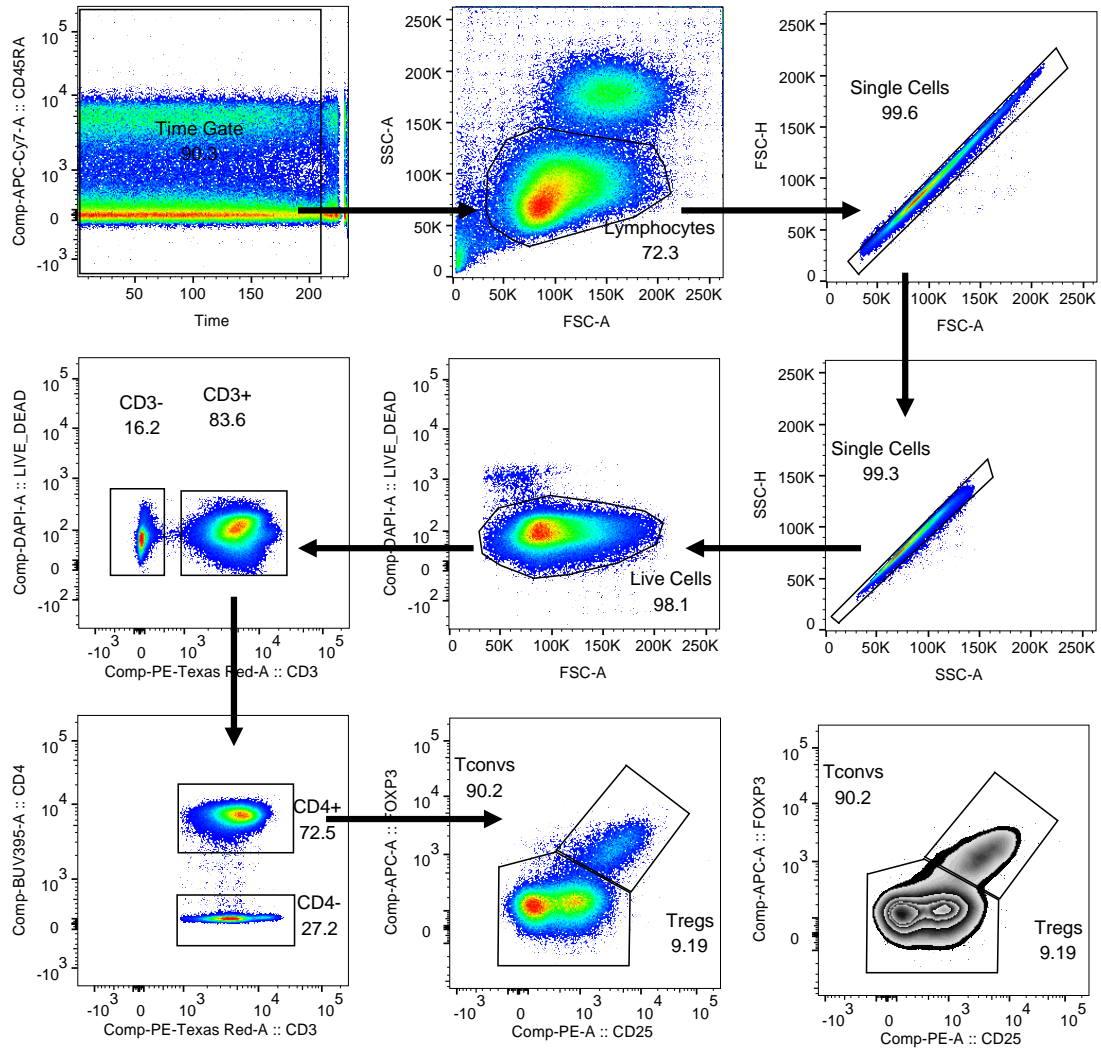


**Figure 5-1 Gating scheme for Treg and Teff in immunophenotyping panel 1.** First all events were gated across time. Then lymphocytes were selected based on size and granularity in the FSC-A and SSC-A axis. Doublets, debris and dead cells were excluded by first gating on single cells and then cells negative for the viability dye in the DAPI channel. Finally, Treg and Teff were identified as CD3<sup>+</sup>CD4<sup>+</sup>CD25<sup>hi/+</sup>FoxP3<sup>+</sup> and CD3<sup>+</sup>CD4<sup>+</sup>CD25<sup>+</sup>FoxP3<sup>-</sup> respectively.

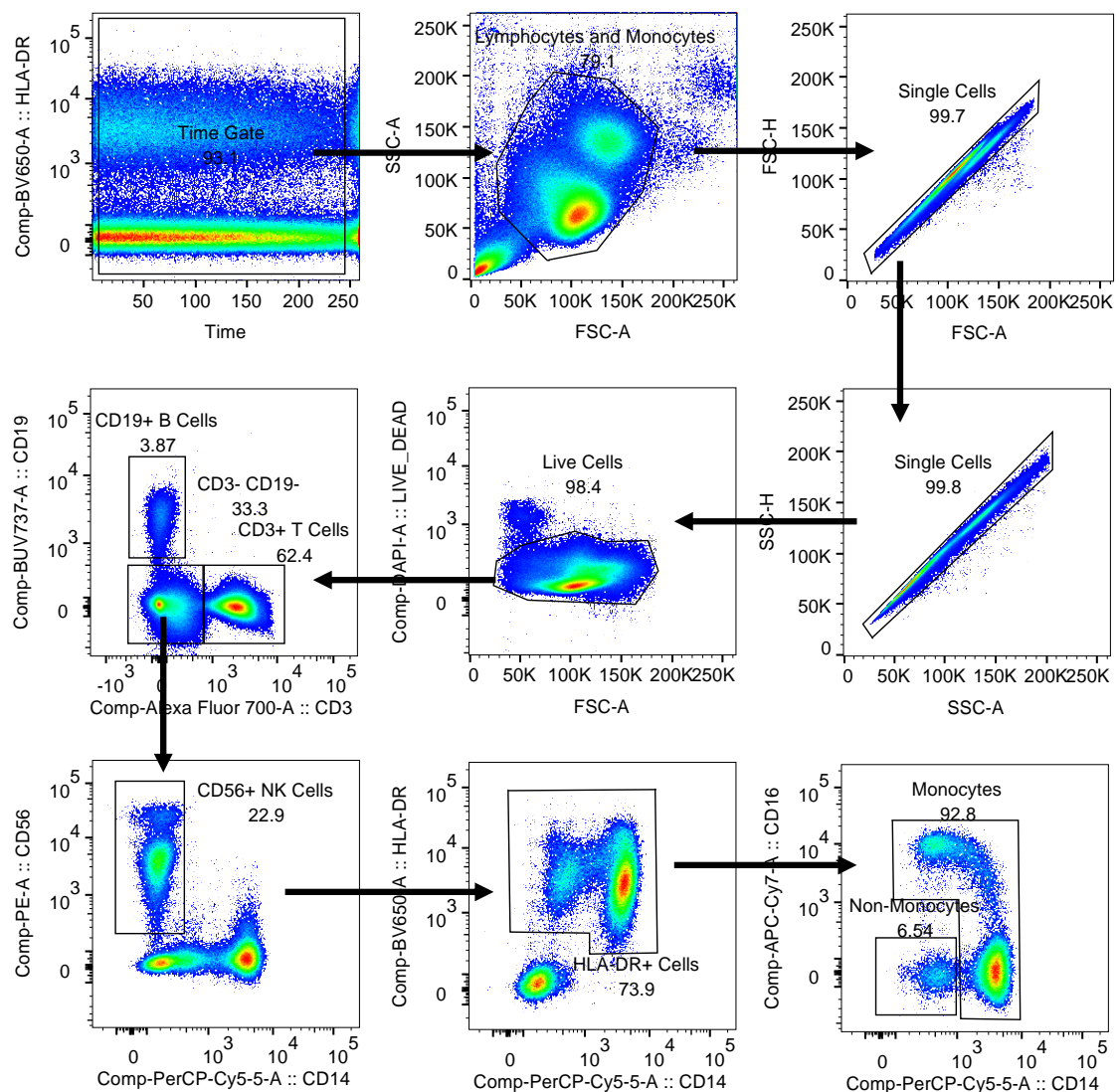


**Figure 5-2 Gating scheme for NK and monocytes in immunophenotyping panel 2.** First all events were gated across time. Then lymphocytes and monocytes were selected based on size and granularity in the FSC-A and SSC-A channels. Doublets, debris and dead cells were excluded by first gating on single cells and then cells negative for the viability dye in the DAPI channel. Then, NK cells were identified as CD3<sup>-</sup>CD19<sup>+</sup>CD56<sup>+</sup> and monocytes were identified as CD3<sup>-</sup>CD19<sup>-</sup>CD56<sup>-</sup>HLA-DR<sup>+</sup>.

To identify subpopulations within the gated cell types, Phenograph analysis was performed with Euclidean distance using k=200 nearest neighbours setting on concatenated patient samples. We used the Uniform Manifold Approximation and Projection (UMAP) algorithm to visualise the subpopulations in 2-D space. FlowSOM analysis was then performed on each patient sample (Arcsinh scaling,

argument 150, minimum scale value -1000) in a single analysis experiment using the parameters in table 5-3.

|                        | Treg | Teff | NK   | Monocytes |
|------------------------|------|------|------|-----------|
| Events to sample       | 3500 | 9000 | 5000 | 6000      |
| Metacluster number     | 18   | 17   | 21   | 16        |
| Iterations             | 10   | 10   | 10   | 10        |
| Hierarchical consensus | Yes  | Yes  | Yes  | Yes       |

**Table 5-3. Parameters used in FlowSOM analysis of Treg, Teff, NK and Monocytes.** All patient samples for one particular population were analysed in the same experiment. Manually selected parameters for analysis include the number of events to sample per file, the number of metaclusters to identify (obtained from Phenograph analysis), number of iterations to be performed per sample and hierarchical consensus.

Statistical analysis of metacluster frequencies was performed using GraphPad Prism. Data distribution was assessed using D'Agostino & Pearson normality and lognormality test. Changes between visits in each treatment group were assessed using a student's t-test or a Wilcoxon matched-pairs signed rank test depending on the normality test result. Group comparisons of changes in subpopulation frequencies were assessed using a two-way ANOVA or mixed-effects analysis with Tukey multiple comparisons test was used to assess differences in subpopulation frequencies between treatment groups. Unbiased hierarchical clustering of marker expression intensities on subpopulations was performed using the "pheatmap" package in R.

### 5.3. Results.

The steps taken to analyse the patient data in this section are outlined in figure 5-3.

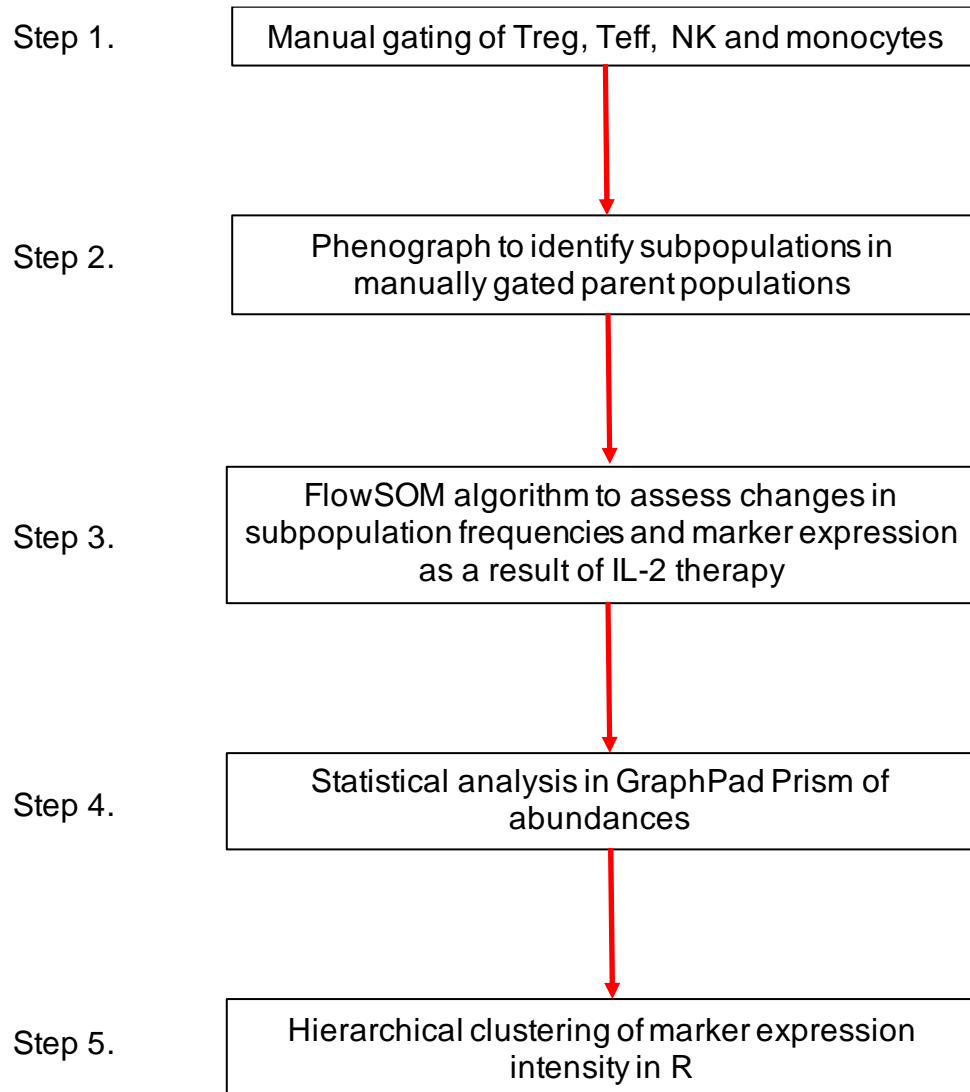


**Figure 5-3 Summary of the data analysis protocol for assessing changes in Treg, Teff, NK and monocyte subpopulations as a result of IL-2 therapy.** Treg, Teff, NK and monocytes were gated in patient samples using FlowJo. Subpopulations within gated parent populations were identified using Phenograph. Subpopulation frequencies and marker expression were determined using FlowSOM. Statistical analysis of changes in subpopulation abundances were assessed in GraphPad Prism. Hierarchical clustering of subpopulation marker expression was performed using an R script.

### 5.3.1. Experimental quality control.

A total of 144 patient samples needed to be analysed by flow cytometry in this chapter, as a result the experiments had to be carried out in a number of batches.

Similar to the approaches in the previous chapters, we mitigated against any influence of day-to-day variation in assay performance by:

1. Assessing all timepoints for an individual on the same day.
2. Assessing a random allocation of individuals in each batch.
3. A single blood draw QC was used to assess any day-to-day variation in assay performance allowing to detect any systematic drift in results.

QC data collected for the frequencies of Treg, Teff, NK and monocytes show excellent day-to-day experimental reproducibility, determined by %CV of <10% (table 5-4).

| Repeat      | Treg<br>(% CD4 <sup>+</sup> ) | Teff<br>(% CD4 <sup>+</sup> ) | NK<br>(% Live) | Monocytes<br>(% Live) |
|-------------|-------------------------------|-------------------------------|----------------|-----------------------|
| 1           | 8.26                          | 90.1                          | 7.71           | 18                    |
| 2           | 9.36                          | 90                            | 7.8            | 16.5                  |
| 3           | 9.45                          | 90.1                          | 7.63           | 17.6                  |
| 4           | 9.24                          | 90.3                          | 7.61           | 17.3                  |
| 5           | 9.28                          | 90.2                          | 7.93           | 15.4                  |
| 6           | 9.5                           | 89.7                          | 7.79           | 16.9                  |
| 7           | 9.3                           | 90                            | 7.89           | 16.4                  |
| 8           | 9.21                          | 90.1                          | 7.72           | 17.1                  |
| 9           | 9.25                          | 90.1                          | 7.92           | 14.7                  |
| 10          | 9.61                          | 89.9                          | 7.82           | 16.5                  |
| 11          | 9.45                          | 90                            | 7.8            | 17.4                  |
| <b>Mean</b> | <b>9.26</b>                   | <b>90.14</b>                  | <b>7.78</b>    | <b>16.71</b>          |
| <b>SD</b>   | <b>0.36</b>                   | <b>0.36</b>                   | <b>0.11</b>    | <b>0.97</b>           |
| <b>% CV</b> | <b>3.84</b>                   | <b>0.39</b>                   | <b>1.39</b>    | <b>5.81</b>           |

Table 5-4 Frequencies of Treg, Teff, NK, Monocytes, B Cells and DC of QC PBMC used in IMODALS sample flow cytometry.

### **5.3.2. Parent populations of Treg, NK and monocytes are comprised of several, heterogenous subpopulations in IMODALS trial participants.**

Prior to addressing the hypotheses of this chapter, we manually gated and concatenated each parent population, for every trial participant, in FlowJo. Using the Phenograph algorithm, we identified 18 subpopulations within total Treg, 21 subpopulations within total NK and 15 subpopulations within total monocytes and visualised them in 2D space using UMAP (figure 5-4 A (i) to C (i)). Analysis performed on total Teff identified 17 subpopulations (data not shown). There were no significant changes in Teff subset frequency in any of the treatment groups, as a result data Teff data is not presented in this chapter. To better understand the phenotypic characteristics of Treg, NK and monocyte subpopulations, we performed hierarchical clustering based on marker expression using R (figure 5-4 A (ii) to C (ii)), which shows:

1. Subpopulations with similar expression profiles clustering together.
2. Protein expression levels of subpopulations.

We observed several, phenotypically heterogenous subsets within total Treg, NK and monocytes. As expected, Treg are the most heterogenous population of cells in this analysis, largely made up of CD45RA<sup>-</sup> subsets, that are either activated, proliferating or both. NK and monocytes appear to be less heterogenous than Treg, with clustering largely driven by the expression of CD56 and CD16 respectively.

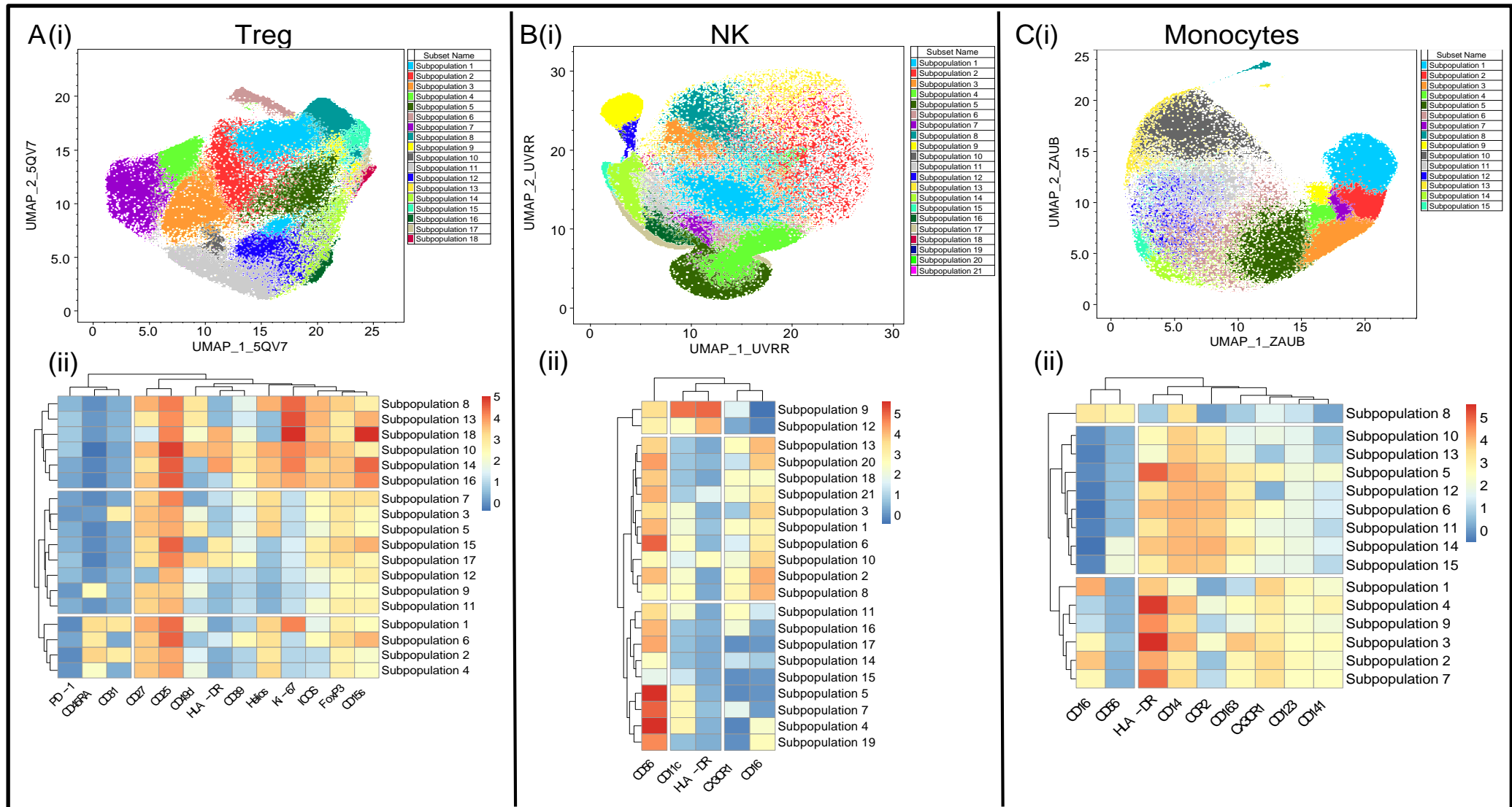
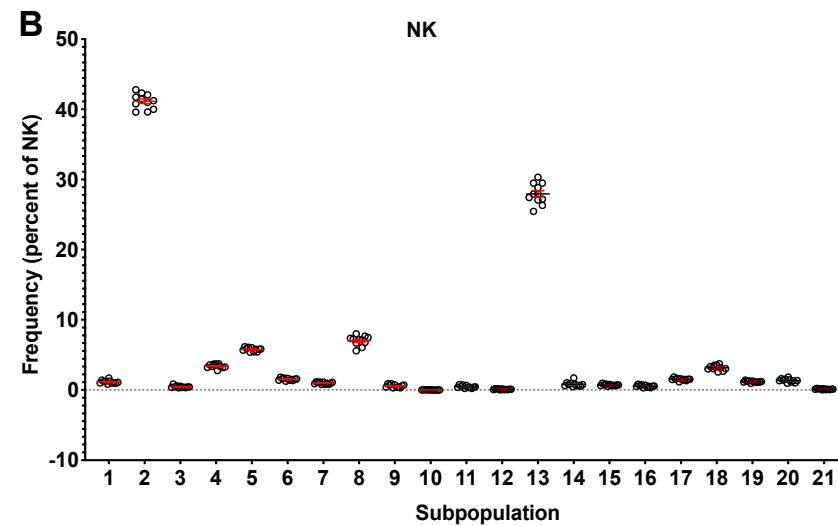
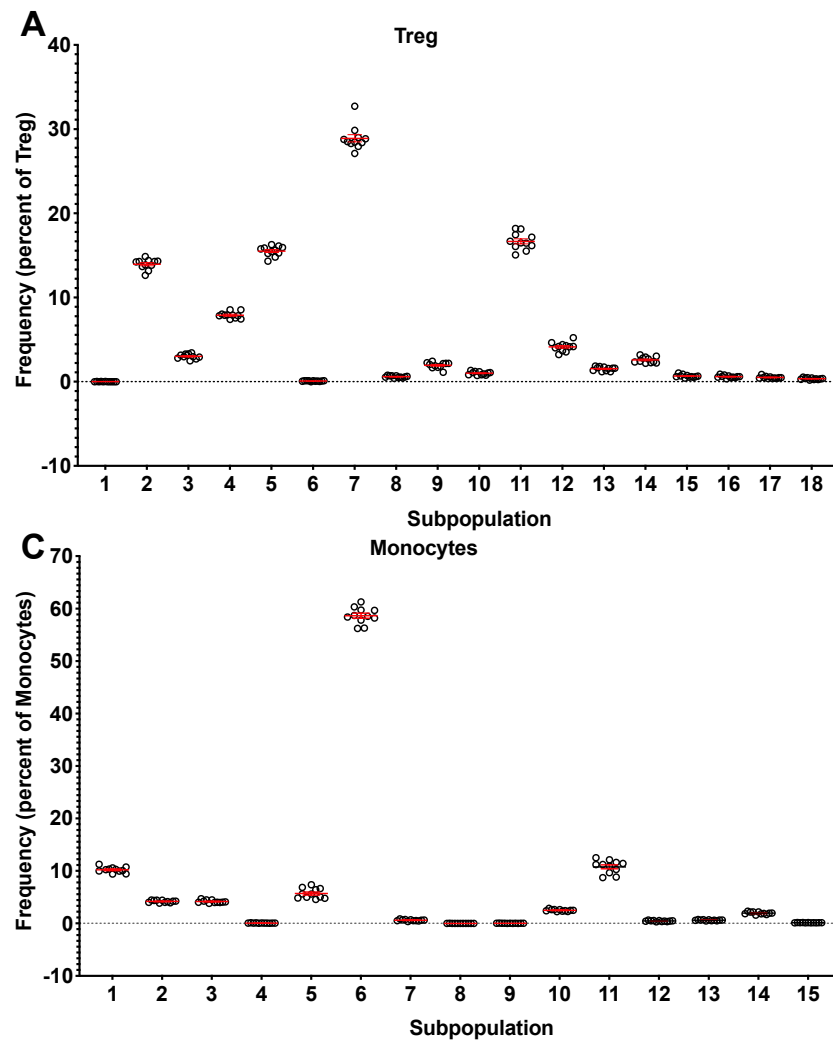


**Figure 5-4 Unbiased hierarchical clustering analysis of Treg, NK and monocyte subpopulations of IMODALS trial participants.** Panels A (i) to C(i): UMAP analysis of Treg, NK and monocyte subpopulations previously identified by Phenograph analysis. Panels A (ii) to C(ii): Unbiased hierarchical clustering of marker expression intensity of Treg, NK and monocyte subpopulations using R.

### **5.3.3. Treg, NK and monocyte subpopulation analysis in QC PBMC across the experimental batches.**

Having identified 18, 21 and 15 subpopulations in total Treg, NK and monocytes of IMODALS trial participants, we assessed the reproducibility of this data by analysing the subpopulation frequencies of these cells in our QC PBMC sample. We adapted the FlowSOM analysis template from tracking changes in subpopulations across trial visits, to assessing the frequencies of each subpopulation of Treg, NK and monocytes at each experimental batch for the QC PBMC sample. As before, we calculated the mean, standard deviation and %CV for all subpopulations. On average, we observe good day-to-day experimental reproducibility with %CV <25% for most of the Treg, NK and monocyte subpopulations (figure 5-5 A to D). However, we also observe increased variance in some populations which are present at extremely low levels, <1%. For Treg, this is the case for subpopulations 1, 6 and 18. For NK we see an increased variance for subpopulations 3, 9, 10, 11, 12, 14, 16 and 21. Finally, in total monocytes the % CV is >25% for subpopulations 4, 8 and 9 (figure 5-5 D (i, ii, iii)). Coefficient of variation assesses the spread of the data around the mean value, and this is particularly sensitive when the values which make up the mean are small. A good example of this is Treg subpopulation 1, which at 8 of the 11 experimental batches was measured at 0% by FlowSOM. While at 3 of the 11 experimental batches it was determined to be 0.03% thus resulting in a %CV of 163.299%. This is not observed when we see a 0.03% increase or decrease in frequency in a subpopulation that is present at greater frequencies, such as Treg subpopulation 3, which is found between 2.5% - 3.5%. Furthermore, subpopulation 1 is not normally present in those not undergoing IL-2 therapy.



- D**
- (i). **Treg Subpopulation (%CV):** 1 (**163.299**), 2 (4.27), 3 (8.93), 4 (4.53), 5 (3.6), 6 (**47.4**), 7 (4.73), 8 (19.18), 9 (17.84), 10 (19.19), 11 (5.72), 12 (12.45), 13 (14.59), 14 (13.06), 15 (24.67), 16 (24.02), 17 (27.17), 18 (**28.31**).
  - (ii). **NK Subpopulation (%CV):** 1 (19.9), 2 (2.49), 3 (**31.96**), 4 (8.06), 5 (4.49), 6 (10.53), 7 (13.27), 8 (9.63), 9 (**35.67**), 10 (**144.69**), 11 (**36.6**), 12 (**51.93**), 13 (5.02), 14 (**39.78**), 15 (16.33), 16 (**29.33**), 17 (11.32), 18 (10.77), 19 (9.59), 20 (18.07), 21 (**51.25**).
  - (iii). **Monocyte Subpopulation (%CV):** 1 (5.09), 2 (5.02), 3 (6.28), 4 (**49.95**), 5 (16.27), 6 (2.54), 7 (22.31), 8 (**98.44**), 9 (**49**), 10 (7.12), 11 (11.17), 12 (20.5), 13 (14.15), 14 (11.4), 15 (20.59).

**Figure 5-5 QC PBMC Treg, NK and Monocyte subpopulation analysis in experimental batches.** Panels A-C: Frequency of 18 Treg, 21 NK and 15 monocyte subpopulations in each experimental batch. Panel D i to iii: %CV of each Treg, NK and monocyte subpopulation. 1 circle = 1 experimental batch, error bars indicate mean with SEM.

### **5.3.4. LD-IL-2 selectively activates specific Treg subpopulations, some of which are maintained for up to three months after the final dose.**

To address the first hypothesis, we assessed the changes in Treg subpopulation frequency at day 1 and day 64. At 2MIU IL-2, we observe significant changes in subpopulations 1 ( $p=0.0021$ ), 5 ( $p<0.0001$ ) and 11 ( $p<0.0001$ ). At 1MIU IL-2, the frequency of subpopulations 7 ( $p=0.0006$ ), 8 ( $p=0.0027$ ) and 11 ( $p<0.0001$ ) was significantly altered. No significant changes were observed in the placebo group (figure 5-6 A to C). This analysis reveals subpopulation changes in each group, to confirm if these are treatment induced, we calculated the change in frequency for each subset and compared these between treatment groups. Comparisons for placebo versus 1MIU, and placebo versus 2MIU showed significant increases were observed in subpopulations 1 ( $p=0.0301$  and  $p=0.0162$ ), 8 ( $p=0.0173$  and  $p=0.0004$ ) and 10 ( $p<0.0001$  and  $p=0.0028$ ) while significant decreases are seen in subpopulations 5 ( $p=0.0023$  for 2MIU), 7 ( $p=0.0102$  and  $p=0.0004$ ), 11 ( $p=0.0020$  and  $p=0.0010$ ) and 12 ( $p=0.0114$ ). We also observed dose-dependent changes in subpopulations 8 ( $p=0.0019$ ), 5 ( $p=0.0397$ ), and 11 ( $p=0.0020$ ) between 1MIU and 2MIU groups (figure 5-6 D). These Treg subpopulations display an activated phenotype, based on their expression of markers such as CD25, CD49d, ICOS, CD15s and Helios as determined hierarchical clustering. Furthermore, the IL-2 expanded subsets (1, 8, 10) show high expression of Ki-67, a marker of T cell proliferation. Interestingly, one of these subpopulations (1) co-expresses CD45RA and CD31, markers associated with Treg recently emigrated from the thymus (figure 5-6 E). These data:

1. Show IL-2 expanded Treg are highly activated and proliferative.
2. Suggest an IL-2 induced Treg generation in the thymus.

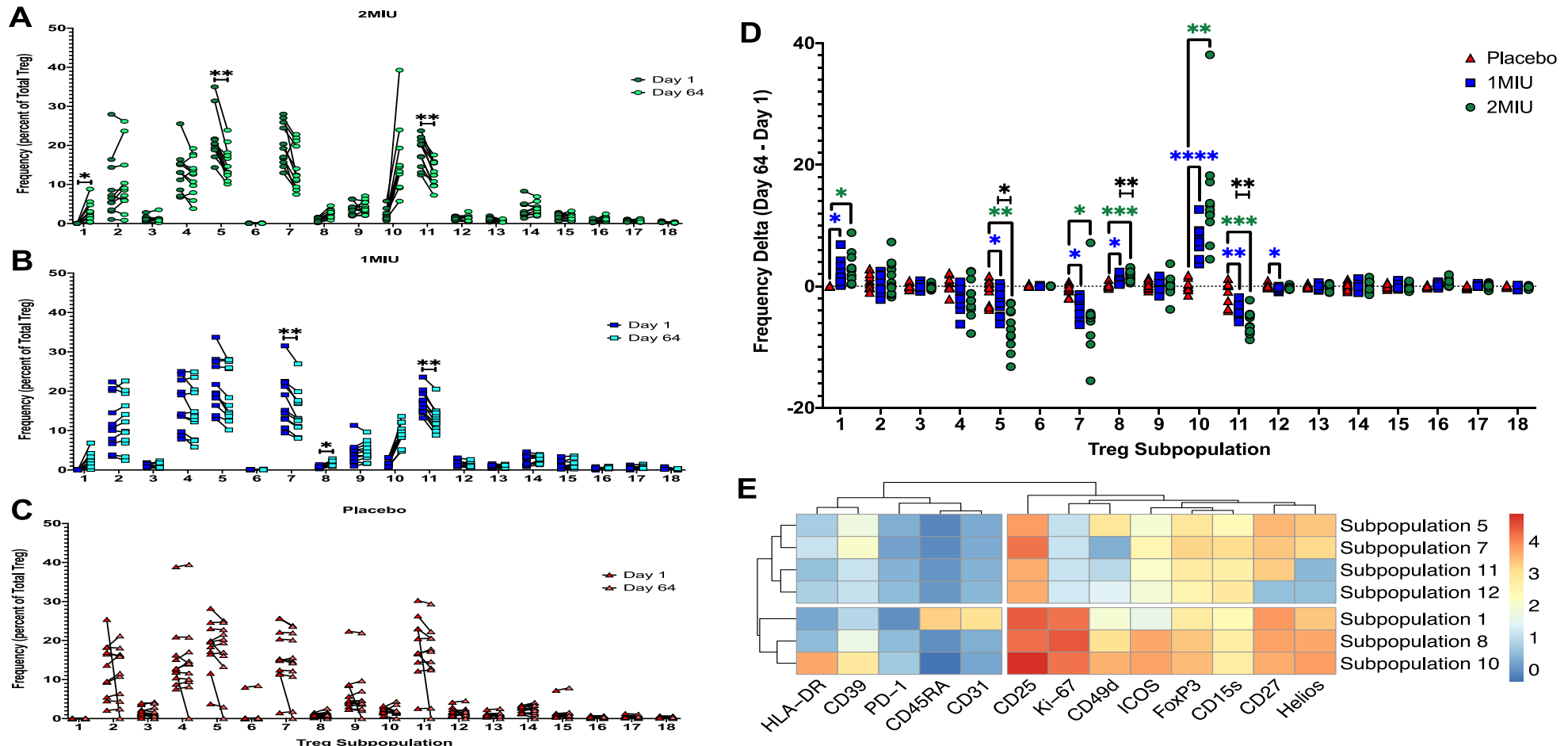


**Figure 5-6 Analysis of change in Treg subpopulation frequency and their expression profiles at day 64.** Panels A-C: Individual analysis of Treg subpopulation frequencies at day 1 and day 64 per treatment group (multiple t-tests with Bonferroni multiple comparisons test). Panel D: Change in Treg subpopulation frequency compared between treatment groups (mixed-effects analysis with Tukey multiple comparisons), \* 1MIU vs Placebo, \* 2MIU vs Placebo, \* 1MIU vs 2MIU. Panel E: Unbiased clustering analysis of expression profiles in R of cells altered in frequency at day 64. \*\*\*\*p<0.0001, \*\*\*p<0.001, \*\*p<0.01, \*p<0.05.

To confirm the phenotype of populations expanded by IL-2 therapy which had been identified by this unbiased analysis we:

1. Downloaded cells within a given cluster and examined expression of key markers.
2. Performed manual gating on the original flow cytometry files using key marker characteristics of each cell subpopulation.

An example of this analysis is shown in figure 5-7. Here, we manually gated cells that share key phenotypic characteristics of cells present in Treg subpopulation 1, recent thymic emigrants (RTE), in total Treg using expression of CD45RA, Helios, CD31 and Ki-67 in combination with the overlay function in FlowJo (figure 5-7 A). Pairwise comparisons of this subpopulation frequency at day 1 versus day 64 shows significant increases at day 64 in both 2MIU ( $p=0.0010$ ) and 1MIU ( $p=0.0020$ ) IL-2 treated and no change in the placebo group (figure 5-7 B to D). As with Treg subpopulations, we assessed the change in frequency at day 64 of the manually gated subpopulation 1 and compared this between treatment groups. We observe a mean increase of 2.78% at 1MIU and 4.22% at 2MIU at day 64. This change is significantly different in the 1MIU when compared to placebo ( $p=0.0111$ ) and 2MIU versus placebo ( $p=0.0001$ ) but not when comparing 1MIU and 2MIU (figure 5-7 E).

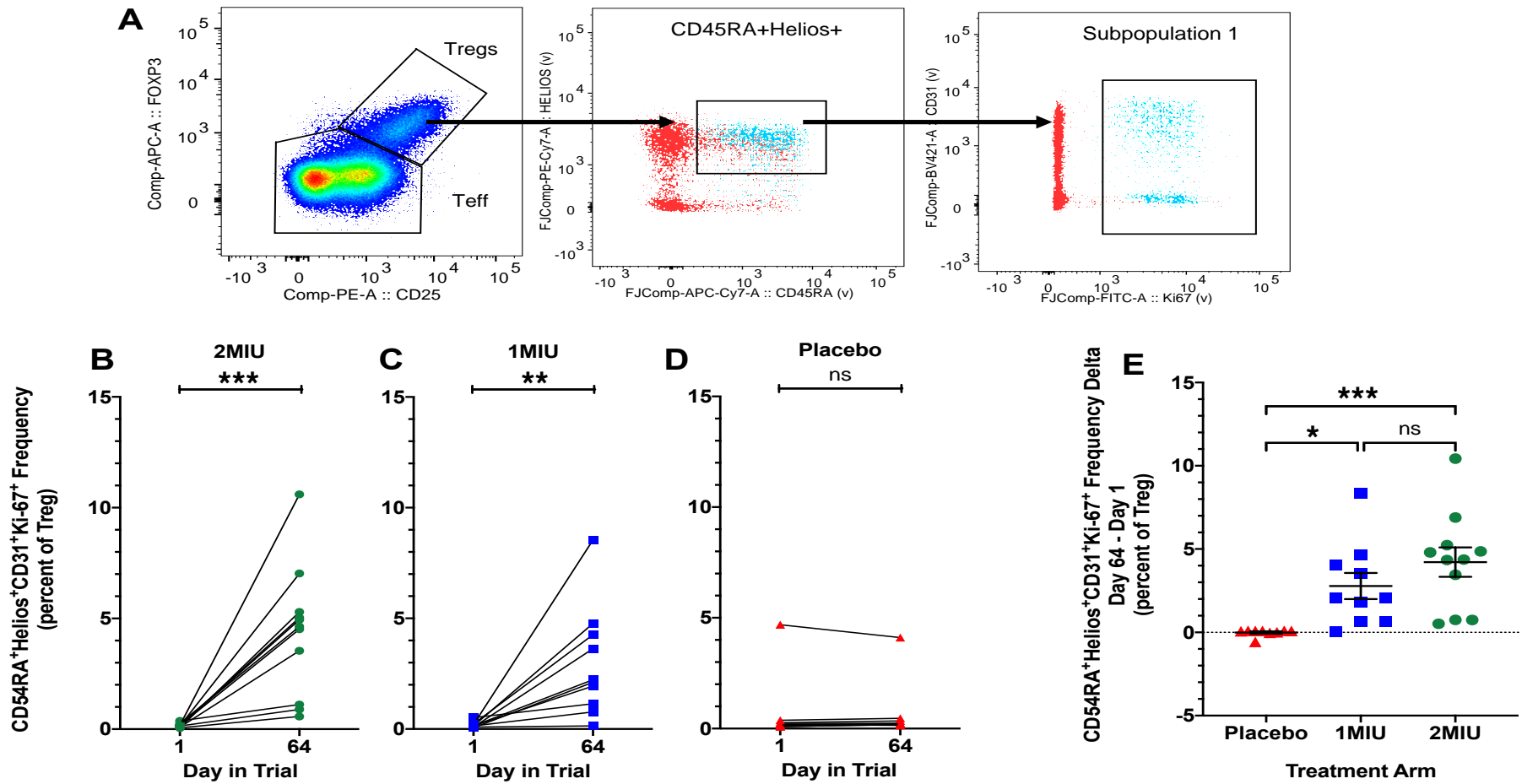


**Figure 5-7 The effects of IL-2 therapy on CD45RA<sup>+</sup>Helios<sup>+</sup>CD31<sup>+</sup>Ki-67<sup>+</sup> Treg at day 64.** Panel A: Cells corresponding to subpopulation 1 were downloaded and manually identified in FlowJo using key marker expression of CD45RA, Helios, CD31 and Ki-67. Panels B-D: Before and after analysis of subpopulation 1 frequency at day 1 and day 64 for each trial participant per treatment group. Panel E: Subpopulation 1 frequency change at day 64 for placebo, 1MIU and 2MIU groups. Error bars indicate mean with SEM. \*\*\*p<0.001, \*\*p<0.01, \*p<0.05, ns – not significant. Panels B to D – Wilcoxon test; Panel E – Kruskal-Wallis test. Red triangles – placebo; blue squares – 1MIU; green circles – 2MIU.

To look for long term effects of IL-2 on Treg subsets, we performed the same analysis at days 85 and 169 as we did at day 1. There were no significant changes in subpopulation frequency at 1MIU or placebo. At 2MIU IL-2, there were significant changes in subpopulations 2 ( $p=0.0007$ ), 7 ( $p=0.0002$ ) and 9 ( $p=0.0005$ ) (figure 5-8 A to C). These subsets were not significantly altered at day 64, suggesting a shift in the balance of Treg subsets as the effects of IL-2 subside. This is also evident in group comparisons of change in subset frequency. From day 64, only subpopulations 5 and 7 remain significantly reduced in frequency ( $p=0.0048$  and  $p<0.0001$  respectively) by day 85, but only between 2MIU and placebo groups. This reduction is dose-dependent ( $p=0.0007$  for subset 5;  $p=0.0470$  for subset 7) when compared to 1MIU IL-2 treated. We also observed increases in subsets that were not present at day 64, namely subpopulations 2 (placebo vs 1MIU  $p=0.0384$ ; placebo vs 2MIU  $p=0.0005$ ; 1MIU vs 2MIU  $p=0.0280$ ), 4 (placebo vs 2MIU  $p=0.0362$ ), 9 (placebo vs 1MIU  $p=0.0104$ ; placebo vs 2MIU  $p=0.0002$ ; 1MIU vs 2MIU  $p=0.0470$ ) and 18 (placebo vs 1MIU  $p=0.0305$ ; placebo vs 2MIU  $p=0.0010$ ) (figure 5-8 D). Marker expression analysis shows that, unlike at day 64, with the exception of subpopulation 18, these altered subsets have low proliferative activity (low Ki-67), express low levels of markers associated with activation (ICOS, CD39, HLA-DR, CD49d). These data show that following the height of treatment, the balance of Treg subsets shifts towards a less active, less proliferative, but still a stable and highly suppressive phenotype as determined by the expression of Helios and CD15s (Zabransky *et al.*, 2012; Miyara *et al.*, 2015). Furthermore, the proliferation of cells sharing characteristics with RTE at day 64 (subpopulation 1), appears to have added to the circulating RTE pool (subpopulation 2) at day 85 (figure 5-8 E)/

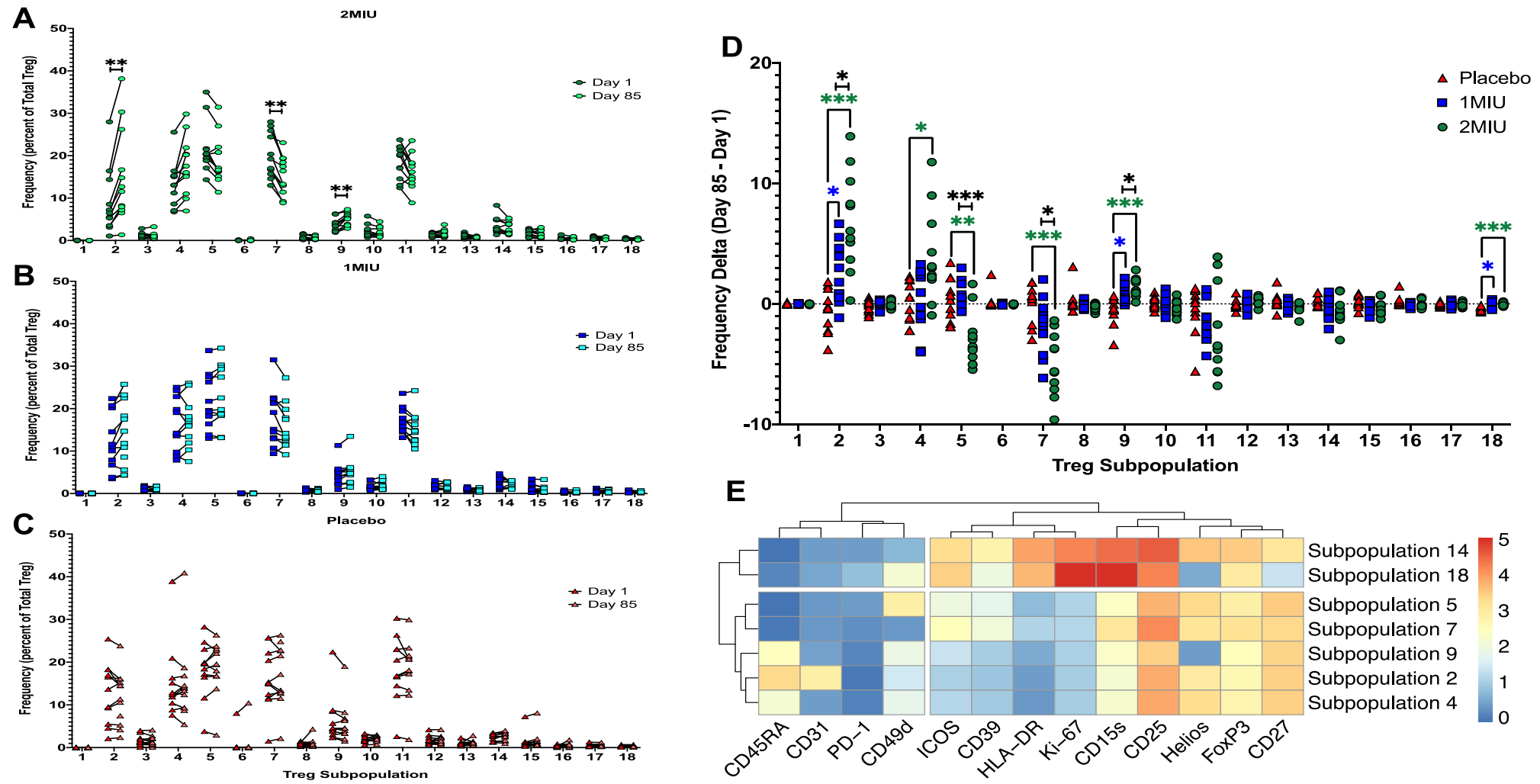


**Figure 5-8 Analysis of change in Treg subpopulation frequency and their expression profiles at day 85.** Panels A-C: Individual analysis of Treg subpopulation frequencies at day 1 and day 85 per treatment group (multiple t-tests with Bonferroni multiple comparisons test). Panel D: Change in Treg subpopulation frequency compared between treatment groups (2way ANOVA with Tukey multiple comparisons), \* 1MIU vs Placebo, \*\* 2MIU vs Placebo, \*\*\* 1MIU vs 2MIU. Panel E: Unbiased clustering analysis of expression profiles in R of cells altered in frequency at day 85. \*\*\*p<0.001, \*\*p<0.01, \*p<0.05.

As we did previously, we sought to confirm the increase in subpopulation 2 at day 85 by manually identifying this Treg subset based on the expression of CD45RA, Helios, CD31 and negative expression of Ki-67 (figure 5-9 A). Analysis of frequency of this manually gated subpopulation showed no significant changes at day 64 when compared to day 1 in any of the treatment groups, which is in line with our unbiased analysis (data not shown). However, at day 85 we observed significant increases at 2MIU ( $p=0.0010$ ) and (1MIU  $p=0.0111$ ) with no significant changes in placebo treated individuals (figure 5-9 B to D). Using unbiased methods, we did not observe a significant change in this subset at 1MIU while using manual assessment we did. This could be the effect of multiple testing, as in our unbiased analysis section we are performing statistics on 18 subpopulations simultaneously, which is not the case in our manual analysis. Assessment of change in frequency at day 85 shows a mean increase of 2.57% at 1MIU and 6.99% at 2MIU from day 1 which is significantly greater at 2MIU when compared to placebo ( $p=0.0002$ ) (figure 5-9 E).

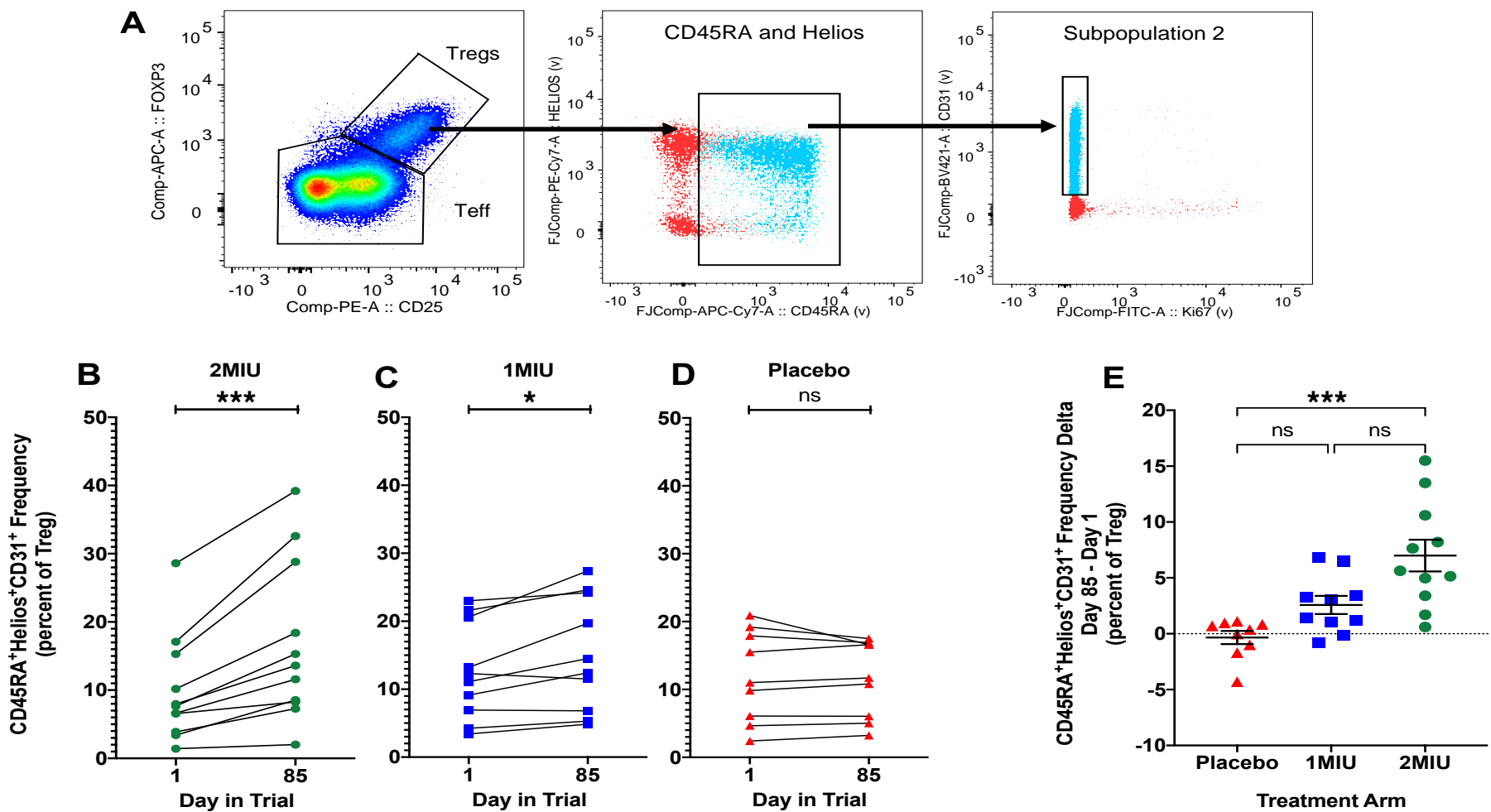


**Figure 5-9 The effects of IL-2 therapy on CD45RA<sup>+</sup>Helios<sup>+</sup>CD31<sup>+</sup> Treg at day 85.** Panel A: Cells corresponding to subpopulation 2 were downloaded and manually identified in FlowJo using key marker expression of CD45RA, Helios, CD31 and Ki-67. Panels B-D: Before and after analysis of subpopulation 2 frequency at day 1 and day 85 for each trial participant per treatment group. Panel E: Subpopulation 2 frequency change at day 85 for placebo, 1MIU and 2MIU groups. Error bars indicate mean with SEM. \*\*\*p<0.001, \*p<0.05, ns – not significant. Panels B to D – Wilcoxon test; Panel E – Kruskal-Wallis test. Red triangles – placebo; blue squares – 1MIU; green circles – 2MIU.

At day 169, subpopulations 2 and 9 remained significantly elevated when compared to day 1 ( $p=0.0019$  and  $p=0.0014$ ) in the 2MIU treated group with no significant changes observed 1MIU or those receiving placebo (figure 5-10 A to C). Group analysis shows significant changes in 3 out of the 18 Treg subsets. Greater levels of subpopulation 2 (placebo vs 2MIU  $p=0.0062$ ) and 9 (1MIU vs 2MIU  $p=0.0276$ ). Significantly lower levels of subpopulation 7 (placebo vs 1MIU  $p=0.0165$ ; placebo vs 2MIU  $p=0.0292$ ) follow on from day 85 (figure 5-10 D). Clustering analysis of marker expression shows the same phenotypic characteristics as it did in day 85 for these two Treg subsets (figure 5-10 E). The findings for subpopulation 2 by unbiased algorithms are further supported by manual analysis, where the frequency of this subset is confirmed to be significantly greater at day 169 at 2MIU ( $p=0.0010$ ) and 1MIU ( $p=0.0108$ ), with no change in placebo treated (figure 5-11 A to C). Analysis of frequency change shows that at 2MIU, the mean frequency remained 3.81% greater than at day 1 and this was significantly greater when compared to placebo group (0.0049) (figure 5-11 D). Collectively, these data show:

1. IL-2 selectively expands memory Treg with a highly activated and proliferating phenotype.
2. IL-2 also appears to have induced generation of new Treg in the thymus.
3. Three weeks after therapy, the balance of Treg subsets shifts from the highly activated, proliferative state, to a stable, activated, resting state.
4. IL-2 has a long-lasting effect on Treg recently emigrated from thymus, which remain at elevated levels at three weeks and three months after the therapy has stopped.
5. Unbiased analysis can effectively guide manual analysis.

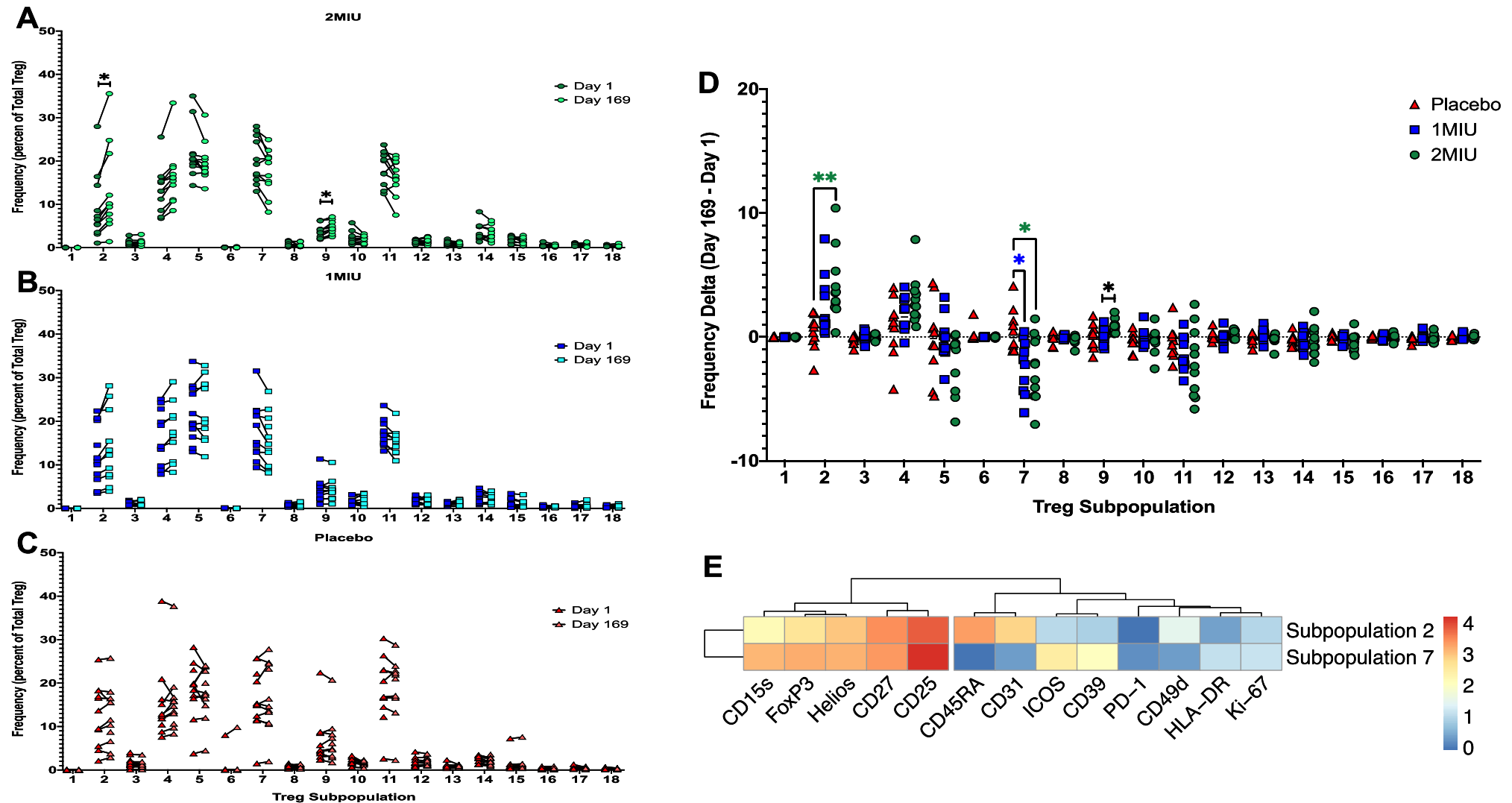


**Figure 5-10 Analysis of change in Treg subpopulation frequency and their expression profiles at day 169.** Panels A-C: Individual analysis of Treg subpopulation frequencies at day 1 and day 169 per treatment group (multiple t-tests with Bonferroni multiple comparisons test). Panel D: Change in Treg subpopulation frequency compared between treatment groups (mixed-effects analysis with Tukey multiple comparisons), \* 1MIU vs Placebo, \* 2MIU vs Placebo, \* 1MIU vs 2MIU. Panel E: Unbiased clustering analysis of expression profiles in R of cells altered in frequency at day 169. \*\*p<0.01, \*p<0.05.

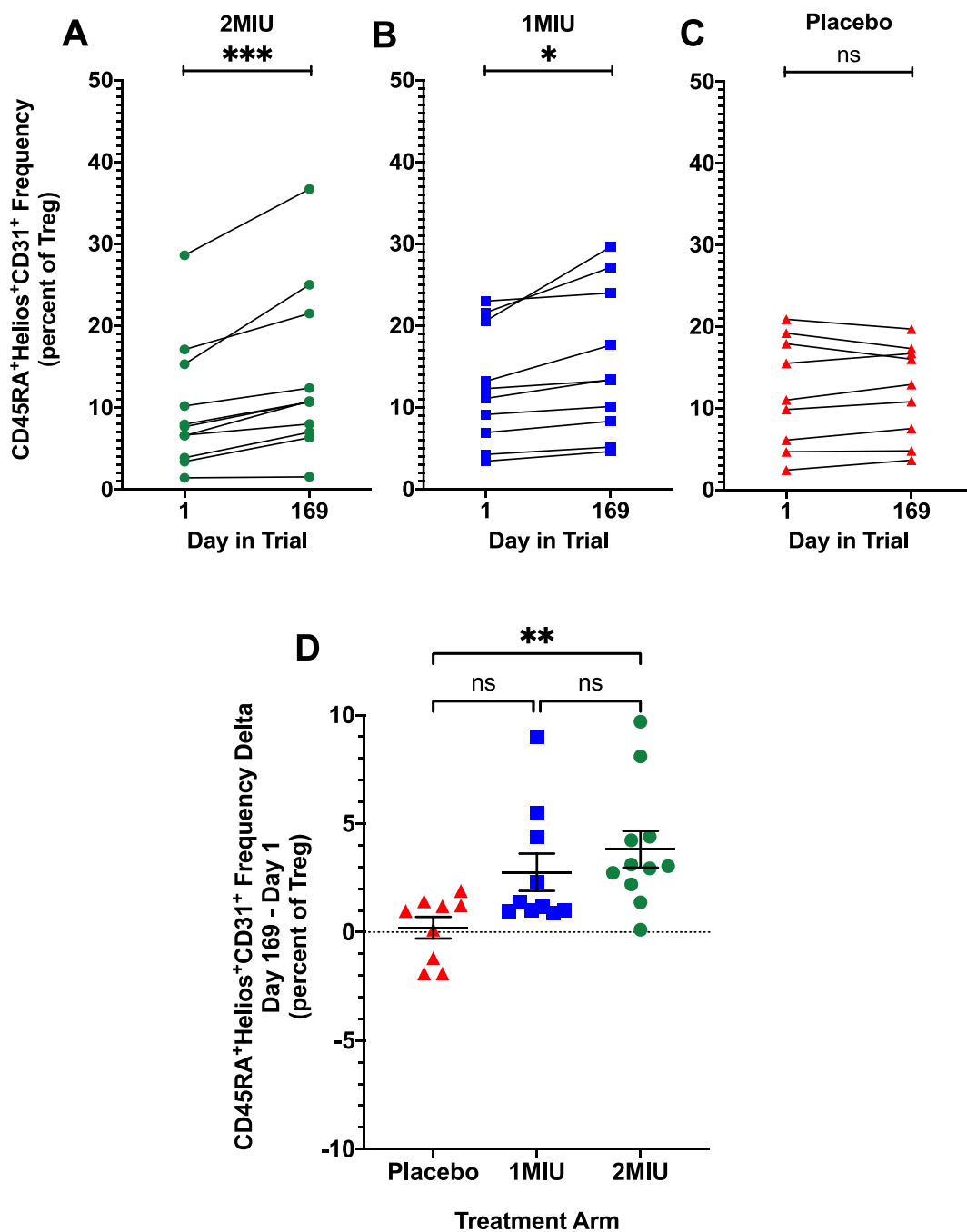


**Figure 5-11 The effects of IL-2 therapy on CD45RA<sup>+</sup>Helios<sup>+</sup>CD31<sup>+</sup> Treg at day 169.** Panels A-C: Before and after analysis of subpopulation 2 frequency at day 1 and day 169 for each trial participant per treatment group. Panel D: Subpopulation 2 frequency change at day 169 for placebo, 1MIU and 2MIU groups. Error bars indicate mean with SEM. \*\*\*p<0.001, \*\*p<0.01, \*p<0.05, ns – not significant. Panels A to C – Wilcoxon test; Panel D – Kruskal-Wallis test. Red triangles – placebo; blue squares – 1MIU; green circles – 2MIU.

### **5.3.5. In ALS patients, IL-2 expands CD56<sup>bright</sup> NK subpopulations associated with an immunoregulatory, NK2, phenotype.**

Part of the first hypothesis in this chapter was to also assess the effects of IL-2 therapy on NK subpopulations, given their reported responsiveness to IL-2 in published works as well as our own observations in chapter 2. First, we assessed changes in NK subsets at day 64. At 2MIU, we observe a significant increase in subpopulation 8 ( $p=0.0021$ ) and a significant decrease in subpopulation 9 ( $p=0.0010$ ). The same change in balance is observed in those treated with 1MIU IL-2, significant increase in subpopulation 5 ( $p=0.0016$ ) and decrease in subpopulation 6 ( $p=0.0012$ ). No significant changes are observed in patients on placebo (figure 5-12 A to C). As with Treg data, we assessed changes in subpopulation frequency and compared this between groups. Significantly greater frequencies 2MIU are observed in subpopulations 4 (placebo vs 1MIU  $p=0.0372$ ; placebo vs 2MIU  $p=0.0352$ ), 5 (placebo vs 1MIU  $p=0.0297$ ; placebo vs 2MIU  $p=0.0266$ ), 6 (placebo vs 1MIU  $p=0.0033$ ; placebo vs 2MIU  $p=0.0320$ ), 7 (placebo vs 1MIU  $p=0.0196$ ; placebo vs 2MIU  $p=0.0031$ ) and 19 (placebo vs 2MIU  $p=0.0244$ ). The same comparisons also show significant reductions in frequency of subpopulations 2 (placebo vs 1MIU  $p=0.0094$ ; placebo vs 2MIU  $p=0.0234$ ), 9 (placebo vs 2MIU  $p=0.0062$ ) and 18 (placebo vs 2MIU  $p=0.0192$ ). Furthermore, a dose-dependent decrease in frequency is also observed in subpopulation 9 (1MIU vs 2MIU  $p=0.0225$ ) (figure 5-12 D). As with Treg subsets, we are observing an IL-2 induced change in the balance of NK subsets. Clustering analysis of marker expression shows that IL-2 selectively expands CD56<sup>bright</sup> NK subsets. These expanded NK subsets do not express CX3CR1 or HLA-DR but show low expression of CD11c (figure 5-12 E).

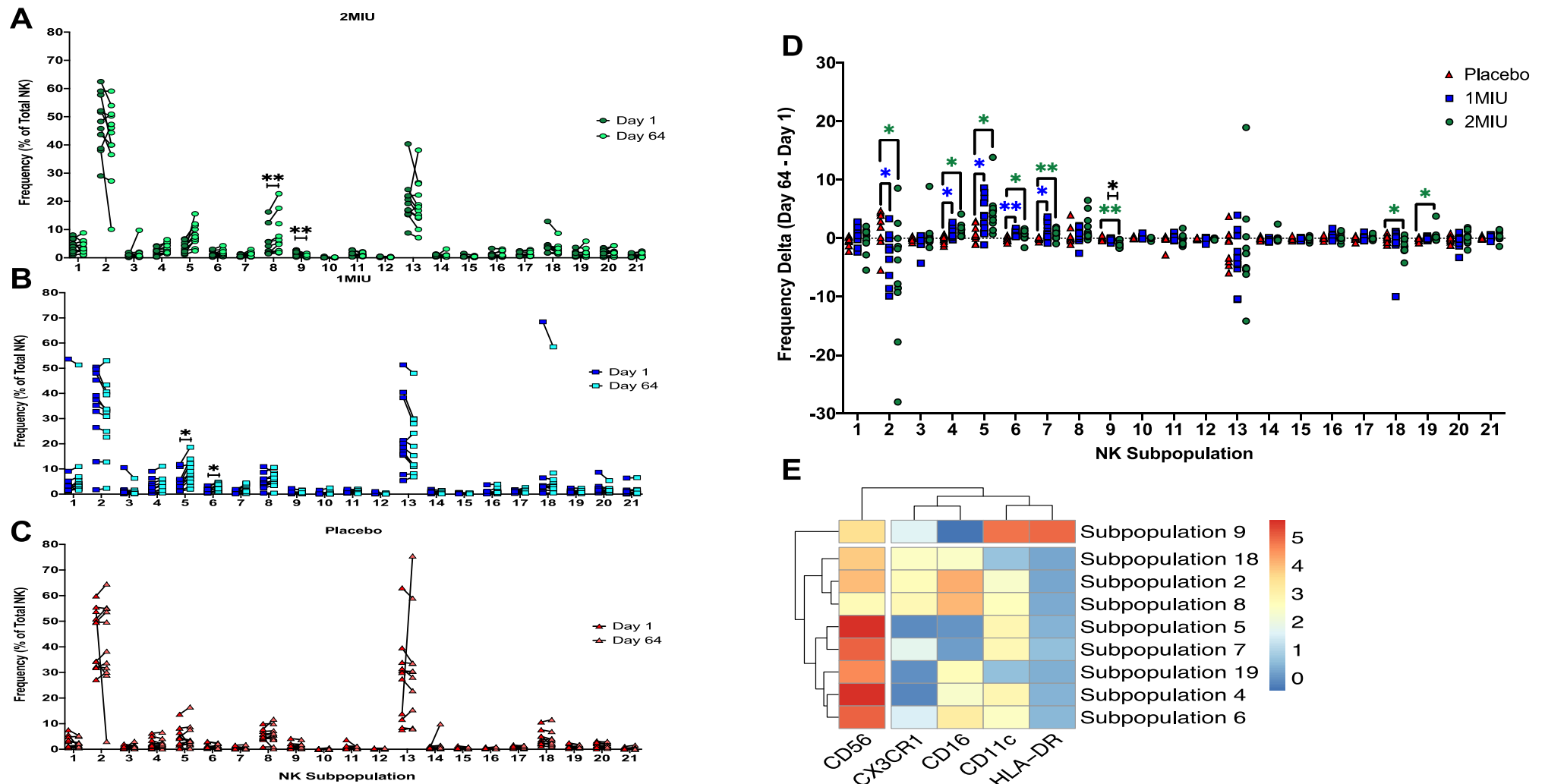


**Figure 5-12 Analysis of change in NK subpopulation frequency and their expression profiles at day 64.** Panels A-C: Individual analysis of NK subpopulation frequencies at day 1 and day 64 per treatment group (multiple t-tests with Bonferroni multiple comparisons test). Panel D: Change in NK subpopulation frequency compared between treatment groups (mixed-effects analysis with Tukey multiple comparisons), \* 1MIU vs Placebo, \* 2MIU vs Placebo, \* 1MIU vs 2MIU. Panel E: Unbiased clustering analysis of expression profiles in R of cells altered in frequency at day 64. \*\*p<0.01, \*p<0.05.

When investigating whether these changes persisted after the therapy has stopped, we do not observe any significant difference in NK subset frequency between days 1 and 85 (figure 5-13 A to C) nor between day 1 and 169 (data not shown) in the three treatment groups. Group comparisons show that the change in the frequency of subpopulation 9 is still significantly different at day 85 between placebo and 2MIU ( $p=0.0270$ ) and 1MIU and 2MIU ( $p=0.0300$ ), this is not observed at day 169 (figure 5-13 D and E). We also see that the frequency of subpopulation 18 is significantly greater at day 169 between placebo and 1MIU ( $p=0.0166$ ) (figure 5-13 E). Compared to the NK subset data at day 64, these changes are marginal. Although the CD56<sup>bright</sup> NK, like total Treg, are highly expanded by IL-2, as seen in chapter 2, the long-term effects of IL-2 on NK subsets are far fewer and less consistent than Treg subsets. Nevertheless, our data has shown that IL-2 selectively expands NK subsets expressing high levels of CD56. These subsets are negative for CX3CR1 and HLA-DR but do express low to moderate levels of CD11c (figure 5-12 E). The relevance of these subsets in ALS is unknown. However, studies in MS patients have shown that NK with high expression of CX3CR1 were more cytotoxic, while differential expression of CD11c may be a phenotype with disease modifying properties (Aranami *et al.*, 2006; Hamann *et al.*, 2011).

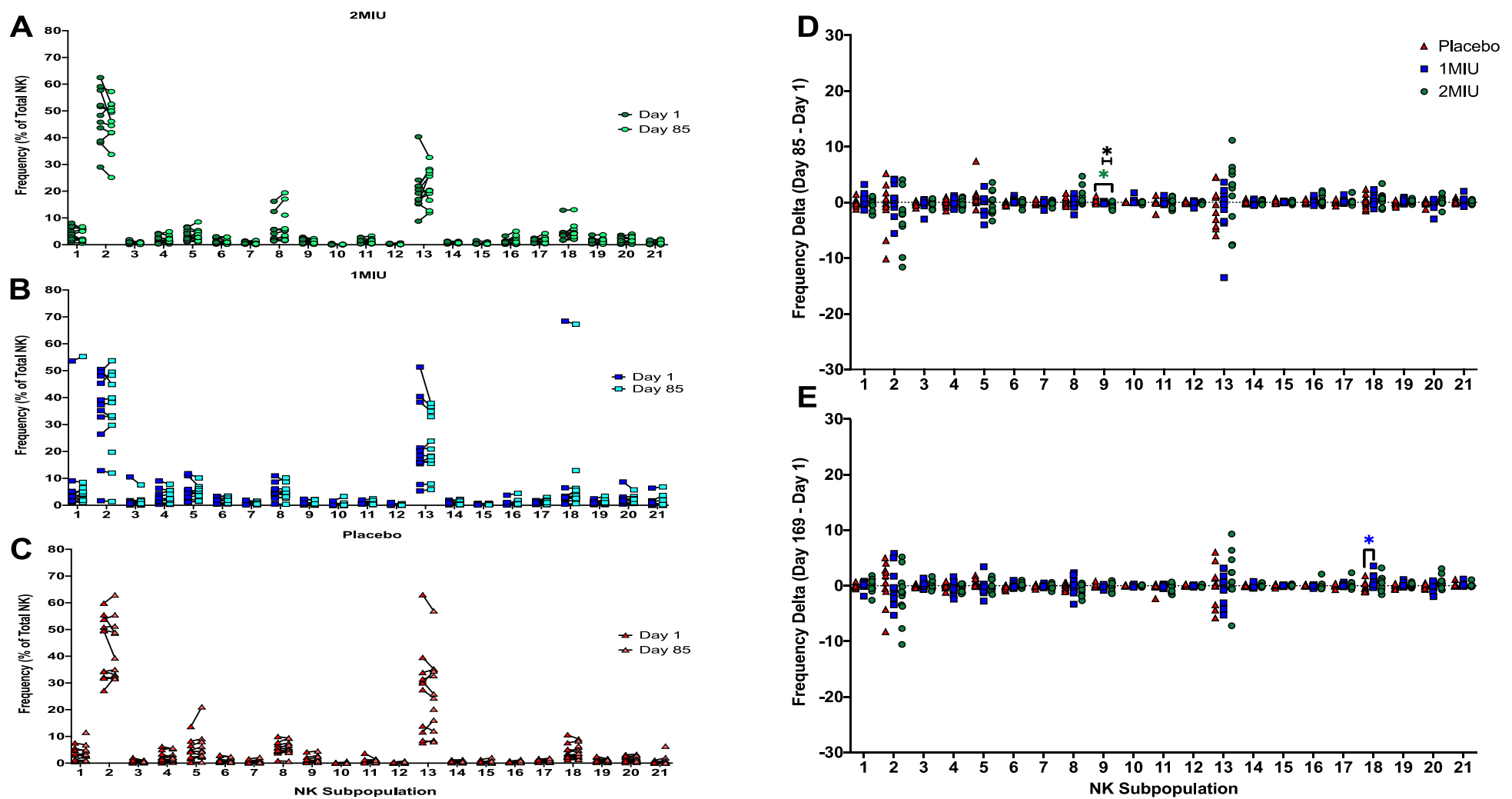


**Figure 5-13 Analysis of change in NK subpopulation frequency and their expression profiles at day 85 and 169.** Panels A-C: Individual analysis of NK subpopulation frequencies at day 1 and day 85 per treatment group (multiple t-tests with Bonferroni multiple comparisons test). Panels D-E: Change in NK subpopulation frequency compared between treatment groups at day 85 (2way ANOVA with Tukey multiple comparisons) and day 169 (mixed-effects analysis with Tukey multiple comparisons), \* 1MIU vs Placebo, \* 2MIU vs Placebo, \* 1MIU vs 2MIU. \* $p<0.05$ .

### **5.3.6. IL-2 therapy induced a decrease in monocytes with high migratory potential.**

To address the final hypothesis of this chapter, we assessed changes and expression profiles on monocyte subsets in ALS patients following IL-2 therapy. Analysis of subpopulation frequency in each group between days 1 and 64 shows a significant decrease in subpopulation 2 ( $p=0.0004$ ) in the 2MIU group and subpopulation 13 ( $p=0.0030$ ) in the 1MIU group. We also observed an increase in subpopulation 6 ( $p=0.0009$ ) in the 1MIU group and no significant changes were observed in the placebo group (Figure 5-14 A to C). When assessing the change in frequency of these subpopulations between treatment groups, we observe no significant differences. This analysis did show an increase in subpopulation 14 in the 1MIU group, this was significantly different when compared to placebo ( $p=0.0477$ ) (figure 5-14 D). As expected, these findings are less clear than for Treg and NK subsets as there are no reports showing the effects of IL-2 therapy on monocytes. Furthermore, the objective of this analysis was to further investigate the phenotype of the monocyte population that was reduced in number, reported in chapter 2. In this regard, the decrease in frequency of subpopulation 2 at 2MIU IL-2 indicates that this is the monocyte subsets of interest. This is further confirmed by marker expression profiles of subpopulation 2, showing that in addition to expressing high levels of CD163, CD16 and HLA-DR, this subset is also positive for CD14, CD123, CD141 and CX3CR1 (figure 5-14 E).

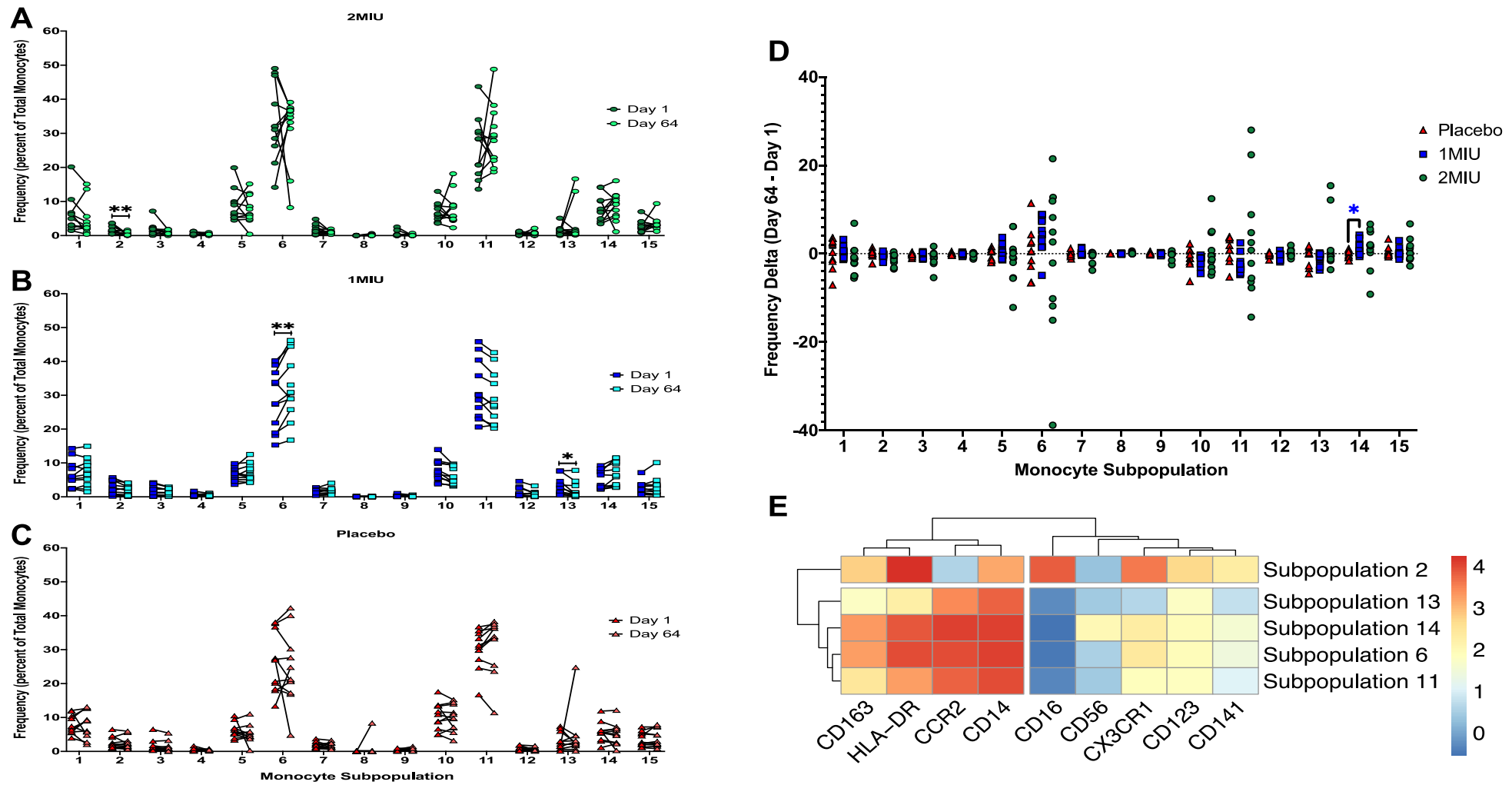


**Figure 5-14 Analysis of change in monocyte subpopulation frequency and their expression profiles at day 64.** Panels A-C: Individual analysis of monocyte subpopulation frequencies at day 1 and day 64 per treatment group (multiple t-tests with Bonferroni multiple comparisons test). Panel D: Change in monocyte subpopulation frequency compared between treatment groups (mixed-effects analysis with Tukey multiple comparisons), \* 1MIU vs Placebo. Panel E: Unbiased clustering analysis of expression profiles in R of cells altered in frequency at day 64. \*\* $p<0.01$ , \* $p<0.05$ .

The relevance of CD123 and CD141 on monocyte subsets is unknown as these markers are expressed on DC (Collin and Bigley, 2018). Our marker expression analysis is also affected by the fact that we had to exclude CD206 (protective) and CD68 (inflammatory) monocyte makers from this analysis, as we observed no heterogenous expression of these between the monocyte subsets. This is due to CD206 being exclusively expressed on macrophages and DC. Focussing on markers that these cells do express, the combination of CD16, CD163, CD14 and no CCR2 suggests that these are not classical, but rather resemble a combination of the intermediate and non-classical monocytes, as classical monocytes have high expression of CCR2. The high expression of CX3CR1 also suggests that the decrease we observe is a result of these cells migrating out of the blood. Based on published research, our data suggests that IL-2 therapy resulted in migration out of the periphery of non-classical monocytes. No significant changes in monocyte subsets were observed at days. 85 and 169.

As with Treg, we sought to confirm this finding by manually identifying monocyte subpopulation 2. Cells corresponding to this subset were downloaded and manually gated within the total monocyte subpopulation using the overlay function and key marker expression characteristics in FlowJo. As marker expression obtained by unbiased analysis shows, these cells are not exclusively non-classical monocytes, but rather occupy the space between non-classical and intermediate monocytes (figure 5-15 A). Analysis of frequency shows a significant decrease at day 64 in the 2MIU group ( $p=0.0137$ ), which is in line our unbiased findings, with no significant changes seen in the 1MIU, placebo nor between treatment groups (figure 5-15 B to E).

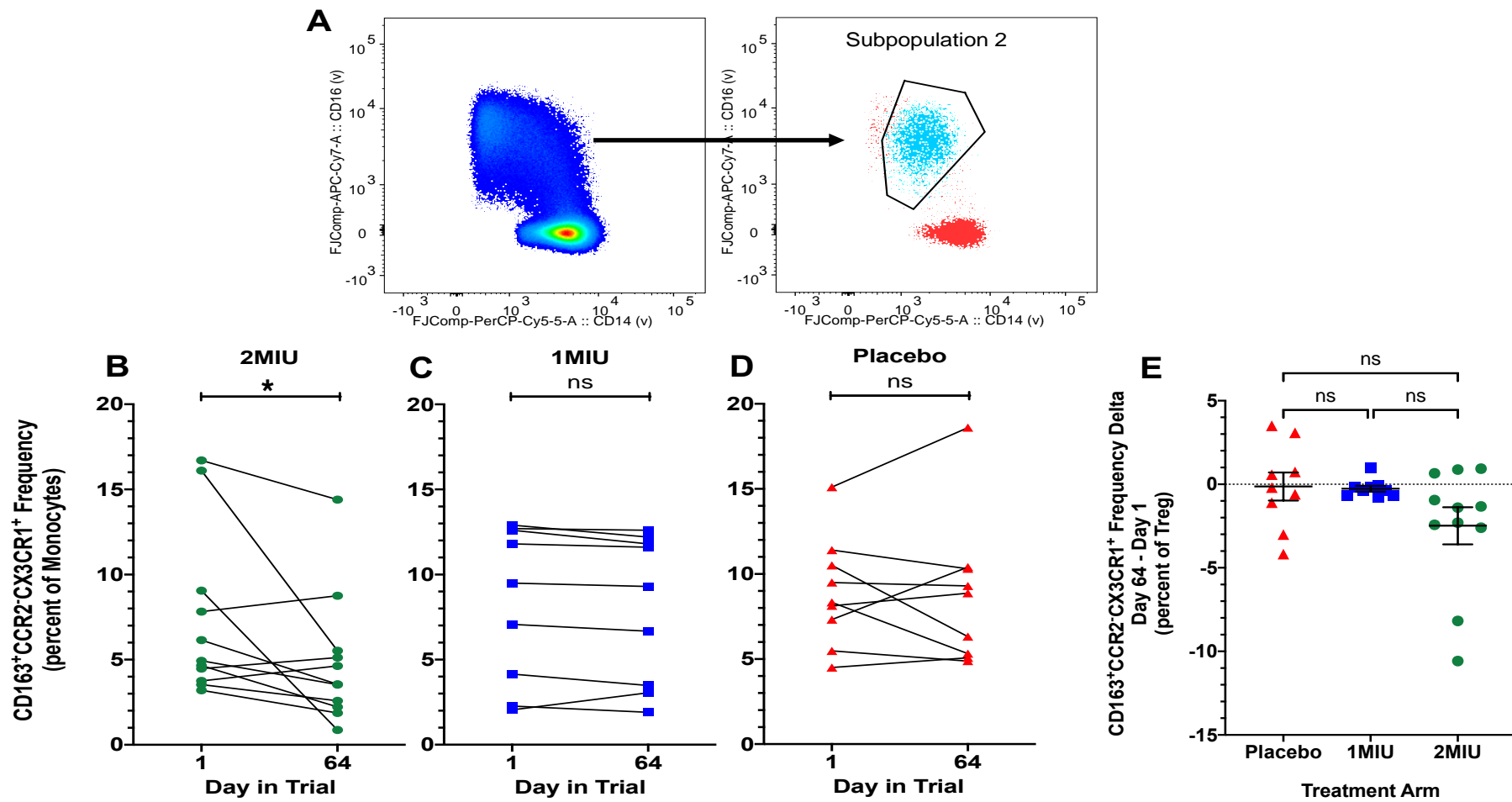


**Figure 5-15 The effects of IL-2 therapy on CD163<sup>+</sup>CCR2<sup>+</sup>CX3CR1<sup>+</sup> monocytes at day 64.** Panel A: Cells corresponding to subpopulation 2 were downloaded and manually identified in FlowJo using the overlay function in their CD14 and CD16 profiles. Panels B-D: Before and after analysis of subpopulation 2 frequency at day 1 and day 64 for each trial participant per treatment group. Panel E: Subpopulation 2 frequency change at day 64 for placebo, 1MIU and 2MIU groups. Error bars indicate mean with SEM. \* $p<0.05$ , ns – not significant. Panels B to D – Wilcoxon test; Panel E – Kruskal-Wallis test. Red triangles – placebo; blue squares – 1MIU; green circles – 2MIU.

#### **5.4. Discussion.**

In this chapter, we set out to design and optimise an experimental protocol that would allow comprehensive phenotyping of Treg, NK and monocytes leading to subsequent assessment of the effects of IL-2 therapy on these subpopulations. Given the volume of IL-2 trials being conducted to improve Treg numbers in particular, the broader effects of IL-2 on specific populations of these cells are largely unknown. We, and others, have previously shown that IL-2 expands several white blood cell populations *in vivo*. The observed expansion is greatest in total Treg and NK cells when compared Teff and CD8<sup>+</sup> T cells, as observed in chapter 2. As total Treg numbers have been implicated in diseases such as T1D, GVHD and ALS, subsequent IL-2 therapy trials in these conditions, including IMODALS, have greatly focussed on selective expansion of total Treg with little regard to the effects of IL-2 on specific Treg subpopulations (Koreth *et al.*, 2011; Hartemann *et al.*, 2013; Camu *et al.*, 2020). Advances in techniques such as flow and mass cytometry have allowed for simultaneous assessment of multiple surface and intracellular proteins on several white blood cells populations. As such it is now evident that Treg are a very heterogenous population of cells, with a recent study showing Treg are comprised of 22 phenotypically distinct subpopulations in a small cohort of healthy volunteers (Mason *et al.*, 2015). As previously stated, some aspects of Treg phenotype with regards to IL-2 have been addressed in IL-2 studies in GVHD, showing that IL-2 selectively expands Helios<sup>+</sup> memory and naïve Treg (Hirakawa *et al.*, 2017). While greater numbers of PD-1<sup>+</sup> Treg in a different GVHD cohort post expansion correlated with better clinical responses (Asano *et al.*, 2017). In addition to Helios and PD-1, Treg express several other markers associated with greater suppressive ability,

activation, stability and maintenance of FoxP3 expression under inflammatory conditions, and whether IL-2 selectively expands these is still unclear. Other than Treg, we also observed IL-2 expansion of NK and an effect on a monocyte subpopulation. As alluded to previously, both NK and monocyte numbers significantly vary in ALS when compared to healthy controls, with some monocyte subsets bearing an association with disease burden (Murdock *et al.*, 2016, 2017; Gustafson *et al.*, 2017; Zhao *et al.*, 2017). Published evidence also shows that NK and monocytes are also heterogenous populations of cells, although to a lesser extent than Treg. NK cells and monocytes alike can be further subdivided in pro- and anti-inflammatory phenotypes based on the expression of markers. Proteins such as CD56, CD11c, CX3CR1 for NK cells and in addition to HLA-DR, CD14 and CD16, markers such as CX3CR1, CD206, CD163, CCR2 and CD68 have been used to distinguish inflammatory and protective monocyte phenotypes and as with Treg, the effects of IL-2 on these phenotypes is also unknown (Infante-Duarte *et al.*, 2005; Aranami *et al.*, 2006; Hamann *et al.*, 2011; Italiani and Boraschi, 2014; Fukui *et al.*, 2018; Hou *et al.*, 2018; Trombetta *et al.*, 2018). Investigating the effects of IL-2 on these cell subpopulations will allow us to better understand the specific effects of immunotherapy, data that can potentially guide analysis in future IL-2 trials as well as studies assessing immune signatures in ALS. For our investigation we elected to use flow cytometry. It is the most widely used technique for assessing immune profiles and biomarker discovery in various diseases. It can be performed using low cell numbers, and with the advent of advanced analysers, over 20 different markers can be assessed in a single PBMC sample (Gadalla *et al.*, 2019). Data gathered for Treg, Teff, NK and monocytes from our QC PBMC sample shows that it is a robust and reproducible

experimental protocol with low day-to-day variation in results as determined by %CV of <10% for all variables. Similarly, good reproducibility is shown when assessing Treg, NK and monocyte subpopulations in the QC PBMC sample across the 11 experimental batches. Although variance does increase in subpopulations which are present at very low numbers <2%. This does not necessarily indicate that our subpopulation data is inaccurate. Percentage CV is a sensitive measure, solely reliant on the mean and standard deviation of gathered data. As such, a subpopulation of cells with a mean frequency of 0%, will yield a high %CV value if one of the measures is recorded at 0.03% in some experimental batches, which would not be observed if the mean value of a subpopulation was for example, 20%. Nevertheless, this should be approached with some caution as it could be interpreted that subpopulations with low frequencies are not accurately enumerated day-to-day. However, by assessing each time point per participant on the same day allowed us to mitigate for this.

To address the first hypothesis, we used unbiased clustering analysis, and identified that trial participant Treg are comprised of 18 phenotypically distinct subpopulations. By assessing the delta change we observed significant expansion in 3 subpopulations in both IL-2 treated groups at day 64. All 3 expanded subpopulations express high levels of Ki-67, a marker of proliferation, indicating that these cells are growing and dividing (Scholzen and Gerdes, 2000). Two of these, subpopulations 8 and 10 harbour a memory (CD45RA<sup>-</sup>) phenotype, expressing CD25, CD49d, ICOS, CD15s, CD27 and Helios. In addition to these markers, subpopulation 10 also expresses HLA-DR and CD39. The third subset,

subpopulation 1, harboured a recent thymic emigrant (RTE) phenotype, in addition to CD25, Ki-67, CD15s, CD27 and Helios also expressing high levels of CD45RA and CD31 (Junge *et al.*, 2007). Whether these Treg subsets are beneficial in ALS is unknown as Treg phenotype has not been related to disease burden in patients on a longitudinal basis. In more general terms, the expansion of these subsets appears to be beneficial. As published articles report that high expression of CD15s represents a subset of Treg that is highly suppressive, while expression of Helios corresponds with a highly activated state with enhanced suppressive capabilities (Zabransky *et al.*, 2012; Miyara *et al.*, 2015). ICOS is involved in FoxP3<sup>+</sup> Treg generation and promoting proliferation, HLA-DR<sup>+</sup> Treg are involved in contact dependent suppression, Treg positive for CD39 can maintain stable FoxP3 expression and thus suppressive function under inflammatory conditions, while CD49d<sup>+</sup> Treg were found to be more effective at suppressing naïve Teff (Baecher-Allan *et al.*, 2006; Kraczyk *et al.*, 2014; Gu *et al.*, 2017; Li and Xiong, 2020). From these findings we can conclude that three cycles of 1MIU and 2MIU IL-2 selectively expanded 2 subpopulations of Treg across both groups with an antigen experienced, activated, highly stable, highly suppressive and proliferative phenotype. Which, in a disease where low Treg numbers and diminished suppressive function are correlative with disease burden, may be indicative of positive outcomes such as reducing progression rates, a longitudinal assessment may shed more light onto this (Henkel *et al.*, 2013; Beers *et al.*, 2017). As for the RTE-like subpopulation, our findings suggest that IL-2 therapy induced thymic generation of naïve Treg. This is in line with a recent study where GVHD patients were administered daily doses of IL-2 (ranging from  $3.0 \times 10^5$  IU/m<sup>2</sup> to  $1.5 \times 10^6$  IU/m<sup>2</sup> per day) for 8 weeks, also showed a

significant increase in RTE. Furthermore, this continuous administration of IL-2 resulted in further increases in Treg RTE, which were maintained at significantly greater levels 2 weeks after the final infusion (Matsuoka *et al.*, 2013). Conversely, our analysis at days 85 and 169 for Treg RTE-like cells (subpopulation 1) show the frequency has returned to baseline levels. However, at these timepoints, significantly elevated frequencies of subpopulation 2 are observed. Based on marker expression profiles we can deduce that this subset is closely related to Treg RTE-like cells from day 64 with regards to co-expression of CD45RA, CD31, CD27, CD25, Helios, FoxP3 and CD15s. The key difference being the level of Ki-67 expression, where unlike subpopulation 1, subpopulation 2 does not express this protein. These data indicate that the initial expansion of proliferating Treg RTE-like cells at day 64, has resulted in a lasting expansion of circulating, non-proliferating Treg RTE-like cells (subpopulation 2) for up to three months after therapy. Although CD45RA and CD31 are good indicators of RTE in circulation, further analysis is needed to confirm their lineage. A good way of assessing RTE is by measuring the levels of T cell receptor excision circle (TREC) by polymerase chain reaction (PCR) (Kohler and Thiel, 2009). TREC are formed during TCR rearrangement in the thymus, and are diluted with each cell division when in circulation therefore, greater expression of TREC on Treg would indicate recent thymic generation (Junge *et al.*, 2007). TREC analysis was performed in the IL-2 GVHD study by Matsuoka and colleagues 2013, hence the continuous tracking of Treg RTE across time (Matsuoka *et al.*, 2013). For our analyses, investigating TREC expression may aid in discovering what proportion of subpopulation 2 is directly descended from subpopulation 1 however, performing this analysis post-hoc would require us to commit precious clinical trial samples, which are not

readily available, for one experimental analysis. Regardless of TREC, whether these subsets are beneficial in ALS patients remains to be seen, however work published recently has shown that expression of CD31 in particular may be essential to maintaining Treg numbers and immunosuppressive function (Huang *et al.*, 2017). In patients with coronary heart disease, where Treg are supposed to play an atheroprotective role but are decreased in number and impaired in their suppressive function, reported that CD31<sup>+</sup> Treg are able to maintain stable FoxP3 expression after activation and that these Treg display an enhanced proliferative and immunosuppressive capacity, thus maintaining or improving the numbers of CD31<sup>+</sup> Treg could be the answer to regulating bulk Treg numbers and in turn, improving immunoregulation (Huang *et al.*, 2017). Treg subset analysis at day 85 also showed significant increases in subpopulations 4, 9 and 18. As with subpopulations 8 and 10 at day 64, these present with a memory, activated, stable and highly suppressive phenotype (CD15s<sup>+</sup>Helios<sup>+</sup>CD27<sup>+</sup>CD45RA<sup>-</sup>) however, are not proliferating as determined by low expression of Ki-67. Throughout this analysis we also observed significant decreases in some Treg subpopulations. However, it is unlikely to be caused by IL-2, given that we reported total Treg number and frequency to be significantly increased by IL-2 in chapter 2. It is likely the cause of reporting subpopulation frequencies as percentages of total Treg, hence a decrease in one subpopulation, is caused by an increase in another. Reporting our data this way has allowed us to observe shifts in the balance of Treg subsets, where Treg analysed directly after IL-2 show an activated, stable and highly suppressive phenotype, but as IL-2 washout takes place, the balance of Treg subsets shifts again towards a non-proliferating, non-naïve, but still activated and highly suppressive phenotype. One other

consideration to take into account is thymic involution, particularly in older individuals undergoing IL-2 therapy. Age is a contributing factor to progressive diminishment in thymus size and structure, leading to a decrease in T lymphocyte production and resulting in abundances of memory phenotypes over naïve (Gu *et al.*, 2012). Whether this has significant bearing on RTE induction by *in vivo* IL-2 is yet unclear. The same is true for the imbalance of memory over naïve T cells. If so, IL-2 dose/frequency may also need to be adapted based on thymic output. To our knowledge, such comprehensive assessment of IL-2 on Treg subsets has not been previously assessed, and aside from Treg RTE, sustained effects of IL-2 on other Treg subsets has also not been shown.

Part of the hypothesis testing in this chapter was also focussed on assessing the effects of IL-2 therapy on NK subsets. In ALS, the relevance of NK subsets has not yet been identified but studies have shown significantly greater numbers of circulating NK when compared to healthy controls, whether these numbers have any bearing on disease progression is not yet known as studies have largely focussed on Treg (Gustafson *et al.*, 2017; Murdock *et al.*, 2017). Other IL-2 immunotherapy trials in T1D and SLE have shown significant expansion of total NK following IL-2, particularly observed in the CD56<sup>bright</sup> NK, without deeper focus on NK subsets (Todd *et al.*, 2016; He *et al.*, 2020). The CD56<sup>bright</sup> NK are thought to exert immunoregulatory activities on cells of the innate and adaptive immune system through cytokine secretion when activated (Michel *et al.*, 2016). Analysis of NK cell subsets in ALS patients resulted in identification of 21 NK subsets using unbiased algorithms. As with Treg, IL-2 therapy resulted a shift in the balance of these NK subsets, where significant expansion was observed in subpopulations

with high expression of CD56, and moderate to low expression of CD11c. This resulted in a reduction in frequency of NK subsets with moderate expression of CD56, CX3CR1 and in the case of subpopulation 9, high expression of HLA-DR. Research from other pathologies indicates that in our cohort, IL-2 induced an expansion of NK cells associated with a regulatory, protective, disease modifying phenotype, at the expense of NK cell subsets associated with high cytotoxicity. NK cells can be further subdivided into natural killer type-1 and type 2 (NK1 and NK2) cells. The NK2 subset is thought to possess regulatory functions, such as prohibiting Th1 activation through production of cytokines such as IL-5 and IL-13 (Kimura and Nakayama, 2005). CD11c could be used to characterise the NK2 as NK cells have been shown to differentially express CD11c ( $CD11c^{low}$  and  $CD11c^{high}$ ) in MS patients who are in remission, and these  $CD11c^{low}$  NK cells express significantly greater levels of IL-5 when compared to  $CD11c^{high}$  NK cells of MS patients and healthy controls. Furthermore,  $CD11c^{low}$  NK cells may possess disease modifying properties as fewer numbers of  $CD11c^{low}$  MS patients developed exacerbated disease when compared to  $CD11c^{high}$  patients, which presented with a clinical relapse (Aranami *et al.*, 2006). Similarly, differential expression of CX3CR1 has been associated with different NK cell states. As previously discussed, CX3CR1 and its ligand CX3CL1 mediates cell recruitment to tissue (Ferretti *et al.*, 2014). CX3CR1<sup>high</sup> NK are more cytotoxic *in vitro* against their target K562 cell line when compared to CX3CR1<sup>negative/low</sup> counterparts, which express significantly greater levels of IL-5, a marker of NK2 cells. Furthermore, CX3CR1<sup>negative/low</sup> NK express greater levels of CD25 and are highly responsive to IL-2 induced proliferation when compared to CX3CR1<sup>high</sup> NK (Infante-Duarte *et al.*, 2005; Hamann *et al.*, 2011). These research studies

indicate that in ALS patients, IL-2 expanded NK cell subsets associated with the NK2 phenotype ( $CD11c^{low}CX3CR1^{negative}$ ) which have been shown to have immunoregulatory properties, at the expense of cytotoxic NK ( $CX3CR1^{high}$ ) cells. Given that total NK are significantly elevated in ALS patients when compared to healthy individuals, future studies of immune signatures in ALS disease progression would benefit from incorporating makers of NK2 cell phenotype into their analysis, while also assessing their cytotoxicity characteristics *in vitro* against motor neurones, which have been shown to be HLA-I deficient and thus can be targeted by NK (Song *et al.*, 2016).

The final hypothesis testing of this chapter was centred around comprehensive analysis of monocyte phenotypes and their responses to IL-2 *in vivo*. This analysis was prompted by a previous observation where a significant reduction in  $CD163^+$  non-classical monocytes was observed in both IL-2 treated groups. Therefore, to further investigate any effect of IL-2 on monocyte phenotype, in addition to CD163 and CCR2, we incorporated markers previously associated with monocyte phenotypes such as CX3CR1, CD68 and CD206 (Italiani and Boraschi, 2014; Fukui *et al.*, 2018; Hou *et al.*, 2018; Trombetta *et al.*, 2018). We identified 15 subpopulations residing within total monocytes of IMODALS trial participants using the Phenograph algorithm. We observed significant changes in three monocyte subpopulations however, unlike with Treg and NK, these changes are not consistently present in both IL-2 treated groups, nor are these changes similar in magnitude. In our quest to further assess whether IL-2 had any significant effect on non-classical monocytes, we observed a significant decrease in subpopulation 2 at the highest dose, which, as suggested by

published reports, may play protective role in ALS. High expression of CD16, CD163 and no CCR2 suggests that this subset is closely related to the CD163<sup>+</sup> non-classical monocyte subset we observed a reduction in previously. This subset also expressed CD14, indicating that it confers to the intermediate monocyte phenotype, rather than the non-classical monocyte phenotype exclusively, as confirmed by manual gating. Furthermore, we observe high levels of CX3CR1, a marker associated with migration (Fukui *et al.*, 2018; Trombetta *et al.*, 2018). In ALS, greater expression of CX3CR1 on CD16<sup>+</sup> and CD16<sup>-</sup> monocytes alike, has been shown to be associated with slower disease progression in a recent study of peripheral immunity in 119 ALS patients and 50 healthy controls (Murdock *et al.*, 2017). The mechanisms by which this is mediated are still unknown as detailed analysis of monocyte mediated neuronal death or preservation is lacking in this field. However, CX3CR1 mediates myeloid and lymphoid cell migration into tissue, and cells of the monocytic lineage, as determined by expression of CD169 (a marker not expressed on CNS resident microglia), have been identified in lumbar spinal cords of live ALS patients, at significantly greater numbers than healthy controls (Zondler *et al.*, 2016). In other experimental settings, non-classical monocytes have been shown to give rise to alternatively activated macrophages and promote skin healing *in vitro* (Idzkowska *et al.*, 2015). Therefore, it is possible that IL-2 therapy induced the migration of these monocytes to tissue and once there, these monocytes provide anti-inflammatory signals. However, to confirm this, simultaneous analysis of CSF samples would have been necessary, which was not collected in the IMODALS trial. Whether this is the case or not, the question of biological significance of this monocyte subpopulation, as well as the Treg and NK subsets we have shown to

be selectively affected by IL-2 in ALS remains unknown. Several studies in ALS have focussed on a broad range of peripheral immune parameters and attempted to correlate these with disease progression and have been successful in doing so. However, our data indicates that future studies would benefit from a more focussed approach, where comprehensive analyses of specific immune cell phenotypes, as well as their cytotoxic or protective behaviours in the CNS, which could first be assessed *in vitro*, would better the understanding of the role the immune system may play in ALS.

In this chapter we have shown that IL-2 selectively expands certain Treg and NK subpopulations and with regards to Treg, sustained effects of IL-2 are observed up to three months after the cessation of therapy. Similarly, we were able to better understand the characteristics of the monocyte subset that was affected by IL-2 in chapter 2. These findings can aid future IL-2 clinical trials as well as studies of immune signatures in ALS by providing a backbone for the types of phenotypic analysis white blood cells should be subjected to. However, as with studies in other diseases, findings in the periphery should be approached with caution, as the events taking place in blood are not necessarily indicative of the processes occurring in the tissue. Hence, future studies could use our data as a guide for investigating inflammation and immune regulation in the CNS of ALS patients.

## **Chapter 6. Integrated analysis and final discussion.**

### **6.1. Integrated analysis of chapter data.**

Having identified changes in several immune parameters in ALS patients after IL-2 therapy, we sought to assess whether there is a relationship between any of the immune parameters that we observed to be changed by therapy. It was necessary to address this as this could allow to better understand the link, if any, between the frequency, phenotype and functional data. Having observed significant expansion of Treg and an improvement in Treg function, we sought to assess whether these changes are related to one another. It was important to address this as both immune parameters have been shown to inversely correlate with ALS progression (Henkel *et al.*, 2013; Beers *et al.*, 2017). We observe a significant correlation ( $p<0.0001$ ) between percent change in Treg number and percent change in suppressive function (figure 6-1). Thus IL-2 therapy results in more Treg which in turn drives an increase in functional ability and these changes may slow disease progression, although that remains to be determined. Interestingly, those on placebo present with a reduction in both number and function, further outlining the benefit of IL-2 in ALS.

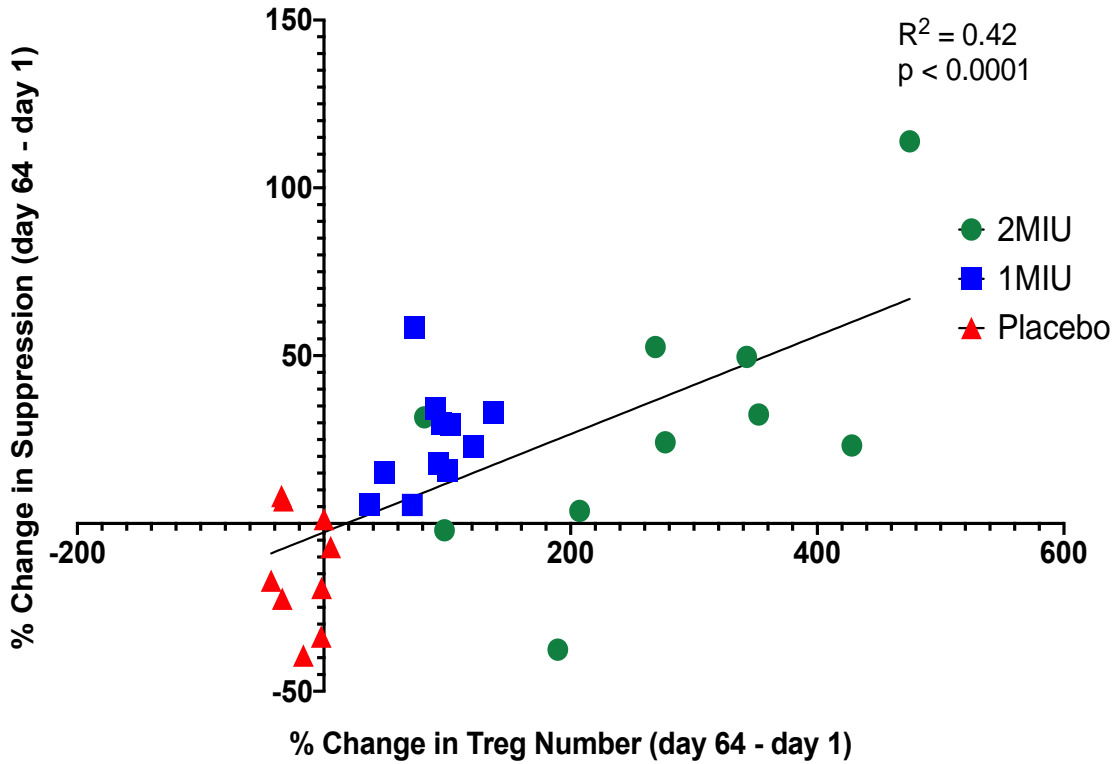


**Figure 6-1 Analysis of percentage change in Treg number and suppressive function.** Percentage change was calculated for Treg number and suppressive function at day 64. The two variables were correlated using simple linear regression.  $R^2 = 0.42$ ,  $p < 0.0001$ . Red triangles = placebo; blue squares = 1MIU IL-2; green circles = 2MIU IL-2.

We wished to take this analysis further and apply it to all the immune parameters affected by IL-2 therapy. One of the reasons for doing this is to assess whether some individuals are simply more responsive to IL-2, regardless of the variables that are changed, be it Treg number, Treg function, NK cell number etc. For such multivariate analysis, rather than manually correlating each finding, we elected to use principal component analysis (PCA). PCA is an unsupervised algorithm used to reduce the dimensionality and simplify large sets of data by identifying patterns, without prior knowledge of treatment group, phenotypic differences or where the samples were obtained. PCA reduces large data sets by extracting linear combinations between the variables and projects them onto lower dimensions

called principal components (PCs). The contribution of each variable to the PCs is then calculated, determining how much of the variation in the data is explained by each PC. The variables are then projected onto the two PCs with the highest percentage variation in the data, usually PC1 and PC2 (Stein *et al.*, 2006; Lever *et al.*, 2017). By using two PCs to explain large data sets, scientists were able to identify key differences in immune cell populations between the periphery and lymph nodes in T1D patients (Yang *et al.*, 2019). In the case of our data set, we wished to assess the relationships between all the immune parameters for Treg and non-Treg cells that we observed to be affected by therapy across the data chapters. Furthermore, as Treg were one of the pivotal cell types in this thesis, we could also use this analysis to investigate what drives the long-term effects of IL-2 on Treg we previously observed. As such, we expect the resultant data to be driven by treatment however, we believe this will:

- a. Show clusters of immune parameters preferentially affected by different IL-2 doses.
- b. Identify relationships between immune findings from different chapters.
- c. Address whether Treg variables at one visit, are associated with changes at later visits.

#### **6.1.1. Overview of PCA analysis.**

To address the aforementioned points, we performed three PCA analyses on:

1. All Treg changes at day 64.
2. All Treg and non-Treg changes at day 64.
3. All Treg parameters across the all the visits where they are altered.

The variables used in PCA analysis are outlined in table 6-1. Using R, data from different chapters was scaled using the “prcomp” function to normalise the readouts. The PCA analysis was performed using the “factoextra” package.

| Treg at Day 64          | Treg and non-Treg at day 64                      | Treg at key visits                 |
|-------------------------|--|------------------------------------|
| Total Treg #            | Total Treg #                                     | <b>D8</b> total Treg #             |
| Treg subpopulation 1 *  | Treg subpopulation 1 *                           | <b>D64</b> total Treg #            |
| Treg subpopulation 8*   | Treg subpopulation 8 *                           | <b>D64</b> Treg subpopulation 1 *  |
| Treg Subpopulation 10 * | Treg Subpopulation 10 *                          | <b>D64</b> Treg subpopulation 8 *  |
| Treg CD25 MFI           | Treg CD25 MFI                                    | <b>D64</b> Treg subpopulation 10 * |
| Suppression at 1:2      | Suppression at 1:2                               | <b>D64</b> Treg CD25 MFI           |
| Suppression at 1:4      | Suppression at 1:4                               | <b>D64</b> suppression at 1:2      |
|                         | Total NK #                                       | <b>D64</b> suppression at 1:4      |
|                         | CD56 <sup>dim</sup> NK #                         | <b>D85</b> total Treg #            |
|                         | CD56 <sup>bright</sup> NK #                      | <b>D85</b> Treg subpopulation 2 *  |
|                         | NK subpopulation 4 *                             | <b>D85</b> Treg subpopulation 4 *  |
|                         | NK subpopulation 5 *                             | <b>D85</b> Treg subpopulation 9 *  |
|                         | NK subpopulation 6 *                             | <b>D85</b> Treg subpopulation 18 * |
|                         | NK subpopulation 7 *                             | <b>D85</b> suppression at 1:2      |
|                         | Total Teff #                                     | <b>D85</b> Treg CD25 MFI           |
|                         | Teff CD25 MFI                                    | <b>D85</b> Treg IL-2 signalling    |
|                         | Total CD8 <sup>+</sup> #                         | <b>D169</b> Treg subpopulation 2 * |
|                         | Monocyte subpopulation 2 *                       |                                    |
|                         | CD163 <sup>+</sup> CCR2 <sup>-</sup> monocytes # |                                    |

**Table 6-1 List of immune parameters used in PCA analysis.** Each parameter is calculated as a change from the baseline visit (day 1). Each column represents the parameters used for each of the three PCA's. Symbol # indicates that the variable is expressed as a number per µL of blood. Symbol \* indicates the variable is expressed as a frequency of the parent population. **D** = day in trial.

In all three analyses, we observe treatment driven patient clusters with PC1, which describes 59.6%, 43.6% and 47.6% of the variation in the data for Treg, Treg and non-Treg, and Treg immune parameters at key visits respectively (figures 6-2, 6-3 and 6-4). Furthermore, PC1 is observed as the main discriminator between those on placebo versus those on IL-2 in each case. In all instances, we observe overlap in patient clusters receiving either dose of IL-2, indicating similarities in treatment associated changes. By contrast, PC2 which accounts for 17% (Treg), 12.8% (Treg and non-Treg) and 10.4% (all Treg) of the variation in data is the main discriminator between individual trial participant responses to IL-2. PC2 is also the main discriminator between the changes in immune parameters we observe after IL-2 therapy (figures 6-2, 6-3 and 6-4).

### **6.1.2. PCA analysis on Treg at day 64.**

For Treg related changes (figure 6-1), we observe two clusters of immune parameters:

1. Cluster consisting of change in total Treg number, Treg CD25 MFI, Treg subpopulation 8 and 10.
2. Cluster consisting of change in Treg function and subpopulation 1.

This indicates a relationship between Treg function and subpopulation 1, which warrants further investigation, particularly as yet unpublished data from our laboratory suggest that CD31<sup>+</sup>CD45RA<sup>+</sup> Treg are better at suppressing autologous Teff than total Treg. Furthermore, the size and direction of the ellipses drawn around each patient cluster indicate that:

- a. As observed in previous data chapters, greater variability in responses is observed in those on 2MIU IL-2 when compared to 1MIU IL-2.

- b. The responses of those on 1MIU IL-2 are preferentially driven towards an increase in Treg function and subpopulation 1.

Although both doses resulted in expansion of total Treg and their subsets, upregulation of CD25 expression and increases in Treg ability to suppress autologous Teff, these data indicate that the 1MIU IL-2 dose may be more beneficial if the goal of therapy is to invoke a steady increase in specific aspects of Treg.

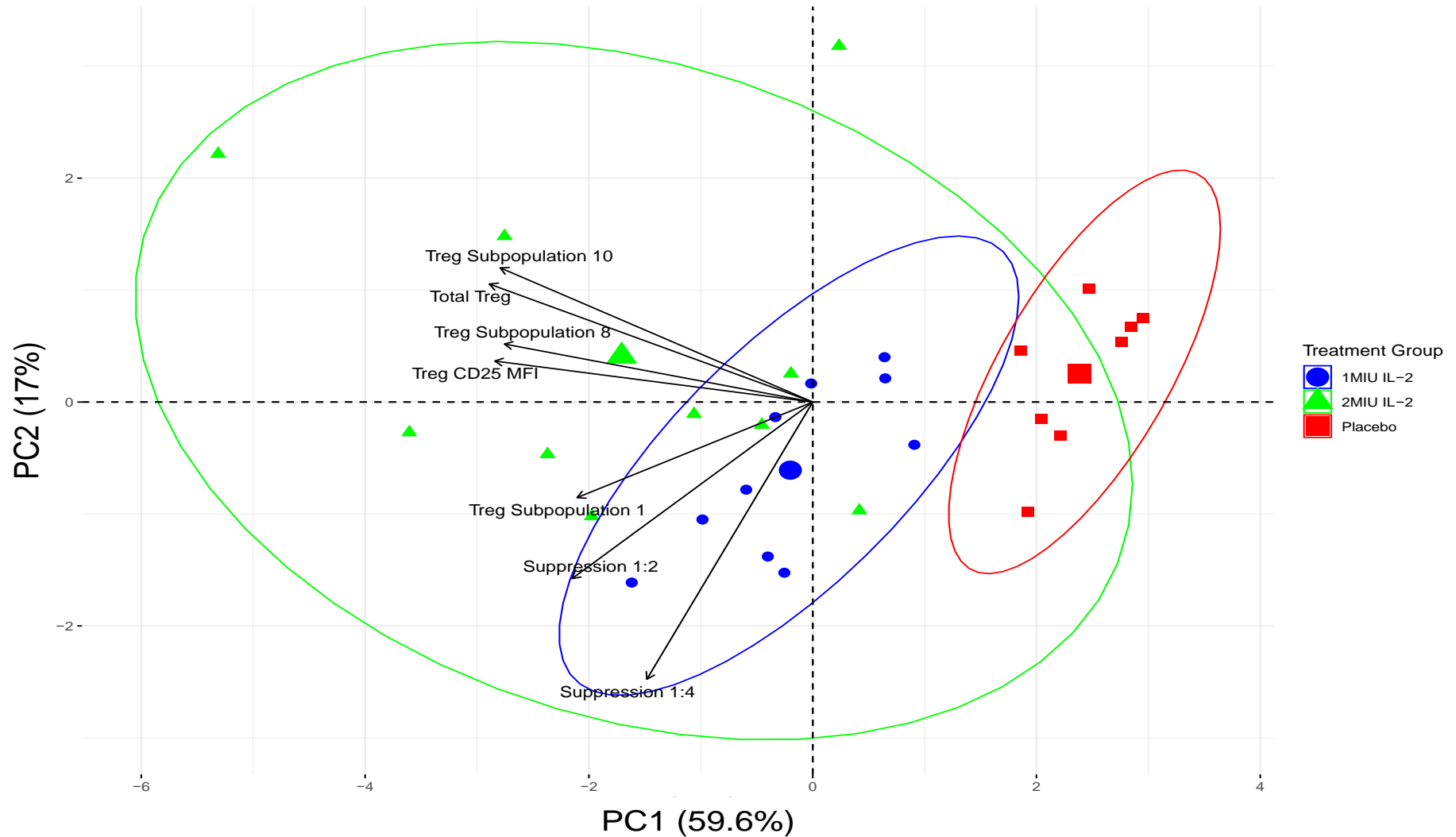


**Figure 6-2 PCA analysis of findings significantly altered by IL-2 therapy at day 64 in Treg cells.** PCA was performed on immune parameters affected by IL-2 therapy ( $n = 7$ ) resulting in two major principal components of our immunologic findings at day 64. Shaded areas represent ellipses drawn assuming a multivariate t-distribution of data. Arrows represent the contribution of each parameter to either principal component.

### **6.1.3. PCA analysis on Treg and non-Treg cells at day 64.**

This is further strengthened by PCA data for Treg and non-Treg cell findings (figure 6-2). In this instance, we observe two clusters of immune parameters:

1. Changes in parent populations of total NK (CD56<sup>bright</sup> and CD56<sup>dim</sup>), total Teff, total CD8<sup>+</sup> T cells, total Treg and their subpopulations 8 and 10, and CD25 expression on Treg and Teff.
2. Changes in NK subpopulations 4, 5, 6 and 7, Treg subpopulation 1, Treg suppression at 1:2 and 1:4.

The two monocyte variables, CD163<sup>+</sup>CCR2<sup>-</sup> monocytes and monocyte subpopulation 2 should not be classed as a separate cluster, as they are loaded in the opposite direction based on their expression as negative values, they go down in those with 2MIU IL-2. Being located in close proximity to one another indicates a good correlation between these two variables, further indicating that, as alluded to in chapter 5, monocyte subpopulation 2 closely resembles the CD163+CCR2- non-classical monocytes from chapter 2. Furthermore, If these were considered as positive values, these variables may be loaded in the vicinity of cluster 2, indicating a relationship between these monocytes and changes in NK subsets and Treg function.

As with Treg cell PCA analysis, those on 2MIU IL-2 show variable responses driven by changes in all immune parameters. While those on 1MIU IL-2 present with a directional shift towards cluster 2, consisting of NK, Treg function, Treg subpopulation 1, while the changes in monocyte subsets are pertinent to the 2MIU IL-2 dose. This once again indicates that 1MIU IL-2 can promote a more pronounced regulatory response, not only in terms of Treg RTE and suppressive

function, but also NK subsets (4, 5, 6 and 7) which are deemed to possess regulatory and disease modifying phenotypes. Furthermore, the clustering of these NK subsets closely with Treg suppressive function suggests a relationship between these immune parameters. Whether it's the change in Treg attributes upregulating the NK subsets, or vice versa, is yet to be determined. This is not to discount the use of the 2MIU IL-2 dose, as we previously reported both doses to be safe, well tolerated and effective at increasing Treg numbers and function. All these data indicate is that we can promote different aspects of the immune system using two different IL-2 doses. This in turn can aid future IL-2 trial design.

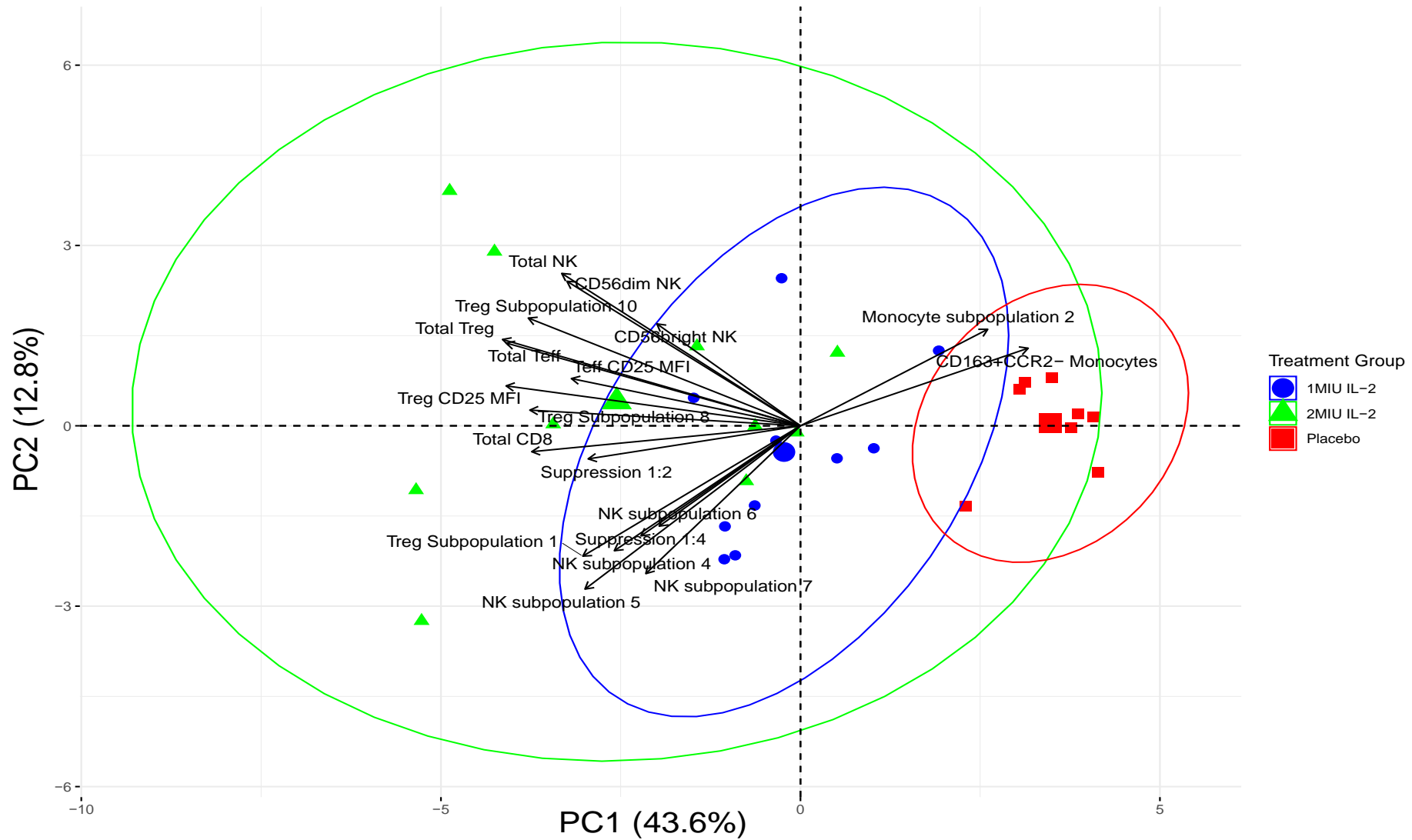


**Figure 6-3 PCA analysis of findings significantly altered by IL-2 therapy at day 64 in Treg and non-Treg cells.** PCA was performed on immune parameters affected by IL-2 therapy ( $n = 19$ ) resulting in two major principal components of our immunologic findings at day 64. Shaded areas represent ellipses drawn assuming a multivariate t-distribution of data. Arrows represent the contribution of each parameter to either principal component.

#### **6.1.4. PCA analysis on Treg at all timepoints where they are altered.**

For our final PCA analysis, we wished to investigate whether the long-term changes we see in Treg parameters, are driven by increases observed at earlier timepoints. For this, we clustered all Treg parameters at all timepoints where they were altered (figure 6-4). In this instance, we observe two main clusters:

1. Cluster of changes in Treg number and subset frequencies. These responses are dominant in patients on 2MIU IL-2.
2. Cluster of changes in Treg function and increase in Treg CD25 MFI. As before, these are more pertinent to participants receiving 1MIU IL-2.

As with monocytes previously, the change in Treg IL-2 signalling and Treg CD25MFI at day 85, is not seen as a separate cluster as it is the result of these variables expressed as negative values. Whether this will affect Treg expansion with subsequent cycles is yet to be determined.

These data indicate:

- a. The increase in Treg subsets at day 64 is associated with the increase in total Treg at day 8 and subsequently 64.
- b. The increase in total Treg number at days 8 and 64 drive the maintenance of elevated total Treg and their subset levels at day 85.
- c. The one remaining Treg subset at day 169 (subpopulation 2) is closely associated to the initial increase in Treg number at day 8 and their subsequent maintenance above baseline at day 85.
- d. As before, Treg function parameters cluster closely together.
- e. The reduction in Treg IL-signalling, observed in participants receiving 2MIU IL-2, is closely related to the reduction of CD25 expression on Treg.

A relationship we briefly explored in chapter 4.

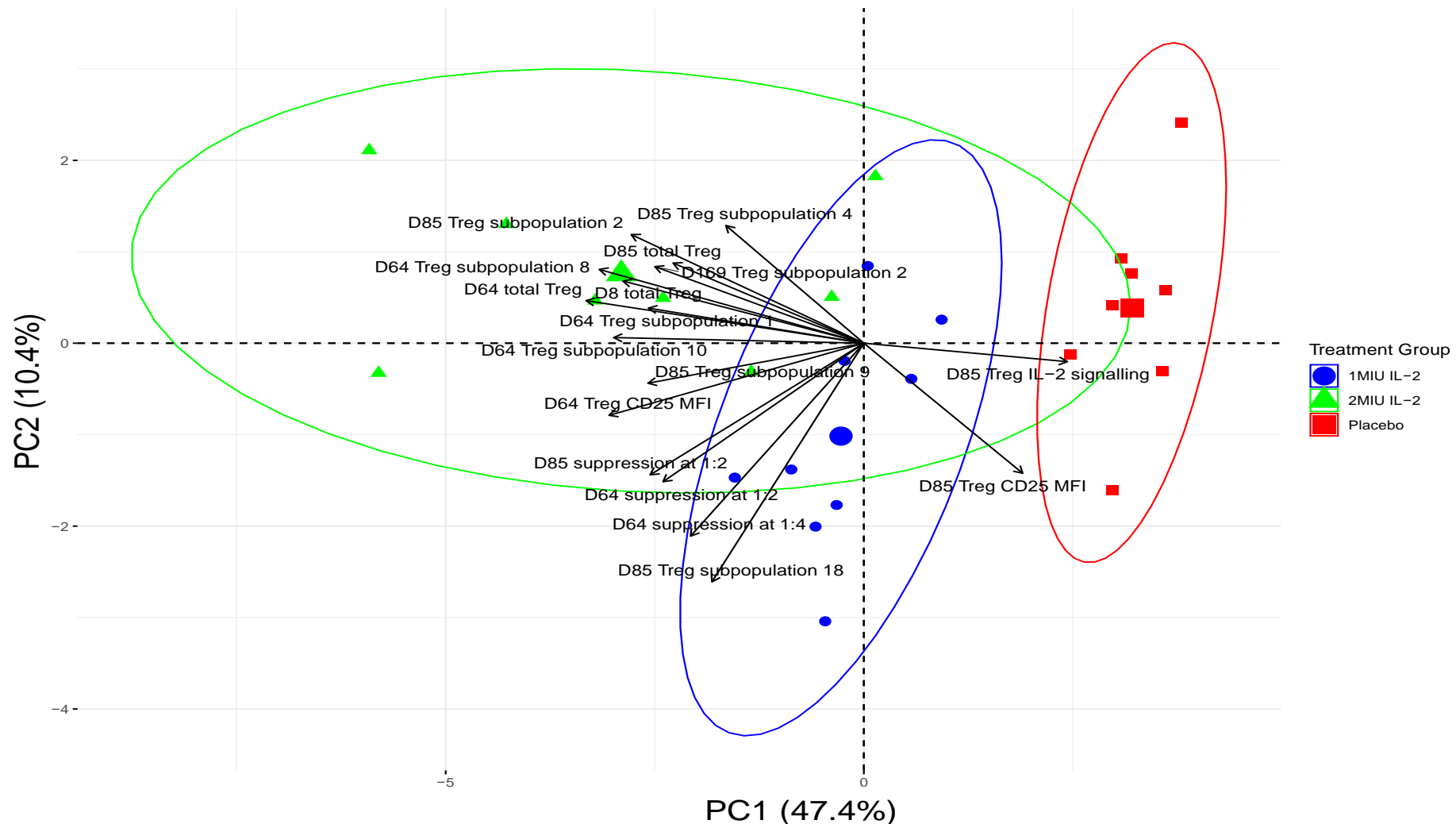


**Figure 6-4 PCA analysis of Treg findings at clinical trial visits where they were significantly altered.** PCA was performed on immune parameters affected by IL-2 therapy ( $n = 17$ ) resulting in two major principal components of our immunologic findings at day 64. Shaded areas represent ellipses drawn assuming a multivariate t-distribution of data. Arrows represent the contribution of each parameter to either principal component. D= day in trial.

### **6.1.5. Summary of PCA analyses.**

With regards to the aims we set out prior to the PCA analysis; the three PCA analyses showed:

1. When day 64 Treg parameters are analysed, two main data clusters are formed, representing a change in total Treg and 2 activated Treg subsets and the other, relating to Treg function, which is closely associated with induction of RTE. Which is in line with yet unpublished findings from our laboratory, where sorted RTE are shown to be better at suppressing autologous Teff proliferation than total Treg.
2. Overlaying non-Treg cell parameters onto Treg at day 64, shows that the change in RTE and Treg function, is closely associated with the change in NK subsets with disease modifying properties. With change in total cell numbers forming a separate cluster.
3. The initial expansion of Treg at day 8 and 64, correlates with the maintenance of Treg levels above baseline at day 85, which also associated with the significantly greater frequency of Treg subset 2, we observed at three months post final IL-2 injection.
4. Treg IL-2 signalling is affected by continuous therapy and this may be monitored by measuring CD25 expression on Treg, rather than performing signalling assays at every timepoint.
5. Those on 2MIU IL-2 present with greater variability in responses than those on 1MIU IL-2, and the 1MIU IL-2 dose results in preferential responses in Treg generation in the thymus, Treg function and potentially protective NK subsets.

Although these data were gathered in a small ALS cohort, over a relatively short period of time, it has provided valuable insight into the plethora of IL-2 mechanisms on the peripheral immune system. These data suggest that in order to improve Treg function (at least when assessed *in vitro*), we may be better off targeting RTE expansion. We have identified subsets of CD56<sup>bright</sup> NK subsets expanded by IL-2 which have shown some disease modifying activity in MS, raising the question of whether these subsets should be followed up on in ALS patients when performing disease progression studies, as is commonly done with Treg. Identified that in order to have long-term Treg effects, a good initial response to IL-2 is needed in terms of Treg expansion, further driving the need for identification of responders versus non-responders prior to the start of IL-2, or dose adjustment based on the initial response. We showed that at the highest dose, there is an indication of monocyte polarisation and possibly migration in ALS however, whether this is a direct or indirect effect of IL-2 is not known, nor is where the cells end up if they do migrate out of the periphery. Finally, although both doses target the same cell types, selecting either the 1MIU or 2MIU may invoke slightly different responses, useful insight depending on the aim of therapy, or if it does become possible to identify responders versus non-responders. Several of these aspects will be tested in the longitudinal IL-2 in ALS study termed MIROCALS.

## **6.2. Summary of thesis findings and outstanding questions.**

As the data presented in each individual chapter was discussed thereafter, the following are brief summaries of the main findings from data chapters 2-5 and the integrated analysis.

## **Chapter 2 – Investigating the effects of IL-2 therapy on immune cells in blood of ALS patients.**

Given that the published evidence from patients and healthy cohorts suggest that ALS may be an immune driven disease, particularly with regards to Treg, we set out to assess the safety and activity of LD-IL-2 (1MIU and 2MIU) in ALS patients along with its effects on the major cell populations of the immune system.

### **Key findings:**

- IL-2 safe and well tolerated at both doses.
- Selective expansion of Treg which increased with repeated cycles.
- Significant expansion of non-Treg cells bearing the IL-2R subunits, namely Teff, CD8<sup>+</sup> T and NK (CD56<sup>bright</sup> and CD56<sup>dim</sup>) cells.
- Significant reduction in CD163<sup>+</sup> non-classical monocytes, a subset which may possess anti-inflammatory properties.

### **Outstanding questions:**

- Do these findings have a significant effect on clinical efficacy of IL-2 in ALS?

## **Chapter 3 – Evaluating the effects of LD-IL-2 therapy on Treg suppressive function *in vitro*.**

Along with number, diminished Treg suppressive function also plays a role in ALS progression. As a result of the Treg findings in chapter 2, we set out to assess whether this increase in number resulted in an improvement in Treg ability to suppress autologous Teff *in vitro*.

*Key findings:*

- No significant change in Teff proliferation after IL-2.
- Increase in Treg suppressive function at both IL-2 doses, highly significant at 1MIU IL-2, and correlative with an increase in CD25 expression on Treg.
- Those on IL-2 able to maintain Treg suppressive function at baseline levels long-term, while those on placebo present with a decline in suppressive function.
- Those on 2MIU IL-2 present with a decline in CD25 expression on Treg after IL-2 cessation.

*Outstanding questions:*

- As before, does the increase in Treg function modify disease burden and survival time?

**Chapter 4 – Investigating the effects of LD-IL-2 therapy on IL-2 signalling in Treg and non-Treg cells.**

We, and several other studies have shown that IL-2 can effectively expand total Treg numbers however, the observed expansion vary greatly between individuals. Therefore, we set out to assess whether we could predict Treg and non-Treg cell expansion and study the effects of continuous IL-2 therapy on IL-2 signalling.

*Key findings:*

- No significant correlation between IL-2 signalling at day 1 and the expansion of Treg, Teff and NK cells at day 64.

- Significant correlation between CD8<sup>+</sup> T cell IL-2 signalling at day 1, and CD8<sup>+</sup> T cell number at day 64 in those receiving 2MIU IL-2.
- Reduced IL-2 signalling on CD45RA<sup>-</sup> Treg with the opposite effect observed on CD8<sup>+</sup>CD45RA<sup>-</sup> T cells at day 85.

*Outstanding questions:*

- If not IL-2 signalling as assessed *in vitro*, what other factors influence the Treg and non-Treg cell responses to IL-2 in trial participants?
- Are interim dose escalations necessary to influence greater Treg expansion as a result of the decreased IL-2 signalling?
- Will a dose escalation lead to a greater expansion of CD8<sup>+</sup> T cells given their increased sensitivity to IL-2?

**Chapter 5 – Comprehensive phenotyping of Treg and non-Treg cells before and after LD-IL-2.**

Given the heterogeneity of Treg and non-Treg cells, and the effects of IL-2 on the phenotype of these cells being relatively unknown, in the final data chapter we wished to focus on the effects of IL-2 therapy on the make-up of Treg and non-Treg cell subpopulations.

*Key findings:*

- Selective expansion of activated and proliferating Treg subpopulations.
- Activated Treg phenotypes are maintained for up to three weeks post therapy.

- IL-2 induced thymic Treg generation (RTE), which added to the already circulating RTE pool, maintaining elevated frequencies of this subset for up to three months post final IL-2 injection.
- Significant expansion of CD56<sup>bright</sup> NK subsets which are reported to have disease modifying effects in other neurological conditions.
- Significant reduction in a non-classical monocyte subset exhibiting high migratory potential (CX3CR1<sup>+</sup>).

*Outstanding questions:*

- What role do these peripheral blood subsets play in modifying ALS progression and survival?
- Rather than expanding total numbers of cell populations, should IL-2 be used to target specific cell phenotypes for better efficacy?
- Are these subsets present in the CNS, if so, are they involved in neuronal protection/degeneration?

### **6.3. Concluding remarks and future directions.**

This thesis aimed to investigate the effects of IL-2 therapy on a broad range of immune parameters in ALS patients, which could provide valuable insight for future IL-2 trials and also for investigations of the role of immune system in ALS disease progression. With Treg having a significant bearing on ALS progression, in the course of our research, we report that IL-2 was safe and well tolerated in all trial participants, observed significant expansion of Treg and their subsets, and improved functional ability, as well as a reduction in IL-2 signalling following continuous IL-2 therapy. We also observed significant expansion of non-Treg

cells such as NK. Subset analysis showed that the expanded NK possess the NK2 cell phenotype, with research showing these cells to prolong remission states in MS patients. Interestingly, we also observed a treatment induced reduction in a subset of non-classical monocytes, indicating their potential recruitment to tissue, with their respective modes of action yet to be fully defined.

With our findings in mind, future directions of ALS should focus on:

1. Investigating the clinical efficacy of IL-2.
2. Assessing the role of the immune cell phenotypes expanded by IL-2 (identified in this thesis) on ALS disease progression.
3. Modifying IL-2 dose/frequency to optimise Treg improvement.
4. Using modified IL-2 drugs for optimal Treg expansion.
5. Translation of immune parameters from the periphery to processes in the CNS, as this is where neuronal death and inflammation takes place in ALS patients.
6. Adoptive Treg cell therapy by generating Treg with desired characteristics, such as homing to CNS, or potentially injecting these into the CNS directly.
7. If life-long IL-2 injections are required, how can the burden of self-administration be eased, particularly as neuronal function declines.

Currently the MIROCALS clinical trial is assessing this in 208 newly diagnosed ALS patients (104 on 2MIU IL-2 and 104 on placebo) using the same dosing schedule as IMODALS repeated over an 18-month period. This trial will show if IL-2 therapy has an effect on disease progression and survival in ALS by investigating a wide set of biomarkers of neuroinflammatory processes in blood and CNS, assessing their relationship with treatment response and disease

activity. This study is also powered to identify IL-2 responders versus non-responders by assessing changes in gene expression signatures as a result of riluzole and IL-2. These blood, CNS and genetic characteristics can then be built on in future IL-2 trials, be it to adapt the IL-2 dose/frequency or use modified IL-2 drugs (IL-2 muteins) to optimise Treg expansion. Adaptation of IL-2 dose/frequency was successfully employed in T1D patients to design a well-tolerated dosing regimen for optimal Treg expansion (Seelig *et al.*, 2018). While the use of IL-2 muteins, synthesised for enhanced *in vivo* half-life or improved conjugation to Treg, have shown improved selective Treg expansion in animals, when compared to their wild type counterparts (Peterson *et al.*, 2018; Khoryati *et al.*, 2020).

As for assessment of immune cell activity in CNS, CSF sample analysis can detect the presence of immune cells. In IMODALS this was not possible as CSF was not collected. However, the MIROCALS partners kindly provided us with some matched PBMC and CSF samples from patients who have withdrawn from the study. Flow cytometry analysis shows the presence of Treg and Teff in the CSF (figure 6-5) as well as CD8<sup>+</sup> T cells, NK and B cells (data not shown), indicating immune cell infiltration.

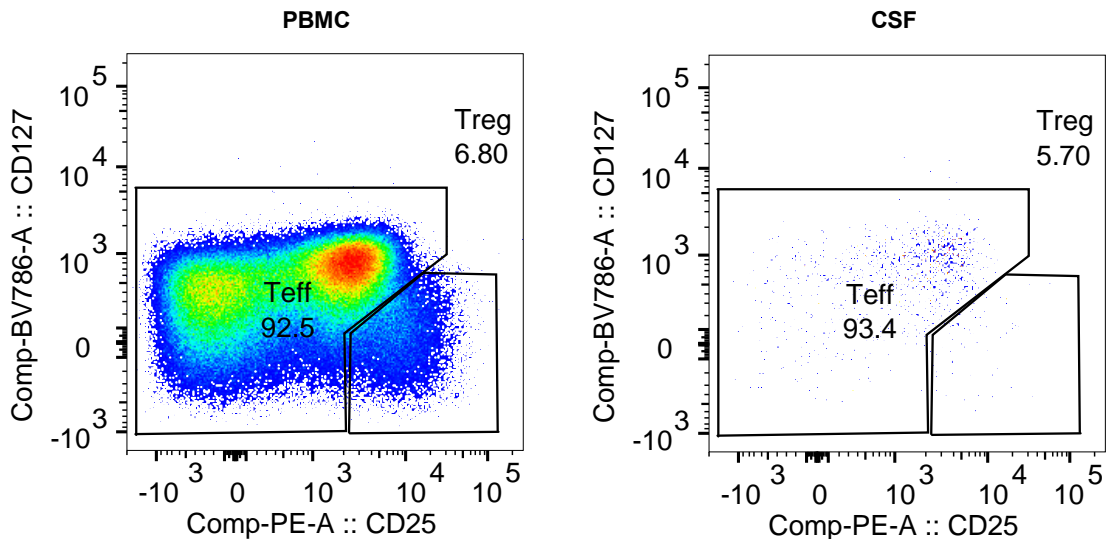


**Figure 6-5 Flow cytometry analysis of matched PBMC and CSF samples from ALS patients in the MIROCALS trial.** Immune cells such as Treg and Teff (shown above) as well as NK, B and CD8<sup>+</sup> T cells (not shown) were identified based on their expression of CD45 in PBMC and CSF samples using the same staining protocol. Panels represent the positive staining for Treg and Teff and PBMC (left) and CSF (right).

Therefore, future analyses should focus on identifying immune cell activities in the CNS of ALS patients, their role in initiating and mediating inflammation, how this affects neuronal cell survival and whether IL-2 can modulate neuronal protection through recruitment of immune cells. Furthermore, these investigations should utilise techniques single-cell transcriptional profiling. As these techniques, when combined with flow cytometry, can not only identify target cell populations in patient samples, but also assess the expression profile, allowing us to relate the presence of immune cells with the role they might play in the inflammatory processes in CNS of ALS patients. Identification of specific Treg subsets in the CNS could pave the way for adoptive Treg therapy, where cells with specific properties such as CNS homing could be developed *in vitro* and subsequently injected into the blood or the CNS. Adoptive transfer of autologous total Treg has been briefly attempted in ALS in a small cohort of patients showing some

improvement in Treg number and function (Thonhoff *et al.*, 2018). However, several caveats to this approach remain, mainly the high skill level and time required to perform such therapy, as well as the high cost of each adoptive transfer, thus, currently the conventional approach of IL-2 injections remains the favoured one. To that end, if life-long IL-2 treatment is required to maintain clinical efficacy, continuous self-administration can become problematic, particularly in ALS where motor function declines. To ease this burden, approaches currently employed in T1D should be considered, where currently many individuals with T1D make use of an insulin pump, a small device delivering rapid amounts of insulin via a catheter under the skin. This device negates the need for multiple daily insulin injections and gives the user increased ability to control blood sugar levels by the press of a button. The same approach could be adapted to IL-2, where an IL-2 pump would deliver a predetermined, daily or bi-daily dose of IL-2, negating for inability to self-administer, or forgetting to self-administer.

The final thought of the work presented in this thesis is that IL-2 may not be a cure for ALS however, by modulating the immune parameters related to disease progression, it may be an effective way to prolong survival while one is found.

## References.

- Abe, K. et al. (2014) 'Confirmatory double-blind, parallel-group, placebo-controlled study of efficacy and safety of edaravone (MCI-186) in amyotrophic lateral sclerosis patients', *Amyotrophic Lateral Sclerosis and Frontotemporal Degeneration*. Taylor and Francis Ltd, 15(7–8), pp. 610–617. doi: 10.3109/21678421.2014.959024.
- Abe, K. et al. (2017) 'Safety and efficacy of edaravone in well defined patients with amyotrophic lateral sclerosis: a randomised, double-blind, placebo-controlled trial', *The Lancet Neurology*. Lancet Publishing Group, 16(7), pp. 505–512. doi: 10.1016/S1474-4422(17)30115-1.
- Abel, A. M. et al. (2018) 'Natural killer cells: Development, maturation, and clinical utilization', *Frontiers in Immunology*. Frontiers Media S.A., p. 1. doi: 10.3389/fimmu.2018.01869.
- Ahmed, S. et al. (2019) 'Standardizing T-Cell Biomarkers in Type 1 Diabetes: Challenges and Recent Advances.', *Diabetes*. American Diabetes Association, 68(7), pp. 1366–1379. doi: 10.2337/db19-0119.
- Ajami, B. et al. (2007) 'Local self-renewal can sustain CNS microglia maintenance and function throughout adult life', *Nature Neuroscience* 2007 10:12. Nature Publishing Group, 10(12), pp. 1538–1543. doi: 10.1038/nn2014.
- Ajroud-Driss, S. and Siddique, T. (2015) 'Sporadic and hereditary amyotrophic lateral sclerosis (ALS)', *Biochimica et Biophysica Acta (BBA) - Molecular Basis of Disease*, 1852(4), pp. 679–684. doi: 10.1016/j.bbadi.2014.08.010.

Akkaya, B. et al. (2019) 'Regulatory T cells mediate specific suppression by depleting peptide–MHC class II from dendritic cells', *Nature Immunology*. Nature Publishing Group, 20(2), pp. 218–231. doi: 10.1038/s41590-018-0280-2.

Alrafiah, A. R. (2018) 'From mouse models to human disease: An approach for amyotrophic lateral sclerosis', *In Vivo*. International Institute of Anticancer Research, pp. 983–998. doi: 10.21873/invivo.11339.

Alroqi, F. J. and Chatila, T. A. (2016) 'T Regulatory Cell Biology in Health and Disease', *Current Allergy and Asthma Reports*, 16(4). doi: 10.1007/s11882-016-0606-9.

Aranami, T., Miyake, S. and Yamamura, T. (2006) 'Differential Expression of CD11c by Peripheral Blood NK Cells Reflects Temporal Activity of Multiple Sclerosis', *The Journal of Immunology*. The American Association of Immunologists, 177(8), pp. 5659–5667. doi: 10.4049/jimmunol.177.8.5659.

Araya, R. E. and Goldszmid, R. S. (2020) 'Characterization of the tumor immune infiltrate by multiparametric flow cytometry and unbiased high-dimensional data analysis', in *Methods in Enzymology*. Academic Press Inc., pp. 309–337. doi: 10.1016/bs.mie.2019.11.012.

Arce-Sillas, A. et al. (2016) 'Regulatory T Cells: Molecular Actions on Effector Cells in Immune Regulation', *Journal of Immunology Research*. Hindawi Limited. doi: 10.1155/2016/1720827.

Arthur, K. C. et al. (2016) 'Projected increase in amyotrophic lateral sclerosis from 2015 to 2040.', *Nature communications*. Nature Publishing Group, 7, p. 12408. doi: 10.1038/ncomms12408.

Asano, T. *et al.* (2017) 'PD-1 modulates regulatory T-cell homeostasis during low-dose interleukin-2 therapy', *Blood*. American Society of Hematology, 129(15), pp. 2186–2197. doi: 10.1182/blood-2016-09-741629.

Bachiller, S. *et al.* (2018) 'Microglia in neurological diseases: A road map to brain-disease dependent-inflammatory response', *Frontiers in Cellular Neuroscience*. Frontiers Media S.A., p. 488. doi: 10.3389/fncel.2018.00488.

Baecher-Allan, C., Wolf, E. and Hafler, D. A. (2006) 'MHC Class II Expression Identifies Functionally Distinct Human Regulatory T Cells', *The Journal of Immunology*. The American Association of Immunologists, 176(8), pp. 4622–4631. doi: 10.4049/jimmunol.176.8.4622.

Bakker, L. A. *et al.* (2017) 'Assessment of the factorial validity and reliability of the ALSFRS-R: a revision of its measurement model', *Journal of Neurology*. Dr. Dietrich Steinkopff Verlag GmbH and Co. KG, 264(7), pp. 1413–1420. doi: 10.1007/s00415-017-8538-4.

Balandina, A. *et al.* (2005) 'Functional defect of regulatory CD4(+)CD25+ T cells in the thymus of patients with autoimmune myasthenia gravis.', *Blood*. NIH Public Access, 105(2), pp. 735–41. doi: 10.1182/blood-2003-11-3900.

Barbeito, A. G., Mesci, P. and Boillée, S. (2010) 'Motor neuron-immune interactions: the vicious circle of ALS.', *Journal of neural transmission (Vienna, Austria : 1996)*. Inserm, 117(8), pp. 981–1000. doi: 10.1007/s00702-010-0429-0.

Baron, P. *et al.* (2005) 'Production of monocyte chemoattractant protein-1 in amyotrophic lateral sclerosis', *Muscle & Nerve*. John Wiley & Sons, Ltd, 32(4), pp. 541–544. doi: 10.1002/mus.20376.

Bayer, A. L., Pugliese, A. and Malek, T. R. (2013) 'The IL-2/IL-2R system: From basic science to therapeutic applications to enhance immune regulation', *Immunologic Research*. NIH Public Access, 57(1–3), pp. 197–209. doi: 10.1007/s12026-013-8452-5.

Beers, D. R. et al. (2008) *CD4 T cells support glial neuroprotection, slow disease progression, and modify glial morphology in an animal model of inherited ALS*. Available at: [www.pnas.org/cgi/doi/10.1073/pnas.0807419105](http://www.pnas.org/cgi/doi/10.1073/pnas.0807419105) (Accessed: 8 August 2019).

Beers, D. R. et al. (2011) 'Endogenous regulatory T lymphocytes ameliorate amyotrophic lateral sclerosis in mice and correlate with disease progression in patients with amyotrophic lateral sclerosis', *Brain*. Narnia, 134(5), pp. 1293–1314. doi: 10.1093/brain/awr074.

Beers, D. R. et al. (2017) 'ALS patients' regulatory T lymphocytes are dysfunctional, and correlate with disease progression rate and severity', *JCI Insight*. American Society for Clinical Investigation, 2(5). doi: 10.1172/JCI.INSIGHT.89530.

Bellingham, M. C. (2011) 'A Review of the Neural Mechanisms of Action and Clinical Efficiency of Riluzole in Treating Amyotrophic Lateral Sclerosis: What have we Learned in the Last Decade?', *CNS Neuroscience and Therapeutics*. Wiley-Blackwell, pp. 4–31. doi: 10.1111/j.1755-5949.2009.00116.x.

Bensimon, G., Lacomblez, L. and Meininger, V. (1994) 'A Controlled Trial of Riluzole in Amyotrophic Lateral Sclerosis', *New England Journal of Medicine*. Massachusetts Medical Society, 330(9), pp. 585–591. doi: 10.1056/nejm199403033300901.

Bhandari, R., Kuhad, A. and Kuhad, A. (2018) 'Edaravone: a new hope for deadly amyotrophic lateral sclerosis', *Drugs of Today*, 54(6), p. 349. doi: 10.1358/dot.2018.54.6.2828189.

Bianconi, V. et al. (2018) 'The regulation and importance of monocyte chemoattractant protein-1.', *Current opinion in hematology*, 25(1), pp. 44–51. doi: 10.1097/MOH.0000000000000389.

Bielekova, B. et al. (2011) 'Intrathecal effects of daclizumab treatment of multiple sclerosis', *Neurology*. Lippincott Williams and Wilkins, 77(21), pp. 1877–1886. doi: 10.1212/WNL.0b013e318239f7ef.

Van Blitterswijk, M., Dejesus-Hernandez, M. and Rademakers, R. (2012) 'How do C9ORF72 repeat expansions cause amyotrophic lateral sclerosis and frontotemporal dementia: Can we learn from other noncoding repeat expansion disorders?', *Current Opinion in Neurology*. NIH Public Access, pp. 689–700. doi: 10.1097/WCO.0b013e32835a3efb.

Bluestone, J. A. et al. (2015) 'Type 1 diabetes immunotherapy using polyclonal regulatory T cells.', *Science translational medicine*. NIH Public Access, 7(315), p. 315ra189. doi: 10.1126/scitranslmed.aad4134.

Booth, N. J. et al. (2010) 'Different Proliferative Potential and Migratory Characteristics of Human CD4 + Regulatory T Cells That Express either CD45RA or CD45RO', *The Journal of Immunology*. The American Association of Immunologists, 184(8), pp. 4317–4326. doi: 10.4049/jimmunol.0903781.

Bosco, M. et al. (1994) 'The gamma subunit of the interleukin-2 receptor is expressed in human monocytes and modulated by interleukin-2, interferon gamma, and transforming growth factor beta 1', *Blood*. American Society of Hematology, 83(12), pp. 3462–3467. doi: 10.1182/blood.v83.12.3462.3462.

Bosco, M. C. et al. (2000) 'IL-2 Signaling in Human Monocytes Involves the Phosphorylation and Activation of p59 hck 1', *The Journal of Immunology*. The American Association of Immunologists, 164(9), pp. 4575–4585. doi: 10.4049/jimmunol.164.9.4575.

Boylan, K. B. et al. (2013) 'Phosphorylated neurofilament heavy subunit (pNF-H) in peripheral blood and CSF as a potential prognostic biomarker in Amyotrophic Lateral Sclerosis', *Journal of Neurology, Neurosurgery and Psychiatry*. BMJ Publishing Group, 84(4), pp. 467–472. doi: 10.1136/jnnp-2012-303768.

Boyman, O. and Sprent, J. (2012) 'The role of interleukin-2 during homeostasis and activation of the immune system', *Nature Reviews Immunology*. Nature Publishing Group, pp. 180–190. doi: 10.1038/nri3156.

Bozzoni, V. et al. (2016) 'Amyotrophic lateral sclerosis and environmental factors', *Functional Neurology*. CIC Edizioni Internazionali s.r.l., pp. 7–19. doi: 10.11138/FNeur/2016.31.1.007.

Braza, F. et al. (2015) 'Central role of CD45RA- Foxp3hi memory regulatory T cells in clinical kidney transplantation tolerance', *Journal of the American Society of Nephrology*. American Society of Nephrology, 26(8), pp. 1795–1805. doi: 10.1681/ASN.2014050480.

Breiner, A., Zinman, L. and Bourque, P. R. (2020) 'Edaravone for amyotrophic lateral sclerosis: Barriers to access and lifeboat ethics', *CMAJ. Canadian Medical Association*, pp. E319–E320. doi: 10.1503/cmaj.191236.

Brettschneider, J. et al. (2012) 'Microglial activation correlates with disease progression and upper motor neuron clinical symptoms in amyotrophic lateral sclerosis', *PLoS ONE*. Public Library of Science, 7(6). doi: 10.1371/journal.pone.0039216.

Brown, R. H. and Al-Chalabi, A. (2017) 'Amyotrophic Lateral Sclerosis', *New England Journal of Medicine*. Edited by D. L. Longo, 377(2), pp. 162–172. doi: 10.1056/NEJMra1603471.

Brubaker, S. W. et al. (2015) 'Innate Immune Pattern Recognition: A Cell Biological Perspective', *Annual Review of Immunology*. Annual Reviews, 33(1), pp. 257–290. doi: 10.1146/annurev-immunol-032414-112240.

Brusko, T. M. et al. (2005) 'Functional defects and the influence of age on the frequency of CD4 +CD25+ T-cells in type 1 diabetes', *Diabetes*. American Diabetes Association, 54(5), pp. 1407–1414. doi: 10.2337/diabetes.54.5.1407.

Caldirola, M. S. et al. (2018) 'Primary immunodeficiencies unravel the role of IL-2/CD25/STAT5b in human natural killer cell maturation', *Frontiers in Immunology*. Frontiers Media S.A., 9(JUN), p. 22. doi: 10.3389/fimmu.2018.01429.

Camu, W., Mickunas, M., Veyrune, J.-L., et al. (2020) 'Repeated 5-day cycles of low dose aldesleukin in amyotrophic lateral sclerosis (IMODALS): A phase 2a randomised, double-blind, placebo-controlled trial', *EBioMedicine*, 59, p. 102844. doi: 10.1016/j.ebiom.2020.102844.

Camu, W., Mickunas, M., Veyrune, J. L., et al. (2020) 'Repeated 5-day cycles of low dose aldesleukin in amyotrophic lateral sclerosis (IMODALS): A phase 2a randomised, double-blind, placebo-controlled trial', *EBioMedicine*. Elsevier B.V., 59. doi: 10.1016/j.ebiom.2020.102844.

Canè, S. et al. (2019) 'The Endless Saga of Monocyte Diversity', *Frontiers in Immunology*. Frontiers, 0, p. 1786. doi: 10.3389/FIMMU.2019.01786.

Castela, E. et al. (2014) 'Effects of Low-Dose Recombinant Interleukin 2 to Promote T-Regulatory Cells in Alopecia Areata', *JAMA Dermatology*. American Medical Association, 150(7), p. 748. doi: 10.1001/jamadermatol.2014.504.

Cedarbaum, J. M. et al. (1999) 'The ALSFRS-R: A revised ALS functional rating scale that incorporates assessments of respiratory function', *Journal of the Neurological Sciences*. J Neurol Sci, 169(1–2), pp. 13–21. doi: 10.1016/S0022-510X(99)00210-5.

Cerosaletti, K. et al. (2013) 'Multiple Autoimmune-Associated Variants Confer Decreased IL-2R Signaling in CD4+CD25hi T Cells of Type 1 Diabetic and Multiple Sclerosis Patients', *PLoS ONE*. Edited by S. Jacobson. Public Library of Science, 8(12), p. e83811. doi: 10.1371/journal.pone.0083811.

Ceuppens, J. L. *et al.* (1988) 'Human T cell activation with phytohemagglutinin. The function of IL-6 as an accessory signal.', *The Journal of Immunology*, 141(11).

Chadi, G. *et al.* (2017) 'Genetic analysis of patients with familial and sporadic amyotrophic lateral sclerosis in a Brazilian Research Center', *Amyotrophic Lateral Sclerosis and Frontotemporal Degeneration*. Taylor & Francis, 18(3–4), pp. 249–255. doi: 10.1080/21678421.2016.1254245.

Chaplin, D. D. (2010) 'Overview of the immune response', *Journal of Allergy and Clinical Immunology*. NIH Public Access, 125(2 SUPPL. 2), p. S3. doi: 10.1016/j.jaci.2009.12.980.

Chen, J. J. (2020) 'Overview of Current and Emerging Therapies for Amyotrophic Lateral Sclerosis', *American Journal of Managed Care*. Ascend Media, pp. S191–S197. doi: 10.37765/AJMC.2020.88483.

Chen, X. *et al.* (2014) 'Evidence for peripheral immune activation in amyotrophic lateral sclerosis', *Journal of the Neurological Sciences*. Elsevier, 347(1–2), pp. 90–95. doi: 10.1016/J.JNS.2014.09.025.

Chen, X. *et al.* (2018) 'Cerebrospinal Fluid Inflammatory Cytokine Aberrations in Alzheimer's Disease, Parkinson's Disease and Amyotrophic Lateral Sclerosis: A Systematic Review and Meta-Analysis', *Frontiers in Immunology*. Frontiers, 9, p. 2122. doi: 10.3389/fimmu.2018.02122.

Cheng, G. *et al.* (2013) 'IL-2R Signaling Is Essential for Functional Maturation of Regulatory T Cells during Thymic Development', *The Journal of Immunology*. The American Association of Immunologists, 190(4), pp. 1567–1575. doi: 10.4049/jimmunol.1201218.

Cheng, G., Yu, A. and Malek, T. R. (2011) 'T-cell tolerance and the multi-functional role of IL-2R signaling in T-regulatory cells', *Immunological Reviews*. NIH Public Access, pp. 63–76. doi: 10.1111/j.1600-065X.2011.01004.x.

Chiu, S. and Bharat, A. (2016) 'Role of monocytes and macrophages in regulating immune response following lung transplantation', *Current Opinion in Organ Transplantation*. Lippincott Williams and Wilkins, pp. 239–245. doi: 10.1097/MOT.0000000000000313.

Collin, M. and Bigley, V. (2018) 'Human dendritic cell subsets: an update', *Immunology*. Wiley-Blackwell, 154(1), p. 3. doi: 10.1111/IMM.12888.

Cooper, M. D. and Alder, M. N. (2006) 'The evolution of adaptive immune systems', *Cell*. Elsevier, pp. 815–822. doi: 10.1016/j.cell.2006.02.001.

Cortez, J. T. *et al.* (2020) 'CRISPR screen in regulatory T cells reveals modulators of Foxp3', *Nature*. Nature Publishing Group, pp. 1–5. doi: 10.1038/s41586-020-2246-4.

Cudkowicz, M. E. *et al.* (2006) 'Trial of celecoxib in amyotrophic lateral sclerosis', *Annals of Neurology*. John Wiley and Sons Inc., 60(1), pp. 22–31. doi: 10.1002/ana.20903.

Van Damme, P., Robberecht, W. and Van Den Bosch, L. (2017) 'Modelling amyotrophic lateral sclerosis: Progress and possibilities', *DMM Disease Models and Mechanisms*. Company of Biologists Ltd, pp. 537–549. doi: 10.1242/dmm.029058.

Danikowski, K. M., Jayaraman, S. and Prabhakar, B. S. (2017) 'Regulatory T cells in multiple sclerosis and myasthenia gravis.', *Journal of neuroinflammation*. BioMed Central, 14(1), p. 117. doi: 10.1186/s12974-017-0892-8.

DeJesus-Hernandez, M. et al. (2011) 'Expanded GGGGCC Hexanucleotide Repeat in Noncoding Region of C9ORF72 Causes Chromosome 9p-Linked FTD and ALS', *Neuron*, 72(2), pp. 245–256. doi: 10.1016/j.neuron.2011.09.011.

Dendrou, C. A. et al. (2009) 'Cell-specific protein phenotypes for the autoimmune locus IL2RA using a genotype-selectable human bioresource', *Nature Genetics*. Nature Publishing Group, 41(9), pp. 1011–1015. doi: 10.1038/ng.434.

Deng, Q. et al. (2019) 'The emerging epigenetic role of CD8+T cells in autoimmune diseases: A systematic review', *Frontiers in Immunology*. Frontiers Media S.A., p. 856. doi: 10.3389/fimmu.2019.00856.

Deshmane, S. L. et al. (2009) 'Monocyte chemoattractant protein-1 (MCP-1): An overview', *Journal of Interferon and Cytokine Research*, pp. 313–325. doi: 10.1089/jir.2008.0027.

Dharmadasa, T. and Kiernan, M. C. (2018) 'Riluzole, disease stage and survival in ALS'. doi: 10.1016/S1474-4422(18)30069-3.

DiGiuseppe, J. A. *et al.* (2018) 'PhenoGraph and viSNE facilitate the identification of abnormal T-cell populations in routine clinical flow cytometric data', *Cytometry Part B - Clinical Cytometry*. John Wiley and Sons Inc., 94(5), pp. 588–601. doi: 10.1002/cyto.b.21588.

Donnelly, C. *et al.* (2018) 'Optimizing human Treg immunotherapy by Treg subset selection and E-selectin ligand expression', *Scientific Reports*. Nature Publishing Group, 8(1), p. 420. doi: 10.1038/s41598-017-17981-z.

Dunkelberger, J. R. and Song, W. C. (2010) 'Complement and its role in innate and adaptive immune responses', *Cell Research*. Nature Publishing Group, 20(1), pp. 34–50. doi: 10.1038/cr.2009.139.

Duque, G. A. and Descoteaux, A. (2014) 'Macrophage cytokines: Involvement in immunity and infectious diseases', *Frontiers in Immunology*. Frontiers Media S.A., p. 491. doi: 10.3389/fimmu.2014.00491.

Fang, T. *et al.* (2018) 'Stage at which riluzole treatment prolongs survival in patients with amyotrophic lateral sclerosis: a retrospective analysis of data from a dose-ranging study'. doi: 10.1016/S1474-4422(18)30054-1.

Feneberg, E. *et al.* (2018) 'Multicenter evaluation of neurofilaments in early symptom onset amyotrophic lateral sclerosis', *Neurology*. Lippincott Williams and Wilkins, 90(1), pp. e22–e30. doi: 10.1212/WNL.0000000000004761.

Ferretti, E., Pistoia, V. and Corcione, A. (2014) 'Role of fractalkine/CX3CL1 and its receptor in the pathogenesis of inflammatory and malignant diseases with emphasis on B cell malignancies', *Mediators of Inflammation*. Hindawi Publishing Corporation. doi: 10.1155/2014/480941.

Finneran, D. J. and Nash, K. R. (2019) 'Neuroinflammation and fractalkine signaling in Alzheimer's disease', *Journal of Neuroinflammation*. BioMed Central Ltd., p. 30. doi: 10.1186/s12974-019-1412-9.

Flajnik, M. F. (2018) 'A cold-blooded view of adaptive immunity', *Nature Reviews Immunology*. Nature Publishing Group, pp. 438–453. doi: 10.1038/s41577-018-0003-9.

Forsberg, K. et al. (2019) 'Misfolded SOD1 inclusions in patients with mutations in C9orf72 and other ALS/FTD-associated genes', *Journal of Neurology, Neurosurgery and Psychiatry*. BMJ Publishing Group, 90(8), pp. 861–869. doi: 10.1136/jnnp-2018-319386.

Fukui, S. et al. (2018) 'M1 and M2 Monocytes in rheumatoid arthritis: A contribution of imbalance of M1/M2 monocytes to osteoclastogenesis', *Frontiers in Immunology*. Frontiers Media S.A., 8(JAN). doi: 10.3389/fimmu.2017.01958.

Fung, M. M., Rohwer, F. and McGuire, K. L. (2003) 'IL-2 activation of a PI3K-dependent STAT3 serine phosphorylation pathway in primary human T cells', *Cellular Signalling*. Elsevier Inc., 15(6), pp. 625–636. doi: 10.1016/S0898-6568(03)00003-2.

Gadalla, R. et al. (2019) 'Validation of CyTOF Against Flow Cytometry for Immunological Studies and Monitoring of Human Cancer Clinical Trials', *Frontiers in Oncology*. Frontiers Media S.A., 9(MAY), p. 415. doi: 10.3389/fonc.2019.00415.

Gaffen, S. L. and Liu, K. D. (2004) 'Overview of interleukin-2 function, production and clinical applications', *Cytokine*. Academic Press, 28(3), pp. 109–123. doi: 10.1016/j.cyto.2004.06.010.

Gagliardi, D. et al. (2019) 'Diagnostic and prognostic role of blood and cerebrospinal fluid and blood neurofilaments in amyotrophic lateral sclerosis: A review of the literature', *International Journal of Molecular Sciences*. MDPI AG. doi: 10.3390/ijms20174152.

Le Gallou, S. et al. (2012) 'IL-2 Requirement for Human Plasma Cell Generation: Coupling Differentiation and Proliferation by Enhancing MAPK–ERK Signaling', *The Journal of Immunology*. The American Association of Immunologists, 189(1), pp. 161–173. doi: 10.4049/jimmunol.1200301.

Garg, G. et al. (2012) 'Type 1 Diabetes-Associated IL2RA Variation Lowers IL-2 Signaling and Contributes to Diminished CD4 + CD25 + Regulatory T Cell Function', *The Journal of Immunology*. The American Association of Immunologists, 188(9), pp. 4644–4653. doi: 10.4049/jimmunol.1100272.

Van Gassen, S. et al. (2015) 'FlowSOM: Using self-organizing maps for visualization and interpretation of cytometry data', *Cytometry Part A*. Wiley-Liss Inc., 87(7), pp. 636–645. doi: 10.1002/cyto.a.22625.

Gautier, E. L., Jakubzick, C. and Randolph, G. J. (2009) 'Regulation of the migration and survival of monocyte subsets by chemokine receptors and its relevance to atherosclerosis', *Arteriosclerosis, Thrombosis, and Vascular Biology*. NIH Public Access, pp. 1412–1418. doi: 10.1161/ATVBAHA.108.180505.

Gazon, H. et al. (2018) 'Hijacking of the AP-1 signaling pathway during development of ATL', *Frontiers in Microbiology*. Frontiers Media S.A., p. 2686. doi: 10.3389/fmicb.2017.02686.

Ghasemi, N., Razavi, S. and Nikzad, E. (2017) *Multiple Sclerosis: Pathogenesis, Symptoms, Diagnoses and Cell-Based Therapy Citation: Ghasemi N, Razavi Sh, Nikzad E. Multiple sclerosis: pathogenesis, symptoms, diagnoses and cell-based therapy, CELL JOURNAL(Yakhteh)*.

Ghelani, A. et al. (2020) 'Defining the Threshold IL-2 Signal Required for Induction of Selective Treg Cell Responses Using Engineered IL-2 Muteins', *Frontiers in Immunology*. Frontiers Media S.A., 11, p. 1106. doi: 10.3389/fimmu.2020.01106.

Gille, B. et al. (2019) 'Inflammatory markers in cerebrospinal fluid: independent prognostic biomarkers in amyotrophic lateral sclerosis?', *Journal of neurology, neurosurgery, and psychiatry*. BMJ Publishing Group Ltd, p. jnnp-2018-319586. doi: 10.1136/jnnp-2018-319586.

Ginhoux, F. and Jung, S. (2014) 'Monocytes and macrophages: Developmental pathways and tissue homeostasis', *Nature Reviews Immunology*. Nature Publishing Group, pp. 392–404. doi: 10.1038/nri3671.

De Giorgio, F. et al. (2019) 'Transgenic and physiological mouse models give insights into different aspects of amyotrophic lateral sclerosis', *DMM Disease Models and Mechanisms*. Company of Biologists Ltd. doi: 10.1242/dmm.037424.

Gonzalez-Mejia, M. E. and Doseff, A. I. (2009) 'Regulation of monocytes and macrophages cell fate', *Frontiers in Bioscience*. Front Biosci (Landmark Ed), 14(7), pp. 2413–2431. doi: 10.2741/3387.

Gordon, P. H. et al. (2007) 'Efficacy of minocycline in patients with amyotrophic lateral sclerosis: a phase III randomised trial', *Lancet Neurology*. Elsevier, 6(12), pp. 1045–1053. doi: 10.1016/S1474-4422(07)70270-3.

Gough, S. and Simmonds, M. (2009) 'The HLA Region and Autoimmune Disease: Associations and Mechanisms of Action', *Current Genomics*. Bentham Science Publishers Ltd., 8(7), pp. 453–465. doi: 10.2174/138920207783591690.

Grant, P., Song, J. Y. and Swedo, S. E. (2010) 'Review of the use of the glutamate antagonist riluzole in psychiatric disorders and a description of recent use in childhood obsessive-compulsive disorder', *Journal of Child and Adolescent Psychopharmacology*. Mary Ann Liebert, Inc., pp. 309–315. doi: 10.1089/cap.2010.0009.

Gregg, R. et al. (2005) 'The number of human peripheral blood CD4+ CD25high regulatory T cells increases with age', *Clinical and Experimental Immunology*. Wiley-Blackwell, 140(3), pp. 540–546. doi: 10.1111/j.1365-2249.2005.02798.x.

Grimm Tse-Kuan Yu, A., Caudell, E. G. and Smid, C. (2000) 'MKK1/2/ERK But Not p38 Kinase Pathway IL-2 Activation of NK Cells: Involvement of', *J Immunol References*, 164, pp. 6244–6251. doi: 10.4049/jimmunol.164.12.6244.

Gu, J. et al. (2017) 'Human CD39hi regulatory T cells present stronger stability and function under inflammatory conditions', *Cellular & Molecular Immunology*. Nature Publishing Group, 14(6), pp. 521–528. doi: 10.1038/cmi.2016.30.

Guerrero, E. N. et al. (2016) 'TDP-43/FUS in motor neuron disease: Complexity and challenges', *Progress in Neurobiology*. Elsevier Ltd, pp. 78–97. doi: 10.1016/j.pneurobio.2016.09.004.

Gui, J. et al. (2012) 'Thymus size and age-related thymic involution: Early programming, sexual dimorphism, progenitors and stroma', *Aging and Disease*. International Society on Aging and Disease, pp. 280–290. Available at: /pmc/articles/PMC3375084/ (Accessed: 17 May 2021).

Guilliams, M., Mildner, A. and Yona, S. (2018) 'Immunity Review Developmental and Functional Heterogeneity of Monocytes'. doi: 10.1016/j.immuni.2018.10.005.

Gustafson, M. P. et al. (2017) 'Comprehensive immune profiling reveals substantial immune system alterations in a subset of patients with amyotrophic lateral sclerosis.', *PloS one*. Public Library of Science, 12(7), p. e0182002. doi: 10.1371/journal.pone.0182002.

Hamann, I. et al. (2011) 'Analyses of phenotypic and functional characteristics of CX3CR1-expressing natural killer cells', *Immunology*. Wiley-Blackwell, 133(1), pp. 62–73. doi: 10.1111/j.1365-2567.2011.03409.x.

Harada, H. et al. (2001) 'p70S6 kinase signals cell survival as well as growth, inactivating the pro-apoptotic molecule BAD', *Proceedings of the National Academy of Sciences of the United States of America*. National Academy of Sciences, 98(17), pp. 9666–9670. doi: 10.1073/pnas.171301998.

Hardiman, O. and van den Berg, L. H. (2017) 'Edaravone: a new treatment for ALS on the horizon?', *The Lancet Neurology*. Lancet Publishing Group, pp. 490–491. doi: 10.1016/S1474-4422(17)30163-1.

Hartemann, A. et al. (2013) 'Low-dose interleukin 2 in patients with type 1 diabetes: A phase 1/2 randomised, double-blind, placebo-controlled trial', *The Lancet Diabetes and Endocrinology*. doi: 10.1016/S2213-8587(13)70113-X.

Hayes, E., Hagan, C. and Campbell, D. (2019) 'Treg cells maintain selective access to IL-2 and immune homeostasis despite substantially reduced CD25 function', *bioRxiv*. Cold Spring Harbor Laboratory, p. 786228. doi: 10.1101/786228.

He, J. et al. (2016) 'Low-dose interleukin-2 treatment selectively modulates CD4+ T cell subsets in patients with systemic lupus erythematosus', *Nature Medicine*. Nature Publishing Group, 22(9), pp. 991–993. doi: 10.1038/nm.4148.

He, J. et al. (2020) 'Efficacy and safety of low-dose IL-2 in the treatment of systemic lupus erythematosus: A randomised, double-blind, placebo-controlled trial', *Annals of the Rheumatic Diseases*. BMJ Publishing Group, 79(1), pp. 141–149. doi: 10.1136/annrheumdis-2019-215396.

Heneka, M. T. et al. (2015) 'Neuroinflammation in Alzheimer's disease', *The Lancet Neurology*. Lancet Publishing Group, pp. 388–405. doi: 10.1016/S1474-4422(15)70016-5.

Henkel, J. S. et al. (2004) 'Presence of dendritic cells, MCP-1, and activated microglia/macrophages in amyotrophic lateral sclerosis spinal cord tissue', *Annals of Neurology*. John Wiley & Sons, Ltd, 55(2), pp. 221–235. doi: 10.1002/ana.10805.

Henkel, J. S. *et al.* (2013) 'Regulatory T-lymphocytes mediate amyotrophic lateral sclerosis progression and survival', *EMBO Molecular Medicine*. John Wiley & Sons, Ltd, 5(1), pp. 64–79. doi: 10.1002/emmm.201201544.

Hirakawa, M. *et al.* (2017) 'Low-dose IL-2 selectively activates subsets of CD4+ Tregs and NK cells', *JCI Insight*. American Society for Clinical Investigation, 1(18). doi: 10.1172/JCI.INSIGHT.89278.

Hoenstein, R. *et al.* (2001) 'Interleukin-2 activates human peripheral blood eosinophils', *Cellular Immunology*. Academic Press Inc., 210(2), pp. 116–124. doi: 10.1006/cimm.2001.1808.

Hou, J. *et al.* (2018) 'Circulating CD14 + CD163 + CD206 + M2 monocytes are increased in patients with early stage of idiopathic membranous nephropathy', *Mediators of Inflammation*. Hindawi Limited, 2018. doi: 10.1155/2018/5270657.

Hou, P. F. *et al.* (2017) 'Age-related changes in CD4+CD25+FOXP3+ regulatory T cells and their relationship with lung cancer', *PLoS ONE*. Public Library of Science, 12(3). doi: 10.1371/journal.pone.0173048.

Hu, Y. *et al.* (2017) 'Increased peripheral blood inflammatory cytokine levels in amyotrophic lateral sclerosis: a meta-analysis study', *Scientific Reports*. Nature Publishing Group, 7(1), p. 9094. doi: 10.1038/s41598-017-09097-1.

Huang, L. *et al.* (2017) 'Decreased frequencies and impaired functions of the CD31+ subpopulation in Treg cells associated with decreased FoxP3 expression and enhanced Treg cell defects in patients with coronary heart disease', *Clinical and Experimental Immunology*. Blackwell Publishing Ltd, 187(3), pp. 441–454. doi: 10.1111/cei.12897.

Huang, Y. et al. (2018) 'Repopulated microglia are solely derived from the proliferation of residual microglia after acute depletion', *Nature Neuroscience* 2018 21:4. Nature Publishing Group, 21(4), pp. 530–540. doi: 10.1038/s41593-018-0090-8.

Hulme, M. A. et al. (2012) 'Central role for interleukin-2 in type 1 diabetes', *Diabetes*. American Diabetes Association, pp. 14–22. doi: 10.2337/db11-1213.

Hwang, J. R. et al. (2020) 'Recent insights of T cell receptor-mediated signaling pathways for T cell activation and development', *Experimental and Molecular Medicine*. Springer Nature, pp. 750–761. doi: 10.1038/s12276-020-0435-8.

Idzkowska, E. et al. (2015) 'The Role of Different Monocyte Subsets in the Pathogenesis of Atherosclerosis and Acute Coronary Syndromes', *Scandinavian Journal of Immunology*. Blackwell Publishing Ltd, 82(3), pp. 163–173. doi: 10.1111/sji.12314.

Ilse, B. et al. (2014) 'Relationships Between Disease Severity, Social Support and Health-Related Quality of Life in Patients with Amyotrophic Lateral Sclerosis', *Social Indicators Research*. Kluwer Academic Publishers, 120(3), pp. 871–882. doi: 10.1007/s11205-014-0621-y.

Infante-Duarte, C. et al. (2005) 'Frequency of blood CX 3 CR1-positive natural killer cells correlates with disease activity in multiple sclerosis patients', *The FASEB Journal*. Wiley, 19(13), pp. 1902–1904. doi: 10.1096/fj.05-3832fje.

Italiani, P. and Boraschi, D. (2014) 'From monocytes to M1/M2 macrophages: Phenotypical vs. functional differentiation', *Frontiers in Immunology*. Frontiers Research Foundation, p. 514. doi: 10.3389/fimmu.2014.00514.

Ito, Hidefumi *et al.* (2008) 'Treatment with edaravone, initiated at symptom onset, slows motor decline and decreases SOD1 deposition in ALS mice', *Experimental Neurology*. Academic Press, 213(2), pp. 448–455. doi: 10.1016/j.expneurol.2008.07.017.

Iwasaki, A. and Medzhitov, R. (2010) 'Regulation of adaptive immunity by the innate immune system', *Science*. American Association for the Advancement of Science, pp. 291–295. doi: 10.1126/science.1183021.

Jiang, T., Zhou, C. and Ren, S. (2016) 'Role of IL-2 in cancer immunotherapy', *Oncolimmunology*. Taylor and Francis Inc. doi: 10.1080/2162402X.2016.1163462.

Junge, S. *et al.* (2007) 'Correlation between recent thymic emigrants and CD31+ (PECAM-1) CD4+ T cells in normal individuals during aging and in lymphopenic children', *European Journal of Immunology*. John Wiley & Sons, Ltd, 37(11), pp. 3270–3280. doi: 10.1002/eji.200636976.

Kaiko, G. E. *et al.* (2008) 'Immunological decision-making: How does the immune system decide to mount a helper T-cell response?', *Immunology*. Wiley-Blackwell, pp. 326–338. doi: 10.1111/j.1365-2567.2007.02719.x.

Kalia, V. and Sarkar, S. (2018) 'Regulation of Effector and Memory CD8 T Cell Differentiation by IL-2-A Balancing Act', *Frontiers in immunology*. NLM (Medline), p. 2987. doi: 10.3389/fimmu.2018.02987.

Kalliolias, G. D. and Ivashkiv, L. B. (2008) 'IL-27 Activates Human Monocytes via STAT1 and Suppresses IL-10 Production but the Inflammatory Functions of IL-27 Are Abrogated by TLRs and p38', *The Journal of Immunology*. The American Association of Immunologists, 180(9), pp. 6325–6333. doi: 10.4049/jimmunol.180.9.6325.

Kapellos, T. S. et al. (2019) 'Human monocyte subsets and phenotypes in major chronic inflammatory diseases', *Frontiers in Immunology*. Frontiers Media S.A., p. 2035. doi: 10.3389/fimmu.2019.02035.

Katyal, N. and Govindarajan, R. (2017) 'Shortcomings in the current amyotrophic lateral sclerosis trials and potential solutions for improvement', *Frontiers in Neurology*. Frontiers Media S.A., p. 1. doi: 10.3389/fneur.2017.00521.

Khairoalsindi, O. A. and Abuzinadah, A. R. (2018) 'Maximizing the Survival of Amyotrophic Lateral Sclerosis Patients: Current Perspectives', *Neurology Research International*. Hindawi Limited, 2018. doi: 10.1155/2018/6534150.

Khalid, S. I. et al. (2017) 'Immune modulation in the treatment of amyotrophic lateral sclerosis: A review of clinical trials', *Frontiers in Neurology*. Frontiers Media S.A., p. 486. doi: 10.3389/fneur.2017.00486.

Khalil, M. et al. (2018) 'Neurofilaments as biomarkers in neurological disorders', *Nature Reviews Neurology*. Nature Publishing Group, 14(10), pp. 577–589. doi: 10.1038/s41582-018-0058-z.

Khoryati, L. et al. (2020) ‘An IL-2 mutein engineered to promote expansion of regulatory T cells arrests ongoing autoimmunity in mice’, *Science Immunology*.

American Association for the Advancement of Science, 5(50). doi: 10.1126/SCIIMMUNOL.ABA5264.

Kiernan, M. C. et al. (2011) ‘Amyotrophic lateral sclerosis’, in *The Lancet*. Elsevier, pp. 942–955. doi: 10.1016/S0140-6736(10)61156-7.

Kim, H. P., Imbert, J. and Leonard, W. J. (2006) ‘Both integrated and differential regulation of components of the IL-2/IL-2 receptor system’, *Cytokine and Growth Factor Reviews*, pp. 349–366. doi: 10.1016/j.cytofr.2006.07.003.

Kim, H. P., Kelly, J. and Leonard, W. J. (2001) ‘The basis for IL-2-induced IL-2 receptor α chain gene regulation: Importance of two widely separated IL-2 response elements’, *Immunity*. Cell Press, 15(1), pp. 159–172. doi: 10.1016/S1074-7613(01)00167-4.

Kimura, K. (2020) ‘Regulatory T cells in multiple sclerosis’, *Clinical and Experimental Neuroimmunology*. Wiley-Blackwell, pp. 148–155. doi: 10.1111/cen.12591.

Kimura, M. Y. and Nakayama, T. (2005) ‘Differentiation of NK1 and NK2 cells’, *Critical Reviews in Immunology*. Crit Rev Immunol, pp. 361–374. doi: 10.1615/CritRevImmunol.v25.i5.20.

Klatzmann, D. and Abbas, A. K. (2015) ‘The promise of low-dose interleukin-2 therapy for autoimmune and inflammatory diseases’, *Nature Reviews Immunology*. Nature Publishing Group, pp. 283–294. doi: 10.1038/nri3823.

Kohler, S. and Thiel, A. (2009) 'Life after the thymus: CD31 and CD31 human naive CD4 T-cell subsets'. doi: 10.1182/blood-2008-02-139154.

Koreth, J. et al. (2011) 'Interleukin-2 and Regulatory T Cells in Graft-versus-Host Disease', *New England Journal of Medicine*. Massachusetts Medical Society, 365(22), pp. 2055–2066. doi: 10.1056/NEJMoa1108188.

Koreth, J. et al. (2016) 'Efficacy, durability, and response predictors of low-dose interleukin-2 therapy for chronic graft-versus-host disease.', *Blood*. The American Society of Hematology, 128(1), pp. 130–7. doi: 10.1182/blood-2016-02-702852.

Kraczyk, B., Remus, R. and Hardt, C. (2014) 'CD49d treg cells with high suppressive capacity are remarkably less efficient on activated CD45RA - than on naive CD45RA + teff cells', *Cellular Physiology and Biochemistry*. Cell Physiol Biochem Press, 34(2), pp. 346–355. doi: 10.1159/000363004.

Kumar, D. R. et al. (2011) 'Jean-Martin Charcot: the father of neurology.', *Clinical medicine & research*. Marshfield Clinic, 9(1), pp. 46–9. doi: 10.3121/cmr.2009.883.

Kušnierová, P. et al. (2019) 'Neurofilament levels in patients with neurological diseases: A comparison of neurofilament light and heavy chain levels', *Journal of Clinical Laboratory Analysis*. John Wiley and Sons Inc., 33(7). doi: 10.1002/jcla.22948.

Lacomblez, L. et al. (1996) 'Dose-ranging study of riluzole in amyotrophic lateral sclerosis', *Lancet*. Lancet Publishing Group, 347(9013), pp. 1425–1431. doi: 10.1016/S0140-6736(96)91680-3.

Lamikanra, A. A. *et al.* (2020) 'The Migratory Properties and Numbers of T Regulatory Cell Subsets in Circulation Are Differentially Influenced by Season and Are Associated With Vitamin D Status', *Frontiers in Immunology*. Frontiers Media S.A., 11. doi: 10.3389/fimmu.2020.00685.

Lannes, N. *et al.* (2017) 'Microglia at center stage: a comprehensive review about the versatile and unique residential macrophages of the central nervous system.', *Oncotarget*. Impact Journals, LLC, 8(69), pp. 114393–114413. doi: 10.18632/oncotarget.23106.

Lawson, J. M. *et al.* (2008) 'Increased resistance to CD4+CD25hi regulatory T cell-mediated suppression in patients with type 1 diabetes', *Clinical and Experimental Immunology*. John Wiley & Sons, Ltd, 154(3), pp. 353–359. doi: 10.1111/j.1365-2249.2008.03810.x.

Lee, M. *et al.* (2018) 'Tissue-specific role of CX3CR1 expressing immune cells and their relationships with human disease', *Immune Network*. Korean Association of Immunologists. doi: 10.4110/in.2018.18.e5.

Lever, J., Krzywinski, M. and Altman, N. (2017) *Principal component analysis*, Nature Publishing Group. doi: 10.1038/nmeth.4346.

Levine, J. H. *et al.* (2015) 'Data-Driven Phenotypic Dissection of AML Reveals Progenitor-like Cells that Correlate with Prognosis', *Cell*. Cell Press, 162(1), pp. 184–197. doi: 10.1016/j.cell.2015.05.047.

Li, D. W. *et al.* (2018) 'Diagnostic performance of neurofilaments in Chinese patients with amyotrophic lateral sclerosis: A prospective study', *Frontiers in Neurology*. Frontiers Media S.A., 9(AUG), p. 726. doi: 10.3389/fneur.2018.00726.

Li, D. Y. and Xiong, X. Z. (2020) 'ICOS+ Tregs: A Functional Subset of Tregs in Immune Diseases', *Frontiers in Immunology*. Frontiers Media S.A., p. 2104. doi: 10.3389/fimmu.2020.02104.

Li, J. et al. (2019) 'The coordination between B cell receptor signaling and the actin cytoskeleton during B cell activation', *Frontiers in Immunology*. Frontiers Media S.A., p. 3096. doi: 10.3389/fimmu.2018.03096.

Li, M. et al. (2014) 'Mutations in the HFE gene and sporadic amyotrophic lateral sclerosis risk: A meta-analysis of observational studies', *Brazilian Journal of Medical and Biological Research*. Associacao Brasileira de Divulgacao Cientifica, 47(3), pp. 215–222. doi: 10.1590/1414-431X20133296.

Li, Q. and Barres, B. A. (2018) 'Microglia and macrophages in brain homeostasis and disease', *Nature Reviews Immunology*. Nature Publishing Group, pp. 225–242. doi: 10.1038/nri.2017.125.

Li, Z. et al. (2015) 'FOXP3+ regulatory T cells and their functional regulation', *Cellular and Molecular Immunology*. Nature Publishing Group, 12(5), p. 558. doi: 10.1038/CMI.2015.10.

Liao, W., Lin, J. X. and Leonard, W. J. (2013) 'Interleukin-2 at the Crossroads of Effector Responses, Tolerance, and Immunotherapy', *Immunity*. NIH Public Access, pp. 13–25. doi: 10.1016/j.jimmuni.2013.01.004.

Liberal, R. et al. (2015) 'Regulatory T cells: Mechanisms of suppression and impairment in autoimmune liver disease', *IUBMB Life*. Blackwell Publishing Ltd, 67(2), pp. 88–97. doi: 10.1002/iub.1349.

Liblau, R. S. et al. (2002) 'Autoreactive CD8 T cells in organ-specific autoimmunity: Emerging targets for therapeutic intervention', *Immunity*. Cell Press, pp. 1–6. doi: 10.1016/S1074-7613(02)00338-2.

Lindley, S. et al. (2005) 'Defective suppressor function in CD4+CD25+ T-cells from patients with type 1 diabetes', *Diabetes*. American Diabetes Association, 54(1), pp. 92–99. doi: 10.2337/diabetes.54.1.92.

Lindqvist, C. A. et al. (2010) 'T regulatory cells control T-cell proliferation partly by the release of soluble CD25 in patients with B-cell malignancies', *Immunology*. Wiley-Blackwell, 131(3), pp. 371–376. doi: 10.1111/j.1365-2567.2010.03308.x.

Liu, W. et al. (2006) 'CD127 expression inversely correlates with FoxP3 and suppressive function of human CD4+ T reg cells.', *The Journal of experimental medicine*. The Rockefeller University Press, 203(7), pp. 1701–11. doi: 10.1084/jem.20060772.

Liu, X. et al. (2019) 'A comparison framework and guideline of clustering methods for mass cytometry data', *Genome Biology*. BioMed Central Ltd., 20(1), pp. 1–18. doi: 10.1186/s13059-019-1917-7.

Logroscino, G. et al. (2018) 'Global, regional, and national burden of motor neuron diseases 1990–2016: a systematic analysis for the Global Burden of Disease Study 2016', *The Lancet Neurology*. Lancet Publishing Group, 17(12), pp. 1083–1097. doi: 10.1016/S1474-4422(18)30404-6.

Long, S. A. *et al.* (2010) 'Defects in IL-2R signaling contribute to diminished maintenance of FOXP3 expression in CD4+CD25+ regulatory T-cells of type 1 diabetic subjects', *Diabetes*. American Diabetes Association, 59(2), pp. 407–415. doi: 10.2337/db09-0694.

Long, S. A. *et al.* (2012) 'Rapamycin/IL-2 combination therapy in patients with type 1 diabetes augments Tregs yet transiently impairs β-cell function', *Diabetes*. American Diabetes Association, 61(9), pp. 2340–2348. doi: 10.2337/db12-0049.

Longinetti, E. and Fang, F. (2019) 'Epidemiology of amyotrophic lateral sclerosis: An update of recent literature', *Current Opinion in Neurology*. Lippincott Williams and Wilkins, pp. 771–776. doi: 10.1097/WCO.0000000000000730.

Lopez-Lopez, A. *et al.* (2014) 'CX3CR1 Is a Modifying Gene of Survival and Progression in Amyotrophic Lateral Sclerosis', *PLoS ONE*. Edited by C. Raoul. Public Library of Science, 9(5), p. e96528. doi: 10.1371/journal.pone.0096528.

Lyon, M. S. *et al.* (2019) 'Inflammation, Immunity, and amyotrophic lateral sclerosis: I. Etiology and pathology', *Muscle & Nerve*. John Wiley & Sons, Ltd, 59(1), pp. 10–22. doi: 10.1002/mus.26289.

MacLeod, M. K. L. *et al.* (2009) 'CD4 memory T cells: What are they and what can they do?', *Seminars in Immunology*. NIH Public Access, pp. 53–61. doi: 10.1016/j.smim.2009.02.006.

Maggi, E. *et al.* (2005) 'Thymic regulatory T cells', in *Autoimmunity Reviews*. Elsevier, pp. 579–586. doi: 10.1016/j.autrev.2005.04.010.

Mahmoudpour, S. H. et al. (2019) 'Safety of low-dose subcutaneous recombinant interleukin-2: systematic review and meta-analysis of randomized controlled trials', *Scientific Reports*. Nature Publishing Group, 9(1), pp. 1–9. doi: 10.1038/s41598-019-43530-x.

Maier, A. et al. (2012) 'Online assessment of ALS functional rating scale compares well to in-clinic evaluation: a prospective trial.', *Amyotrophic lateral sclerosis: official publication of the World Federation of Neurology Research Group on Motor Neuron Diseases*. Taylor & Francis, 13(2), pp. 210–6. doi: 10.3109/17482968.2011.633268.

Malek, T. R. (2008) 'The biology of interleukin-2', *Annual Review of Immunology*. Annual Reviews, pp. 453–479. doi: 10.1146/annurev.immunol.26.021607.090357.

Malek, T. R. and Castro, I. (2010) 'Interleukin-2 Receptor Signaling: At the Interface between Tolerance and Immunity', *Immunity*. Elsevier, pp. 153–165. doi: 10.1016/j.jimmuni.2010.08.004.

Mantovani, S. et al. (2009) 'Immune system alterations in sporadic amyotrophic lateral sclerosis patients suggest an ongoing neuroinflammatory process', *Journal of Neuroimmunology*, 210(1–2), pp. 73–79. doi: 10.1016/j.jneuroim.2009.02.012.

Marshall, J. S. et al. (2018) 'An introduction to immunology and immunopathology', *Allergy, Asthma and Clinical Immunology*. BioMed Central Ltd., p. 49. doi: 10.1186/s13223-018-0278-1.

Martin, D., Thompson, M. A. and Nadler, J. V. (1993) 'The neuroprotective agent riluzole inhibits release of glutamate and aspartate from slices of hippocampal area CA1', *European Journal of Pharmacology*. Elsevier, 250(3), pp. 473–476. doi: 10.1016/0014-2999(93)90037-I.

Martin, M. D. and Badovinac, V. P. (2018) 'Defining memory CD8 T cell', *Frontiers in Immunology*. Frontiers Media S.A., p. 2692. doi: 10.3389/fimmu.2018.02692.

Martin, S., Al Khleifat, A. and Al-Chalabi, A. (2017) 'What causes amyotrophic lateral sclerosis?', *F1000Research*. Faculty of 1000 Ltd. doi: 10.12688/f1000research.10476.1.

Martínez-Rodríguez, J. E. et al. (2011) 'Natural killer cell phenotype and clinical response to interferon-beta therapy in multiple sclerosis', *Clinical Immunology*. Academic Press, 141(3), pp. 348–356. doi: 10.1016/j.clim.2011.09.006.

Marwaha, A. K. et al. (2012) 'TH17 cells in autoimmunity and immunodeficiency : Protective orpathogenic?', *Frontiers in Immunology*. Frontiers, p. 129. doi: 10.3389/fimmu.2012.00129.

Mason, G. M. et al. (2015) 'Phenotypic Complexity of the Human Regulatory T Cell Compartment Revealed by Mass Cytometry.', *Journal of immunology (Baltimore, Md. : 1950)*. American Association of Immunologists, 195(5), pp. 2030–7. doi: 10.4049/jimmunol.1500703.

Mass, E. et al. (2016) 'Specification of tissue-resident macrophages during organogenesis', *Science (New York, N.Y.)*. NIH Public Access, 353(6304). doi: 10.1126/SCIENCE.AAF4238.

Matejuk, A. (2018) ‘Skin Immunity’, *Archivum Immunologiae et Therapiae Experimentalis*. Birkhauser Verlag AG, pp. 45–54. doi: 10.1007/s00005-017-0477-3.

Matsuoka, K. I. et al. (2013) ‘Low-dose interleukin-2 therapy restores regulatory T cell homeostasis in patients with chronic graft-versus-host disease’, *Science Translational Medicine*. American Association for the Advancement of Science, 5(179), pp. 179ra43-179ra43. doi: 10.1126/scitranslmed.3005265.

Matsuoka, K. ichi (2018) ‘Low-dose interleukin-2 as a modulator of Treg homeostasis after HSCT: current understanding and future perspectives’, *International Journal of Hematology*. Springer Tokyo, pp. 130–137. doi: 10.1007/s12185-017-2386-y.

McCombe, P. A. et al. (2020) ‘The Peripheral Immune System and Amyotrophic Lateral Sclerosis’, *Frontiers in Neurology*. Frontiers Media S.A., p. 279. doi: 10.3389/fneur.2020.00279.

McCombe, P. A. and Henderson, R. D. (2011) ‘The Role of immune and inflammatory mechanisms in ALS.’, *Current molecular medicine*. Bentham Science Publishers, 11(3), pp. 246–54. doi: 10.2174/156652411795243450.

McGoldrick, P. et al. (2013) ‘Rodent models of amyotrophic lateral sclerosis’, *Biochimica et Biophysica Acta - Molecular Basis of Disease*. Elsevier, pp. 1421–1436. doi: 10.1016/j.bbadi.2013.03.012.

Meng, X. et al. (2016) ‘Regulatory T cells in cardiovascular diseases’, *Nature Reviews Cardiology*. doi: 10.1038/nrcardio.2015.169.

Meucci, N., Nobile-Orazio, E. and Scarlato, G. (1996) 'Intravenous immunoglobulin therapy in amyotrophic lateral sclerosis', *Journal of Neurology*. J Neurol, 243(2), pp. 117–120. doi: 10.1007/BF02444000.

Michel, T. et al. (2016) 'Human CD56 bright NK Cells: An Update', *The Journal of Immunology*. The American Association of Immunologists, 196(7), pp. 2923–2931. doi: 10.4049/jimmunol.1502570.

Miller, K. (1983) 'The Stimulation of Human B and T Lymphocytes by Various Lectins', *Immunobiology*. Urban & Fischer, 165(2), pp. 132–146. doi: 10.1016/S0171-2985(83)80055-2.

Miyara, M. et al. (2015) 'Sialyl Lewis x (CD15s) identifies highly differentiated and most suppressive FOXP3<sup>high</sup> regulatory T cells in humans.', *Proceedings of the National Academy of Sciences of the United States of America*. National Academy of Sciences, 112(23), pp. 7225–30. doi: 10.1073/pnas.1508224112.

Mizoule, J. et al. (1985) '2-Amino-6-trifluoromethoxy benzothiazole, a possible antagonist of excitatory amino acid neurotransmission-I. Anticonvulsant properties', *Neuropharmacology*. Pergamon, 24(8), pp. 767–773. doi: 10.1016/0028-3908(85)90011-5.

Mogensen, T. H. (2009) 'Pathogen recognition and inflammatory signaling in innate immune defenses', *Clinical Microbiology Reviews*. American Society for Microbiology (ASM), pp. 240–273. doi: 10.1128/CMR.00046-08.

Moglia, C. et al. (2017) 'The polymorphisms of CX3CR1 gene influence ALS survival in an Italian population-based study (S3.008)', *Neurology*, 88(16 Supplement).

Monier, A. et al. (2007) 'Entry and Distribution of Microglial Cells in Human Embryonic and Fetal Cerebral Cortex', *Journal of Neuropathology & Experimental Neurology*. Oxford Academic, 66(5), pp. 372–382. doi: 10.1097/NEN.0B013E3180517B46.

Mora, J. S. et al. (2020) 'Masitinib as an add-on therapy to riluzole in patients with amyotrophic lateral sclerosis: a randomized clinical trial', *Amyotrophic Lateral Sclerosis and Frontotemporal Degeneration*. Taylor and Francis Ltd, 21(1–2), pp. 5–14. doi: 10.1080/21678421.2019.1632346.

Moreno-Martinez, L. et al. (2019) 'Are circulating cytokines reliable biomarkers for amyotrophic lateral sclerosis?', *International Journal of Molecular Sciences*. MDPI AG. doi: 10.3390/ijms20112759.

Morrice, J. R., Gregory-Evans, C. Y. and Shaw, C. A. (2018) 'Animal models of amyotrophic lateral sclerosis: A comparison of model validity', *Neural Regeneration Research*. Wolters Kluwer Medknow Publications, pp. 2050–2054. doi: 10.4103/1673-5374.241445.

Morris, J. C. and Waldmann, T. A. (2000) 'Advances in interleukin 2 receptor targeted treatment', in *Annals of the Rheumatic Diseases*. BMJ Publishing Group Ltd, pp. i109–i114. doi: 10.1136/ard.59.suppl\_1.i109.

Moudgil, K. D. and Choubey, D. (2011) 'Cytokines in autoimmunity: Role in induction, regulation, and treatment', *Journal of Interferon and Cytokine Research*. Mary Ann Liebert Inc., pp. 695–703. doi: 10.1089/jir.2011.0065.

Murdock, B. J. et al. (2016) 'Increased ratio of circulating neutrophils to monocytes in amyotrophic lateral sclerosis', *Neurology: Neuroimmunology and NeuroInflammation*. Lippincott Williams and Wilkins, 3(4). doi: 10.1212/NXI.0000000000000242.

Murdock, B. J. et al. (2017) 'Correlation of Peripheral Immunity With Rapid Amyotrophic Lateral Sclerosis Progression', *JAMA Neurology*. American Medical Association, 74(12), p. 1446. doi: 10.1001/jamaneurol.2017.2255.

Nagata, T. et al. (2013) 'Neurological Research A Journal of Progress in Neurosurgery, Neurology and Neuro Sciences Elevation of MCP-1 and MCP-1/VEGF ratio in cerebrospinal fluid of amyotrophic lateral sclerosis patients Elevation of MCP-1 and MCP-1/VEGF ratio in cerebrospinal flu'. doi: 10.1179/016164107X229795.

Nelson, B. H. (2004) 'IL-2, Regulatory T Cells, and Tolerance', *J Immunol References*, 172, pp. 3983–3988. doi: 10.4049/jimmunol.172.7.3983.

Nicolas, A. et al. (2018) 'Genome-wide Analyses Identify KIF5A as a Novel ALS Gene', *Neuron*, 97(6), pp. 1268-1283.e6. doi: 10.1016/j.neuron.2018.02.027.

Nishiki, S. et al. (2004) 'Selective activation of STAT3 in human monocytes stimulated by G-CSF: implication in inhibition of LPS-induced TNF- $\alpha$  production', *American Journal of Physiology-Cell Physiology*. American Physiological Society, 286(6), pp. C1302–C1311. doi: 10.1152/ajpcell.00387.2003.

Olingy, C. E. et al. (2017) 'Non-classical monocytes are biased progenitors of wound healing macrophages during soft tissue injury', *Scientific Reports*. Nature Publishing Group, 7(1), pp. 1–16. doi: 10.1038/s41598-017-00477-1.

Opal, S. M. and DePalo, V. A. (2000) 'Anti-inflammatory cytokines', *Chest*. American College of Chest Physicians, 117(4), pp. 1162–1172. doi: 10.1378/chest.117.4.1162.

Paganoni, S. et al. (2014) 'Diagnostic timelines and delays in diagnosing amyotrophic lateral sclerosis (ALS)', *Amyotrophic Lateral Sclerosis and Frontotemporal Degeneration*. Informa Healthcare, 15(5–6), pp. 453–456. doi: 10.3109/21678421.2014.903974.

Palit, S. et al. (2019) 'Meeting the challenges of high-dimensional single-cell data analysis in immunology', *Frontiers in Immunology*. Frontiers Media S.A., 10(JUL), p. 1515. doi: 10.3389/fimmu.2019.01515.

Pan, X. et al. (2012) 'Increased CD45RA+FoxP3low Regulatory T Cells with Impaired Suppressive Function in Patients with Systemic Lupus Erythematosus', *PLoS ONE*. Edited by F. Rieux-Laucat. Public Library of Science, 7(4), p. e34662. doi: 10.1371/journal.pone.0034662.

Pansarasa, O. et al. (2018) 'SOD1 in Amyotrophic Lateral Sclerosis: "Ambivalent" Behavior Connected to the Disease.', *International journal of molecular sciences*. Multidisciplinary Digital Publishing Institute (MDPI), 19(5). doi: 10.3390/ijms19051345.

Patel, A. A. et al. (2017) 'The fate and lifespan of human monocyte subsets in steady state and systemic inflammation', *Journal of Experimental Medicine*. The Rockefeller University Press, 214(7), pp. 1913–1923. doi: 10.1084/JEM.20170355.

Perdomo-Celis, F. et al. (2016) 'Viability and functionality of cryopreserved peripheral blood mononuclear cells in pediatric dengue', *Clinical and Vaccine Immunology*. American Society for Microbiology, 23(5), pp. 417–426. doi: 10.1128/CVI.00038-16.

Peterson, L. B. et al. (2018) 'A long-lived IL-2 mutein that selectively activates and expands regulatory T cells as a therapy for autoimmune disease', *Journal of Autoimmunity*. Academic Press, 95, pp. 1–14. doi: 10.1016/j.jaut.2018.10.017.

Petrov, D. et al. (2017) 'ALS Clinical Trials Review: 20 Years of Failure. Are We Any Closer to Registering a New Treatment?', *Frontiers in Aging Neuroscience*. Frontiers, 9, p. 68. doi: 10.3389/fnagi.2017.00068.

Phani, S., Re, D. B. and Przedborski, S. (2012) 'The Role of the Innate Immune System in ALS.', *Frontiers in pharmacology*. Frontiers Media SA, 3, p. 150. doi: 10.3389/fphar.2012.00150.

Philips, T. and Rothstein, J. D. (2015) 'Rodent Models of Amyotrophic Lateral Sclerosis.', *Current protocols in pharmacology*. NIH Public Access, 69, pp. 5.67.1-21. doi: 10.1002/0471141755.ph0567s69.

Phillips, B. and Weisrose, E. (1974) 'The mitogenic response of human B lymphocytes to phytohaemagglutinin', *Clinical and experimental immunology*. Wiley-Blackwell, 16(3), pp. 383–38392. Available at: [/pmc/articles/PMC1553944/?report=abstract](https://www.ncbi.nlm.nih.gov/pmc/articles/PMC1553944/?report=abstract) (Accessed: 26 February 2021).

Poesen, K. et al. (2017) 'Neurofilament markers for ALS correlate with extent of upper and lower motor neuron disease', *Neurology*. Lippincott Williams and Wilkins, 88(24), pp. 2302–2309. doi: 10.1212/WNL.0000000000004029.

Poesen, K. and Van Damme, P. (2019) 'Diagnostic and prognostic performance of neurofilaments in ALS', *Frontiers in Neurology*. Frontiers Media S.A., p. 1167. doi: 10.3389/fneur.2018.01167.

Da Pozzo, E. et al. (2019) 'Microglial pro-inflammatory and anti-inflammatory phenotypes are modulated by translocator protein activation', *International Journal of Molecular Sciences*. MDPI AG, 20(18). doi: 10.3390/ijms20184467.

Proudfoot, M. et al. (2016) 'The ALSFRS as an outcome measure in therapeutic trials and its relationship to symptom onset', *Amyotrophic Lateral Sclerosis and Frontotemporal Degeneration*. Taylor and Francis Ltd, 17(5–6), pp. 414–425. doi: 10.3109/21678421.2016.1140786.

Pugliese, A. (2017) 'Autoreactive T cells in type 1 diabetes', *Journal of Clinical Investigation*. American Society for Clinical Investigation, pp. 2881–2891. doi: 10.1172/JCI94549.

Rajabinejad, M. et al. (2020) 'Regulatory T cells for amyotrophic lateral sclerosis/motor neuron disease: A clinical and preclinical systematic review', *Journal of Cellular Physiology*. Wiley-Liss Inc., 235(6), pp. 5030–5040. doi: 10.1002/jcp.29401.

Reijn, T. S. et al. (2009) 'CSF neurofilament protein analysis in the differential diagnosis of ALS', *Journal of Neurology*. Springer, 256(4), pp. 615–619. doi: 10.1007/s00415-009-0131-z.

Rentzos, M. et al. (2012) 'Alterations of T cell subsets in ALS: a systemic immune activation?', *Acta Neurologica Scandinavica*. John Wiley & Sons, Ltd (10.1111), 125(4), pp. 260–264. doi: 10.1111/j.1600-0404.2011.01528.x.

Rezaie, P. et al. (2005) 'Microglia in the Cerebral Wall of the Human Telencephalon at Second Trimester', *Cerebral Cortex*. Oxford Academic, 15(7), pp. 938–949. doi: 10.1093/CERCOR/BHH194.

Richards, D., Morren, J. A. and Pioro, E. P. (2020) 'Time to diagnosis and factors affecting diagnostic delay in amyotrophic lateral sclerosis', *Journal of the Neurological Sciences*. Elsevier B.V., p. 117054. doi: 10.1016/j.jns.2020.117054.

Riviere, M. et al. (1998) 'An analysis of extended survival in patients with amyotrophic lateral sclerosis treated with riluzole', *Archives of Neurology*. American Medical Association, 55(4), pp. 526–528. doi: 10.1001/archneur.55.4.526.

Romano, M. et al. (2018) 'Expanded regulatory T cells induce alternatively activated monocytes with a reduced capacity to expand T helper-17 cells', *Frontiers in Immunology*. Frontiers Media S.A., 9(JUL), p. 1625. doi: 10.3389/fimmu.2018.01625.

Rosen, D. R. et al. (1993) 'Mutations in Cu/Zn superoxide dismutase gene are associated with familial amyotrophic lateral sclerosis', *Nature*. Nature, 362(6415), pp. 59–62. doi: 10.1038/362059a0.

Rosenzwaig, M. et al. (2015) 'Low-dose interleukin-2 fosters a dose-dependent regulatory T cell tuned milieu in T1D patients', *Journal of Autoimmunity*. Academic Press, 58, pp. 48–58. doi: 10.1016/j.jaut.2015.01.001.

Rosenzwajg, M. et al. (2020) 'Low-dose IL-2 in children with recently diagnosed type 1 diabetes: a Phase I/II randomised, double-blind, placebo-controlled, dose-finding study', *Diabetologia*. Springer, 63(9), pp. 1808–1821. doi: 10.1007/s00125-020-05200-w.

Ross, S. H. and Cantrell, D. A. (2018) 'Signaling and Function of Interleukin-2 in T Lymphocytes', *Annual Review of Immunology*. Annual Reviews Inc., 36, pp. 411–433. doi: 10.1146/annurev-immunol-042617-053352.

Rutkove, S. B. (2015) 'Clinical Measures of Disease Progression in Amyotrophic Lateral Sclerosis', *Neurotherapeutics*. Springer New York LLC, pp. 384–393. doi: 10.1007/s13311-014-0331-9.

Saadoun, D. et al. (2011) 'Regulatory T-Cell Responses to Low-Dose Interleukin-2 in HCV-Induced Vasculitis', *New England Journal of Medicine*. Massachusetts Medical Society, 365(22), pp. 2067–2077. doi: 10.1056/nejmoa1105143.

Sakaguchi, S. et al. (2008) 'Regulatory T Cells and Immune Tolerance', *Cell*. Elsevier, pp. 775–787. doi: 10.1016/j.cell.2008.05.009.

Sakaguchi, S. et al. (2010) 'FOXP3 + regulatory T cells in the human immune system'. doi: 10.1038/nri2785.

Saudagar, R. and Garge, L. (2019) 'Amyotrophic Lateral Sclerosis: An Overview', *Journal of Drug Delivery and Therapeutics*, 9(3), pp. 613–616. doi: 10.22270/jddt.v9i3.2874.

De Schaepdryver, M. et al. (2018) 'Comparison of elevated phosphorylated neurofilament heavy chains in serum and cerebrospinal fluid of patients with amyotrophic lateral sclerosis', *Journal of Neurology, Neurosurgery and Psychiatry*. BMJ Publishing Group, 89(4), pp. 367–373. doi: 10.1136/jnnp-2017-316605.

Schmidt, A., Oberle, N. and Krammer, P. H. (2012) 'Molecular mechanisms of reg-mediated cell suppression', *Frontiers in Immunology*. Frontiers, p. 51. doi: 10.3389/fimmu.2012.00051.

Scholzen, T. and Gerdes, J. (2000) 'The Ki-67 protein: From the known and the unknown', *Journal of Cellular Physiology*. J Cell Physiol, pp. 311–322. doi: 10.1002/(SICI)1097-4652(200003)182:3<311::AID-JCP1>3.0.CO;2-9.

Seale, A. C. et al. (2008) 'Effects of cryopreservation on CD4+ CD25+ T cells of HIV-1 infected individuals', *Journal of Clinical Laboratory Analysis*, 22(3), pp. 153–158. doi: 10.1002/jcla.20234.

Seelig, E. et al. (2018) 'The DILfrequency study is an adaptive trial to identify optimal IL-2 dosing in patients with type 1 diabetes', *JCI Insight*. American Society for Clinical Investigation, 3(19). doi: 10.1172/JCI.INSIGHT.99306.

Sheean, R. K. et al. (2018) 'Association of regulatory T-Cell Expansion with progression of amyotrophic lateral sclerosis a study of humans and a transgenic mouse model', *JAMA Neurology*. American Medical Association, 75(6), pp. 681–689. doi: 10.1001/jamaneurol.2018.0035.

Shevyrev, D. and Tereshchenko, V. (2020) 'Treg Heterogeneity, Function, and Homeostasis', *Frontiers in Immunology*. Frontiers Media S.A., p. 3100. doi: 10.3389/fimmu.2019.03100.

Silva-Neta, H. L. et al. (2018) 'CD4+CD45RA-FOXP3<sup>low</sup> Regulatory T Cells as Potential Biomarkers of Disease Activity in Systemic Lupus Erythematosus Brazilian Patients', *BioMed Research International*. Hindawi Limited, 2018. doi: 10.1155/2018/3419565.

Smith, N. C., Rise, M. L. and Christian, S. L. (2019) 'A Comparison of the Innate and Adaptive Immune Systems in Cartilaginous Fish, Ray-Finned Fish, and Lobe-Finned Fish', *Frontiers in Immunology*. Frontiers Media S.A., p. 2292. doi: 10.3389/fimmu.2019.02292.

Smith, S. A. et al. (1994) 'Treatment of ALS with high dose pulse cyclophosphamide', *Journal of the Neurological Sciences*. Elsevier, 124(SUPPL.), pp. 84–87. doi: 10.1016/0022-510X(94)90188-0.

Sojka, D. K., Huang, Y. H. and Fowell, D. J. (2008) 'Mechanisms of regulatory T-cell suppression - A diverse arsenal for a moving target', *Immunology*. Wiley-Blackwell, pp. 13–22. doi: 10.1111/j.1365-2567.2008.02813.x.

Song, S. W. et al. (2016) 'Major histocompatibility complex class I molecules protect motor neurons from astrocyte-induced toxicity in amyotrophic lateral sclerosis', *Nature Medicine*. Nature Publishing Group, 22(4), pp. 397–403. doi: 10.1038/nm.4052.

Song, W. M. and Colonna, M. (2018) 'The identity and function of microglia in neurodegeneration', *Nature Immunology*. Nature Publishing Group, pp. 1048–1058. doi: 10.1038/s41590-018-0212-1.

Soucie, E. L. *et al.* (2016) 'Lineage-specific enhancers activate self-renewal genes in macrophages and embryonic stem cells', *Science (New York, N.Y.)*. NIH Public Access, 351(6274), p. aad5510. doi: 10.1126/SCIENCE.AAD5510.

Von Spee-Mayer, C. *et al.* (2016) 'Low-dose interleukin-2 selectively corrects regulatory T cell defects in patients with systemic lupus Erythematosus', *Annals of the Rheumatic Diseases*. BMJ Publishing Group, 75(7), pp. 1407–1415. doi: 10.1136/annrheumdis-2015-207776.

Spolski, R., Li, P. and Leonard, W. J. (2018) 'Biology and regulation of IL-2: from molecular mechanisms to human therapy', *Nature Reviews Immunology*. Nature Publishing Group, pp. 648–659. doi: 10.1038/s41577-018-0046-y.

Stauber, D. J. *et al.* (2006) 'Crystal structure of the IL-2 signaling complex: Paradigm for a heterotrimeric cytokine receptor', *Proceedings of the National Academy of Sciences of the United States of America*. National Academy of Sciences, 103(8), pp. 2788–2793. doi: 10.1073/pnas.0511161103.

Stein, S. A. M. *et al.* (2006) 'Chapter 13 Principal Components Analysis: A Review of its Application on Molecular Dynamics Data', *Annual Reports in Computational Chemistry*. Elsevier, pp. 233–261. doi: 10.1016/S1574-1400(06)02013-5.

Steinacker, P. *et al.* (2016) 'Neurofilaments in the diagnosis of motoneuron diseases: A prospective study on 455 patients', *Journal of Neurology, Neurosurgery and Psychiatry*. BMJ Publishing Group Ltd, 87(1), pp. 12–20. doi: 10.1136/jnnp-2015-311387.

Stelmaszczyk-Emmel, A. *et al.* (2013) 'Frequency and Activation of CD4+CD25 high FoxP3+ Regulatory T Cells in Peripheral Blood from Children with Atopic Allergy', *International Archives of Allergy and Immunology*. Karger Publishers, 162(1), pp. 16–24. doi: 10.1159/000350769.

Stephenson, J. and Amor, S. (2017) 'Modelling amyotrophic lateral sclerosis in mice', *Drug Discovery Today: Disease Models*. Elsevier Ltd, pp. 35–44. doi: 10.1016/j.ddmod.2018.10.001.

Su, D. L. *et al.* (2012) 'Roles of pro- and anti-inflammatory cytokines in the pathogenesis of SLE', *Journal of Biomedicine and Biotechnology*. doi: 10.1155/2012/347141.

Taams, L. S. *et al.* (2005) 'Modulation of monocyte/macrophage function by human CD4+CD25+ regulatory T cells', *Human Immunology*, 66(3), pp. 222–230. doi: 10.1016/j.humimm.2004.12.006.

Thonhoff, J. R. *et al.* (2018) 'Expanded autologous regulatory T-lymphocyte infusions in ALS', *Neurology - Neuroimmunology Neuroinflammation*. Wolters Kluwer Health, Inc. on behalf of the American Academy of Neurology, 5(4), p. e465. doi: 10.1212/NXI.0000000000000465.

Thonhoff, J. R., Simpson, E. P. and Appel, S. H. (2018) 'Neuroinflammatory mechanisms in amyotrophic lateral sclerosis pathogenesis', *Current Opinion in Neurology*. NLM (Medline), 31(5), pp. 635–639. doi: 10.1097/WCO.0000000000000599.

Tiemessen, M. M. et al. (2007) *CD4 CD25 Foxp3 regulatory T cells induce alternative activation of human monocytes/macrophages*. Available at: [www.pnas.org/cgi/doi/10.1073/pnas.0706832104](http://www.pnas.org/cgi/doi/10.1073/pnas.0706832104) (Accessed: 9 April 2020).

Todd, John A. et al. (2016) 'Regulatory T Cell Responses in Participants with Type 1 Diabetes after a Single Dose of Interleukin-2: A Non-Randomised, Open Label, Adaptive Dose-Finding Trial', *PLOS Medicine*. Edited by T. W. J. Huizinga. Public Library of Science, 13(10), p. e1002139. doi: 10.1371/journal.pmed.1002139.

Todd, John A et al. (2016) 'Regulatory T Cell Responses in Participants with Type 1 Diabetes after a Single Dose of Interleukin-2: A Non-Randomised, Open Label, Adaptive Dose-Finding Trial'. doi: 10.1371/journal.pmed.1002139.

Traynor, B. J. et al. (2000) 'Clinical features of amyotrophic lateral sclerosis according to the El Escorial and Airlie House diagnostic criteria: A population-based study', *Archives of Neurology*. American Medical Association, 57(8), pp. 1171–1176. doi: 10.1001/archneur.57.8.1171.

Traynor, B. J. et al. (2003) 'An outcome study of riluzole in amyotrophic lateral sclerosis: A population-based study in Ireland, 1996-2000', *Journal of Neurology*. J Neurol, 250(4), pp. 473–479. doi: 10.1007/s00415-003-1026-z.

Trojsi, F. et al. (2019) 'ALS Genetics, Mechanisms, and Therapeutics: Where Are We Now?' doi: 10.3389/fnins.2019.01310.

Trombetta, A. C. et al. (2018) 'A circulating cell population showing both M1 and M2 monocyte/macrophage surface markers characterizes systemic sclerosis patients with lung involvement', *Respiratory Research*. BioMed Central Ltd., 19(1), p. 186. doi: 10.1186/s12931-018-0891-z.

Tsai, S., Shameli, A. and Santamaria, P. (2008) 'Chapter 4 CD8+ T Cells in Type 1 Diabetes', *Advances in Immunology*. Academic Press, pp. 79–124. doi: 10.1016/S0065-2776(08)00804-3.

Turner, M. R. et al. (2004) 'Evidence of widespread cerebral microglial activation in amyotrophic lateral sclerosis: An [11C](R)-PK11195 positron emission tomography study', *Neurobiology of Disease*. Academic Press, 15(3), pp. 601–609. doi: 10.1016/j.nbd.2003.12.012.

Turner, M. R. et al. (2013) 'Mechanisms, models and biomarkers in amyotrophic lateral sclerosis.', *Amyotrophic lateral sclerosis & frontotemporal degeneration*. NIH Public Access, 14 Suppl 1(0 1), pp. 19–32. doi: 10.3109/21678421.2013.778554.

Turvey, S. E. and Broide, D. H. (2010) 'Innate immunity', *Journal of Allergy and Clinical Immunology*. NIH Public Access, 125(2 SUPPL. 2), p. S24. doi: 10.1016/j.jaci.2009.07.016.

Umoh, M. E. *et al.* (2016) Comparative analysis of C9orf72 and sporadic disease in an ALS clinic population. Available at: <https://www.ncbi.nlm.nih.gov/pmc/articles/PMC5027809/pdf/NEUROLOGY2016729715.pdf> (Accessed: 7 August 2019).

Valle-Mendiola, A. *et al.* (2016) 'Pleiotropic Effects of IL-2 on Cancer: Its Role in Cervical Cancer', *Mediators of Inflammation*. Hindawi Limited. doi: 10.1155/2016/2849523.

Venken, K. *et al.* (2007) 'A CFSE based assay for measuring CD4+CD25+ regulatory T cell mediated suppression of auto-antigen specific and polyclonal T cell responses', *Journal of Immunological Methods*. Elsevier, 322(1–2), pp. 1–11. doi: 10.1016/j.jim.2007.01.025.

Venken, K. *et al.* (2008) 'Natural Naive CD4 + CD25 + CD127 low Regulatory T Cell (Treg) Development and Function Are Disturbed in Multiple Sclerosis Patients: Recovery of Memory Treg Homeostasis during Disease Progression', *The Journal of Immunology*. The American Association of Immunologists, 180(9), pp. 6411–6420. doi: 10.4049/jimmunol.180.9.6411.

Viglietta, V. *et al.* (2004) 'Loss of Functional Suppression by CD4+CD25+ Regulatory T Cells in Patients with Multiple Sclerosis', *Journal of Experimental Medicine*. The Rockefeller University Press, 199(7), pp. 971–979. doi: 10.1084/jem.20031579.

Vignali, D. A. A., Collison, L. W. and Workman, C. J. (2008) 'How regulatory T cells work', *Nature Reviews Immunology*, pp. 523–532. doi: 10.1038/nri2343.

Villarino, A. V. *et al.* (2015) 'Mechanisms of Jak/STAT Signaling in Immunity and Disease', *The Journal of Immunology*. The American Association of Immunologists, 194(1), pp. 21–27. doi: 10.4049/jimmunol.1401867.

Vu, L. T. and Bowser, R. (2017) 'Fluid-Based Biomarkers for Amyotrophic Lateral Sclerosis', *Neurotherapeutics*. Springer New York LLC, pp. 119–134. doi: 10.1007/s13311-016-0503-x.

Wales, S. *et al.* (2011) 'Seminar Amyotrophic lateral sclerosis', *The Lancet*, 377, pp. 942–955. doi: 10.1016/S0140.

Wallin, M. T. *et al.* (2019) 'Global, regional, and national burden of multiple sclerosis 1990–2016: a systematic analysis for the Global Burden of Disease Study 2016', *The Lancet Neurology*. Lancet Publishing Group, 18(3), pp. 269–285. doi: 10.1016/S1474-4422(18)30443-5.

Wang, Y. *et al.* (2012) 'Regulatory T cell: a protection for tumour cells.', *Journal of cellular and molecular medicine*. Wiley-Blackwell, 16(3), pp. 425–36. doi: 10.1111/j.1582-4934.2011.01437.x.

Waysbort, N. *et al.* (2013) 'Coupled IL-2–Dependent Extracellular Feedbacks Govern Two Distinct Consecutive Phases of CD4 T Cell Activation', *The Journal of Immunology*. The American Association of Immunologists, 191(12), pp. 5822–5830. doi: 10.4049/jimmunol.1301575.

Werdelin, L. *et al.* (1990) 'Immunosuppressive treatment of patients with amyotrophic lateral sclerosis', *Acta Neurologica Scandinavica*. John Wiley & Sons, Ltd, 82(2), pp. 132–134. doi: 10.1111/j.1600-0404.1990.tb01602.x.

Willinger, T. et al. (2005) 'T Cell Subsets Central Memory from Effector Memory CD8 Molecular Signatures Distinguish Human', *The Journal of Immunology*, 175, pp. 5895–5903. doi: 10.4049/jimmunol.175.9.5895.

Wojdasiewicz, P. et al. (2014) 'The Chemokine CX3CL1 (Fractalkine) and its Receptor CX3CR1: Occurrence and Potential Role in Osteoarthritis', *Archivum Immunologiae et Therapiae Experimentalis*. Birkhauser Verlag AG, pp. 395–403. doi: 10.1007/s00005-014-0275-0.

Wolf, S. A., Boddeke, H. W. G. M. and Kettenmann, H. (2017) 'Microglia in Physiology and Disease', *Annual Review of Physiology*. Annual Reviews Inc., 79(1), pp. 619–643. doi: 10.1146/annurev-physiol-022516-034406.

Yadav, A., Saini, V. and Arora, S. (2010) 'MCP-1: Chemoattractant with a role beyond immunity: A review', *Clinica Chimica Acta*. doi: 10.1016/j.cca.2010.07.006.

Yam-Puc, J. C. et al. (2018) 'Role of B-cell receptors for B-cell development and antigen-induced differentiation', *F1000Research*. F1000 Research Ltd. doi: 10.12688/f1000research.13567.1.

Yang, J. H. M. et al. (2015) 'Natural variation in interleukin-2 sensitivity influences regulatory T-cell frequency and function in individuals with long-standing type 1 diabetes', *Diabetes*. American Diabetes Association Inc., 64(11), pp. 3891–3902. doi: 10.2337/db15-0516.

Yang, J. H. M. et al. (2019) 'Phenotypic Analysis of Human Lymph Nodes in Subjects With New-Onset Type 1 Diabetes and Healthy Individuals by Flow Cytometry', *Frontiers in Immunology*. Frontiers Media S.A., 10(OCT), p. 2547. doi: 10.3389/fimmu.2019.02547.

Yao, Y. and Tsirka, S. E. (2014) 'Monocyte chemoattractant protein-1 and the blood-brain barrier.', *Cellular and molecular life sciences : CMLS*. NIH Public Access, 71(4), pp. 683–97. doi: 10.1007/s00018-013-1459-1.

Yatim, K. M. and Lakkis, F. G. (2015) 'A brief journey through the immune system', *Clinical Journal of the American Society of Nephrology*. American Society of Nephrology, 10(7), pp. 1274–1281. doi: 10.2215/CJN.10031014.

Ye, C., Brand, D. and Zheng, S. G. (2018) 'Targeting IL-2: an unexpected effect in treating immunological diseases', *Signal Transduction and Targeted Therapy*. Springer Nature, pp. 1–10. doi: 10.1038/s41392-017-0002-5.

Yoshino, H. and Kimura, A. (2006) 'Investigation of the therapeutic effects of edaravone, a free radical scavenger, on amyotrophic lateral sclerosis (phase II study)', *Amyotrophic Lateral Sclerosis*. Taylor and Francis Ltd., 7(4), pp. 247–251. doi: 10.1080/17482960600881870.

Yu, A. et al. (2000) 'Efficient Internalization of IL-2 Depends on the Distal Portion of the Cytoplasmic Tail of the IL-2R Common  $\gamma$ -Chain and a Lymphoid Cell Environment', *The Journal of Immunology*. The American Association of Immunologists, 165(5), pp. 2556–2562. doi: 10.4049/jimmunol.165.5.2556.

Yu, A. *et al.* (2015) 'Selective IL-2 responsiveness of regulatory t cells through multiple intrinsic mechanisms supports the use of low-dose IL-2 therapy in type 1 diabetes', *Diabetes*. American Diabetes Association Inc., 64(6), pp. 2172–2183. doi: 10.2337/db14-1322.

Zabransky, D. J. *et al.* (2012) 'Phenotypic and Functional Properties of Helios+ Regulatory T Cells', *PLoS ONE*. Edited by C. A. Piccirillo. Public Library of Science, 7(3), p. e34547. doi: 10.1371/journal.pone.0034547.

Zelante, T. *et al.* (2012) 'Interleukin-2 production by dendritic cells and its immuno-regulatory functions', *Frontiers in Immunology*. Frontiers, p. 161. doi: 10.3389/fimmu.2012.00161.

Zhang, J. *et al.* (2018) 'Dynamic changes of CX3CL1/CX3CR1 axis during microglial activation and motor neuron loss in the spinal cord of ALS mouse model', *Translational Neurodegeneration*. BioMed Central Ltd., 7(1), p. 35. doi: 10.1186/s40035-018-0138-4.

Zhang, J. M. and An, J. (2007) 'Cytokines, inflammation, and pain', *International Anesthesiology Clinics*. NIH Public Access, pp. 27–37. doi: 10.1097/AIA.0b013e318034194e.

Zhang, N. and Bevan, M. J. (2011) 'CD8+ T Cells: Foot Soldiers of the Immune System', *Immunity*. Elsevier, pp. 161–168. doi: 10.1016/j.immuni.2011.07.010.

Zhang, R. *et al.* (2006) 'MCP-1 chemokine receptor CCR2 is decreased on circulating monocytes in sporadic amyotrophic lateral sclerosis (sALS)', *Journal of Neuroimmunology*. Elsevier, 179(1–2), pp. 87–93. doi: 10.1016/J.JNEUROIM.2006.06.008.

Zhao, H., Liao, X. and Kang, Y. (2017) 'Tregs: Where We Are and What Comes Next?', *Frontiers in immunology*. Frontiers Media SA, 8, p. 1578. doi: 10.3389/fimmu.2017.01578.

Zhao, W. et al. (2017) 'Characterization of gene expression phenotype in amyotrophic lateral sclerosis monocytes', *JAMA Neurology*. American Medical Association, 74(6), pp. 677–685. doi: 10.1001/jamaneurol.2017.0357.

Ziegler-Heitbrock, L. (2007) 'The CD14+ CD16+ blood monocytes: their role in infection and inflammation', *Journal of Leukocyte Biology*. Wiley, 81(3), pp. 584–592. doi: 10.1189/jlb.0806510.

Zondler, L. et al. (2016) 'Peripheral monocytes are functionally altered and invade the CNS in ALS patients', *Acta Neuropathologica*. Springer Berlin Heidelberg, 132(3), pp. 391–411. doi: 10.1007/s00401-016-1548-y.

Zorn, E. et al. (2006) 'IL-2 regulates FOXP3 expression in human CD4 CD25 regulatory T cells through a STAT-dependent mechanism and induces the expansion of these cells in vivo'. doi: 10.1182/blood-2006-02-004747.